Conceptualising and quantifying the nonlinear, chaotic climate: Implications for climate model experimental design

Stefaan Conradie (CNRWIL004)

Supervisors: Dr. Babatunde J. Abiodun
Dr. Joseph D. Daron
Dr. Tristan P. Hauser

Dissertation presented for the degree of Master of Science in the Department of Environmental and Geographical Science
University of Cape Town

November 27, 2015

Plagiarism Declaration

I know the meaning of plagiarism and declare that all of the work in the dissertation, save for that which is properly acknowledged, is my own.

Signed: Willem Stefaan Conradie (CNRWIL004) _____

Date: _____

Abstract

Uncertainty in climate system initial conditions (ICs) is known to limit the predictability of future atmospheric states. On weather time scales (i.e. hours to days), the separation between two atmospheric model trajectories, initially "indistinguishable" (compared to unavoidable uncertainties) from one another, diverges exponentially-on-average over time, so that the "memory" of model ICs is eventually lost. In other words, there is a theoretical limit in the lead time for skilful weather forecasts. However, the influence of perturbations to climate system model ICs—particularly in more slowly evolving climate system components (e.g., the oceans and ice sheets)—on the evolution of model "climates" on longer time scales is less well understood. Hence, in order to better understand the role of IC uncertainty in climate predictability, particularly in the context of climate change, it is necessary to develop approaches for investigating and quantifying—at various spatial and temporal scales—the nature of the influence of ICs on the evolution of climate system trajectories. To this end, this study explores different conceptualisations and competing definitions of climate and the climate system, focussing on the role of ICs. The influence of ICs on climate quantifications, using probability distributions, is subsequently investigated in a climate model experiments using a low-resolution version of the Community Climate System Model version 4 (CCSM4). The model experiment consists of 11 different 50-member ensemble simulations with constant forcing, and three 50-member ensemble simulations under a climate change scenario with transient forcing. By analysing the output at global and regional scales, at least three distinct levels of IC influence are detected: (a) microscopic influence; (b) interannual-scale influence; and (c) intercentennial-scale influence. Distinct patterns of interannual-scale IC influence appear to be attributable to aperiodic and quasi-periodic variability in the model. It is found that, over some spatial domains, significant ($p < 0.01$) differences in atmospheric variable "climatologies", taken from 60-year distributions of model trajectories, occur due to IC differences of a similar order to round-off error. In addition, climate distributions constructed using different approaches are found to differ significantly. There is some evidence that ensemble distributions of multidecadal temperature response to transient forcing conditions can be influenced by ICs. The implications for quantifying and conceptualising climate are considered in the context of the experimental results. It is concluded that IC ensemble experiments can play a valuable role in better understanding climate variability and change, as well as allowing for superior quantification of model climates.

Acknowledgements

Without the significant ($p < 0.01$), extensive assistance of many individuals and institutions, this study would certainly not have been possible. My first thanks go to Phillip Mukwenha, member of the Climate System Analysis Group (CSAG) IT team, whose essential support of this study may not be acknowledged elsewhere. Phillip helped to me port, set-up, compile and run the Community Earth System Model (CESM) on the numerous platforms used in this study. His tireless assistance with debugging and general software support during the project are greatly appreciated. Thanks Phillip, for always being approachable and ready to help, even with stupid questions!

My supervisors provided extraordinary support, encouragement and assistance to the project. I thank Joseph Daron for suggesting the topic of study to me and giving me an opportunity to explore and engage with aspects of the climate science field I would not otherwise have been able to access. Thanks, in particular, Joe, for remaining available to help and comment, even after having left CSAG and being able to communicate only virtually. Your detailed comments and thorough engagement is great asset to this dissertation. Thanks also to Joe and Babatunde Abiodun for their understanding during the difficult time I had during the first year or so of the study and for keeping faith in my ability to produce a dissertation of some value. Babatunde I must also thank for keeping me grounded and his continued attempts to teach me the need for focus and planning. As he quoted: "you can take a camel to the water, but you cannot force it to drink." This camel has been carefully guided to the water and motivated to drink. These lessons I start to learn now will hopefully be of value to me throughout my life. I thank Tristan Hauser for always being available to answer questions and for his interest in our work. Tristan seemed always to have a comment handy that somehow is thought-provoking, humorous, grounding and motivating at the same time.

Great help and support with running CESM1.2 and using NERSC was also provided by Karthik Kashinath, Travis O'Brien and Daithi Stone. It would not have been possible to do the extensive experiments run without your assistance.

To my sister, Carina, and parents, Ina and Jurie, my heartfelt thanks for your continued love and support through the time of the dissertation, despite how "moeilik" I've often been. Thanks also to my dad for reading through and commenting on much of this document (there are no commas in this sentence...). I could not dream of repaying this support.

I would also like to share my thanks for the many useful conversations and hints from the fellow students with whom I shared office 1.04 ("The Office"): Sabina Abba Omar, Myra Naik, Temitope Egbebiyi, Molulaqhooa Maoyi, Lerato Thakoli and Mankurwana Mahlase. Thanks also for all the not-necessarily-useful-but-interesting/fun conversations and general entertainment. Life will never quite be the same again without the quote board...

The financial assistance of the National Research Foundation (DAAD-NRF) towards this research is hereby acknowledged. Opinions expressed and conclusions arrived at, are those of the author and are not necessarily to be attributed to the DAAD-NRF. I would like to further thank DAAD for the extended support they provided, especially through hosting the DAAD-NRF In-Country scholarship holders meetings.

Computational resources made available for this study by the South African Centre for High Performance Computing (CHPC)—operating as part of South Africa's Centre for Scientific and Industrial Research (CSIR) under South Africa's Department of Science and Technology (DST)—and the National Energy Research Scientific Computing Center (NERSC)—a DOE Office of Science User Facility supported by the Office of Science of the U.S. Department of Energy under Contract No. DE-AC02-05CH11231—were essential and are greatly appreciated. I would also like to thank the CHPC for the valuable Winter and Summer school workshops they host, two of which I have been fortunate to attend during the course of this study. Additional computation was also conducted on the CSAG's "core" cluster. My (and I'm sure all of CSAG's) sincere thanks go to Phillip Mukwenha, Roger Duffet and Chris Jack for their tireless work in maintaining the cluster, supporting students in our use of it and the immense effort involved in ensuring its optimal functioning between load-shedding events.

CESM is used in this study. It is freely available (https://www2.cesm.ucar.edu/) and support is available to users through the CESM forum (https://bb.cgd.ucar.edu/). I would like to thank the developers and maintainers of the CESM project for making the model widely available and for all forum users who provided valuable answers and input in response to questions I posed regarding this study. The CESM project is supported by the National Science Foundation and the Office of Science (BER) of the U.S. Department of Energy.

And finally, thanks to Johann Sebastian Bach and Wolfgang Amadeus Mozart for writing the music that kept me motivated while writing up this dissertation.

Contents

List of Figures

List of Tables

Chapter 1

Introduction

As understanding and predicting climate variability and climate change take on ever increasing importance for political, economic, ecological and social decision making (IPCC, 2013b, 2014), interrogating remaining conceptual ambiguities in the climate discourse becomes an urgent task. This study aims to explore fundamental questions arising from inconsistent and often imprecise formulations of the definition of climate. A nonlinear dynamical systems perspective is adopted to assess how contrasting conceptualisations and approaches to quantification of the climate affect our understanding and perceptions of the behaviour of the climate system, with a particular focus on the role of initial conditions (ICs). To this end, assumptions relating to various conceptualisations of "climate", are explored using output from IC ensemble simulations of a climate system model (CSM), both under stationary and transient forcing conditions.

In section 1.1, the need to review definitions of climate is considered. The idea of a definition is considered in a broad sense to include attempts at conceptualising or characterising—especially through quantification—the relevant entity. The reasons for applying a low-dimensional nonlinear dynamical systems approach is presented in section 1.2. The framework for the conceptual component of the study is presented in section 1.3. Its relation to the experimental component is addressed in section 1.4. The study aim, objectives and research question are presented in section 1.5.

1.1 Why Consider Definitions of Climate and The Climate System?

Many definitions have been proposed for climate and the climate system in the literature (e.g., Werndl, 2015; Lucarini, 2002; Kraus, 1984; Lovejoy, 2013; Lorenz, 1995), in introductory works on the subject (e.g., McGuffie and Henderson-Sellers, 2005; Goosse et al., 2013; Monin, 1986) and by national and international scientific organisations (e.g., IPCC, 2013a;

AMS, 2013; WMO, 2010).

There has recently been debate in the literature about the value of assessing potential definitions of climate (e.g., Werndl, 2014b) and perceived conventional approaches to conceptualising (e.g., Lovejoy, 2013; Lovejoy et al., 2013; Lovejoy, 2014) and quantifying (e.g., Daron and Stainforth, 2013, 2015) climate. Why, then, do we consider it necessary to review definitions of climate? For many of the central concepts in climate science, there do not appear to be any widely accepted definitions (Todorov, 1986; Daron, 2012; Werndl, 2015). One might argue that definitions used are broadly similar, that there appears to be consensus on the intuitive idea of climate (Leith, 1985, see subsection 2.1.2) and that the descriptions used are generally "good enough" for the specific contexts in which they are applied. However, Lorenz (1995) notes that "certain questions regarding climate may be answered either affirmatively or negatively, according to the precise [definition of climate used]". Furthermore, Lorenz (1995) suggests that in different contexts—across which the nature of the available data varies—the definition that would lead to the most meaningful characterisation of a given climatic state, may differ (see also Schneider and Dickinson, 1974). For example, a key distinction explored in this dissertation is between definitions applicable to individual climate trajectories sampled over time, on the one hand, and, on the other hand, definitions applicable only to ensembles of climate model trajectories, either at a particular "instant" or over a period of time. In this work, ensembles considered are IC ensembles, but definitions involving perturbed physics and multi-model ensemble output could also be proposed; in particular, it could be argued that the IPCC (2013b) apply a multi-model ensemble definition in quantifying projected future climates. This argument is further developed in section 1.3, where five Conceptualisations of climate, which it will be argued in section 2.1 represent distinct ways of thinking about "climate" and/or "the climate", are introduced.

While the field of climate science continues to expand rapidly, it may be useful to reconsider how we conceptualise and quantify a non-stationary climate (Daron and Stainforth, 2013, 2015; Werndl, 2015). Refining and enhancing our understanding of the nature of the climate system—and our models of it—would be valuable in this regard (Held, 2005). Exploring the question of which avenues of investigation might help to fulfil this goal is the primary focus of this study. Particularly, how one might incorporate into our conceptualisation of climate ideas derived from our enhanced understanding of the climate system, its internal interactions and its—presumably (see section 1.2)—nonlinear dynamical nature (Tsonis, 2001; Selvam, 2012), requires further investigation. This study explores particular examples of such concepts, considered in the context of low-dimensional conceptual models by Daron (2012) and Daron and Stainforth (2013, 2015).

Definitions of climate play an important role—often implicitly—in shaping the discussion of related terms. This applies, in particular, to terms applied in the climate change discourse (e.g., Lorenz, 1995; Todorov, 1986; Werndl, 2015). These are often expressed in terms of climate and/or the climate system (e.g., IPCC, 2013a).

Precise definitions would improve comparability between studies and are a valuable

tool in mathematical investigations of climate, including climate modelling (Schneider and Dickinson, 1974). While actually establishing a single definition of climate appropriate in all climatic subdisciplines is clearly not within reach of this investigation—and it is quite possible that any attempt to do so will prove fruitless (Lorenz, 1995)—it is hoped that this study contributes to the discussion around the conceptual framework within which different climatic definitions are developed, chosen and applied. An attempt is also made to interrogate some of those assumptions regarding definitions of climate which are generally made, but often remain implicit or imprecisely stated.

Definitions of climate which are applicable in observational studies, are not necessarily the most useful in theoretical or modelling studies (Lorenz, 1995; Schneider and Dickinson, 1974; Leith, 1978). Hence, understanding of the differences in climatic characterisations that could be produced by different approaches to defining climate, should be explored and considered in experimental design and interpretation of results (Lorenz, 1995). This study aims to contribute to the discussion on preferable future approaches to climate model experimental design (see section 1.4), following Daron and Stainforth (2013, 2015).

1.2 Utility of a Nonlinear Dynamical Systems Perspective in Climate System Investigation

The equations which are believed to describe the assumed "physical laws" (Lorenz, 1964, p.1) governing the behaviour of the climate system and, in particular, the dynamics of the atmosphere (Lorenz, 1964), are nonlinear (e.g., Rind, 1999). Climate models, being essentially solvers of these nonlinear equations (e.g., Goosse et al., 2013), are thus necessarily nonlinear systems. The nature of the real system is more difficult to assess, given the complicated interplay between constantly changing, uncertain "forcing conditions" and internal variability (Tsonis et al., 1994; Stainforth et al., 2007a). However, there is evidence that the climate system displays signs of nonlinearity (e.g., Rial et al., 2004; Lovejoy, 2014)—for example in the strength of the the Atlantic Meridional Overturning Circulation (AMOC) (e.g., Stommel, 1961; Hawkins et al., 2011; Drijfhout, 2014; Boulton et al., 2014). Furthermore, it is widely considered very likely that at least some features of the climate system's behaviour are chaotic (e.g., Lorenz, 1990, 1995; Palmer, 1996; Lucarini, 2002; Teng et al., 2011; Branstator and Teng, 2012; Daron, 2012, section 2.1.2).

In this study, the climate system—and in particular the output of a climate system model—is considered as a complex nonlinear system, certain qualitative aspects of the behaviour of which can be studied and understood by analogy with the behaviour of simple nonlinear systems. For this purpose, concepts developed to explore and explain the behaviour of such systems—especially those of Lorenz (1963, 1984)—are used.

Such a nonlinear paradigm can enhance qualitative understanding of the nature of climate changes and shifts in patterns of variability (e.g., Palmer, 1999; Hauser et al.,

2015). However, the extent to which nonlinearity influences predictability and uncertainty in the system is unknown and poorly understood (Katzav et al., 2012), as is its role in the response of the climate system to external forcing and anthropogenic influence (Lorenz, 1976, 1991a; Andrews et al., 2015; Rind, 1999; Rial et al., 2004).

Understanding of the behaviour of nonlinear dynamical systems has rapidly grown during a period of exponential growth of computational power (Strogatz, 1994). Ideas from meteorology (especially Lorenz, 1963) played an essential part in the initial motivation for this development (Tsonis, 2001; Strogatz, 1994; Shilnikov et al., 1998). Subsequently, valuable applications of chaos and nonlinear dynamical systems theory in atmospheric and climate science have been found (Tsonis, 1996, 2001; Sivakumar, 2004; Broer and Vitolo, 2008). Numerous potential future applications appear to be promising, warranting further investigation, which could lead to improved qualitative understanding of the system (Tsonis, 1996, 2001; Broer and Vitolo, 2008; Lovejoy et al., 2009). It has been widely suggested that nonlinear dynamical systems approaches are undervalued in climate science (e.g., Lovejoy et al., 2009; Rial et al., 2004; Daron and Stainforth, 2013).

Challenges in applying nonlinear dynamical systems approaches arise in practice, given that the equations describing planetary climate are partial differential equations (PDEs) (Goosse et al., 2013; Spiegel, 1987), rather than the ordinary differential equations (ODEs), in terms of which "classical" chaos and low-dimensional nonlinear dynamical systems theory is framed (Broer and Vitolo, 2008). However, there are conditions under which ODEs can be considered useful approximations to climatic processes (e.g., Lorenz, 1984, 1990). Furthermore, through spatial discretisation, prior to temporal discretisation, climate models are transformed into solvers of systems of ODEs (Lorenz, 1964; Dijkstra and Ghil, 2005; Goosse et al., 2013). The value of low-dimensional dynamical systems theory for climate system investigation is considered in greater detail in subsection 2.2.1. It remains a subject of contention (e.g., Tsonis, 2001; Lovejoy et al., 2009; Lovejoy, 2014).

It should be noted that this work is intended to serve as an investigation of concepts derived from the study of nonlinear systems (Daron, 2012), explored here using a CSM, which is related to a Coupled Model Intercomparison Project phase 5 (CMIP5; Taylor et al., 2012) member model (CCSM4). It therefore does not involve the application of advanced nonlinear analysis techniques, as explored in the global circulation model (GCM) or CSM context by, for example, Dijkstra and Ghil (2005), Thies et al. (2009), Tsonis and Swanson (2012), Tantet and Dijkstra (2014) and Lovejoy et al. (2013).

1.3 Overview of Conceptual Component

The concept of IC "influence" is central to this study. IC uncertainty (ICU; Stainforth et al., 2007a) is intimately related to observations. The quality of observations is not considered in depth, here. The distinction between microscopic and macroscopic ICU is of particular value, in part because there is good reason to expect ICUs of particular

kinds to reflect in characteristic ways in the subsequent evolution of climate trajectories (Stainforth et al., 2007a). Consequently, a central goal of this study (see section 1.5) is to explore how IC differences of particular types, from different locations in the model state space, reflect in the subsequent behaviour of climate system evolution and, hence, how different quantifications of climate are influenced. In this context, the term IC influence is used to refer to the effects of IC differences on climate trajectories and quantifications. IC influence could be quantified by the length of time it takes for the "IC footprint" in climate system trajectories to decay to the extent that the system behaviour can no longer be directly attributed to particular aspects of the ICs used. Quantification of IC influence is discussed at greater length in subsection 5.1.2 and section 6.1. IC influence could also be seen as reflecting the extent of qualitatively different behaviours of the system which are consistent with a particular ICU. IC influence describes the differences in subsequent climate that emerge when choosing a particular IC from an uncertainty domain in state space (following Lorenz (1995)), rather than some other IC from within that domain.

A related key concept is that of potential predictability. For a variable $v(t)$, given some information, I about the state of $v(t)$ or a quantity influencing $v(t)$, potential predictability is considered to exist when the probability distribution of $v(t)$, given I, is detectably different from the probability distribution of $v(t)$, in the absence of I. This definition is similar to that used by, for example, Branstator and Teng (2010) and Daron and Stainforth (2015). Understanding the relationship between IC influence, potential predictability and quantifications of climate, is a prominent theme of this study.

Perceived key assumptions relating to conceptualisations and quantification of climate are discussed in chapters 2 and 6, representing the primary conceptual component of this study. This component is presented in the framework of a number conceptual questions, and conceptualisations and notions of climate. Firstly, we suggest that the following represent key conceptual questions, which need to be addressed prior to deciding upon a precise definition or quantification of "climate":

Conceptual Questions

(CQ1) Is climate simply a statistical construct, or does it represent a collection of physical properties of the Earth system?

(CQ2) Can a meaningful distinction between "weather" and "climate" time scales be found?

(CQ3) Which components or subsets of the "climate system" or "Earth system" should be considered when defining climate? In particular, should we include variables of immediate practical relevance, or all variables considered to have a significant impact on the distributions of these variables?

(CQ4) Should it be possible for climate to vary significantly in the absence of net external forcing?

(CQ5) Are the answers to (CQ1)–(CQ4) different for the "real" climate system and climate models?

(CQ6) Do the answers to (CQ1)–(CQ4) depend on whether one considers global, regional or local spatial scales?

Prominent conceptualisations of climate considered are:

Conceptualisations

(C1) Climate as "average weather", or more generally "statistics of weather variables".

(C2) Climate as some set of conditions which determine the weather "possibility space".

(C3) Climate as an "attractor" in some—potentially unknown, high-dimensional—climate system phase space. This Conceptualisation could be considered a special case of (C2).

(C4) Climate as a collection of processes acting on distinct time scales and producing distinct patterns of behaviour to "weather". "Climatic state" can then be thought of as similar to "climate" as defined by (C1) (Lovejoy, 2014).

(C5) Climate as the collective behaviour of coupled climate subsystems (Tsonis and Swanson, 2012).

The extent of understanding of climate change, at a global scale, that can be gained from consideration of a few time series—which nonetheless require immense resource and time expenditure, and ingenuity to assemble and study—appears to contradict the widely acknowledged notion that climate has high dimensionality (e.g., Bryson, 1997). However, if the answer to (CQ6) is affirmative, it may help resolve this apparent contradiction. In particular, we note that the term "climate" can be used to refer to at least four distinct, scale-dependent notions:

Notions

(N1) Local "climates";

(N2) Classification of spatial domains into climatic zones;

(N3) The nature of global energy budgets and exchanges of climate system components; and

(N4) The state and behaviour of a spatiotemporal dynamical system, referred to as the "climate system".

Admittedly, the boundaries between Notions (N1)–(N4) are rather fluid. Perhaps a more in-depth investigation into distinct conceptualisations held by researchers in climate-related fields would help to establish a more meaningful distinction between them. However, this is beyond the scope of the present work.

There are clear associations between Conceptual Questions (CQ1)–(CQ6), Conceptualisations (C1)–(C5) and Notions (N1)–(N4). For example, conceptualising climate as per (C2) or (C3) is clearly not consistent with a notion of climate as (N1). However, applying (C2) or (C3) to (N3) or (N4) could provide interesting results.

Following Lorenz (1995), it is suggested that any definition of climate should correspond generally to the idea that "climate is what you expect", given that this is the general perception of what the concept is which one is attempting to characterise in defining a climate.

1.4 Modelling Experiments and Defining Climate

Experimental design refers here to the development and running of numerical climate models of various types (Claussen et al., 2002; McGuffie and Henderson-Sellers, 2005; Goosse et al., 2013). This is often done for qualitative or quantitative predictive purposes (Kirtman et al., 2013; Collins et al., 2013). Such predictions are considered decision-relevant by various sectors of society (Stainforth et al., 2007a; Smith, 2002) and are increasingly being applied at various temporal and spatial scales (Frigg et al., 2015; Branstator and Teng, 2010).

In this study, large IC ensemble simulations of the Community Earth System Model (CESM), version 1.2 (Hurrell et al., 2013; Vertenstein et al., 2013) are run at coarse horizontal resolution, to minimise computational expense. Details of the experimental design are provided in section 3.3. The focus of the computational component is to address the following questions, for the chosen model configuration:

Modelling Questions

(MQ1) Can one identify distinct "levels" of IC influence (see Stainforth et al., 2007a, for a discussion of levels of ICU)?

(MQ2) Is the kairodic assumption of Daron and Stainforth (2014) (stating, roughly-speaking, that climate variable distributions sampled over time are indistinguishable from climate variable distributions sampled from multiple "possible" climate model trajectories at the same model time) valid? What time scales should be considered "long enough" for single model run trajectories to explore enough of the model state space to be able to accurately represent the range of possible system states?

(MQ3) Could, in a stationary climate (i.e., where external forcing is constant), in a transitive state (i.e., where "jumps" between different model attractors is not possible), ensemble climate statistics be sensitively dependent on IC sampling? If so, how much, when and how?

(MQ4) Is there evidence to suggest that particular model subsystems are intransitive or display "almost-intransitivity" (Lorenz, 1968)?

(MQ5) How are the answers to the above questions affected by the domains over which they are assessed?

1.5 Aims and Objectives

1.5.1 Research Question

What role, if any, should ICs play in our conceptualisation and approaches to quantifying climate?

1.5.2 Aim

To explore different possible influences of ICs on climate variable distributions, using a nonlinear dynamical systems framework.

1.5.3 Objectives

1. Develop a comprehensive overview of definitions of climate that have been—and continue to be—applied in the climate discourse and review the literature on their utility.

2. Consider aspects of the current state of understanding of variability and uncertainty in the climate system, which have implications for conceptualisations and quantification of climate.

3. Run a set of large IC ensemble simulations of a CSM, with the intention of sampling a range of possible IC influences on the model climate, under stationary and transient forcing conditions.

4. Explore the nature of the atmospheric variability produced by the model control runs, to inform assessment of the likely connections between IC influence and modes of variability.

5. Investigate the nature of IC influence apparent in atmospheric variable time series.
6. Analyse regional-mean atmospheric data to assess the validity of the kairodic assumption in this model.
7. Consider possible evidence of interaction between IC influence and transient climate change response.

1.6 Layout of the Dissertation

This study is composed of a conceptual component and a modelling component. A general background to—and discussion of—the conceptual component is provided in section 2.1. Conceptual questions relating more directly to the modelling component are addressed in section 2.2. The set-up of the modelling experiment is described in chapter 3. Context for the analysis of the ensemble run results is provided by chapter 4 and Appendix B, in which control run results are presented and discussed. Findings of the ensemble experiment are presented in chapter 5. A discussion of key implications is presented in chapter 6. The extent to which the research objectives were met is addressed in chapter 7.

Chapter 2

Literature Review

This chapter is composed of two parts. Literature related to key ideas raised in sections 1.3 and section 1.4 is reviewed in section 2.1. In section 2.2, literature related more directly to the modelling experiments performed is reviewed.

2.1 Part A: Exploring Definitions of Climate

In the discussion which follows, emphasis is placed on aspects of our conceptualisation of the climate system which are considered to require further attention, as we seek to develop more informative climate model experiments and projections, and more meaningfully interpret their results.

Before definitions of climate are explored, some requirements which Werndl (2015) suggests such a definition should satisfy, are summarised in subsection 2.1.1. A general introduction to definitions of climate is then given in subsection 2.1.2. In subsection 2.1.3, examples of definitions of climate which have previously been applied are discussed and broadly classified, according to the Conceptualisations introduced in section 1.3. Different Notions with which climate may be equated are explored in subsection 2.1.4. More precise aspects of definitions of climate are considered in subsection 2.1.5. Together, these sections address the Conceptual Questions posed in section 1.3.

2.1.1 Purpose of a Definition in the Present Context

Definitions should be precise, unambiguous and avoid circular reasoning (Werndl, 2015). Werndl (2015, section 3) suggests five further "desiderata" which a rigorous definition of climate should satisfy. Werndl (2015) describes these desiderata as "fairly weak". They can be summarised as stating that such a definition should:

Desiderata

1. Allow the Earth's climate over a particular period to be empirically determined;
2. Allow one to detect changes that would be universally regarded as climatic;
3. Be independent of the degree of uncertainty that exists regarding the climate system;
4. Be applicable to any period; and
5. Not be mathematically meaningless.

These desiderata present challenges in conceptualising and quantifying model climates, which are explored in this dissertation.

2.1.2 Climate as "Average Weather"

The exploration of the concept of climate is perhaps best approached by first considering what could be thought of as an approximate intuitive definition of climate proposed by, for example, Leith (1978) and IPCC (2013a), characterising climate as "average weather". Lorenz (1995) quotes a saying which is similar in its message: "Climate is what you expect, weather is what you get", before attempting a more precise formulation as "Climate is...what you ought to expect, when you are not in a position to make a skillful weather forecast". Lorenz (1995) suggests that this may be the best intuitive definition of climate that one could give, and should serve as a reference for all more precise definitions of climate. Accordingly, to gain an understanding of the climate, one would do well to consider the weather first (Goosse et al., 2013).

Although it describes climate "in a narrow sense" in terms of weather, IPCC (2007, 2013a) does not include a definition of "weather". The World Meteorological Organisation (WMO) defines weather as the "[s]tate of the atmosphere at a particular time, as defined by the various meteorological elements ([a]tmospheric variable[s] or phenomen[a] which characterize the state of the weather at a specific place at a particular time (e.g., air temperature, pressure, wind, humidity, thunderstorm and fog))" (WMO, 2012). The American Meteorological Society (AMS), in turn, proposes the following definition for weather: "The state of the atmosphere, mainly with respect to its effects upon life and human activities," adding that, in contrast to climate, "weather consists of the short-term (minutes to days) variations in the atmosphere", most often described with reference to the variables "temperature, humidity, precipitation, cloudiness, visibility, and wind" (AMS, 2013). The AMS distinguishes between the above use of the word in terms of "atmospheric state" and its use in the context of "surface weather observations", where weather is defined as "a category of individual and combined atmospheric phenomena that must be drawn upon to describe the local atmospheric activity at the time of observation" (AMS, 2013). Presumably, climate is intended to refer to a statistical description of the former.

Although weather is defined in terms of atmospheric state, the "weather" in the turbosphere, for example, is rarely discussed, yet it is generally considered part of the atmosphere. The troposphere is often described as the portion of the atmosphere in which weather occurs (e.g., IPCC, 2013a). The comment by the AMS (2013) that weather is usually discussed with reference to the impact of the atmosphere on people suggests that a description of weather involves mostly the near-surface "atmospheric state". One might argue that what occurs throughout the atmosphere impacts upon measured weather elements, but so does the oceanic circulation, though this is not widely considered as an entity whose state should be included in a *description* of the weather. It is, however, sometimes included in a description of climate.

An alternative definition for weather is implicitly given in the AMS glossary entry on "atmosphere", where it is noted that "[f]luid dynamical instabilities play a large role in [the atmospheric general circulation] and are crucial in determining the fluctuations in [the atmospheric general circulation] that we call 'weather' " (AMS, 2013). This would suggest a fundamentally different way of thinking about the relationship between weather and climate; one in which weather is considered to be high-frequency "noise" superimposed upon a stable background "climate state." These ideas are discussed further in subsubsection 2.1.4.2.

A number of noteworthy points emerge from the formulation of the above definitions. The use of examples and clarifying phrases is suggestive of a lack of consistency in precisely how the term is applied. Additionally, the WMO definition applies circular reasoning, in that it defines the weather in terms of entities whose definition refers to "weather"; as a result, the definition provides little information other than example state variables.

2.1.3 Common Definitions of Climate

In this subsection, some examples of definitions of climate which have been proposed and applied in the climate literature are given. Together with definitions discussed in subsection 2.1.4, these examples are intended to be representative of Conceptualisations (C1)–(C5) (page 6) and different approaches to quantifying climate thus conceptualised. It is suggested that there is scope to explore the implications of these different definitions. Wallace (1996a) notes that the conceptual differences in views of climate exist between different climatic subdisciplines, as a result of the nature of the data they encounter.

2.1.3.1 Temporal Statistics and Climate Normals

More precise definitions of climate often employ the concept of "climatological standard normals" (Guttman, 1989; Huang et al., 1996; Goosse et al., 2013): mean values of atmospheric variables measured at meteorological stations, which are computed over successive, non-overlapping 30-year periods, starting from 1 January 1901 (AMS, 2013;

WMO, 1988). Hence, the most recent period is 1961-1990. The practice of computing climatological standard normals was established in order to standardise the presentation of climate information, thus improving comparability between locations internationally (Trewin, 2007). The arbitrary period of 30 years was chosen primarily as it was considered to be the longest period for which sufficient data coverage existed at the time (WMO, 2010; Trewin, 2007). However, the WMO (2010) acknowledge that there are shortcomings in using only statistics derived during these 30-year periods in formulating our knowledge of climatic variable states—a matter explored by, among others, Trewin (2007); Lamb and Changnon Jr (1981) and Livezey et al. (2007).

Additionally, mean statistics cannot fully characterise climatic states. They do not, for example, give any indication of the frequency or duration of threshold exceedances, which identify rare or extreme events (Guttman, 1989). Hence, it has been suggested that other distributional statistics be incorporated into descriptions of climate states (WMO, 2010). As such, a complete, optimal, standard framework for the statistical description of climate remains elusive (Livezey et al., 2007). It could even be considered impossible to establish, due to, for example, spatially and temporally variable optima (Huang et al., 1996).

Approximations of the first two statistical moments (mean and variance) and percentile values of weather variable distributions, are commonly used in descriptions of climate. However, information about distributional skewness and kurtosis (the third and fourth moments) has only recently begun to receive more attention (Leith, 1978), as can be seen by comparing the second (WMO, 1983) and third (WMO, 2010) editions of the WMO's "Guide to Climatological Practices". Skewness statistics can provide insight into the mechanisms, low-frequency modulations, spatial structure and degree of nonlinearity of El Niño-Southern Oscillation (ENSO) behaviour (Burgers and Stephenson, 1999; Jin et al., 2003; An and Jin, 2004; An, 2009; Zhang and Sun, 2014). Niño sea surface temperature (SST) indices display significant, spatially and temporally highly variable skewness, with eastern Pacific SST tending to be positively skewed and western Pacific SST negatively skewed (An, 2009). This "ENSO asymmetry" is generally poorly simulated by CSMs and (Zhang et al., 2009; Zhang and Sun, 2014). Burgers and Stephenson (1999) also advocate for the use of kurtosis to characterise the nature of climate mode fluctuations.

A more general approach than specifying a finite collection of distributional statistics would be to define the climate as the probability distributions of the variables of interest (e.g. Guttorp, 2014). In practice these would then be estimated by empirical distribution functions (e.g., Werndl, 2015, section 4). The approach of using distributions to characterise climate variables is used in this study; definitions using distributions of a single model trajectory, sampled over time, are referred to as temporal definitions. It can also be applied to ensemble studies; see subsubsection 2.1.3.2.

In the context of present climate change, it is of particular relevance that the use of distributions and distributional statistics derived by sampling over time has the potential to be very misleading in the presence of nonlinear, secular trend (e.g., Livezey et al., 2007; Trewin, 2007; Daron and Stainforth, 2013, 2015). This is acknowledged by Werndl (2015),

who proposes defining climate as "the distribution over time under a regime of varying external conditions" (Werndl, 2015). However, Werndl (2014a,b, 2015) acknowledges that it would be a non-trivial task to stipulate how to identify distinct regimes of forcings.

Under the common assumption that temperatures are approximately normally distributed (Trewin, 2007), specifying the first two statistical moments is sufficient to entirely characterise such a distribution. However, the assumption does not always hold even for temperature distributions, locally and regionally; for example, the Niño temperature indices discussed above and Lenhard and Baum (1954) and Harmel et al. (2002).

2.1.3.2 Ensemble Statistics

Schneider and Dickinson (1974) propose a definition of climate as "averages over a hypothetical ensemble of internal states that is nearly in equilibrium with ... external influences".Leith (1978) proposes the use of "ensemble simulations", by analogy with Statistical Mechanics, in quantifying and predicting climatic conditions, suggesting a definition of climate "in terms of averages over the ensemble". Such definitions are only valid for simulated climate, since there do not exist alternative "Earths" to experiment on (Leith, 1978; Werndl, 2015). Ensembles may be initialised from a range of different ICs. Potentially, alternative definitions using perturbed parameter ensembles (e.g., Teng and Branstator, 2011; Teng et al., 2011) or multi-model ensembles could conceivably be employed (see subsections 2.2.1.3 and 6.2.1).

The definition originally proposed by Leith (1978) conforms generally to Definition 4 of Werndl (2015). Leith (1978) and Lorenz (1995) suggest that this definition is of considerable value in conceptual and theoretical studies. However, Werndl (2015) points out that, as with temporal distributions defined with fixed external forcings, the applicability to the real climate system is limited, since external forcings in reality never remain fixed. Daron and Stainforth (2015) show that periodic forcings of certain frequencies produce distributions very different from distributions with constant external forcings in the Lorenz-63 model (L63; Lorenz, 1963). There is some evidence that such behaviour may occur in the real system, in that internal variability interacts with diurnal (e.g., McCormack et al., 2010) and annual cycles (e.g., Wu et al., 2008; Neelin et al., 1998, section 6.2). Hence, even in the case of what is generally considered "stationary" parameters (i.e including only diurnal and annual cycle changes), the use of conventional autonomous dynamical systems theory to understand the nature of climate is problematic (Werndl, 2015).

In response, a non-autonomous ensemble definition is proposed by Werndl (2015, as Definition 5). Similarly, Daron and Stainforth (2015), for example, define the "time-dependent [model] climate" as the "[ensemble] frequency distributions of model variables".

Theoretically, IC ensemble definitions may be formulated in terms of infinite-member ensembles (Werndl, 2015), but practically finitely many ICs need to be sampled from a subset of the state space. It is non-trivial to decide from which subset of the model state

space to sample ICs. Often the aim of ensemble simulations is to quantify uncertainty from a particular source (Stainforth et al., 2007a); in particular, IC ensembles are widely used to investigate uncertainty related to internal variability, due to uncertainty in initial state (e.g., Hansen et al., 1997; Daron and Stainforth, 2013). Lorenz (1995) suggests that IC ensembles be initialised from a collection of states indistinguishable from a particular "best-guess" observed state, within observational uncertainty. To Werndl (2015) this presents a problem: referring in a definition of climate to the present degree of uncertainty in climate system observations would seem to violate her Desideratum (3) (see subsection 2.1.1).

Considering the distinction between micro- and macroscopic ICU, introduced by Stainforth et al. (2007a, see also section 1.3), could help resolve this problem. This represents a focal line of inquiry in this study. Microscopic ICU refers to uncertainties about climate system state which are essentially insensitive to our state of knowledge. As Smith (2000a,b, 2002) notes, even if models were perfect representations of reality, initialised from accurate observations, with complete spatial coverage—which, even theoretically, is unachievable—round off error in measurement and computation would still lead to propagation of error over time. Lorenz (1969b) found that climate-like systems may exhibit the property that, for a given "lead time" (the simulation time prior to computing ensemble statistics), IC predictability cannot be improved through finite reductions in the IC error. Hence, it is likely that CSM IC ensemble distributions evaluated after a lead time appropriate for climate assessments, would be relatively insensitive to the magnitude or nature of atmospheric IC perturbations applied (Palmer, 2009; Palmer et al., 2014). In other words, the extent of knowledge and observational coverage of the atmospheric state might not significantly affect climate estimates from ensemble definitions. This possibility is explored with one of the ensembles run for this study; see section 3.3 for details.

An important consideration for evaluating ensemble distributions is optimal lead times, addressed in subsubsection 2.1.4.4. A potential extension of ensemble definitions would be to use an "ensemble-temporal" distribution obtained by sampling over ensemble members and over a period of time. This is suggested by Stainforth et al. (2007a), as a pragmatic approach to quantifying model climate under rapidly evolving external forcings, in the absence of sufficiently large ensembles. An adaptation of this approach is used in this study. Such ensemble-temporal definitions are viewed as a general approach to subsume possible long-lasting quasi-periodic signals (see subsubsection 2.2.2.4), thus reducing the influence of a possibly too short lead time.

2.1.3.3 Time Scales and Processes

Climate can also be characterised in a manner similar to Conceptualisation (C4); i.e. by processes acting on distinct time scales. Often this involves attempting to explicitly differentiate between weather and climate time scales (e.g., Schneider and Dickinson, 1974; Pitcock, 1978) or between processes considered to be "weather processes" and "climate processes". An example of the latter approach was suggested by Hasselmann (1976).

The "coupled ocean-atmosphere-cryosphere-land system" also referred to as the "complete weather-climate system", is conceptualised as being described by a state vector $\mathbf{z}$, which can be separated into $\mathbf{x}$ and $\mathbf{y}$. These are the state vectors of the "weather system" and the "climate system", respectively. The state of rapidly varying components of $\mathbf{z}$—essentially the atmosphere—is quantified by $\mathbf{x}$. Slowly varying variables—quantifying the state of "the ocean, cryosphere, land vegetation, etc."—are contained in $\mathbf{y}$. This assumes the existence of a meaningful distinction of climate and weather time scales, thus answering Conceptual Question (CQ2) affirmatively. It is noteworthy that Hasselmann's characterisation of climate in terms of the evolution of $\mathbf{y}$ excludes any explicit reference to atmospheric variables. Hence, it circumvents the need to compute statistics by considering only slowly varying variables. Investigating the mechanisms believed to be responsible for climate system processes is a vital facet of climate research (von Storch and Zwiers, 1999, pg.1). Defining climate in terms of these mechanisms implies regarding climate as not simply a statistical convenience (see subsubsection 2.1.4.2). Such an approach is taken by McGregor (2006), stating that "climate is the long-term manifestation of the interaction between the atmosphere and the [E]arth's surface and of processes arising from other causes that are internal and external to the climate system." Definitions of the "climate system" are reviewed in subsubsection 2.1.4.1.

Lovejoy (2013, 2014), building on results from (Lovejoy and Schertzer, 1986), considers the climate system as an infinite-dimensional nonlinear system, exhibiting "scale-invariance" through "cascade processes", best investigated in the framework of "stochastic chaos" (Lovejoy and Schertzer, 1998, 2010). Scaling analysis is performed on time series assumed to describe atmospheric variability, covering a wide range of temporal scales. It is suggested that these series are characterised by different atmospheric temporal "scaling regimes". It is proposed that these be referred to as "weather" (acting on time scales up to roughly 10 days, i.e. $\tau \lesssim 10$ days), "macroweather" (10 days $\lesssim \tau \lesssim 40$ years, although this may vary between a decade and a century, depending on the extent of anthropogenic forcing), "climate" (40 years $\lesssim \tau \lesssim 8 \times 10^4$ years), "macroclimate" (8×10^4 years $\lesssim \tau \lesssim 5 \times 10^5$ years) and megaclimate ($\tau \gtrsim 5 \times 10^5$ years). The "weather", "climate" and "megaclimate" regimes are characterised by variations which increase with increasing temporal scale and thus do not yield stationary temporal statistics. Conversely, "macroweather" and "macroclimate" series tend to be amenable to meaningful averaging; statistics over the "macroweather" time scales are regarded as determining the "climate state", which evolves through climate time scales under the influence of distinct climatic processes. Consequently, Lovejoy (2013, 2014) suggests that "climate is not what you expect". It should be noted that, as explained in section 1.3 (see also, subsection 2.1.2), this work investigates the idea of climate as "what one should expect". In accordance with a conceptual perspective following the work of Lorenz (1968, 1970, 1976, 1991a, 1995), this expectation should be allowed to vary—even in the absence of variable external forcing, due to the possibility of almost-intransitivity.

2.1.4 Conceptualising Climate

2.1.4.1 Climates, The Climate and The Climate System

In this section, Notions (N1)–(N4) (page 6), as they are applied in the literature, are discussed. Definitions of the climate system and Earth system are then reviewed.

Notion (N1) (of local climates) is characterised by its reference to essentially zero-dimensional data (if one disregards the convention of representing statistics for seasons, months, weeks or dates separately). It involves analysing spatially localised time series statistically, thus quantifying climate as in subsubsection 2.1.3.1). However, as McGregor (2006) notes, "the climate of a location is influenced by the balance between large and local scale factors". Furthermore, "the climate of a location or region is the product of the interaction between the surface and a range of thermodynamic and dynamical variables." Hence, there is a prominent link between (N1) and (N4).

Notion (N2) (of climatic zones), the most famous example of which was proposed by Köppen (1900), is intended to provide maps depicting regions which experience similar "climates" (Martyn and Senn, 1992; von Storch and Zwiers, 1999), usually as defined according to (N1) (Martyn and Senn, 1992). However, Martyn and Senn (1992) suggest that regional climate classification would be less arbitrary and more useful if considered in terms of (N4).

Notion (N3) (in terms of energy budgets) primarily involves the evolution of globally aggregated time series. It can be studied by using, among other approaches, energy balance models (EBMs, see subsubsection 2.2.1.1). Studies of (N3) often employ observational (e.g., Cowtan and Way, 2014) or proxy (e.g., Phipps et al., 2013) time series over as extensive a period as data is relatively reliably available for. These series are intended to capture globally influential characteristics of the climate system. Usually the quantities investigated are means or integrals over a surface—such as global-mean surface temperature (GMST; as used in, e.g., IPCC, 2013b; Estrada et al., 2013; Dai et al., 2015)—or a volume—such as ocean heat content (OHC; as used in, e.g., IPCC, 2013b; Meehl et al., 2011; Watanabe et al., 2013).

Notion (N4) (of the climate as a system) involves consideration of dynamical and physical processes, teleconnections and their regional expressions. This approach to climate is described by McGregor (2006) as "climate system theory". Conceptualised thus, "climate is the manifestation of the interaction among the major climate system components of the atmosphere of hydrosphere, cryosphere, biosphere and land surface and external forcings such as solar variability and long term earth-sun geometry relationships."

Spatial patterns and structures, investigated in studies of (N4), influence the energy exchanges studied in relation to (N3). Park and Mann (2000) assert that it is likely that "multidecadal (50–70 year)...intrinsic oscillatory climate processes...largely redistribute heat over the surface of the globe...projecting weakly onto global...warmth", following work by,

among others, Mann and Park (1994); Mann et al. (1995). This could be interpreted as justification for treating of (N3) and (N4) as largely distinctive fields of study on sufficiently long time scales. However, the influence of patterns of internal variability on global climate (N3) appears to be gaining prominence, as more evidence comes to light supporting the notion that GMST evolution at multidecadal time scales is sensitive to patterns of spatial variability (e.g., Rose et al., 2014; Dai et al., 2015; Tantet and Dijkstra, 2014), although this is still a matter of considerable debate (e.g., Mann et al., 2014; Kravtsov et al., 2014). This debate can be conceptualised as being about the necessity of considering (N4) in studies of (N3).

IPCC (2013a) differentiates between climate "in a narrow sense" (as discussed in subsection 2.1.2) and climate "in a wider sense". The latter is defined as "the state, including a statistical description, of the climate system." Similarly, Bryson (1997) distinguishes between "Climate" and "climates". A climate is "the statistical assemblage of the weather in a region or at a place", clearly corresponding to (N1) or (N2). "Climate", which is considered equivalent to "climatic status", is defined as "the thermodynamic/hydrodynamic status of the global [boundary conditions (BCs)] that determine the concurrent array of weather patterns". Climate thus defined could be considered to refer to aspects of (N3) and (N4). Similarly, Lorenz (1995) draws a distinction between defining "climate" and applying such a definition to determine the "climatic state". Such a distinction is also implicit in the use of these terms by Lovejoy (2013, 2014). Perhaps determining "climatic state" may be seen as part of the study of (N1) and (N3), whereas (N4) is employed in studies of "climate". This distinction could be useful in understanding connections between different conceptualisations of climates, the climate and the climate system.

Until recently, characterisations of the climate system were often relatively narrow. For example, Peixóto and Oort (1984) characterised the "internal [climate] system" as including only the atmosphere. Rind (1999) states that "climate system consists of interactions between the atmosphere and ocean". Lorenz (1995) considered the climate system to be composed of " the atmosphere, the ocean and the upper layers of the land".

Recent definitions of the climate system are often similar to that of Kutzbach (1976), who proposes that the climate system "consist[s] of the atmosphere, oceans, cryosphere..., lithosphere and biomass". A similar definition is endorsed by IPCC (2013b) and, consequently, Goosse et al. (2013). Schellnhuber (1999), Kabat et al. (2004) and Rial et al. (2004) propose a more extensive definition: "Earth's climate system includes the natural spheres (e.g., atmosphere, biosphere, hydrosphere and geosphere), the anthrosphere (e.g., economy, society, culture), and their complex interactions." However, there appears to be some inconsistency, as Rial et al. (2004) sometimes refer to such a system as the "Earth system". The view of humans as internal to the climate system is certainly not universally accepted; for example, Lovejoy (2013) refers to anthropogenic influences as external forcings, whereas Cornell et al. (2012) suggests that including the "anthroposphere...as a distinctive subset of the biosphere" could be considered an "extention" of a conventional Earth system conceptualisation. Considering the biosphere in conjunction

with the "geosphere" (composed of atmosphere, hydrosphere, cryosphere and lithosphere) forms the basis for the "Earth system".

However, Schneider and Dickinson (1974) already asserted that "[w]e generally think of climate in reference to the average behavior of the land-ocean-atmosphere-cryosphere system over relatively long periods". Note that climate thus defined corresponds to Notion (N4). It implies an inclusive answer to Conceptual Question (CQ3), in contrast to definitions discussed in subsection 2.1.2, which involve only the near-surface elements. A similar view is suggested by the "climate system theory" definition of McGregor (2006) (see above) and by Guttorp (2014), who claims that, "[f]or a statistician, climate is the distribution of weather and other variables that are part of the climate system." Definitions of climate in terms of climate system state have generally become more widely applied, as our understanding of the importance of climate system component interactions grows (Goosse et al., 2013). Emphasis is also placed in IPCC (2013b) on climate change as involving changes in the climate system (i.e. on changes in climate "in a wider sense"). In contrast, Werndl (2015) asserts that not all climate system variables are "climate variables"—even though processes occurring throughout the climate system influence climatic state.

2.1.4.2 Climate as the "Possibility Space" for Weather or Climate as the Statistics of Weather?

In this section Conceptual Question (CQ1) (page 5) is addressed. To this end, Conceptualisations (C1) and (C2) (page 6), as employed in the literature, are compared and contrasted.

It could be argued that a statistical description of weather data is simply a convenient means of estimating the possibility space of weather. It will be argued here that this is not always the case. Consider, for example, the points of view of Larson (2012), and Kraus (1984). Larson (2012) claims that "[c]limate is a statistical construct computed from meteorological state data sampled over a predefined period". Kraus (1984) suggests that "[c]limatology is not a science in its own right, it is only a special way of considering the state, changes and processes in the atmosphere, i.e. the science of meteorology". Thus he claims that climate is simply the consideration of weather variables on suitably large "time- and space-scales" (thus combining aspects of Conceptualisations (C1) and (C4)). On the other hand, Bryson (1997), after reviewing and critiquing some definitions in the spirit of Kraus (1984), suggests that "Climate"—as he defines it (see subsubsection 2.1.4.1)—identifies "climatology as a distinctive atmospheric science". This view appears to arise from a view of climate consistent with Conceptualisation (C2).

McGregor (2006) endorses this view. He remarks that such a conceptualisation of climate "reverses the abstract notion that climate is 'average weather' ", noting that it is also more compatible with the metaphorical use of the term "climate". Stone et al. (2009)

suggest that conventional definitions, involving "statistics of weather...over...30 years" are unsatisfactory as working definitions of "climate", in part because "[they are] purely based on measurement rather than some integral property of a system." Following Allen (2003), Stone et al. (2009) then suggests that climate be defined as "the statistical properties of possible weather," noting that this implies that "the actual observed weather [is] just one realization of many possible realizations within a given climate." This definition—consistent with Conceptualisation (C2)—appears to encourage the use of ensembles to quantify "a given climate".

Werndl (2014b) remarks that the reliance on BCs in "Bryson's definition goes against how one intuitively thinks about climate, where climate is some kind of distribution of the temperature, the surface pressure, etc." It should also be noted that Bryson's definition of "Climate" implicitly assumes that the range of possible atmospheric behaviours is uniquely determined by BCs. In this context, BCs are probably intended to include what in a dynamical systems setting would be considered as "control parameters". The assumption that climate prediction is a BC problem has been questioned by, for example, Pielke Sr. (1998), Lovejoy (2013, 2014), and, implicitly, by Lorenz (1970) and Daron and Stainforth (2013), who note the possibility of the climate system being intransitive. The associated possibility that boundaries between basins of attraction may be fractal, would imply an extreme form of IC sensitivity (McDonald et al., 1985).

2.1.4.3 Climate as an Attractor

Viewing the climate system conceptually as a low-dimensional nonlinear dynamical system leads naturally to a conceptualisation of "climate" as a strange attractor in the theoretical climate system state space (see Conceptualisation (C3) on page 6). Lorenz (1995) proposes that climate could be defined as "[t]he attractor of the dynamical system—the set of all states that can occur or be closely approximated again and again as time progresses, after possible transient effects introduced by the choice of [ICs] have died out." Lorenz (1995) notes that the climate system is dissipative and that "[i]n a dissipative system[,] arbitrarily chosen initial states generally represent transient or 'unreasonable' patterns, and will subsequently be avoided in favour of a few 'reasonable' states, which form the attractor." In accordance with Conceptualisation (C2), this surface would closely approximate the system's possibility space, once the influence of the initial transient has become negligible.

Conceptualising climate as a strange attractor is applicable "[i]n the context of constant [BCs], and specifically no changes in atmospheric [greenhouse gases (GHGs)] and therefore radiative forcing" (Stainforth et al., 2007a). Then, "weather is chaotic and climate may be taken as the distribution of states on some 'attractor' of weather" (Stainforth et al., 2007a). Similarly, Daron and Stainforth (2013) suggest that "[i]f the [BCs] were fixed, then the 'climate' of [the ocean-atmosphere system] could be considered as the variable distributions on [its] attractor." More often, conceptualisations of climate in terms of attractors remain implicit, involving references to "the climatic attractor" (e.g., Branstator

and Teng, 2010, see also subsubsection 2.2.1.4).

In the more realistic setting of variable external forcing, considering climate as an attractor is problematic. Hence, Stainforth et al. (2007a) suggests defining climate as "the image of the initial attractor under the transient forcing". Quantitatively, this could be estimated in climate model worlds with large ensembles sampled from the attractor for constant forcings (Stainforth et al., 2007a).

A broader discussion of questions involved in conceptualising climate in terms of attractors is presented in subsubsection 2.2.1.4.

2.1.4.4 What Should Constitute Climate Change?

Lorenz (1995) suggests that lead times for ensemble definitions of model climates should be sufficiently short that the climate does not change in the interim. Important parameters in definitions of climate, therefore, are determined by notions of what should constitute a change in climate.

In the 19$^{\text{th}}$ and early 20$^{\text{th}}$ Centuries, climate was widely considered to be an unchanging entity (Lenhard and Baum, 1954; Guttman, 1989; Lamb, 1972, Introduction); standard climate normals were introduced with the intention of capturing assumed stable infinite-term statistics (with a particular emphasis on the mean) of weather, based on available data (Guttman, 1989; Livezey et al., 2007). Changes in climate statistics during the 20$^{\text{th}}$ Century, as well as investigations of paleoclimatic records, revealed, increasingly, that such a view was inconsistent with observations (e.g., Lorenz, 1968; Lamb, 1972; Bryson, 1997; McGregor, 2006). Leith (1978) and Werndl (2015) point out the consequent problems with equating the idea of climate with infinite-term statistics. A question which remains more openly contested to the present, however, is: to what extent can "climate" change in the absence of monotonic changes in external forcings? Differences in what is considered internal to the climate system influence answers to this question (see subsubsection 2.1.4.1).

The concept of almost-intransitivity, introduced by Lorenz (1968), has important implications for such questions. A distinction is drawn between transitive and intransitive systems. The former refers to systems (including specifications of control parameters or forcings) possessing a unique attractor; in the latter case, even under specified parameters, the attractor set towards which the system evolves is dependent on the ICs. The "[closure of] the set of all ICs which" evolve towards a given attractor, is defined as the basin of attraction of that attractor (McDonald et al., 1985). Intransitivity could result in hysteresis (Strogatz, 1994, pg.68); if control parameters are varied, the attractor to which a system evolves, given particular parameter value, could be influenced by the system's "memory" of its previous states. However, Lorenz (1990) suggests that intransitivity in the true climate system is unlikely. A more relevant possibility is that of almost-intransitivity: a transitive system which displays the characteristic of spending extended—but finite—periods of time in a particular subset of the system's attractor, before transitioning to a different

attractor subset, thus creating the impression of having moved between distinct attractors. Lorenz (1970, 1976, 1991a) points out the difficulties this presents to what would now be considered detection and attribution studies (e.g., Stone et al., 2009). Recently, studies of "long-term persistence" or "long-range dependence", have found evidence of such behaviour in the real system and the link to almost-intransitivity has been pointed out (Franzke et al., 2015, and references therein).

An important question is which "changes" or "shifts" in climate system state should constitute climate change and which can be considered to fall within climate time scales. Making such decisions are particularly important for Conceptualisation (C4) (see subsubsection 2.1.3.3). Lorenz (1995) suggests that changes in the ENSO phase should not be considered as climatic changes, although he acknowledges that this view is not universally accepted. In particular, ensemble statistics should not be considered representative of a climatological distribution when forecast lead times do not exceed the limit of potential predictability of ENSO. He suggests rather that changes in the nature of ENSO variability should constitute climate changes. However, as Wittenberg et al. (2014) points out, such changes may not be reflected in ensemble simulations, as, to a large extent, they may reflect almost-intransitivity of the (model) system.

This poses the question of whether changes in the "phase" of other modes of internal variability, for which the associated mechanisms are qualitatively similar to some aspects of ENSO variability, but for which potential predictability may be much longer (see subsubsection 2.2.2.4), should be considered as climatic changes. The case of low-frequency variability over the Pacific (Minobe, 1997, 1999), which has been referred to as the Pacific Decadal Oscillation (PDO; Mantua et al., 1997) or Pacific Decadal Variability (PDV; preferred here, as in Deser et al., 2012b), is of particular interest. Shifts in PDV are possibly linked to changes in ENSO variability (e.g., Trenberth, 1990; Trenberth and Hurrell, 1994; Mann and Park, 1994; Zhang et al., 1997; Gu and Philander, 1997; Rodgers et al., 2004; Deser et al., 2004; Clement et al., 2011). These shifts have been associated with changes in GMST trend (Tsonis et al., 2007; Swanson and Tsonis, 2009), global top of the atmosphere (TOA) energy balance (Brown et al., 2014) and distribution of climate system heat content (Meehl et al., 2011; Balmaseda et al., 2013). Some evidence suggests that such regime shifts may occur at a frequency of approximately 4 to 5 per century (Minobe, 1999; Gedalof and Smith, 2001). However, although the PDV appears to have 2 pronounced spectral peaks around 17 and 60 years (e.g., Minobe, 1997, 1999; Deser et al., 2004), it has a significant "red-noise" component (Deser et al., 2004, 2012b).

If one would want each PDV regime to correspond to a single climate—thus providing predictive advantages—the length of time over which temporal definitions of climate are computed may have to be adjusted, perhaps continuously. If they should be subsumed within a given climate, longer periods would have to be considered to account for all the different types of variability that may occur under different regimes of such low-frequency modes. Additionally, the predictability of such a shift would influence lead time considerations for ensemble definition model climates; if the shifts are not predictable,

ensembles will tend to capture multiple regimes at a given time. At particular lead times, ensembles may be able to quantify probabilities of being in particular regimes, especially if ensemble-temporal definition, as used in this study, are considered.

As pointed out by Lorenz (1995) and discussed in detail by Werndl (2015), the definition of climate one uses influences what one would regard as climate change. Lovejoy (2013) suggests that, given that 30-years is a near-optimal averaging period for describing "macroweather" in an anthropogenically forced climate, it naturally follows that climate change occurs when successive normals differ significantly. If the climate is conceptualised as a strange attractor (as in Conceptualisation (C3); see subsubsection 2.1.4.3), climate change could occur because (a) a system trajectory moves from one attractor to another (in an intransitive system) or (b) the shape of the attractor changes in response to applied forcing (Daron, 2012, pp. 52–78; see also subsubsection 2.2.1.2). Hence, in intransitive systems, defining climate as a strange attractor faces the difficulty that "the climate" is not uniquely defined (Lorenz, 1995; Daron and Stainforth, 2013).

As the above discussion highlights, the question of stationarity of climate is intimately related to the evolution of conceptualisations of climate. Questions regarding whether climate changes at all—and if so, over which time periods and in response to which, if any, identifiable causes—are inherently answered in the framework of an existing conceptualisation. Answers to these questions can also bring about changes in the way we think about climate.

2.1.5 Quantifying Climate

2.1.5.1 Temporal Statistics vs Ensemble Statistics

Examples of temporal and ensemble definitions of climate, and motivations for employing them, are presented in subsection 2.1.3. This subsubsection explores some of their relative advantages and disadvantages. The kairodic assumption is discussed.

Strict adherence to Desideratum (1) of Werndl (2015), would imply that ensemble distributions cannot be used as climate definitions. Werndl (2014a, 2015) also raises other concerns regarding ensemble definitions of climate. However, the theoretical value of ensemble distributions (noted in subsubsection 2.1.3.2) is acknowledged and a preferred ensemble "concept of climate"(Werndl, 2014a) is selected: "climate as the future ensemble distribution when the external conditions vary as in reality" at a finite (but not precisely specified) lead time. The question of optimal lead times for ensemble definitions is discussed in subsubsection 2.1.4.4. Noting multiple concerns regarding ensemble quantification, Werndl (2014a) suggests that they be regarded "just refer[ring] to a distribution which is useful for predictive purposes", rather than "defining the climate".

Diurnal and annual cycles present a challenge for climate quantifications. In the case of temporal definitions, it must be decided which periods of the year should be

considered together when computing statistics. Should climate variable statistics be presented separately by time of day, or should summary statistics (such as minimum, maximum and mean daily temperatures (e.g., Larson, 2012)) be quoted? Should they be presented by date, by month, by season, or per annum? Should the length of the record and/or the geographic location (e.g., Lenhard and Baum, 1954) be considered when making such assessments? Does this have an implication for which data should be used for model validation? Climate normals (see subsection 2.1.2), as dictated by the WMO, are computed at monthly temporal resolution (Arguez and Vose, 2011), but alternatives have also been suggested or used (e.g., Quinlan, 1986; Lamb and Changnon Jr, 1981; Huang et al., 1996; Livezey et al., 2007; Larson, 2012).

For ensemble definitions, there is the question of whether temporal averaging or summing should be done prior to computing ensemble statistics; i.e. should we consider daily mean sea-level pressure (PSL) or monthly precipitation totals from simulations as the quantities for which climatological distributions should be determined, or should ensemble climatologies be produced for each time point of interest, for example, wind speed at 18:00 on July 7, 2015? Alternatively, one could use an ensemble-temporal sample to compute statistics; for example, one might consider daily mean temperature over the 30 days of June 2016, sampled from each member of a 30-member IC ensemble, initialised at some prior time, as representative of the climatological distribution for June 2016. This approach is used here, although all data used are annual means, so that complexities related to the diurnal and annual cycles (see subsubsection 2.2.1.4) are ignored. However, this may be an important avenue for future work to explore.

The possibility of climate-like dynamical systems being intransitive is discussed in subsubsection 2.1.4.2. A related attribute of dynamical systems, often equated with transitivity (e.g., Leith, 1978; Peixóto and Oort, 1984), is ergodicity (for a Mathematical overview, see Eckmann and Ruelle, 1985). Under the ergodic hypothesis, a single trajectory in a system's state space, over infinite time and under fixed parameter values, will visit all "reasonable" (see subsubsection 2.1.4.3) locations in the state space. Roughly speaking, an ergodic system would have the property that statistics derived from a single infinite-time trajectory should be equal to those derived from an infinite, representative IC ensemble. As with questions of transitivity, the infinite term properties of the system are not necessarily those that are of greatest practical importance in studies of climate. Daron and Stainforth (2014) therefore introduce the "kairodic assumption", which states that finite-time temporal statistics from a single trajectory should be indistinguishable from those derived from an IC ensemble which samples microscopic ICU. Intuitively, the kairodic assumption is to the ergodic assumption what almost-intransitivity is to intransitivity.

The kairodic assumption is explored further in subsection 5.1.3. It should be noted that whether the kairodic assumption holds depends on the particular time scales considered. Generally, following Lorenz (1968), one may consider the climatologically relevant scales here to be decadal, multidecadal and perhaps centennial. The focus in this study is on 60-year periods, equal to two consecutive climate normal periods. The extent to which the

kairodic assumption holds has important implications for the interpretation of ensemble and temporal statistics (Daron and Stainforth, 2013, 2015).

2.1.5.2 Temporal Scale Considerations

The "more rigorous [narrow]" IPCC (2013a) definition of climate, "as the statistical description in terms of the mean and variability of relevant quantities over a period of time ranging from months to thousands or millions of years", highlights the range of temporal scales that the term "climate" is applied to. The qualification that "[t]he classical period for averaging these variables is 30 years, as defined by the [WMO]", is, however, added. Some discussion of this topic, to the extent that it relates to the question of climatic stationarity, is presented in subsubsection 2.1.4.4.

Many studies, using metrics that attempt to quantify particularly the predictive value of climatological means, have suggested that climate normals, or certain generalisations of the concept, would be best computed over shorter periods than the 30-year standard (e.g., Lamb and Changnon Jr, 1981; Changnon Jr, 1985; Todorov, 1985, 1986; Angel et al., 1993; Huang et al., 1996). These studies often relate to particular sectors applying climatic data. It is common for such studies to advocate more regular updating of quantifications of climate than is conventional (e.g., Todorov, 1985, 1986; Huang et al., 1996; Arguez and Vose, 2011). Generalisations of the conventional climate normal, which incorporate trends and/or autocorrelation metrics into descriptions of climate time series, have also been suggested (e.g., Trewin, 2007; Livezey et al., 2007; Arguez and Vose, 2011).

In contrast to studies focussing on improvements in short-term predictive skill, Quinlan (1986) points out that valuable information can be gained from consideration of all available data. It would help in gaining understanding of all variability and trends that are captured in the local or regional observational record, which may be of value in future. Todorov (1986) responds that changes in observational and measurement practices may make this task impractical.

A more advanced approach to the problem is proposed by Larson (2010). An information theoretic measure is applied to decide on the optimal length of time over which to compute climatological statistics, from an estimated probability density function (PDF). The work is only in an exploratory stage. However, Larson (2012) suggests the use of time-dependent, N-year "windowed" PDF estimates to characterise evolving climate variable distributions.

2.1.5.3 Spatial Scale Considerations and Variables Considered

According to the WMO (2010), climate entails "statistical descriptions of the central tendencies and variability of relevant elements...[, or] combinations of elements, such as weather types and phenomena, that are typical to a location, region or the world for any time period." Hence a range of spatial scales of consideration are included, covering Notions

(N1)–(N4) (page 6). Both the IPCC (2013a) and WMO (2010) distinguish between climate in a "narrow sense"—defined by the WMO (2010) "as the average weather conditions for a particular location and period of time"(i.e. Notion (N1))—and a broader view of climate. IPCC (2013a) state that variables considered in the "narrow" definition of climate "are most often surface variables such as temperature, precipitation and wind." WMO (2010) include among "the relevant [climatic] elements...temperature, precipitation, atmospheric pressure, humidity, and winds". McGregor (2006) point out that, traditionally, temperature and precipitation have dominated climatic quantification, both because of their relevance and ease of measurement. The variables mentioned thus far are all surface variables, but Trewin (2007) includes a discussion of normals (i.e. relating to climate in a "narrow" sense) of upper tropospheric data, as well.

The Intergovernmental Panel on Climate Change (IPCC) "wider sense" definition applies to the climate system as a whole (see subsubsection 2.1.4.1), suggesting variation in conceptualisations of climate used, depending on the spatial scales considered. Perhaps as a consequence, approaches to quantifying climate on different scales are largely distinct. This applies, in particular, to the time scales considered, possibly explaining the large range of time scales included in the IPCC (2013a) definition (see subsubsection 2.1.5.2). Werndl (2015) surmises that "the vagueness [of the IPCC definition] may well be intended to subsume under one characterization the various different definitions of climate".

Global or hemispheric scale assessments often employ quantifications consistent with Notion (N3), discussed in subsubsection 2.1.4.1. Local definitions generally assess shorter periods, as discussed in subsubsection 2.1.5.2. Surface variables of practical interest are described through perceived societally relevant statistical analysis. Such analysis is often conducted by meteorological or agrometeorological institutes, under WMO guidelines (e.g., WMO, 1988, 2010; Trewin, 2007). Large-scale spatial analyses often consider variables of particular dynamical relevance and/or indices that attempt to capture the state of modes of variability. This is because these quantities are widely regarded as dictating the nature and patterns of climatic variability and trend on regional scales (e.g., Philander et al., 1984; Fedorov and Philander, 2000; Marini et al., 2011; Malherbe et al., 2014, see also references discussing SAM and AMOC variability in subsubsection 2.2.2.5 and ENSO variability and PDV in subsubsection 2.1.4.4).

Peixóto and Oort (1984) distinguish between "additive" (or roughly conserved) properties of the climate system, such as "the volume, internal energy, mass of individual [climate system] components, and angular momentum"; and "intensive" properties, more often associated with weather states. Additive quantities are of greater relevance at a global scale, whereas intensive variables—examples of which are discussed above in relation to the "narrow sense" definitions of the IPCC and WMO, are relevant at all scales.

As noted by, for example, Peixoto et al. (1992), Lucarini (2002) and WMO (2010), climatology is also concerned with the associations and correlations between variables. Thus, such statistics could be included, together with distributional estimates, autocorrelation (see subsubsection 2.1.5.2) and quantifications of variability of seasonality (e.g., Douglass,

2011), in quantifying climate at various scales (see also section 6.2).

2.2 Part B: Conceptual Questions in Modelling the Climate System

In this section, connections between the Conceptual Questions introduced in section 1.3, and the experimental component of this study are considered in the context of past theoretical and experimental studies.

Literature on relevant methodologies, applied in climate science and developed in a nonlinear dynamical systems framework, is reviewed in subsection 2.2.1. Climate variability and predictability is briefly reviewed in subsection 2.2.2, considering evidence from observational and modelling studies. Literature relating to practical aspects of the modelling experiment conducted, is reviewed in subsection 2.2.3. In subsection 2.2.4, the value IC ensemble studies are considered from a climate projection uncertainty perspective.

2.2.1 Nonlinear Approaches

2.2.1.1 Conceptual Models and the Climate Modelling Hierarchy

It has frequently been suggested that climate science would benefit from wide application of a "hierarchy of models" of various levels of complexity (e.g., Schneider and Dickinson, 1974; Ghil, 2001; Dijkstra, 2013). This approach could be used to address various qualitative and quantitative questions, including ones regarding robustness and uncertainty in climate projections (Claussen et al., 2002; Held, 2005). The climate model hierarchy consists of EBMs (e.g., Budyko, 1969; Sellers, 1969, as discussed by Lorenz (1995) and adapted in Dijkstra and Viebahn (2015)), conceptual "general circulation models" (Lorenz, 1984, 1990, and numerous developments hereof), climate models of intermediate complexity (e.g., Claussen et al., 2002) and high-dimensional GCMs, CSMs and Earth system models (ESMs). The value of low-dimensional models in this hierarchy includes their much lower computational cost, which allows for the running of large IC ensembles(Lorenz, 1982, 1987), as in Daron and Stainforth (2013, 2015).

In the context of dynamical systems theory, investigation of low-dimensional conceptual climate models has contributed greatly to qualitative understanding of possible climate system behaviour at various time scales (Daron and Stainforth, 2015). Low-dimensional "climate-like" models of various climate system features have been used to explore possible qualitative behaviours of climate (e.g., Lorenz, 1963, 1990; Broer et al., 2002). Lorenz (1976, 1995) and Werndl (2014a, 2015) use such models to illustrate issues involved in employing various conceptualisations and approaches to quantification of climate and climate change. Recent studies have also used IC ensemble simulations of low-dimensional

models to investigate climate variable distributions and ICU in an abstract setting (e.g., Daron and Stainforth, 2013, 2015; Palmer, 1993).

It is important that conceptual questions raised by studies of low-dimensional models be evaluated in more complex models in the climate model hierarchy (Bódai and Tél, 2012), including those models which are used to inform policy directly (Daron, 2012; Oreskes et al., 2010; Frigg et al., 2015). This study aims to address some of these questions in a low-resolution version of a CMIP5 CSM.

2.2.1.2 Nonlinear Dynamical Systems and Conceptualising Climate Change

Describing a "nonlinear dynamical perspective" on prediction of anthropogenic climate change, Palmer (1993, 1996, 1999) suggests an essential role for interaction between internal variability and external forcing in determining the nature of climate change. Considering the climate system as a nonlinear dynamical system, Palmer (1999) predicts that climate change should be detectable in variables representing modes of climate variability primarily through changes in the modality and modal frequencies of their PDFs. Such distributional responses would represent changes in the frequency of occurrence of climatic "regimes". Stone et al. (2001) suggest that linear translation of climate regimes is the dominant response to monotonically evolving forcing in the model system they consider. However, Corti et al. (1999) and Hsu and Zwiers (2001) do find evidence of shifts in the frequency of occurrence climate regimes, although Hsu and Zwiers (2001) point out the need to apply a methodology that does not falsely detect apparently distinct regimes that are the consequence of small samples from highly autocorrelated time series.

2.2.1.3 IC Ensemble Approaches

IC ensembles are increasingly being used to probe the relative roles of internal variability and external forcing in climate evolution (e.g., Deser et al., 2012a), especially in the context of the recent "pause" or "slow-down" in global warming (e.g., Hawkins et al., 2014). A prominent example of this approach is the CESM Large Ensemble Project (CESM-LE; Kay et al., 2014). CESM-LE involves a 30-member ensemble, integrated over a 181-year period (1920-2100). CESM-LE uses a relatively high resolution ESM, which is a substantial development of the model used in this study. Because much of the data from the CESM-LE project is available to the climate community, a valuable extension of this study may be to apply similar analyses to CESM-LE data.

In this study we aim to explore a range of possible model responses to changes in ICs. Hence the use of numerous larger ensembles is vital. Similarly, Wittenberg et al. (2014) use sets of 40-member ensembles to explore ENSO variability, predictability and modulations, each ensemble starting from ICs obtained from a period exhibiting distinct patterns of ENSO variability. They find that the level of ENSO variability captured by ICs in their

model represents essentially microscopic IC influence (see subsubsection 2.1.3.2).

Wittenberg et al. (2014) note that the computational cost of running n ensembles for m years is lower than for that of running a single simulation for $n \times m$ years. This is due to the imperfect parallelisability of climate model implementations and the large number of cores usually required for operational climate model studies. Hence, Wittenberg et al. (2014) suggest that, for a particular mode of variability, ensemble approaches could represent a more efficient means of estimating a model's possibility space than long individual runs.

2.2.1.4 Is There a Climate Attractor in Reality or in Climate Models?

The idea of climate evolving on a strange attractor is often invoked, sometimes implicitly, to illustrate qualitative aspects of theories and conjectures regarding the climate system's behaviour (e.g., Lorenz, 1995; Palmer, 1996, 1999; Corti et al., 1999; Branstator and Teng, 2010; Stainforth et al., 2007a). Hence, it is considered relevant to discuss the utility of such a conceptualisation (cf. Conceptualisation (C3)), both in the context of the Earth's climate system and the climates of model worlds.

After a method for estimating the dimensions of strange attractors was documented by Grassberger and Procaccia (1983), numerous studies (e.g., Nicolis and Nicolis, 1984, 1986; Fraedrich, 1986) suggested that the climate system evolves on a low-dimensional ($n \lesssim 5$) attractor. The practice of applying such methods to climate proxy time series was, however, widely questioned (e.g., Grassberger, 1986; Lorenz, 1991b; Tsonis et al., 1993). Given the degree of spatiotemporal complexity of the climate system as a whole, it is unlikely to possess an attractor with low dimensionality (e.g Lorenz, 1991b; Sahay and Sreenivasan, 1996). Rather, attractors found using climate proxy series are more likely to represent climate subsystems (Tsonis and Elsner, 1989; Lorenz, 1991b; Fraedrich and Wang, 1993). Tsonis and Elsner (1989) and Lorenz (1991b) posit that such subsystems may be "loosely coupled" together, thus producing the observed "climate" (cf. Conceptualisation (C5)).

Tsonis (1996, 2001) suggests that it is "naive" to expect an attractor on which the entire climate system evolves (a so-called "grand attractor") to exist. Even if a grand attractor does exist, it would not necessarily have practical value; given the high dimensionality it is almost certain to possess, determining which quantities should be used to describe its evolution would likely be an intractable problem (Sahay and Sreenivasan, 1996). Furthermore, the existence of an attractor of the system does not guarantee uniqueness; Earth's climate system, or certain climate model system with particular choices of control parameters, may be intransitive (see subsubsection 2.1.4.4).

Additionally, as noted in subsubsection 2.1.4.3, strange attractors are well-defined only under fixed forcings. Given the prominence of annual (e.g., Lorenz, 1990) and diurnal forcing in climate and the system's nonlinear response to forcing, it is not clear whether—even if a climatic attractor "exists" in the real system or model systems—their climate trajectories ever evolve "on" the attractor. In this study, only annual mean quantities

are considered, deferring consideration of such questions. However, much of the coupled system's dynamic variability is necessarily subsumed and there exist, as far as the authors are aware, no dynamical models attempting to compute meteorological or climatological variable values with an annual time step, in a manner that accounts for the influences of variability on shorter time scales.

Nonlinear dynamical systems theory, in the context of which the concept of a strange attractor developed, relates to finite-dimensional ODE systems (see section 1.2). However, it is not impossible for finite-dimensional attractors to exist in dissipative PDE systems (Sahay and Sreenivasan, 1996, and references therein). Presently, however, network (e.g., Tsonis et al., 2006; Tsonis and Swanson, 2012) and nonlinear stochastic modelling (see e.g. Majda, 2012; Selvam, 2012) approaches appear to be preferred frameworks for understanding climate variability as arising in complex spatiotemporal systems.

Accordingly, when considering the possibility of attractors in GCMs, CSMs or ESMs, what is considered to be the "model"—particularly what stage of spatial and temporal discretisation PDEs are considered at—is of central importance (see section 1.2). Lorenz (1980), considering a $\sim 10^5$-dimensional (spatially discretised) GCM from that time, suspected that a strange attractor should exist for at least some control parameter values and that it should have $\sim 10^2$ dimensions. However, in the ever higher-dimensional models presently in use—particularly in coupled models in which different components evolve with very different characteristic time scales (e.g., Daron and Stainforth, 2013)—the idea of a model's strange attractor appears to be of use primarily in conceptual arguments.

2.2.2 Variability and Predictability of the Climate System

Literature on the nature of observed (subsubsection 2.2.2.1) and modelled (subsubsection 2.2.2.3) climate system variability is briefly reviewed. The connection between climate system variability, the central questions addressed by this study (subsubsection 2.2.2.2) and decadal predictability (subsubsection 2.2.2.4) are also considered.

2.2.2.1 The Nature of Climate System Variability

Observational evidence suggests that climate system temporal variability occurs at all time scales, from fractions of a second to millions of years (e.g., Lovejoy, 2014; Pelletier, 1997; Ghil, 2002; Bryson, 1997). This variability is composed of a periodic component (the diurnal and annual cycles), a "quasi-periodic" component (including ENSO) and an aperiodic continuum (Wallace, 1996b). Wallace (1996b) claims that the importance of prediction in atmospheric sciences has inclined researchers to focus particularly on broad spectral peaks. These are likely to be associated with identifiable mechanisms of variability, and thus can contribute towards predictability on longer time scales (Wallace, 1996b). However, some observational studies suggest that only a small proportion of total climate

system variability is explained by quasi-periodic modes; instead, most of the variability is claimed to be attributable to a spectral continuum suggestive of a "red-noise" process (e.g., Shackleton and Imbrie, 1990; Wunsch, 2003; Lovejoy, 2014). Generally, which mechanisms are responsible for particular attributes of lower-frequency variability is poorly understood (Tantet and Dijkstra, 2014).

Interactions between climate system components exhibiting distinct characteristic time scales are widely considered to contribute significantly to climate system variability (e.g., Hasselmann, 1976; Daron and Stainforth, 2013; Trenberth and Hurrell, 1994). Dommenget and Latif (2008) use a simplified ocean model coupled to a low-resolution atmospheric GCM to show that essentially random atmospheric forcing, combined with the large thermal inertia of the near-surface ocean, can produce a so-called "global climate hypermode", consistent with the predictions of the stochastic climate theory of Hasselmann (1976). Hence, the mechanism primarily responsible for this variability does not involve ocean circulation. Theoretical considerations suggest that this mechanism should be able to produce ever increasing levels of variability with characteristic time scales beyond the millennial. The associated variance spectrum shows increasing power until well after a fitted first-order autoregressive (AR(1)) spectrum has flattened. This implies non-stationarity of the mode up to multimillennial scales, which could have important implications for conceptualisations of climate (see also subsubsection 2.1.4.4 and subsubsection 2.1.3.3).

The hypermode is seen in detrended observations and control run model integrations (see subsubsection 2.2.3.2), on multidecadal time scales. It seems to have a global footprint, although it appears to originate in the northern Pacific.

2.2.2.2 Relevance to Conceptualisation of the Climate System

The importance of considering the nature of modes of climate system variability in defining climate is highlighted in subsubsection 2.1.4.4. In predictability studies, ICs and modes of variability can also be important. Meehl et al. (2014) find that initialised CMIP5 decadal predictions perform significantly better than uninitialised equivalents over certain domains, for lead times up to about 5 years. Initialising simulations with the correct phase of prominent quasi-periodic modes of variability, such as ENSO, provide improved hindcasts of GMST evolution (Risbey et al., 2014). Interrogating the relationships between such IC predictability (ICP), the degree of IC influence apparent in climate time series, and modes of variability, is an area of focus in this study.

2.2.2.3 Variability in Climate Models and Interactions Between Forced and Unforced Variability

It has been widely suggested that CSMs and ESMs underestimate the extent or amplitude of low- to very low-frequency variability in the climate system, as well as its propensity

for sudden shifts (e.g., Kravtsov et al., 2008; Swanson et al., 2009; Lovejoy et al., 2013; Kravtsov et al., 2014; Ghil, in press, 2015; Katzav et al., 2012). However, the relative contributions of internal processes and external forcings to recent observed variability are difficult to distinguish (Wu et al., 2011; DelSole et al., 2011; Kravtsov et al., 2014). Given the nonlinear interactions that are likely to occur between internal processes and externally imposed radiative imbalances (Andrews et al., 2015; Meehl et al., 2009; Corti et al., 1999; Brown et al., 2014), the extent to which such signals can be distinguished remains unclear (Lorenz, 1970, 1976, 1991b). The possibility of interactions between ICs and ensemble response to applied forcings in our experiment is considered in subsection 5.2.2.

Lovejoy et al. (2013) suggest that variability falling in the macroweather regime (see subsubsection 2.1.4.3) is the lowest frequency variability which GCMs are capable of reproducing, possibly owing to their origins in weather forecasting. Lovejoy (2014) claims that climate variability (a regime he classifies as extending to $\sim 10^5$ years) could only be the result of interactions between internal modes of climate system variability and external forcings, involving mechanisms not represented in GCMs or CSMs (Lovejoy, 2014).

Such underestimation of low-frequency variability and sensitivity to IC perturbations in CSMs could have implications for their ability to capture larger scale IC influence.

2.2.2.4 Decadal Predictability

One of the central aims of CMIP5 is to explore climate predictability on decadal time scales (Taylor et al., 2012). This task has been approached by placing greater emphasis on the accuracy of ICs used (Branstator and Teng, 2010), as these are considered likely to influence the climate evolution on decadal time scales. Decadal climate prediction is generally considered to be an initial-boundary value problem (I-BVP; Meehl et al., 2009), in which both ICs and forcings need to be considered.

Decadal predictability studies often make the "perfect model" assumption (e.g., Smith, 2000a), as is done in this study. It can be thought of as stating that one of the model trajectories represents "the true climate". One can then explore how well one would be able to predict variable states along that trajectory, given imperfect knowledge of its ICs. Studies making the perfect model assumption can only provide an upper bound to the predictive potential of a model for a given physical system (Teng et al., 2011).

Using the information theoretic criterion of entropy, Branstator and Teng (2010) show that, in the Community Climate System Model, version 3 (CCSM3), on ocean basin scales, the influence of ICs on extratropical boundary layer ocean temperature dominates forced predictability for approximately 7 years. Applying similar techniques to AMOC and northern Atlantic boundary layer temperature, using 4 40-member IC ensembles, it is found that ICP in these quantities may extend beyond a decade (Teng et al., 2011). After $\lesssim 10$ years, in both studies, ICP is exceeded by predictability due to GHG forcings. Other studies (including Corti et al., 2012; DelSole et al., 2013b; Bellucci et al., 2015) suggest

similar time frames.

In a further related study, Teng and Branstator (2011) use ICs which project strongly onto prominent northern Pacific oceanic modes of variability in CCSM3 for three IC ensemble simulations. Modes of variability are represented by emperical orthogonal functions (EOFs). The interaction between the two leading EOFs is responsible for a "propagating mode", which appears to be predictable up to decadal scales. For one of the three ensembles, ICP of the propagating mode, as well as the leading EOF, appears to extend beyond two decades. In their other ensembles, ICP for the leading EOF lasts for only about six years. These findings suggest that the degree of what might be considered "macroscopic" IC influence could vary significantly depending on the locations of the ICs in the model state space. Such state dependence of IC influence should not be surprising in a nonlinear dynamical system (Smith, 2000b). It is also observed by Daron and Stainforth (2015) in a simple, chaotic, climate-like system and is investigated further in chapter 5.

Branstator and Teng (2010) and Teng and Branstator (2011) distinguish between "signal" and "dispersion" components of predictability. For IC ensembles, the former is related primarily to the ensemble mean and the latter to the ensemble "spread". The latter is more conventionally associated with ICP (Kleeman, 2002; Teng and Branstator, 2011). Teng and Branstator (2011) and Teng et al. (2011) show that in the Northern Hemispheric ocean basins, deviations of the ensemble mean from the "background" or "climatological" mean are predictable for longer than reduced spread.

Subsequent studies by Branstator et al. (2012) and Branstator and Teng (2012) found that the duration of detectable ICP varies substantially between CMIP5 models and on sub-basin scales within models. There remains substantial scope, therefore, for further investigation into the influence of climate system ICs in CSM behaviour and predictability. Additionally, further investigation is required to translate the findings of perfect model assumption studies to the real climate system context; however, observational analysis is beyond the scope of the present study.

2.2.2.5 Importance of Southern Hemisphere Variability

Ocean-basin scale analyses of climate predictability have generally focussed on one or more of the following three domains (e.g., Meehl et al., 2014; Branstator et al., 2012; Bryan et al., 2006; Collins et al., 2006b; Doblas-Reyes et al., 2013):

1. the tropical Pacific—where ENSO is played out;
2. the northern Pacific—where PDV (see subsubsection 2.1.4.4) is focussed; and
3. the northern Atlantic—where the North Atlantic Oscillation (NAO) and the Atlantic Multidecadal Oscillation (AMO) operate.

These basins appear to display major modes of variability, which have direct impacts on large populations. Relationships between ENSO and NAO have also been identified in observation (e.g., Rogers, 1984; Huang et al., 1998; Jevrejeva et al., 2003; Mokhov and Smirnov, 2006; Brönnimann, 2007). However, the focus on these modes has meant that Southern Ocean variability, especially, remains understudied (Latif et al., 2013).

Evidence, however, suggests that long-term variability over the Southern Ocean (SO), and the remainder of the Southern Hemispheric extratropics, is substantial (e.g., Park and Latif, 2012; Latif et al., 2013) and may be amenable to decadal prediction (e.g., Branstator and Teng, 2010; DelSole et al., 2013a; Latif and Keenlyside, 2011; Boer and Lambert, 2008). Furthermore, temperature variability over SO could exert significant influence on GMST (Brown et al., 2014, 2015). It has been proposed that variability over SO, in Antarctic sea ice extent and in the Antarctic Circumpolar Current can contribute to long-term variability in the northern Atlantic (Martin et al., 2014; Marini et al., 2011; Patara and Böning, 2014) and influence ENSO (Ivchenko et al., 2004, 2006). Variability over Southern Hemispheric mid- to high-latitudes may also play a role in marked regional variability over southern Africa (e.g., Malherbe et al., 2014; Reason and Rouault, 2005; Reason et al., 2006).

The most prominent mode of extratropical variability in the the Southern Hemisphere (SH) is the Southern Annular Mode (SAM; Limpasuvan and Hartmann, 1999), also sometimes referred to as the Antarctic Oscillation (AO or AAO; Gong and Wang, 1999). It is is an important driver of climate system variability—and may be influential in climate change evolution—over the Southern Hemispheric extratropics (Thompson et al., 2011; Abram et al., 2014). Significant recent changes have been observed in SAM, although it is unclear to what extent these are attributable to internal variability, changes in GHG concentrations and stratospheric ozone depletion (Fogt et al., 2009).

Long-term variability over SO is investigated in observations and using a low-resolution multimillennial integration of the Kiel Climate Model (KCM), by Martin et al. (2013, 2014) and Latif et al. (2013). Evidence is found of century-scale variability over the region, which may in turn affect the northern Atlantic, through modulation of AMOC. AMOC is widely considered a primary driver of low-frequency climate system variability (Delworth and Mann, 2000; Latif et al., 2004; Schleussner et al., 2014; Muller et al., 2013; Chylek et al., 2014) and a potential instigator of sudden climatic shifts (Stommel, 1961; te Raa and Dijkstra, 2002; Dijkstra and Ghil, 2005; Lenton et al., 2008, 2009; Hawkins et al., 2011). Strong associations between SO variability and low-frequency SAM variability has also been found (Martin et al., 2013; Latif et al., 2013). Such long-term variability may also mask the anthropogenic warming signal (Latif et al., 2013). It is not clear to what extent the KCM SO variability represents a quasi-periodic mode, distinct from the aperiodic spectrum (Latif et al., 2013).

Martin et al. (2013) and Latif et al. (2013) find that variability in SO is itself largely independent of Northern Hemispheric modes of variability, including AMO and PDV (Martin et al., 2013; Latif et al., 2013). Crowley et al. (2014) also suggest that temperatures

in the Southern Hemispheric high-latitudes are relatively independent of temperatures elsewhere, up to centennial time scales, possibly because of the isolating influence of the Antarctic ice shelf and the well-mixed SO. Long-term persistence of Antarctic temperature was found in Ludescher et al. (2015).

SO variability in the higher resolution, standard version of CCSM4 is discussed in Weijer et al. (2012). The model does not reproduce vertical ocean processes in SO well. This shortcoming is likely to be amplified at lower resolution, so that SO variability will likely be underestimated.

Because these regions have been understudied, despite prominent long-term variability, a number of domains covering the Southern Hemispheric extratropics are included in this study (see subsection 3.6.2). The apparent isolation of extratropical Southern Hemispheric modes of variability also suggests that studying climate variability over these regions may produce qualitatively distinct results from other regions.

2.2.3 Climate Model Experimental Design and Interpretation

2.2.3.1 IC Ensemble Design and Ensemble Size

Climate model IC ensembles are generally "branched off" from long control run simulations (see subsubsection 2.2.3.2), after the model drift in the surface climate has become small (e.g., Haughton et al., 2014; Wittenberg et al., 2014). Alternatively, a single transient run may be branched off from a control run, before initialising an ensemble of runs from the transient run (e.g., Hunt and Elliott, 2004; Teng and Branstator, 2011; Teng et al., 2011; Kay et al., 2014). Ensemble members can be differentiated by imposing small atmospheric perturbations (e.g., Wittenberg et al., 2014; Kay et al., 2014) or by selecting different starting times from a pre-existing run, which does not use the same forcing as the ensemble (e.g., Haughton et al., 2014; Branstator and Teng, 2010). In this study all ensembles are branched from a control run (see section 3.3). Different IC ensembles intended to explore potentially macroscopic IC influence were initialised from different model years, in a manner similar to Haughton et al. (2014), although the approach used here is not systematic (see subsection 3.5.3).

Daron and Stainforth (2013) suggest that ensembles of size at least 100 may be necessary to quantify uncertainty in distributions of climatic variables in a manner relevant to prediction and policy. In this study, a compromise needs to be struck between the size of ensembles run and the number of different ensembles run, because of the computational expense involved. Few GCM, CSM or ESM studies involve IC ensemble sizes greater than 10—far fewer than, for example, Daron and Stainforth (2013, 2015). CMIP5 required only 3 IC members (Taylor et al., 2012). Daron and Stainforth (2013) show that ensembles with fewer than 10 members perform very poorly in constraining the variable possibility space in the low-dimensional coupled model they use (Lorenz, 1984, 1990; Stommel, 1961).

Larger ensembles are particularly useful for understanding extremes (Daron and Stainforth, 2013). In this study, 50-member ensembles are used.

2.2.3.2 Control Run Drift and Variability

Control runs are model simulations run for an extended period with fixed external forcings. Conventionally, control runs, including those conducted with the Community Climate System Model, version 4 (CCSM4; Gent et al., 2011), the low-resolution CCSM4 (Shields et al., 2012) and CMIP5 (Taylor et al., 2012), are run with "pre-industrial" (usually around 1850AD) forcing. Additionally, in contrast with CCSM3—for which parametrisation efforts concentrated on "present day" (usually around 2000AD) control runs (Collins et al., 2006a)—CCSM4, in its high- and low-resolution configurations, was parametrised to achieve approximate TOA energy balance in the pre-industrial control (Gent et al., 2011; Shields et al., 2012). This limits OHC drift, in the control run from which 20$^{\text{th}}$ Century (20C) simulations are initialised (Gent et al., 2011).

However, for this investigation, it is not of primary interest whether the simulated model state is realistic, although variability that is qualitatively similar to that observed is highly desirable (see chapter 4). However, we required a control run from which RCP8.5 (van Vuuren et al., 2011) ensembles could be branched without too great an initial shift in forcings (see subsection 3.5.5). Furthermore, conceptual questions related to defining climate, for practical purposes, are best investigated under conditions approximating those currently experienced, as in Teng et al. (2011); Teng and Branstator (2011); Park and Latif (2008); Martin et al. (2013). Hence we perform control runs with present day forcing. Delworth et al. (2012) and Small et al. (2014) also use present day forcings for their control runs, although this is primarily in order to have more reliable observations to validate model output against—something which is not done in this study.

Model drift in this study is defined as in Sen Gupta et al. (2013), as "spurious long-term changes in general circulation models that are unrelated to either changes in external forcing or internal low-frequency [model system] variability". Note that no particular mechanism is stipulated as being responsible for this model behaviour; rather, model drift refers to trends observed in model output time series. Model drift—which is associated especially with ocean state variables (Sen Gupta et al., 2012)—may occur partially or entirely because of model system relaxation behaviour from imposed ICs derived from observations (Sen Gupta et al., 2013), towards the model's "preferred state". Hirst et al. (2000) suggest that model drift occurring over longer time scales could be related to adjustments towards the model's preferred state of SO deep convetion, citing particularly large drift over SO in their model, as well as that of Fanning and Weaver (1997). Violations of conservation laws and inconsistencies arising in exchanges between coupled model components (e.g., Rahmstorf, 1995; Gordon et al., 2000) can also contribute to drift in model system quantities (Sen Gupta et al., 2013, and references therein).

Comparatively little model drift is observed in control runs of CCSM4, and related models, at various resolutions (Gent et al., 2011; Danabasoglu et al., 2012; Shields et al., 2012; Small et al., 2014). This drift is most apparent in OHC. It is is approximately linear and occurs in conjunction with near-constant TOA radiative imbalances. In contrast, approximately exponential decay is expected to occur in response to IC perturbations away from a model attractor (if one exists), as discussed in subsubsection 2.2.3.3. The apparent linearity may, however, reflect a long characteristic decay time.

There does not seem to be consensus on when a model could be considered to display sufficiently little drift for ensembles to be branched off. Even in studies using multimillennial control runs, detectable model drift may persist throughout much of the simulation (e.g., Stone et al., 2001; Latif et al., 2013; Wittenberg et al., 2014). Often detrending of assumed drift patterns is performed prior to analysing data (e.g., Dommenget and Latif, 2008; Wittenberg et al., 2014). Previously, model drift was commonly corrected for with flux adjustments (Hirst et al., 2000), but improved parameterisations in newer CSMs allow them to be run without flux adjustments (Sen Gupta et al., 2013), as is the case with the model configuration used here. Concerns exist about the influence of flux adjustments on model climates (e.g., Neelin and Dijkstra, 1995; Fanning and Weaver, 1997).

2.2.3.3 IC Perturbation Decay

The difference between ensemble IC variable values and corresponding "climatological" mean values (or preferred state values) can be conceptualised as a perturbation. This notion is made more precise in subsection 5.1.1. This approach is not without problems (not least how to define "the climatology"; see subsection 2.1.5). Nonetheless, it is considered to be of value, especially when the state space distance between ICs and the model's preferred state is particularly large, as is the case for the ensemble discussed in subsection 5.1.4.

The term "relaxation" will be used in this study to refer to the decay of a perturbation imposed, through whatever means, on some collection of variables, away from their preferred state values. The behaviour resulting from the collection of processes acting to induce this perturbation decay will be termed "relaxation behaviour".

Using simple energy balance considerations (e.g., McGuffie and Henderson-Sellers, 2005; Schwartz, 2007), to a first-order approximation, the process of relaxation of near-surface temperature should follow exponential decay, provided that the IC perturbation is sufficiently small (Schwartz, 2007).

Consider a temperature perturbation ΔT, applied to a body B, whose climatological mean temperature is T_p. Let r denote the characteristic decay rate of ΔT and C the effective specific heat capacity of B.

The term "equilibrium climate sensitivity" will be defined here as the change in "equilibrium" GMST per unit change in net radiative forcing. This definition is used

in, for example, Schwartz (2007) and is quantitatively convenient. Note, however, that it is different from the IPCC (2013a) definition, where it is defined as the change in equilibrium GMST resulting from a change in net radiative forcing equivalent to a doubling of atmospheric CO_2 concentrations.

Let λ be the equilibrium climate sensitivity of B. Then r is given by:

$$r = \frac{1}{\lambda C} \tag{2.1}$$

It follows from the above that (e.g., Schwartz, 2007, 2008b, 2012; Schwartz et al., 2010; Knutti et al., 2008)

$$\begin{aligned} \frac{\mathrm{d}T}{\mathrm{d}t} &\approx -r\Delta T \\ \Rightarrow T(t) &\approx T_p + \Delta T e^{-rt} \end{aligned} \tag{2.2}$$

The parameters λ and C, on which r depends, are still very uncertain (e.g., IPCC, 2013b; Knutti and Hegerl, 2008; Otto et al., 2013) for the real climate system. The values of these parameters vary according to the characteristic time scales of relaxation processes (e.g., Lovejoy and Schertzer, 2012; Scafetta, 2008; Schwartz, 2008a), the temporal evolution of spatial temperature anomaly distributions through the climate system (e.g., Andrews et al., 2015; Schwartz, 2012, see also subsection 5.2.2) and possibly various other climate system variables.

2.2.4 Uncertainty and Ensembles

Large uncertainties remain in climate change projections (Katzav et al., 2012; Frigg et al., 2015)—and are likely to persist for the foreseeable future (Smith, 2000b). Uncertainties are larger at smaller scales (Oreskes et al., 2010). To establish meaningful adaptation strategies, based on robust climate information, a good understanding of the future probability distributions of climatic variables is essential. This requires thoroughly exploring all possible substantial sources of uncertainty in climate projections (Oreskes et al., 2010; Stainforth et al., 2007a,b; Daron, 2012; Daron and Stainforth, 2013).

The use of IC ensembles is valuable for understanding and quantifying model variability and ICU (Daron and Stainforth, 2013, 2015). ICU represents a lower bound on total uncertainty, both under fixed and changing external forcing (Daron and Stainforth, 2013; Phipps et al., 2013; Smith et al., 2014). Using IC ensembles contrasts with the more traditional approach of estimating uncertainty bounds by considering multi-model

ensembles, a range of forcing scenarios and/or different model parametrisations (Taylor et al., 2012; Daron, 2012; Randall et al., 2007; Collins et al., 2006a).

It should be noted that there is a distinction between internal variability within "model worlds"—sampled by IC ensembles (Daron and Stainforth, 2013)—and model error (Deser et al., 2012a; Kay et al., 2014). IC ensembles are also entirely distinct from multi-model and perturbed parameter ensembles (see, e.g., Haughton et al., 2014), which sample uncertainty in what Stainforth et al. (2007a) call "model inadequacy" and "model uncertainty", respectively. Means of such ensembles cannot be considered representative of internal variability (Latif et al., 2013; Hawkins et al., 2014).

Chapter 3

Methods

This chapter documents the IC ensemble experiment conducted for this study (in sections 3.2–3.5). A descriptions of methods employed in analysing the model output is then provided in section 3.6.

A short description of the experimental design is presented in section 3.1, which is expanded upon in section 3.3. The model used is discussed in section 3.2, the model control runs in section 3.4 and the ensembles in section 3.5.

3.1 Experimental Overview

A large IC ensemble simulation of the Community Earth System Model, version 1.2 (CESM1.2; Hurrell et al., 2013), was run at very coarse horizontal resolution (see section 3.2). The output is used to explore theoretical concepts discussed in chapter 2 with data which is to some extent representative of the qualitative behaviour of the real climate system.

Control runs were performed to initialise ensembles from. Fourteen IC ensembles—each with fifty members—were run under one of two different forcing scenarios:

- present day constant external forcing (see subsection 3.4.2); or
- a Representative Concentration Pathway (RCP; van Vuuren et al., 2011) scenario forcing (see subsection 3.5.5).

Each ensemble member is run for 60 years to allow for equal, reasonably large sample sizes in comparisons between ensemble and temporal distributions from a given ensemble, from which the first decade of ensemble data is neglected. This duration also corresponds to two periods of standard climatology (WMO, 1988). Some ensemble members were run for somewhat longer (around 100 years in total), so as to judge whether ensemble member trajectories might diverge further from the control run trajectories over longer periods.

3.2 The CESM Model and Configurations Used

The CESM1.2 configuration used in this study corresponds essentially to running the Community Climate System Model, version 4 (CCSM4; Gent et al., 2011). CCSM4 lacks an active carbon cycle, which would have been computationally prohibitively expensive for this study. Hence, CCSM4 would be considered a CSM, rather than an ESM (Flato, 2011; Hurrell et al., 2013; Stevens and Bony, 2013). Additional documentation can be found in the special collection for CESM1 and CCSM4 in the Journal of Climate[1]. In higher resolution configurations, both and CCSM4 formed part of CMIP5. Some further discussion of the model is provided in Appendix A.

3.2.1 Model Components Used

CCSM4 was run in a "fully coupled" configuration. This includes the following components: atmosphere (Community Atmosphere Model, version 4.0 (CAM4.0; Neale et al., 2013)), land (Community Land Model, version 4.0 (CLM4.0; Lawrence et al., 2012)), ocean (Parallel Ocean Program, version 2 (POP2; Danabasoglu et al., 2012)), sea ice (Community Ice Code, version 4 (CICE4; Hunke and Lipscomb, 2008)), and river run-off (RTM). Interactions between components are controlled by the coupler (CPL7), described by Craig et al. (2012). More details are provided in subsection A.1.1.

In order to minimise computational expense, the lowest resolution (`f45gx3`) on which the fully coupled model can be run, is used. Accordingly, CAM and CLM computation is performed by a finite volume (FV) dynamic core (dycore) (Lin, 2004), on a 4x5° latitude-longitude grid. A nominally 3° Greenland pole grid is used by POP2 and CICE, as in the model configuration described by Shields et al. (2012). The same horizontal grid is also used in the CCSM3 configuration documented by Yeager et al. (2006).

It should be noted that active Carbon-Nitrogen cycling (the `CN`-module) is not used. The `CN`-module has a pronounced influence on tropical climates (as determined from test runs; results not shown).

CAM4.0 has 26 vertical levels; POP2 has 60. The time step used is 1800s (30min).

3.2.2 Resolution Considerations

More realistic patterns of variability—particularly of ENSO—are produced by the `T31x3` CCSM4 configuration described by Shields et al. (2012). Initially the decision to use `f45gx3`, was taken with the intention of reducing computational cost, but, due to the superior scaling of the spectral element (SE) dycore (see, for example, Dennis et al. (2012)),

[1] http://journals.ametsoc.org/page/CCSM4/CESMI

computational expense of `T31x3` on multiple compute nodes is similar to that of `f45gx3`. However, for the ensemble runs—responsible for most of the computational cost incurred in this study—individual members were run concurrently, so that scaling was less influential.

The SE dycore used in `T31x3` employs `T31` truncation (implying an approximately $3.75 \times 3.75°$ horizontal resolution) and is used by the CAM and CLM components. The `CN`-module is included with CLM. Model parametrisation in `T31x3` is optimised for use with a low resolution. Shields et al. (2012) point out inherent, severe shortcomings of coarse resolution FV dycores in resolving baroclinic wave development (Jablonowski and Williamson, 2006).

However, the primary intention of this study is not to reproduce or analyse realistic variability or assess predictability in an operational context. Rather, large IC ensemble behaviour of a climate-like system is analysed with the intention of exploring possible qualitative behaviours of model climates. Hopefully this will encourage further study in a more realistic setting, to determine the extent to which these behaviours need to be considered in designing model experiments and interpreting model output. Accordingly, exhaustive scientific validation of the model climate for the `f45gx3` configuration is not conducted, even though this has not previously been done; it is expected that certain aspects of the model behaviour are unrealistic artefacts of the low resolution. Despite these shortcomings, the model should satisfy the requirements of the present study; in fact, to date most studies with a similar approach have been conducted on more conceptual models of climate dynamics (e.g., Daron, 2012; Daron and Stainforth, 2013; van Veen et al., 2001; van Veen, 2003, see also subsubsection 2.2.1.1). However, it is suggested that future studies extending this work apply the `T31x3` configuration (or a similar resolution in an alternative model), to assess the extent to which the qualitative results obtained here transfer to a more realistic model set-up.

3.2.3 Machines Used

CESM1.2.0 model runs were conducted on the Tsessebe Cluster at South African Centre for High Performance Computing (CHPC; `http://www.chpc.ac.za/`). CESM1.2.1 runs were conducted on the Edison machine at the National Energy Research Scientific Computing Center (NERSC; `http://www.nersc.gov/`). This version difference is minor, involving only bug fixes and should not detectably affect the model climate. More details on the machine set-up used is provided in section A.2.

Because of model set-up choices made to improve computational throughput, POP2 output (and hence, due to coupling, output from all other components) will not be bit-for-bit reproducible using a different number of cores. Model run trajectories from different machines, with the same number of cores, also diverge. The rate and extent of divergence is comparable to that produced by (a) using a different number of cores on the same machine; and (b) applying a small IC perturbation to the atmospheric temperature fields.

Similar behaviour was observed by Delworth et al. (2012). Accordingly, although the same ICs (see subsection 3.4.1) were used for the two control runs using present day forcing (see section 3.3), their output trajectories diverge in a manner not dissimilar to the divergence observed between ensemble members of a given ensemble (see chapter 5).

3.3 Experimental Design

3.3.1 Experimental Approach

A 1624-year simulation, using present day forcing, was run at CHPC. This run will be referred to as the CHPC Control. At NERSC, a corresponding 992-year simulation—the NERSC Control—was run. Together, the CHPC and NERSC Controls are referred to as the Present Day Controls (PDCs) see.

IC ensembles were initialised with ICs from different years of these two PDCs (cf. subsubsection 2.2.3.1). Presumably, sampling appreciably different ocean ICs allows us to explore the consequences of macroscopic ICU for model system trajectories (see also subsubsection 2.1.3.2 and subsection 3.5.2). The selection of the IC ensemble starting model years, which provide the model system ICs, was partly strategic and partly arbitrary, as explained in greater detail in subsection 3.5.3. Ensemble member IC differences are intended to be microscopic in nature.

A third control simulation, using pre-industrial forcing conditions, is run for 459 years at CHPC. It is referred to as the Pre-Industrial Control (PIC). The qualitative influence of different constant external forcings is explored by comparing its output to that of the PDCs. No ensembles were initialised from the PIC. Results from this simulation are presented primarily in Appendix B.

3.3.2 IC Ensembles run

The ensembles run, together with some information about their initialisation, is given in Table 3.1. Ensemble names refer to the origin of the restart files used as a basis for the ensemble member ICs. In cases where the ensemble name ends in "RCP", RCP8.5 forcing was used for the ensemble members. Ensembles for which the name does not end in "RCP" use present day forcing. All "years" (abbreviated as Yr") referred to in the ensemble names are equivalent control run model years, to be referred to henceforth as model years. The model year is equal to the total number of years during which ocean circulation has been active.

For model year 186, from which two ensembles were started (both at NERSC), the two ensembles are distinguished from one another by the suffixes "A" and "B". The same

applies for model year 1055, from which two ensembles were started (both at CHPC). For model year 876, an ensemble was started at NERSC and another at CHPC. This is indicated by corresponding suffixes in the ensemble names.

Table 3.1: Table of ensembles run. The ensemble name used, the machine on which the ensemble was run, the magnitude of IC temperature perturbation applied, whether the ensemble is a "primary ensemble" (i.e. whether it was initialised from a control run) and external forcing applied, are indicated. Where the ensemble is a secondary ensemble, the ensemble name and member number (preceded by "r") is shown. Present day forcing is indicated as "2000 AD".

Name	**Machine**	**IC Perturbation**	**Primary Ensemble**	**Forcing**
Yr126	NERSC	$O(10^{-11})$K	Yes	2000 AD
Yr126_RCP	NERSC	$O(10^{-11})$K	Yes	RCP8.5
Yr186A	NERSC	$O(10^{-11})$K	Yr126 r38	2000 AD
Yr186B	NERSC	$O(10^{-11})$K	Yr126 r48	2000 AD
Yr587	CHPC	$O(10^{-11})$K	Yes	2000 AD
Yr587_RCP	CHPC	$O(10^{-11})$K	Yes	RCP8.5
Yr597	CHPC	$O(10^{-11})$K	Yes	2000 AD
Yr647	CHPC	$O(10^{-11})$K	Yr587_RCP r16	2000 AD
Yr876_CHPC	CHPC	$O(10^{-11})$K	Yes	2000 AD
Yr876_NERSC	NERSC	$O(10^{-11})$K	Yes	2000 AD
Yr1055A	CHPC	$O(10^{-11})$K	Yes	2000 AD
Yr1055A_RCP	CHPC	$O(10^{-11})$K	Yes	RCP8.5
Yr1055B	CHPC	$O(10^{1})$K	Yes	2000 AD
Yr1065	CHPC	$O(10^{-11})$K	Yes	2000 AD

Figure 3.1 shows a schematic representation of the various runs conducted for the IC ensemble experiments: the PDCs and the ensembles. Eleven primary ensembles—initialised from PDC output—and three secondary ensembles—initialised from the the final (sixtieth) year output of of a primary ensemble member—are shown. The model years from which output was used as ICs for ensemble simulations are indicated. For each ensemble, five of the fifty members are shown. Note that RCP8.5 transient forcing ensembles (TFEs) were run from only some ICs.

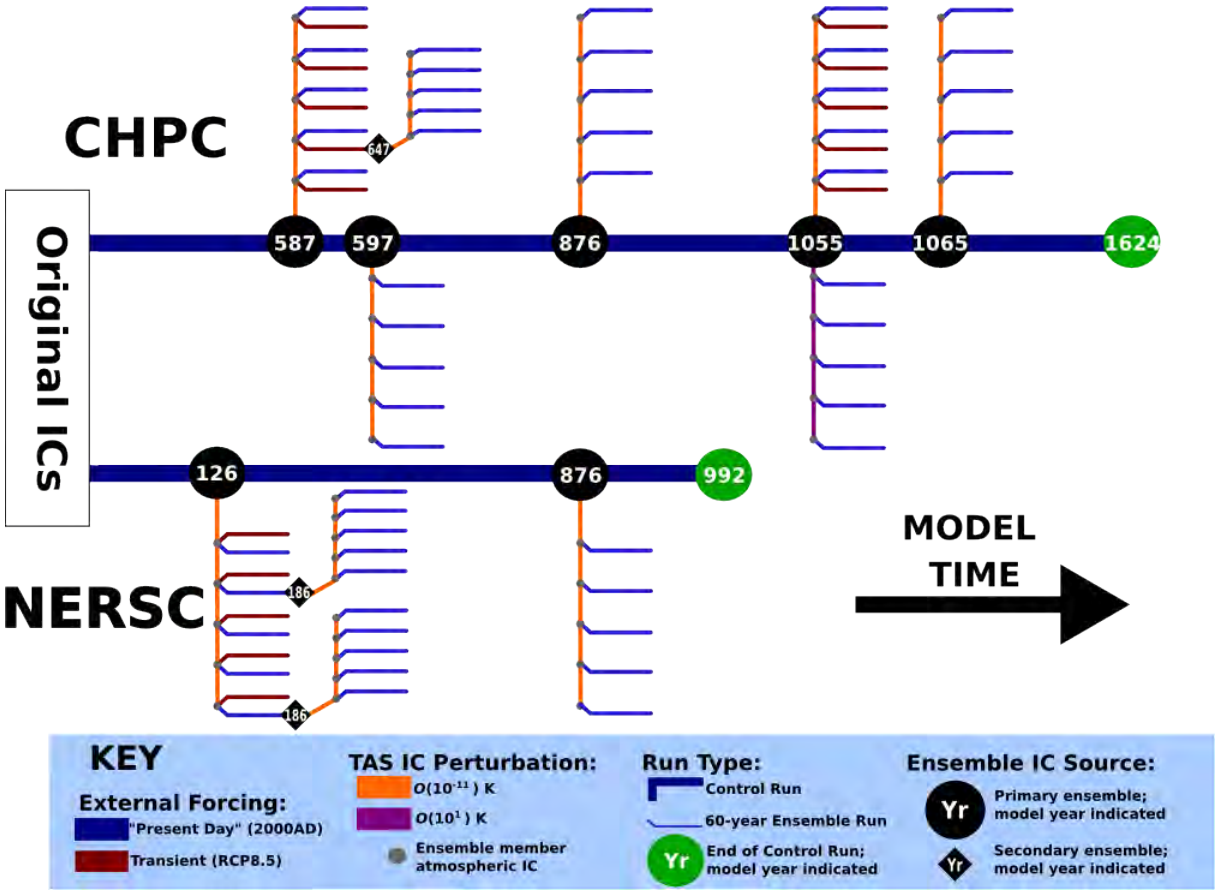

Figure 3.1: Conceptual schematic of ensemble experimental design. Runs in the upper (lower) half were conducted at CHPC (NERSC). See section 3.2.3 for a more complete discussion. Note that the PIC is not shown. Model years indicated are control run model years or corresponding control run model years (see text for details). Primary ensembles are "branched" off from control runs at selected model years (see subsection 3.5.3 for a discussion of the motivation for model years selected). Secondary ensembles are ensemble started from ensemble member output. Note that all ensembles include 50 members, even though only 5 are shown. Each ensemble member is run for 60 years, under either present day (2000 AD) or projected transient RCP8.5 forcing for 2005–2064AD. Note that, as indicated, 11 present day constant forcing ensembles (CFEs) and 3 RCP8.5 transient forcing ensembles (TFEs) were run. See 3.3 for further discussion on the experiment conducted and 3.5 for discussion of the ensemble set up.

3.3.3 Atmospheric IC Perturbations

Each of the 50 ensemble members of each ensemble uses restart output from all CCSM4 components of the model run they are branched off from, other than that an atmospheric IC perturbation is applied to distinguish the members from one another. The mechanism used is equivalent to that applied by Kay et al. (2014) in the CESM-LE.

Starting from the CAM restart state, random perturbations are applied to the 3-dimensional temperature field, given a user-supplied parameter[2], a. For each vertical level k, a random number $p(k)$, is generated. $p(k)$ is approximately uniformly distributed on [-a, a]. Denoting temperature at longitudinal grid point i, latitudinal grid-point j, and vertical level k by $T(i, j, k)$, the perturbed temperature field, $T_P(i, j, k)$, is given by $T_P(i, j, k) = (1 + p(k))(T(i, j, k))$.

For all ensembles other than Yr1055B, the value of a was varied between 1.16×10^{-13} (for run 1) and 9×10^{-13} (for run 50). A constant increment of 1.6×10^{-14} was used between successive members. Hence, if a_i represents the value of a for the i^{th} ensemble member:

$$a_i = 10^{-13} + (1.6 \times 10^{-14})(i) \tag{3.1}$$

For Yr1055B, a was varied between 9.16×10^{-2} and 0.17, using an increment of 1.6×10^{-3} between successive members, so that:

$$a_i = 0.09 + 0.0016(i) \tag{3.2}$$

Given that temperatures near the surface approach 300K, p_{26} (where the lowest level is nearest the surface), for Yr1055B members, could approach 30K. For other ensembles, p_k values are likely not much larger than round-off error order.

During the 43^{rd} model year integration of the 4^{th} member of Yr597, a fatal "CICE monotonicity error" occurred. Hence, a substitute 4^{th} member was run, using $a_4 = 1.6 \times 10^{-13}$, rather than the original 1.64×10^{-13} and the error was avoided. This modification should not qualitatively affect the results.

In addition to these deliberately imposed perturbations, the different number of cores used for control and ensemble simulations (at CHPC) and running ensembles as "hybrid" rather than "branch" restarts, also contribute to divergence between the trajectories of ensemble members and the PDC off which they were branched (Vertenstein et al., 2013). Using hybrid restarts is required to allow perturbations to take effect; however, it implies

[2]This parameter is named `pertlim` in the CAM namelist.

that a bit-for-bit equivalence with the control cannot be achieved. Further, the ocean component integration only starts at the second time step. However, these factors do not contribute to divergence between members of the same ensemble (tests were conducted to confirm this). Consequently, differences between ensemble members can be attributed directly to atmospheric IC perturbations.

3.4 Control Runs

A discussion of the use of control runs in the literature is provided in subsubsection 2.2.3.2. Here, the procedures used in this study are outlined.

3.4.1 Initialisation

All control runs were initialised with default ICs for the model configuration. The ocean is initially at rest (Vertenstein et al., 2013) and potential temperature (θ) and salinity (S) values are from Levitus et al. (1998) and Steele et al. (2001), as described by Danabasoglu et al. (2012).

ICs of other model components are generally considered to be of little consequence to multicentennial simulations (Kay et al., 2014). However, in an intransitive system or one exhibiting almost-intransitivity, even round-off order changes in initial state could produce different rates—or even patterns—of model climate evolution, when considering time periods of up to about centennial-scale. However, it is unlikely that such changes could be attributed to the nature or pattern of ICs; these effects are likely the result of chaotic processes that are relatively insensitive to the scale of IC perturbation (Lorenz, 1969b, see subsection 5.1.2).

3.4.2 External Forcing

The primary control simulations performed used present day forcing: annual-cycle forcing, intended to approximate those forcing conditions that prevailed in 2000 AD. The atmospheric near-surface CO_2 concentration is set to 367 parts per million by volume (ppmv). Insolation is set to $1361.27 \mathrm{W} \cdot \mathrm{m}^{-2}$. For the PIC, forcing conditions approximate those that prevailed in 1850 AD. CO_2 concentrations are set to 284.7 ppmv and insolation is fixed at $1360.89 \mathrm{W} \cdot \mathrm{m}^{-2}$. For all control and ensemble runs, orbital parameters are fixed at 1990 AD values.

3.5 Ensembles

3.5.1 Overview

All ensemble simulations were performed on the same cluster as the simulation from which they are branched. Individually, ensemble members are referred to as "Run$n$" where $n \in \mathbb{N}, 1 \leq n \leq 50$). For all ensembles other than Yr876_NERSC, all members were run for at least 60 years. Due to computational constraints, 4 ensemble members of Yr876_NERSC were not completed. These are Run13 (56 completed years available), Run14 (40 years), Run17 (48 years) and Run34 (58 years). The impact upon results is assumed to be negligible. Unless otherwise indicated, analysis is done on only the first 6 decades of available ensemble member output.

3.5.2 Motivation for Ensemble Selection and Conceptual Approach to Interpretation of Results: Levels of IC Influence

This subsection expands on ideas introduced in subsection 3.3.1. A goal of this study is to explore whether—and if so, how—varying the distribution (in model state space) of ICs can lead to qualitatively different within-ensemble behaviour. By applying equivalent IC perturbations to the different model system states used as ICs for the different ensembles (see subsection 3.5.3), we attempt to establish whether within-ensemble IC influence is affected by macroscopic IC state.

For the model set-up used, an attempt is made to assess how distant—and different in which sense—ICs have to be for particular types, or "levels", of IC influence (see section 1.3) to emerge. In this study, following Stainforth et al. (2007a), it is proposed that IC influence sufficiently large to lead to statistically distinguishable ensemble distributions be considered macroscopic. Consequently, some degree of ICP, observable in annual mean quantities, is required for an IC perturbation to be considered macroscopic. Traditional "weather-scale" IC influence, which produces distinct time series, but statistically similar behaviour, is labelled microscopic. It is of interest whether further meaningful distinctions between different levels of micro- and macroscopic IC influence exist. In order to do address this question, a range of approaches are used to select model system ensemble ICs (see subsection 3.5.3 for details) and two different scales of atmospheric perturbation are applied (see subsection 3.3.3).

In addition to exploring whether meaningful delineations exist between different levels of IC influence, the possibility of qualitatively distinct sets of possible within-ensemble behaviours, produced by qualitatively indistinguishable ICs, is considered.

Multidecadal divergence in the statistical properties of members of a given ensemble can be seen as evidence of almost-intransitivity (Lorenz, 1968, see also subsection 1.5.3) in

a model subsystem. Strictly speaking, almost-intransitivity refers to a single trajectory spending extended periods of time in different regions of the attractor space. However, for most of the ensembles considered here, the difference in ICs between ensemble members is only slightly larger than round-off error order. Consequently, each member trajectory can be considered a possible extension of the original run the ensemble was branched off of, within computational error. Two trajectories diverging for extended periods, therefore, suggest alternative patterns of evolution which the original run could have followed.

Furthermore, there may be value in distinguishing between IC sets that lead to almost-intransitive behaviour resulting from different mechanisms that last for differing time scales. Different degrees of within-ensemble divergence may result from different rates of IC "memory loss", potentially related to long-term persistence (see subsubsection 2.1.4.4).

3.5.3 Ensemble Starting Time Selection

Time series of regional-mean atmospheric quantities (see 3.6.2) of the PDCs were analysed to select model years at which to initialise ensembles. The objective was to sample a range of model states in order to address the key research questions. Primary ensembles initialised from the CHPC Control are discussed in subsubsection 3.5.3.1, before primary ensembles from the NERSC Control in subsubsection 3.5.3.2 and secondary ensembles in subsubsection 3.5.3.3. The intention was first to sample model years from across the range of produced states, with emphasis on years with the largest anomalies, relative to surrounding decades and centuries, and those from different stages of large-scale model drift (see subsubsection 2.2.3.2). Then the influence of presumably intermediate IC differences are explored.

To explore model variability during an arbitrary model period and to compare ensemble output from NERSC and CHPC, a present day constant forcing ensemble (CFE) was initialised with restart output from each of the two PDCs at the beginning of model year 876. These ensembles are named Yr876_NERSC and Yr876_CHPC, respectively. See Figure 3.1 and Table 3.1 for ensemble details.

3.5.3.1 CHPC Control

Model year 586 is the most anomalous year occurring in either of the PDCs, showing large deviations of atmospheric variable values from states prevailing during the surrounding model centuries, across numerous spatial domains. Very high temperatures occurred across much of globe, especially in the eastern Pacific. Temperatures across the Southern Hemispheric extratropics were anomalously low. Model year 1055, in contrast, was anomalously cold, especially over the Northern Hemispheric polar regions and tropical Pacific. It was the coldest year after model year 600, in the PDCs. To investigate the impact of such unusual conditions on ensemble behaviour, both a CFE and a TFE were

initialised from the end of the anomalously hot year (ensembles Yr587 and Yr587_RCP) and from the start of anomalously cold year (ensembles Yr1055A and Yr1055A_RCP). In the interest of investigating whether the scale of atmospheric IC perturbation applied affects qualitative within-ensemble behaviour, a second CFE (Yr1055B) was initialised from model year 1055, using much larger scale IC perturbations (see section 3.3).

Further CFEs were initialised from model years 597 (ensemble Yr597) and 1065 (ensemble Yr1065), 10 years (arbitrarily chosen) after the initialisation of the Yr587 ensembles and Yr1055 ensembles, respectively. They are intended to explore scales of IC influence presumably larger than those produced by atmospheric perturbations and potentially smaller than those produced by long-term secular changes in model climate, or by unusually large anomalies.

3.5.3.2 NERSC Control

As discussed in section 4.1, an early period of relative stability appears to occur in the PDCs. To investigate ensemble behaviour during this period, a CFE and a TFE were initialised from model year 126 (ensembles Yr126 and Yr126_RCP).

3.5.3.3 Secondary Ensembles

Over the Southern Hemispheric extratropics and northern Pacific, divergence between Yr126 ensemble members is relatively large. To investigate the influence of this divergence, ensembles are initialised from the 60th year output (model year 185) of the Yr126 members which were coldest (Yr186A) and warmest (Yr186B) over the the Southern Midlatitudes (SML) (see domain definition in Table 3.4) in the last ensemble decade. The ICs for these ensembles were thus obtained in a manner similar to ensembles II and III from Teng and Branstator (2011) and ensemble A1B(IV) from Teng et al. (2011). Although these ensembles are not strictly speaking IC ensembles, the authors claim that they do behave like IC ensembles.

Yr647 is run under present day forcing, but was initialised with restart files from the 60th ensemble year (model year 646) of the hottest—in terms of global-mean near-surface (2m) air temperature (TAS) (see Table 3.2) over the 6th ensemble decade—member of the Yr587_RCP ensemble. Thus, this ensemble's ICs were produced by first applying present day forcing for 586 model years, followed by 60 years of RCP8.5 forcing, for 2005–2064AD. This ensemble was run to investigate the influence of ICs distant from the region in model state space through which present day trajectories pass. In a hypothetical equivalent low-order nonlinear dynamical system, these Yr647 ICs would be substantially removed from the present day model attractor. Yr647 behaviour is discussed in subsection 5.1.4.

3.5.4 Constant Forcing Ensembles

The eleven CFEs (see Figure 3.1) were run to explore the influence of internal model variability. Forcing conditions for these ensembles are as for the PDCs (see subsection 3.4.2).

3.5.5 Transient Forcing Ensembles

In reality, external forcings are never constant; in particular, currently they are evolving rapidly due to anthropogenic influences (IPCC, 2013b). To explore the influence of transient forcing trajectories, the most rapidly evolving forcing scenario that can be easily implemented with CESM1.2, RCP8.5 is used for three ensembles. RCP8.5 forcing should reveal qualitative differences in ensemble behaviour under stationary and transient conditions clearly. TFEs are initialised from the three most different IC sets described in subsection 3.5.3. Forcings for 2005–2064 AD are used, implying a "jump" of 5 years between the forcing conditions used in the PDCs and at the start of the ensemble runs. This is deliberately imposed to see whether such a forcing discontinuity would influence ensemble evolution.

It is important to note that, in addition to the atmospheric IC perturbations introduced as in the constant forcing ensembles, a perturbation in the CLM ICs was necessitated. This is described in subsection A.1.2.

3.6 Methods for Analysis

Annual averages of selected CAM output variables, from CFEs, TFEs and PDCs are analysed. In this section, the methods used for this of analysis, as well as the variables and regions analysed, are described.

3.6.1 Variables

The CAM variables considered are summarised in Table 3.2. Variable names as output by CAM are given as "CAM Name". In cases where manipulation of raw output is performed, the formula applied is reproduced in this column. The convention used is to present raw output variables in "Typewriter" typeface. Quantities for which units are denoted as "1" are dimensionless.

3.6.2 Spatial Domains

Each of the regional domains is a rectangle in the mapping of the sphere onto Cartesian $\theta - \phi$ space (i.e. the domains include all points on the planetary surface whose longitude (θ) and latitude (ϕ) are bounded by specified respective limits). The convention used is that for any location $\mathbf{r}$ on Earth's surface, $\mathbf{r} = (\theta, \phi) \in \{\mathbb{R}^2 | -180^\circ \leq \theta \leq 180^\circ, -90^\circ \leq \phi \leq 90^\circ\}$.

Table 3.2: CAM variables considered in this study

Variable Descriptive Name	**CAM Name**	**Abbreviated Form**	**Units**
2m Air Temperature	`TREFHT`	SAT	K
Radiative Surface Temperature	`TS`	TS	K
Precipitation	c(`PRECC` + `PRECL`)	PPT	mm $\cdot$ yr $^{-1}$
Sea-level Pressure	`PSL`/100	PSL	hPa
Vertically Integrated Cloud Cover	`CLDTOT`	CLD	1
Meridional (Zonal) Wind	`V` (`U`)	V (U)	m $\cdot$ s $^{-1}$
Meridional (Zonal) Wind Squared	`VV` (`UU`)	VV (UU)	$m^2 \cdot s^{-2}$
Wind Kinetic Energy	`UU` + `VV`	UUVV	$m^2 \cdot s^{-2}$
*where c is a conversion factor from m $\cdot$ s^{-1} to mm $\cdot$ yr^{-1}			

Table 3.3: Domains of regions considered in this study

		Domain Bounds			
Domain Name	**Abbreviated Form**	**West (°E)**	**East (°E)**	**South (°N)**	**North (°N)**
Africa	Af	-25	60	-40	40
Antarctic Circumpolar	ACC	-180	180	-65	-40
Eastern Tropical Pacific	ETP	-150	-80	-20	20
North Atlantic	NAt	-80	0	20	75
North Pacific	NPa	120	-110	20	65
Southern Africa	SA	10	40	-35	-10
South of southern Africa	SSA	-30	70	-60	-40
Western Tropical Pacific	WTP	120	-150	-20	20

The domains used are divided into groups: "latitudinal bands," "regions" and other domains. Latitudinal bands are circumglobal domains, defined by bounding latitudes exclusively. Regions are domains covering important ocean basins, as well as two primarily continental regions. The domains considered are shown in Tables 3.3, 3.4 and 3.5.

The latitudinal bounds used for the Eastern and Western Tropical Pacific, domains are as in Teng and Branstator (2011). The decision to split the tropical Pacific basin in eastern and western sections at the 150°W meridian is somewhat arbitrary, although it does correspond to the western bound of the region used to compute the Niño-3 index (Trenberth, 1997). The standard domains for Niño-1+2, Niño-3, Niño-3.4 and Niño-4 indices (as in, e.g. Trenberth and Hoar, 1996; Trenberth, 1997) are applied (see Table 3.5). The region for Niño-3.5 is defined as in Trenberth and Hoar (1996). The the North Pacific (NPa) and the North Atlantic (NAt) domains are the same as in Branstator and Teng (2010). The the North-West Pacific (NPI) region is defined to correspond to the domain over which PSL is averaged to obtain the North Pacific Index (Trenberth and Hurrell, 1994). Minobe (1997) refers to it as the "Central North Pacific".

Table 3.4: Domains of latitudinal bands considered in this study

		Domain Bounds	
Domain Name	**Abbreviated Form**	**South (°N)**	**North (°N)**
Global	Gl	-90	90
Southern Hemisphere	SH	-90	0
Northern Hemisphere	NH	0	90
Tropics	Tr	-23.5	23.5
Southern Midlatitudes	SML	-60	-30
Northern Midlatitudes	NML	30	60
Southern Polar Region	SP	-90	-66.5
Northern Polar Region	NP	66.5	90

Table 3.5: Other domains considered in this study

		Domain Bounds			
Domain Name	**Abbreviated Form**	**West (°E)**	**East (°E)**	**South (°N)**	**North (°N)**
Niño1+2	Niño1+2	-90	-80	-10	0
Niño3	Niño3	-150	-90	-5	5

Domain Name	Abbreviated Form	West (°E)	East (°E)	South (°N)	North (°N)
Niño3.4	Niño3.4	-170	120	-5	5
Niño3.5	Niño3.5	-180	-120	-10	5
Niño4	Niño4	160	-150	-5	5
North-West Pacific	NPI	160	-140	30	66
Southern Ocean	SO	-180	180	-70	-50

The relatively large region defined to cover the the Antarctic Circumpolar domain (ACC) is based on the following sources: Orsi et al. (1995); Moore et al. (1999); Sen Gupta et al. (2009); Allison et al. (2011) and Meijers et al. (2012). The domain also corresponds to the approximate latitudinal bounds used to compute the SAM PSL index (e.g., Gong and Wang, 1999; Marshall, 2003; Abram et al., 2014). The SO domain is the same as in Latif et al. (2013). The domain labelled "the region South of southern Africa (SSA)" was chosen to capture the region that showed the largest multicentennial change in SST during the period of rapid model drift (discussed in chapter 4). It is situated at the interface between the far south-eastern Atlantic Ocean and Southern Ocean.

The region used for the Southern Africa (SA) and Africa (Af) domains are loosely based on Kalognomou et al. (2013). The mid-latitudes are defined to correspond to the middle third of latitudes in the respective hemispheres.

3.6.3 Indices

Three other sets of CAM variable time-series are considered; these are referred to as "indices" and are listed in Table 3.6. Each index is computed as the difference between zonal or meridional means. For example, the SAM index for a variable v is computed as $\bar{v}_{-40} - \bar{v}_{-65}$, where $\bar{v}_l$ is the mean of v along the latitude l, over all meridians (as indicated by a "meridional extent" of 180°W to 180°E in Table 3.6). SAM definition is based on Gong and Wang (1999), NAO index on Li and Wang (2003) and the Southern Oscillation Index (SOI) on the conventionally used definition of Trenberth (1976).

Note that, strictly-speaking, each of these "indices" correspond to a set of indices—one for each variable for which they are computed (e.g. the SAM TAS index). Only one of these variables (generally PSL), however, is used in the computation of the commonly-used index upon which the index definition—as used here—is based.

Table 3.6: Indices used in this study. Two of the indices are differences in zonal means, over given meridional bands; the other is the difference in meridional means over a defined zonal extent.

		Meridional extent		Latitudes differenced	
Index Reference	**Abbreviated Form**	**West (°E)**	**East (°E)**	**Positive (°N)**	**Negative (°N)**
Southern Annular Mode	SAM	-180	180	-38	-66
North Atlantic Oscillation	NAO	-90	40	38	66

		Zonal extent		Longitudes differenced	
Index Reference	**Abbreviated Form**	**South (°N)**	**North (°N)**	**Positive (°E)**	**Negative (°E)**
Southern Oscillation	SOI	-20	-10	-150	130

3.6.4 Means and Anomalies

Time series considered are of deviations from what will be referred to as the long-term PDC mean, computed as follows. It was determined that after 400 model years model drift had reduced markedly (see chapter 4). Kay et al. (2014) also discarded the first 400 years of their control simulation as spin-up. Hence, the long-term mean value of each variable, over each domain/index (e.g for SAM PSL or ACC TAS), is computed in each PDC, between model years 400 and 992—the final year for which output was available for both PDCs. The means from the two PDCs are then arithmetically averaged to obtain the long-term mean value. Hence, if $\overline{v_{R,i}}$ is the mean of variable v over region R in PDC i:

$$\overline{v_{R,i}} = \frac{1}{992 - 400} \int_{400}^{992} v_{R,i}(t)\,\mathrm{d}t \tag{3.3}$$

where the discretised integral is evaluated using annual averages. If the CHPC Control is PDC 1 and the NERSC Control PDC 2, the corresponding long-term mean $\mu_{v,R}$ is given by:

$$\mu_{v,R} = \frac{1}{2}\left(\overline{v_{R,1}} + \overline{v_{R,2}}\right) \tag{3.4}$$

3.6.5 Wavelet Transforms

Wavelet transforms are performed, in a climate science context, to discern time-dependent patterns of variability (e.g., Torrence and Webster, 1998; Jevrejeva et al., 2003; Maraun and Kurths, 2004; Ujeneza and Abiodun, 2015). They can be viewed as generalisations of a Fourier spectral decomposition, which indicate time periods during which variability with a particular frequency (or equivalently, period) is more or less significant. Further, wavelet transforms allow the evolution of patterns of variability in time series that are not second-order stationary (i.e. have a non-constant temporal first derivative) to be assessed, in 2-D time-frequency space (Torrence and Compo, 1998; Rouyer et al., 2008b).

Morlet wavelet transforms (e.g., Torrence and Compo, 1998) are performed on PSL and radiative surface temperature (TS) variable time series for both PDCs, using all but the first model century of data. Wavelet transforms are implemented using the `R` (R Development Core Team, 2014) package `biwavelet`[3]. See section A.3 for more details.

The Morlet wavelet is complex-valued, implying superior capacity to identify oscillations (Torrence and Compo, 1998). Being a continuous wavelet makes it preferable to discrete wavelets for pattern identification (Grinsted et al., 2004). It is a popular choice as a "mother wavelet" (Cazelles et al., 2008), being a good compromise between localisation in the frequency and time dimensions (Grinsted et al., 2004).

Wavelet power spectra are locally tested against the null hypothesis that they result from an AR(1) time series. Significance is suggestive of greater variability, at a particular frequency, over a particular period, than would be expected from a process with some degree of "memory" of its immediately preceding state. A χ^2-statistics is used, with variable (in time and frequency) degrees of freedom, computed using the approach of Torrence and Compo (1998, section 5). Caution is required in interpreting regions (in time-frequency space) of significance thus produced, given that the computation of the test-statistic assumes a Gaussian distribution of variable values (Torrence and Compo, 1998; Grinsted et al., 2004). This is not always a valid assumption with series analysed here. Unless otherwise indicated, statistical significance is determined at the 5% level for wavelet results.

Towards the temporal boundaries of non-cyclic time series, edge effects play a significant role in determining local wavelet spectra (e.g., Torrence and Compo, 1998; Grinsted et al., 2004). This is especially significant in time series where the discontinuities introduced by merging the time series at the end points are large, as is the case with many of the series

[3]Avaiable for download at `http://biwavelet.r-forge.r-project.org/`

considered here, due to the secular trends introduced by model drift (see section 4.1). The subset of the time-frequency space in which such effects are deemed significant is named the cone of influence (COI). It is usually defined as the region in which the contribution of edge discontinuities to spectral power is greater than e^{-2} times that at the edge (Torrence and Compo, 1998; Grinsted et al., 2004). The COI is indicated on all wavelet figures presented here. Its width increases approximately linearly with period. Variability detected within the COI is likely spurious. The width of the COI also serves as a useful guide of the temporal width a region of significant variability should span to be considered likely to have identified a "real" process, as it approximates the decorrelation time of an isolated random disturbance in the time series at a given frequency (Torrence and Compo, 1998).

3.6.5.1 Wavelet Clustering

For PDCs, wavelet clustering is performed for a representative sample of regions and indices, for PSL, TS or both, considering all model years after year 100. The intention is to find groups of region-variable combinations whose patterns of variability are similar. The clustering is performed on the spectral power of the corresponding time series, normalised by their variance (σ^2), using the distance metric proposed in Rouyer et al. (2008a) and Rouyer et al. (2008b). The clustering method applied is Ward's minimum variance method (Ward, 1963), using the Lance-Williams algorithm (Lance and Williams, 1967).

3.6.5.2 Cross-Wavelets and Wavelet Coherence

For selected combinations of time series, cross-wavelets (Torrence and Compo, 1998; Grinsted et al., 2004) are computed and wavelet coherence (Torrence and Webster, 1998; Grinsted et al., 2004) determined. As in Grinsted et al. (2004), series are standardised (by subtracting the mean and dividing by σ) before the computations are performed. The purpose of applying these techniques is to determine when, how and to what extent time series covary and hence to uncover possible associations between regional modes of variability.

The cross-wavelet transform highlights regions of time-frequency space where two time series share high spectral power, while indicating the phase relationship between concurrent oscillations (Grinsted et al., 2004; Cazelles et al., 2008). Wavelet coherence indicates the degree to which oscillations are locally "phase-locked" (Grinsted et al., 2004; Cazelles et al., 2008). It does not require high spectral power in order to detect relationships between time series (Grinsted et al., 2004).

3.6.6 Frequentist Hypothesis Testing

To explore differences resulting from various approaches to quantifying climate as a probability distribution (see subsubsection 2.1.3.1 and subsection 2.1.5), frequentist hypothesis tests are conducted. To measure differences between distributions, the Kolmogorov-Smirnov (KS) D-statistic (Massey Jr., 1951; see also von Storch and Zwiers (1999, p.81) and Daron and Stainforth (2013)) is used. For two real-valued variables v and w, D is the maximum difference between the cumulative probability density functions of v and w, denoted by $F_v(x)$ and $F_w(x)$. Quantitatively:

$$D = \sup_{x \in \mathbb{R}} |\Pr[v \leq x] - \Pr[w \leq x]| \tag{3.5}$$

Significance values (p-values) for hypothesis tests, taking into account the large range of sample sizes considered in comparisons, are included where it is deemed appropriate. The D-statistic also has value, however, as an absolute measure of difference between probability distributions.

Student's t-tests (measuring differences in location) and Fisher's F-tests (for differences in spread) are also conducted. However, the assumptions of (a) normality (to which the F-statistic is particularly sensitive (Box, 1953; Sawilowsky and Blair, 1992)); and (b) independence of samples—especially when considering distributions of temporal ensemble member distributions—are highly likely to be violated significantly (due in part to autocorrelation) (e.g., von Storch and Zwiers, 1999, p. 114). Hence, these statistics are taken as a rough guide only.

3.6.7 Skewness Calculations

In this study, (sample) skewness (b_1) is defined—as is conventional (Burgers and Stephenson, 1999)—by the standardised third centred moment. For a discrete annual time series $\{X_i\}_1^n$ of length n, with mean $\bar{X} = \frac{\sum_1^n X_i}{n}$ the sample skewness b_1, is computed as follows:

$$b_1 = \frac{\sum_1^n (X_i - \bar{X})^3}{n s^{\frac{3}{2}}} \tag{3.6}$$

where s is the sample standard deviation.

Chapter 4

Present Day Control Run Evolution and Variability

This chapter consists of a presentation and discussion of results obtained from the CAM output of the PDCs. Results from the PIC are detailed in Appendix B. It should be noted that the "climates" of the two PDCs do not appear to differ significantly from one another at any stage during their concurrent integration. The names of the computing centres where the runs were conducted (CHPC and NERSC) are used only to distinguish between the PDCs.

The focus of this study is understanding the influence of ICs on ensemble evolution. It is essential, however, to give context to ensemble behaviour discussed in chapter 5 by exploring the evolving model climate. For example, the ensemble response to transient forcing is shown, in some cases, to depend on model drift (see subsection 5.2.2). It is also suggested that ensemble simulations can help to characterise and quantify regional-scale model drift. Regional within-ensemble behaviour is shown in section 5.1 to depend on the nature of variability exhibited by the model.

In section 4.1, PDC atmospheric time series are analysed to gain insight into the long-term temporal evolution of the model system climate. Two apparently distinct model drift behaviours are found:

1. an initial rapid adjustment;
2. followed by spatially variable, slow temperature increases, at a non-monotonic, but generally decreasing rate.

The latter remains prominent for at least 1200 model years. In between the two model drift regimes, there is a period of relatively stable global mean temperature.

The focus in section 4.2 is on evaluating the model's regional atmospheric variability,

thus addressing objective 4 (see subsection 1.5.3). Wavelet decompositions (see subsection 3.6.5) are used as the primary investigative tool. The model variability is shown to be dominated by its ENSO pattern and strongly associated NAO variability, except in the Southern Hemispheric extratropics. Here—and to a lesser extent over NPa—variability is characteristic of an essentially "red-noise" process, except during anomalous ENSO events of a particular type (see subsection 4.2.2). These factors are invoked in section 5.1 to explain important aspects of ensemble behaviour.

4.1 Pseudo-Steady States and Model Drift

The first 100 years of output is disregarded for all controls, as the model shows strong trends and weak internal variability for much of this time. This behaviour is indicative of an "initial transient", also called a "spin-up" period (as discussed by, for example, Shields et al. (2012) and Kirtman et al. (2012)). During the initial transient the ocean circulation is set in motion and rapid adjustments result (e.g., Small et al., 2014). This is illustrated in Figure 4.1 by global-mean (Gl) TS. Because model TS variability is much smaller over SML (and other domains of the Southern Hemispheric extratropics) the behaviour is more evident in SML TS. Tropical temperature variability is also initially very small (not shown), possibly because of the absence of developed ocean circulation.

Over most regions, the initial transient involves rapid increases in temperature for about 30 years ($\sim$1K·dec^{-1}). This is followed by a short pause and then a less rapid ($\sim$ 0.1K·dec^{-1}) temperature reduction, apparently in response to the initial "overshoot". These patterns are reflected in the Gl behaviour. The exceptions are the NAt and the Arctic (NP) domains, where the initial temperature appears to be too warm. Hence, the initial response involves a rapid temperature decrease. A period of relatively little temperature change follows, well before this occurs over the other domains. The period of most rapid subsequent temperature drift in the PDCs also occurs much earlier over NAt—it starts about 100 years earlier (compare SML and NAt TS in Figure 4.1).

It is hypothesised that most of the initial transient—and perhaps an important component of the subsequent drift—is a consequence primarily of: (a the ocean initially being at rest; and (b the too warm initial temperatures over the northern Atlantic basin and the Arctic Ocean. The newly initialised ocean circulation rapidly distributes this excess surface heat across the globe—especially to Southern Oceans. Subsequently, rapid cooling occurs over NAt and this colder, denser water sinks, before eventually being transported and resurfacing, cooling SSTs across the globe. This hypothesis is supported by the fact that the pattern of initial temperature response over SML and NPa is qualitatively similar in the PDCs and PIC, even though PIC SML TS after the spin-up is almost equal to its IC value.

Similar spin-up behaviour is observed in the Geophysical Fluid Dynamics Laboratory Climate Model version 2.5. Delworth et al. (2012) and Griffies et al. (2014) provide

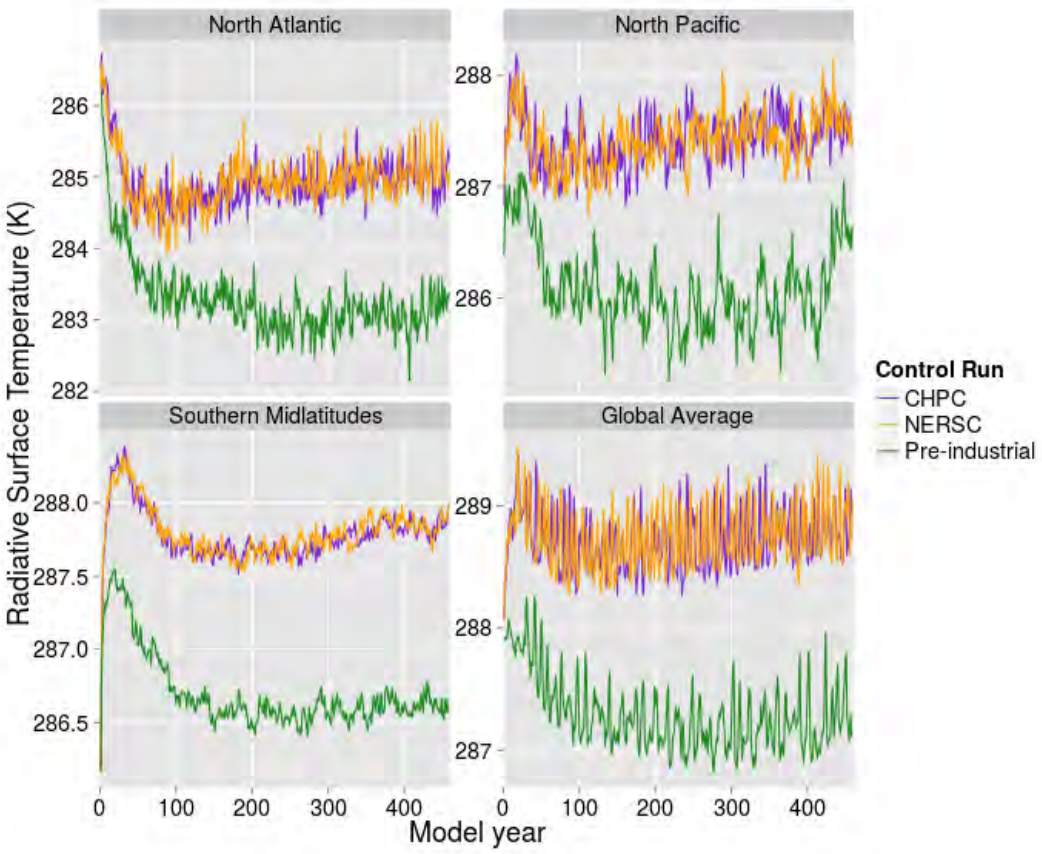

Figure 4.1: Time series plots of TS over the NAt, NPa, SML and Gl domains, for the PDCs and PIC, including the first 459 model years (the length of the PIC).

evidence that such a rapid initial shift in surface climate may be related to a lack of eddy resolving capacity in the ocean model, closely related to horizontal resolution. Subsequent large-scale secular changes are much slower and are regarded as different stages of transient adjustment to ICs and model drift.

A period of relatively little drift occurs in the PDCs, over most regions, approximately between model years 100 and 200 (earlier over the Northern Hemispheric extratropics), before larger trends reappear. The ensembles Yr126, Yr126_RCP, Yr186A and Yr186B are initialised from this model period.

After the initial transient and subsequent period of relative temperature stability, a new regime of model drift ensues in the PDCs. Over all domains studied, it is expressed, on multicentennial time scales, as a slowly decaying temperature increase. It is most prominent in SH. However, temperature changes tend to occur in "jumps" between multidecadal periods of apparent relative stability. This is illustrated by Figure 4.2, which shows the TAS evolution of PDCs and CFEs over SSA and NPa. The most rapid SSA TAS changes

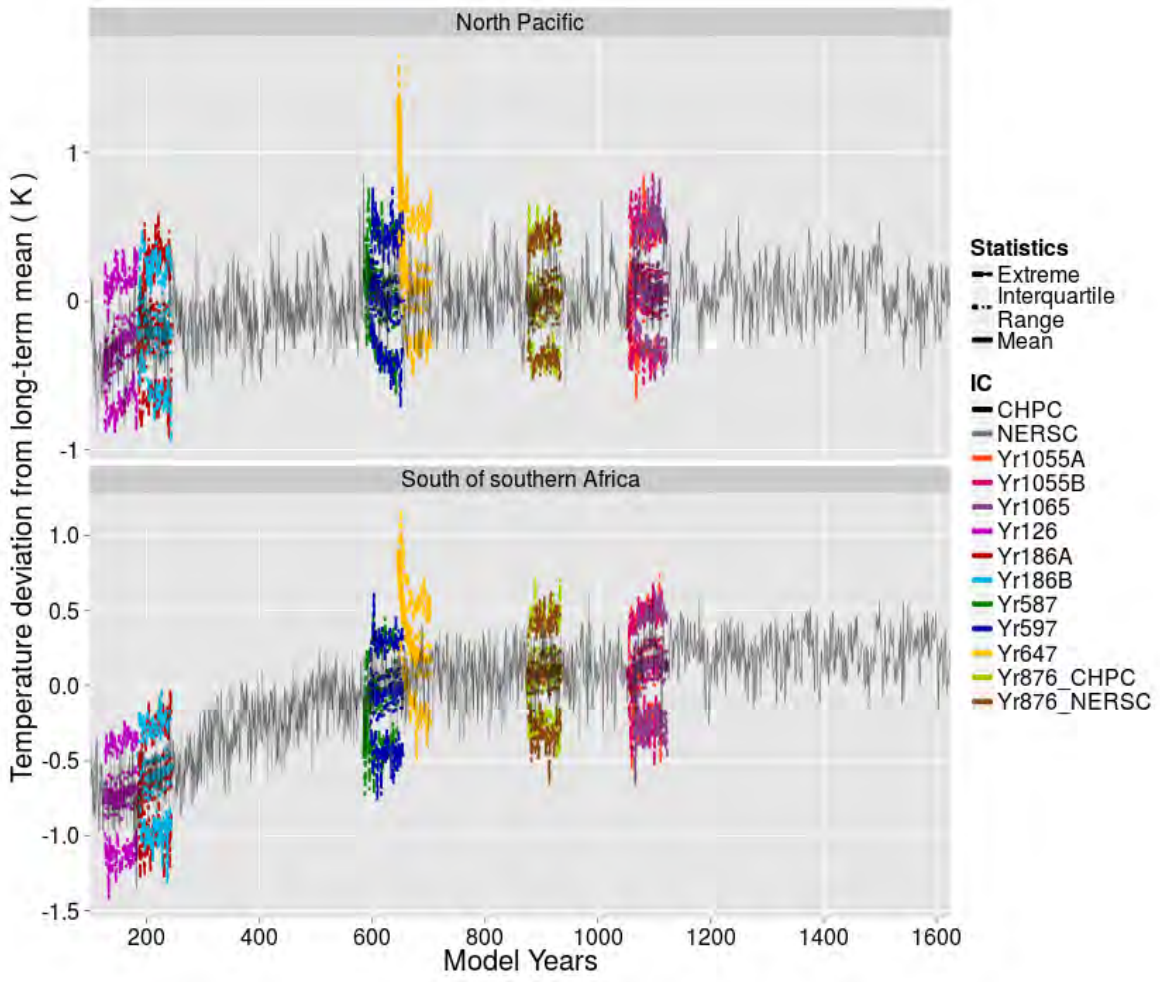

Figure 4.2: Time series of TAS from the PDCs, disregarding the initial transient, for SSA and NPa. The mean, interquartile range and minimum and maximum ensemble TAS values for each CFE are also plotted as a function of model time. Temperatures shown are relative to the long-term mean, computed as described in subsection 3.6.4. Note that the PDCs are depicted by darker (CHPC) and lighter (NERSC) grey lines.

appear to occur between approximately model years 250 and 350, 450 and 550, 800 and 875, and 1050 and 1150 (the last-mentioned in the CHPC Control only). The first of these periods also shows rapid trend in SML TS in Figure 4.1.

As a result of model drift, regional-mean variable time series used to compute long-term mean values (see subsection 3.6.4), are not stationary. Temperatures—especially—do not appear to settle at any stage during either PDC, although the CHPC Control does appear to show less trend in regional mean temperature after about model year 1200. However, it is not at all certain that this is an indications of a "steady state" being approached. A

much longer control run would be required to establish whether a stable model climate with negligible drift is ever established by the model configuration used.

As a consequence of such model drift, ensemble mean values do not necessarily tend to settle around zero, even when present day forcing is applied (see section 5.1); this is most apparent over the Southern Hemispheric extratropics. In particular, for the Yr126 ensemble, temperature anomalies are much more likely to be negative, as this run coincides to a model period prior to most of the (mostly increasing) temperature drift. The apparent lesser degree of drift and accompanying increased variability in the PIC is discussed in Appendix B.

The approximate state around which the PDCs appear to vary is similar between the two PDCs, over most domains considered (illustrated in Figure 4.1). This would appear to suggest that the mechanisms controlling model drift in the model are relatively insensitive to small perturbations. This is less true for TAS over NAt and NPa (see also Figure 4.2), regions where significant multidecadal to centennial temperature variability is at times detectable (see section 4.2). NAt TS variability in the PDCs appear to sometimes be approximately in phase with one another (for example, between model years 300 and 370), and at other times, approximately out of phase (for example, between model years 150 and 200). Similar behaviour is seen in NPa TS. Such changes in the phase relationship of the variability patterns suggest a strong random component to the internal variability, a theme explored further in subsection 5.1.2.

Temperature drift over the Southern Hemispheric extratropical domains (such as SSA TAS in Figure 4.2) appears to continue throughout the length of the PDCs. Increases in ensemble mean temperature, as a function of model time, confirm some degree of model drift continuing in all regions, until at least model year 1115—the final year of the Yr1065 ensemble. Additional support is given to the notion that model drift continues throughout the CHPC Control duration, by NAO and SAM TS indices (not shown). These track zonal temperature differences across the northern Atlantic basin and Southern Ocean, respectively. Both show negative temperature slopes, implying more rapid temperature increases at higher latitudes. A slow decreasing trend appears to continue after model year 1200, in both cases.

Patterns of drift tend to occur over NAt prior to other domains. TAS over NAt and—especially—NPa and NPI, not only do not show positive trend, but appear to exhibit a tendency towards decreasing TAS anomalies after model year 1500 (see NPa TAS in Figure 4.2). It is possible that reduced drift allows patterns of multidecadal to centennial variability to emerge, as also appears to occur in the PIC (see NPa TS in Figure 4.1 and further discussion in Appendix B). Results presented in section 4.2 show that over the northern Atlantic, multidecadal- to centennial-scale variability in NAO TS in the 1624-year CHPC Control, after about model year 900. No significant spectral power at these frequencies is detected either prior to model year 900 in the CHPC Control—when model drift was greater—or in the 992-year NERSC Control.

The results of this section highlight that regional-scale secular changes, presumably related to internal adjustment processes, can continue even when, on a global scale, temperatures have approximately stabilised.

4.2 Variability

4.2.1 Model ENSO

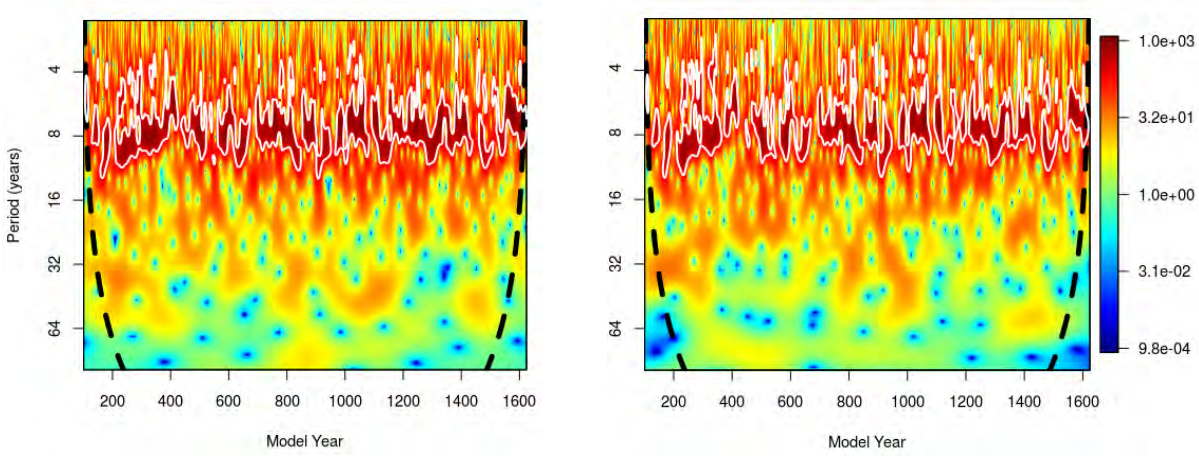

(a) Niño-4 TS

(b) SOI PSL

Figure 4.3: Plots of the normalised (by time series variance), bias-corrected (see section A.3) wavelet power spectra of annual-average quantities from the CHPC Control. The COI lies between the vertical edges and the thick black dashed lines. Regions where the spectral power is significantly different from a "red noise" process at the 5% level, according to the χ^2 test of Torrence and Compo (1998, Section 5), are delineated with thin white lines. See section 3.6 for domain bounds used.

Temporal variability of annual-mean CAM variables is dominated by periodicities of 6–9 years in both PDCs. This appears to be associated with the model's ENSO variability, as the spectral power over these frequencies is most continuous and prominent in TS (essentially SST in these cases) over the Niño domains (particularly Niño-4; see Figure 4.3a) and the SOI PSL index (see Figure 4.3b). This is illustrated by Figure 4.3, which shows wavelet power spectra for SOI PSL and Niño-4 TS from the CHPC Control.

Prominent, near-continuous variability in the same frequency range, in-phase with the SOI PSL index, is observed in the NAO PSL index. This relationship is apparent in both the SOI-NAO PSL wavelet coherence (Figure 4.4) and cross-wavelet transform (Figure 4.5), for both PDCs (one of each is shown). Teleconnections between ENSO and NAO are known to occur (see subsubsection 2.2.2.4), but here they are far stronger. ENSO-like

patterns also dominate temperature variability over the Eastern Tropical Pacific (ETP), the Western Tropical Pacific (WTP), the Tropics (Tr) and—presumably because of the spatial extent of these domains and the high ENSO amplitude—the global-mean.

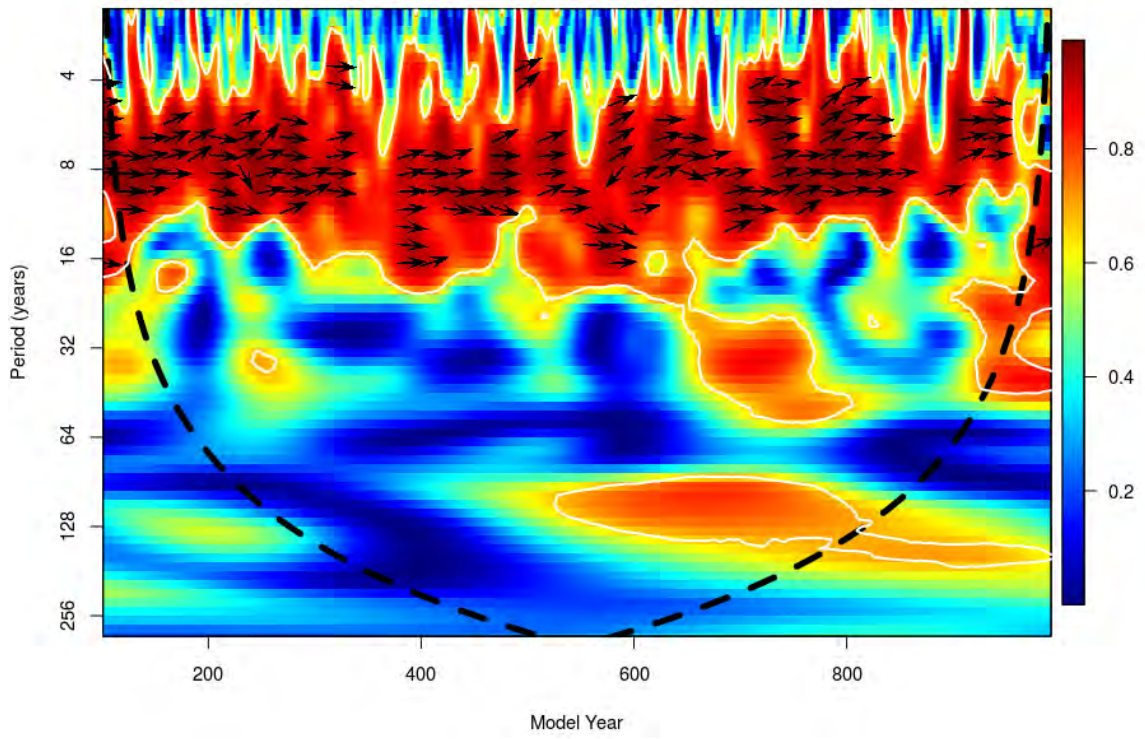

Figure 4.4: As in Figure 4.3, but for squared wavelet coherence between the SOI and NAO PSL indices, from the NERSC Control. Arrows, pointing in the direction of the angle of relative phase between SOI and NAO PSL, are drawn in regions of high coherence. Hence, right-pointing arrows indicate an in-phase relationship, left-pointing arrows imply that SOI and NAO PSL are anti-phase, downward-pointing arrows indicate that SOI PSL leads NAO PSL by a quarter cycle ($\frac{\pi}{2}$) and upward-pointing arrows that NAO PSL leads SOI PSL by a quarter cycle.

There appears to be a general decrease in ENSO period over the model duration in both PDCs (see Figure 4.3). This may be suggestive of a small state dependence of the model variability, even under fixed external forcing conditions. Differences between the PIC and PDC ENSO are discussed in Appendix B.

4.2.2 ENSO Asymmetry

Table 4.1 shows skewness (b_1) values from CHPC Control time series, computed over the last 1000 years of output, during which time comparatively little model drift occurred

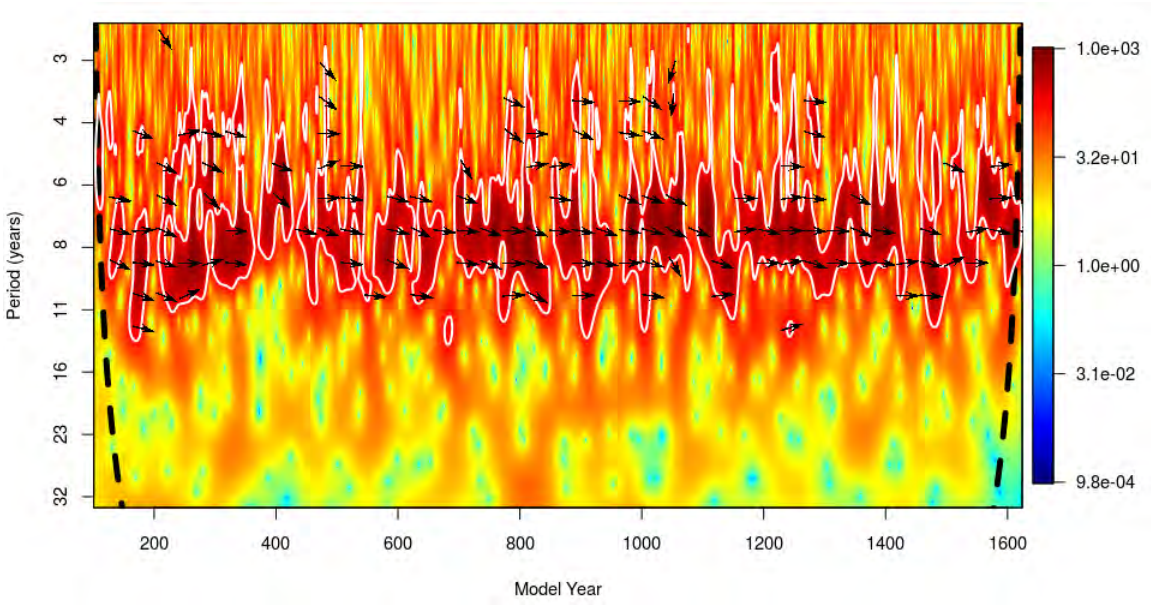

Figure 4.5: As in Figure 4.3, but for the normalised, bias-corrected cross-wavelet spectral power between the SOI and NAO PSL indices, from the CHPC Control. Arrows are used as in Figure 4.4, but are indicated in regions of high spectral power.

Variable	**Skewness**	**Variable**	**Skewness**	**Variable**	**Skewness**
ETP.TS	0.82	WTP.TS	-0.38	Niño-1+2.TS	0.92
SOI.PSL	-0.79	NPa.TS	0.18	Niño-3.TS	0.73
SAM.PSL	-0.34	SO.TS	0.08	Niño-3.4.TS	0.59
NAO.PSL	-0.40	NAt.TS	0.14	Niño-4.TS	0.19
NAO.TS	0.04	SP.TS	0.16	SP.PSL	0.15

Table 4.1: Table of skewness values for selected variable-region combinations from the CHPC Control, between model years 625 and 1624. Regions, abbreviated according to Tables 3.3–3.6, are indicated first, followed by a period, and then the variable name, abbreviated according to Table 3.2.

(see subsection 3.6.7 for details of how b_1 is computed and subsubsection 2.1.3.1 for a brief discussion of ENSO skewness documented in the literature). PDC temperature distributions over ETP are highly positively skewed. Time series of ETP TS and TAS show very large positive excursions from the long-term mean (see subsection 3.6.4) during periods of high ENSO variability, but little change in the magnitude of negative excursions between periods of higher and lower ENSO variability. This is illustrated in Figure 4.7, which shows ETP TS time series of the PDCs, with semi-transparent ensemble time series superimposed. All the eastern Pacific Niño TS indices also exhibit large positive skew.

There is associated large negative skewness in the SOI PSL index. The WTP temperature series are negatively skewed, but with much lower magnitudes of skewness.

The Niño-4 TS index exhibits much lower levels of positive skew than the other Niño TS indices. Niño-4 TS shows clear oscillations between El Niño and La Niña states, away from a near-central mean state, with indications of bimodality. This is illustrated in Figure 4.6, which shows ENSO TS index distributions for all CFEs. The SOI index in the figure shows a spatial *temperature* gradient (see subsection 3.6.2). Ensemble distributions closely approximate long-term PDC distributions (all b_1 values differ by less than 0.06) for these variables, as shown in Figure 4.7. A comparison between ENSO skewness values obtained in this study and the observations of Zhang and Sun (2014) is presented in section C.1.

The correlation between the different Niño TS indices in the PDCs are very high ($\rho > 0.9$) in all cases. For most model years, the largest anomalies (positive and negative) are found over the Niño-3.4 region. For a given Niño TS index, annual anomalies tend to be tightly clustered around a linear scaling of each of the other Niño indices. This is illustrated in Figure 4.8 for the case of the—spatially, and in terms of correlation—most different Niño TS indices: Niño-1+2 and Niño-4.

When comparing a more western Pacific Niño TS (such as Niño-4) to a more eastern Pacific Niño index (such as Niño-1+2), a second, much more sparsely populated, near-linear clustering of years can be identified. It is characterised by comparatively higher TS anomalies in the east (Figure 4.8). These years appear to represent a different type of model ENSO event, during which Niño-1+2 TS anomalies are predominantly near-normal (ENSO-neutral) or above normal (El Niño). Such events will be referred to here as "Eastern Pacific" or "EP" events. Quantitatively, they are identified as years when:

$$T_{N4}(t) - \left(2T_{N12}(t) - 0.28(T_{N12}(t))^2\right) < -0.75\text{K} \tag{4.1}$$

where $T_{N4}(t)$ and $T_{N12}(t)$ are respectively the annual-mean Niño-4 and Niño-1+2 TS anomalies during model year t. The quadratic term is included to account for the apparent plateauing of Niño-4 TS anomalies during particularly warm events, possibly because of physical processes imposing an upper bound on SSTs (e.g., Jin et al., 2003; An, 2009). The relatively uniform distribution across model centuries of EP events suggests that they are not simply a product of different speeds of model drift.

The total number of CHPC Control EP years between model year 101 and 1624 is 59 ($< 4\%$ of years). The longest sequence of EP years is 3 years. This occurs on 5 separate occasions. The number of such occurrences suggests that they are produced by distinct processes—at random, one would expect at most 2 such extended periods of relatively rare events to occur, even over 1524 years ($p < 0.01$). Autocorrelation is also unlikely to explain the propensity for consecutive EP years to occur, given that changes in Niño-1+2 TS values between two consecutive EP years are often much larger than the perpendicular "distance" between the two anomaly clusters (representing EP and non-EP years), in

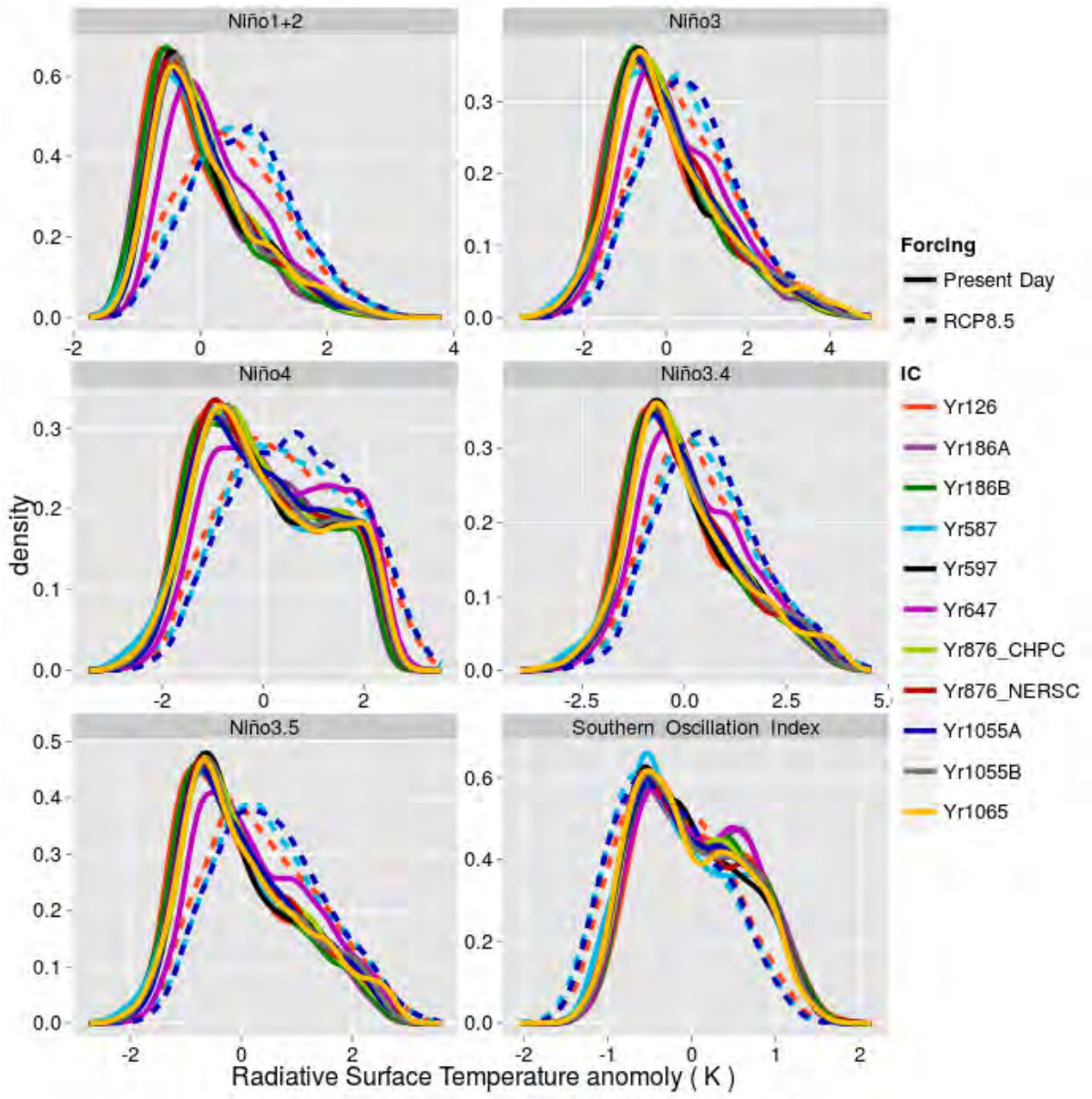

Figure 4.6: Plots of Gaussian kernel density estimates[1] of annual-mean TS, over all years and all ensemble members of each CFE and each TFE, for ENSO TS indices. See Tables 3.5 and 3.6 for details on the domains used. Each curve represents an estimate of the ensemble TS PDF over a particular domain, for a particular ensemble. For each ensemble, all 60 years of all 50 ensemble members are sampled, to give a total sample size of 3000 per ensemble (except in the case of Yr876_NERSC, for which 2962 years are considered, as explained in section 3.5). Ensembles are distinguished by the combination of external forcings applied and ICs used. Small perturbations to the atmospheric temperature fields were applied to differentiate ensemble members (see section 3.3).

[1] using the default `ggplot2` method (Wickham, 2009) in `R` (R Development Core Team, 2014)

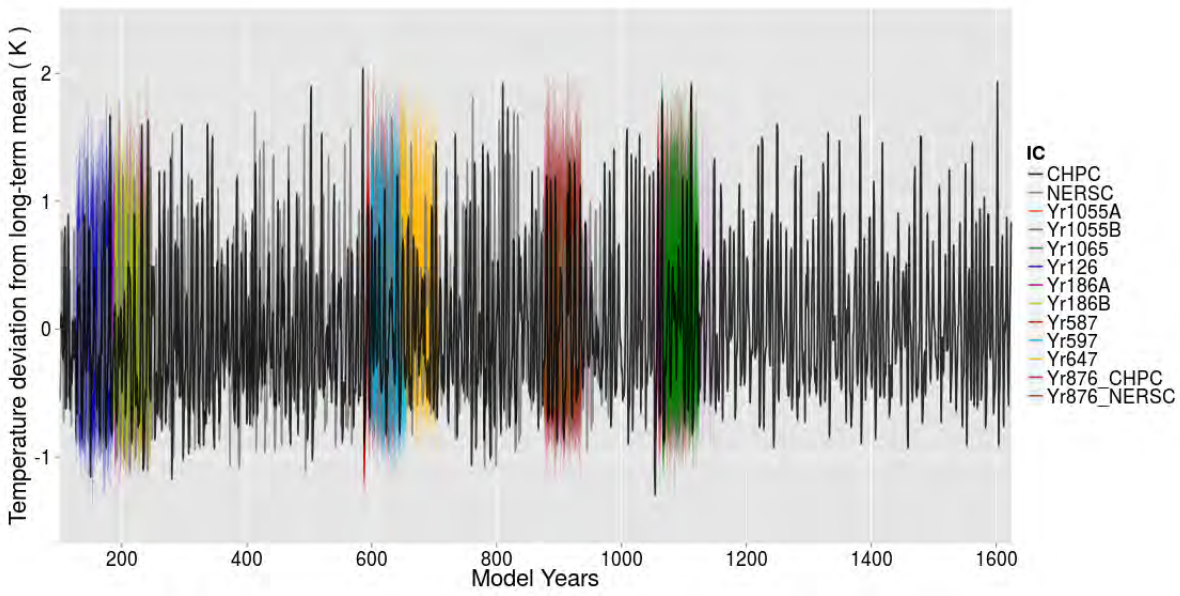

Figure 4.7: Time series of ETP TAS for all CFEs and the PDCs

Niño-1+2 TS-Niño-4 TS space. For example, model years 503 and 504 are EP years, but $T_{N12}(503) - T_{N12}(504) \approx 2\text{K}$.

One 3-year EP event occurs between model years 585 and 587, during which period ensembles Yr587 and Yr587_RCP were initialised. The large anomalies which prompted this decision (see subsubsection 3.5.3.1) appear to be closely related to occurrence of a particularly strong EP event (see Figure 4.8) over this period. See chapter 5 for an analysis of the behaviour observed with these ensembles.

Since the normal distribution is symmetric, lower magnitudes of skew are desirable for time series used for wavelet analysis. Accordingly, the Niño-4 TS index is used as the primary proxy for ENSO state and ENSO variability in the present study. Wavelet significance values obtained from highly skewed data should be treated with caution. Accordingly, the 30-year centred running variance of annual-mean Niño-4 TS is employed as a measure of the level of ENSO variability occurring in the PDCs, as a function of model year (see section C.1). It is shown that low-frequency ENSO modulations are related to NPa TS variability, especially in later model years.

4.2.3 Low-Frequency Variability

Low-frequency variability, with periodicities between 50 and 150 years, appears to become more prominent as model drift is reduced after about model year 1100 in the CHPC Control (see also the discussion in section 4.1). This change is most apparent in the

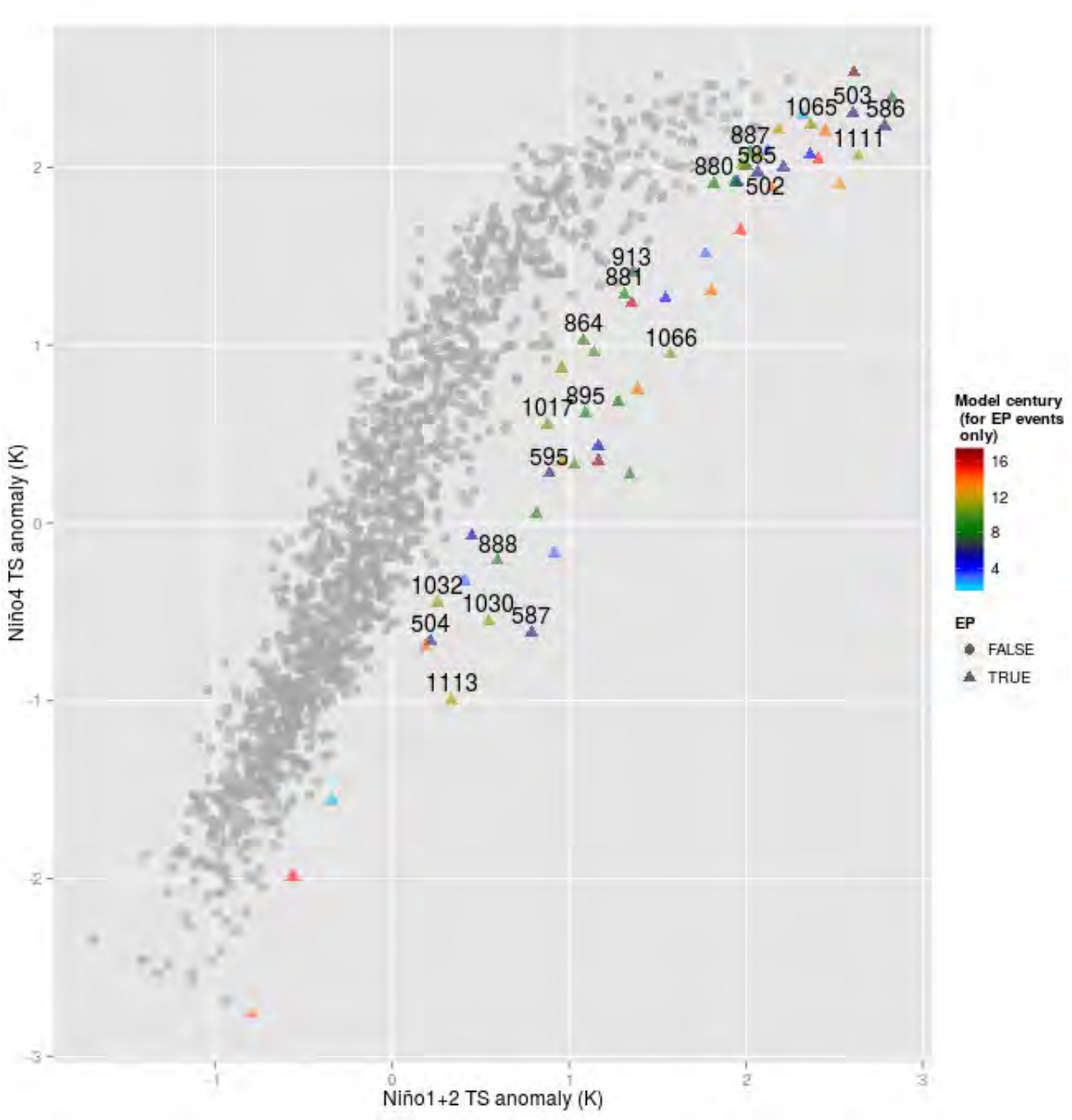

Figure 4.8: Scatter plot of Niño-4 TS against Niño-1+2 TS for the CHPC Control, indicating years with significantly higher than expected (from regression) TS anomalies in the eastern equatorial Pacific as "EP events" (i.e. EP = 'TRUE'; see Equation 4.1 for details). EP years falling between model years 501 and 649, 851 and 949, and 1001 and 1199 (selected to cover periods during which ensembles were run) are also labelled in the figure.

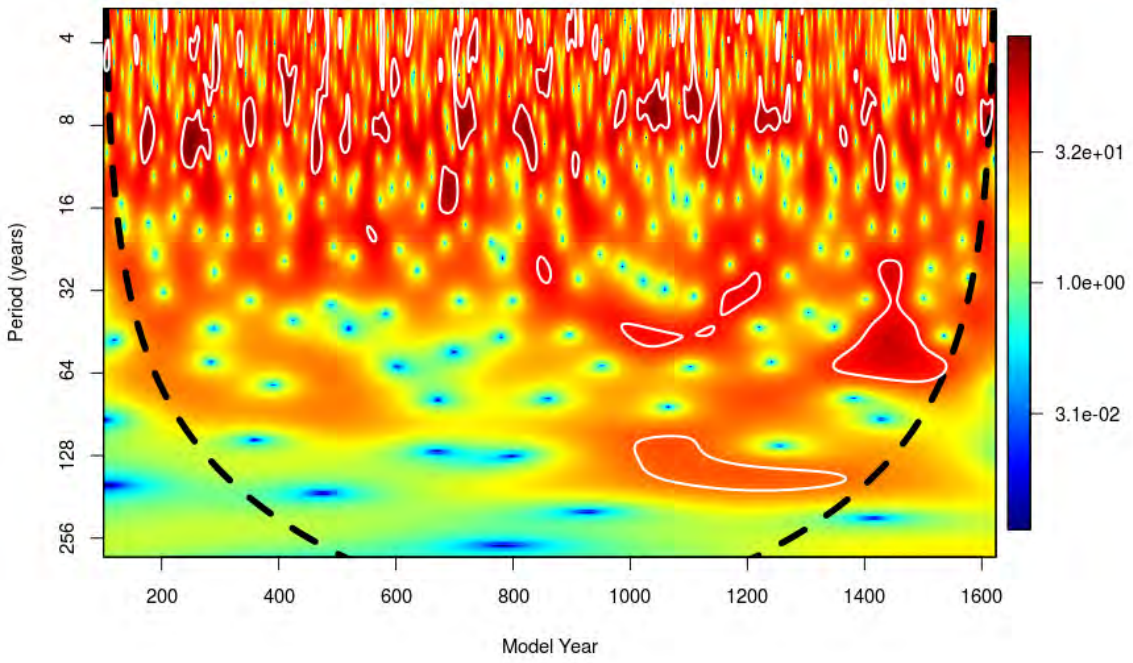

Figure 4.9: As in Figure 4.3, but for the NAO TS index, representing the zonal TS difference across the northern Atlantic basin.

NAO TS wavelet spectrum (Figure 4.9), which shows significant centennial wavelet power ($\frac{1}{150}\text{yr}^{-1} \leq \nu \leq \frac{1}{100}\text{yr}^{-1}$ in this case) for a duration of approximately 400 years, outside the COI. This may simply be a consequence of random fluctuations in the model variability. It may also be indicative of a relationship between model drift and patterns of long-term variability, in this case possibly related to the model AMOC. A longer PDC and investigation of POP2 dynamics would be required to test this hypothesis. Dynamically driven variability at such time scales could potentially lead to long-lasting, substantial IC influence.

4.2.4 Southern Hemispheric Variability

In general, the Southern Hemispheric extratropical regions are the only domains explored where variability is, during most years, essentially independent of the model ENSO and prominent Northern Hemispheric modes of variability (see also subsubsection 2.2.2.5). This is illustrated by the low coherence and generally random phase distribution seen in the wavelet coherence plot of SO against Niño-4 TS (Figure 4.10). However, approximately in-phase decadal variability does, at times, occur; for example, just prior to model year

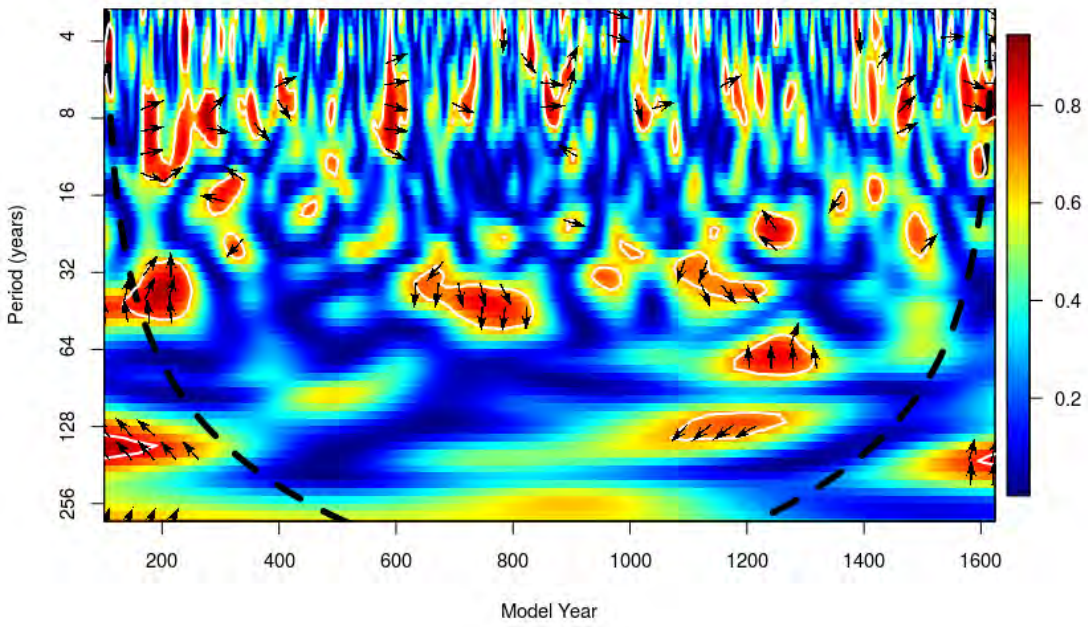

Figure 4.10: As in Figure 4.4, but for the squared wavelet coherence between SO TS and the Niño-4 TS index, from the CHPC Control.

600. Closer inspection reveals that these periods almost all correspond to EP events and that stronger EP events seem to produce greater coherence and cross-wavelet power (not shown). This would be suggestive of a teleconnection pattern co-occurring only with the EP-type ENSO events. This, in turn seems to lead to substantial IC influence (see subsection 5.1.2). Teleconnections to Southern Hemispheric extratropical variability are discussed further in section C.2.

It appears that, predominantly, variability in the Southern Hemispheric extratropics, in the present model configuration, is indistinguishable from red noise. This lends support to postulated Factors driving interannual-level IC influence in subsection 5.1.2.

4.2.5 Wavelet Clustering

Wavelet clustering (see subsubsection 3.6.5.1) performed on the two PDCs suggest similar groupings of variability. Colours in Figures 4.11 and 4.12 show variable-region combinations grouped into four clusters. One cluster (indicated in grey), whose members are identical for the two PDCs, appears to indicate variables most closely connected to ENSO variability. Clustering into two groups separates this cluster from the other considered variables. This

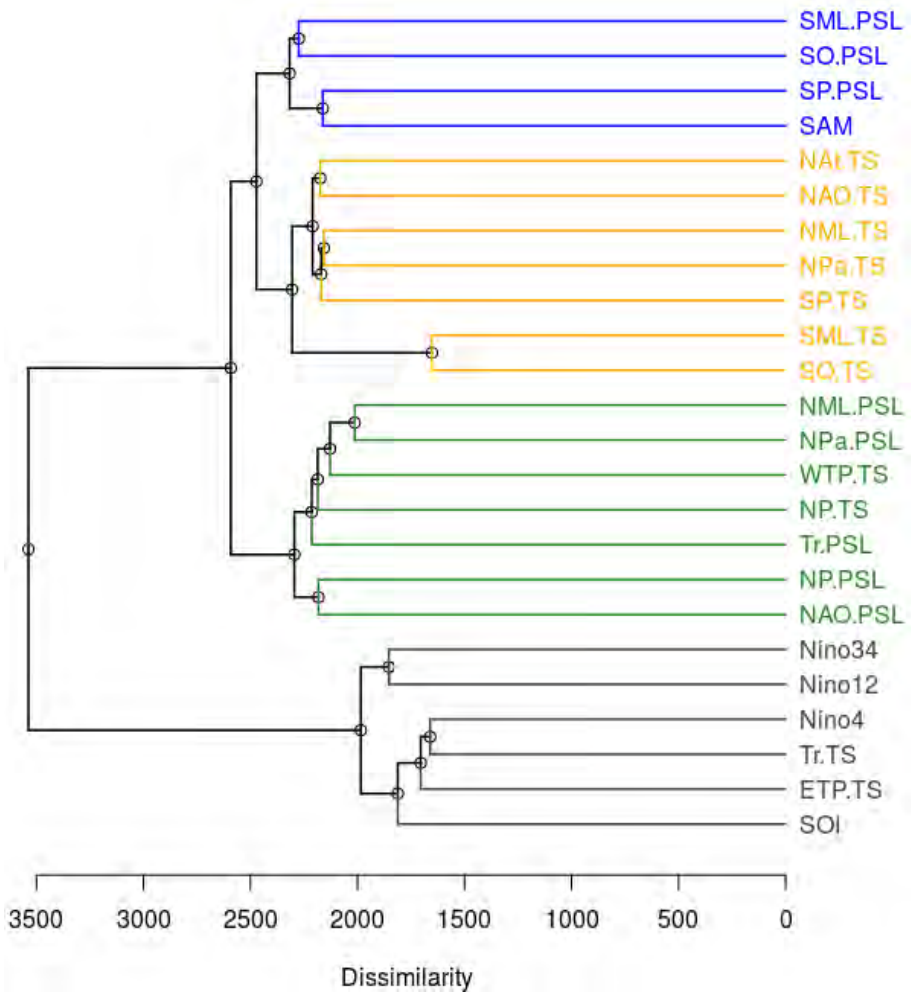

Figure 4.11: Wavelet clustering (see subsection 3.6.5) performed on a selection of 24 variable-region combinations (see Tables 3.2 to 3.6) from the CHPC Control CAM output. The distance metric of Rouyer et al. (2008a,b) is applied to wavelet power spectra, normalised by time series variance. Clustering is performed with Ward's Method.

supports the notion that ENSO represents the primary mode of variability of the model. The group includes regional TS variables and the SOI PSL index, which is in both PDCs closely related to Niño-4 TS, whereas the more skewed Niño-3.4 and Niño-1+2 TS indices (see Table 4.1), are closely associated. This similarity between ENSO indices justifies the use of a single index (Niño-4 TS) to characterise most attributes of the model ENSO.

Interestingly, WTP TS, is grouped not with ENSO variables, but in a cluster that includes the Northern Midlatitudes (NML) PSL, Tr PSL and NP TS. This cluster is—like the model ENSO—dominated by variability with periods of 6-11 years, but the variability is less continuous. Also, slightly stronger variability occurs on the interdecadal scale.

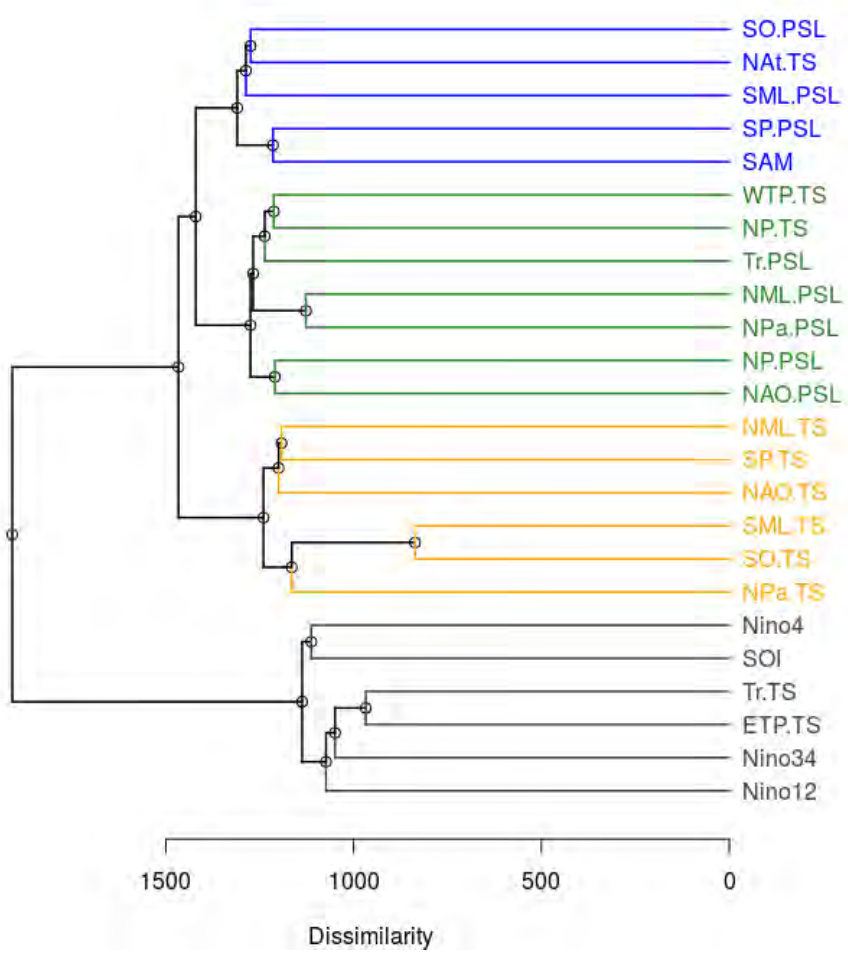

Figure 4.12: As in Figure 4.11, but for the NERSC Control.

Figures 4.4 and 4.5 show that the variability of this cluster is strongly linked to model ENSO variability.

Southern Hemispheric extratropical PSL variability forms a third cluster. Their wavelet spectra are characterised by:

- intermittent, irregular 6-11 year variability, seemingly related to EP events; and
- sporadic interdecadal and multidecadal ($\sim$ 15- and 30-year) peaks, with an apparent shift from the former to the latter over the run duration (see Figure C.4).

The fourth cluster is composed of extratropical TS series (from both hemispheres). Possibly, the relative influence of model drift on variability is in part responsible for this grouping; drift may also contribute to the (relatively minor) differences observed between the CHPC and NERSC clusters.

It will be shown in section 5.1 that the nature of ensemble behaviour is often similar among variables clustered together in this subsection.

Chapter 5

IC Ensembles and IC Influence

In this chapter, CFE (section 5.1) and TFE (section 5.2) results are presented, discussed and then compared in section 5.3.

The discussion in this chapter is focussed around the evolution of ensemble frequency distributions, potential predictability (to be referred to henceforth simply as "predictability"; see section 1.3) and ensemble member divergence.

5.1 Constant Forcing Ensemble Runs

In this section, results obtained from analysis of CFEs are presented. The focus is on investigating how ICs influence variable probability distributions of:

1. entire ensembles as they evolve over six decades (primarily in subsection 5.1.2); and
2. individual ensemble members, years and decades (subsection 5.1.3).

In subsection 5.1.4, the nature and rate of decay of the large perturbation produced by applying strongly imbalanced external forcing prior to the initialisation of Yr647, is discussed. Differences in ensemble behaviour between spatial domains are considered in subsection 5.1.1.

5.1.1 Regional Results

Figures 5.1 and 5.2 show TAS distributions for 8 latitudinal bands and 8 regions, respectively. Only the last 20 years of output is considered, because, by this stage of ensemble evolution, CFE distributions for different years of the same ensemble, over the same

domain, are generally insignificantly different from one another, as determined from KS, Student's t (t) and Fisher (F) tests (see subsection 3.6.6). TFE distributions are also shown, but primary discussion of TFE distributions is deferred to section 5.2.

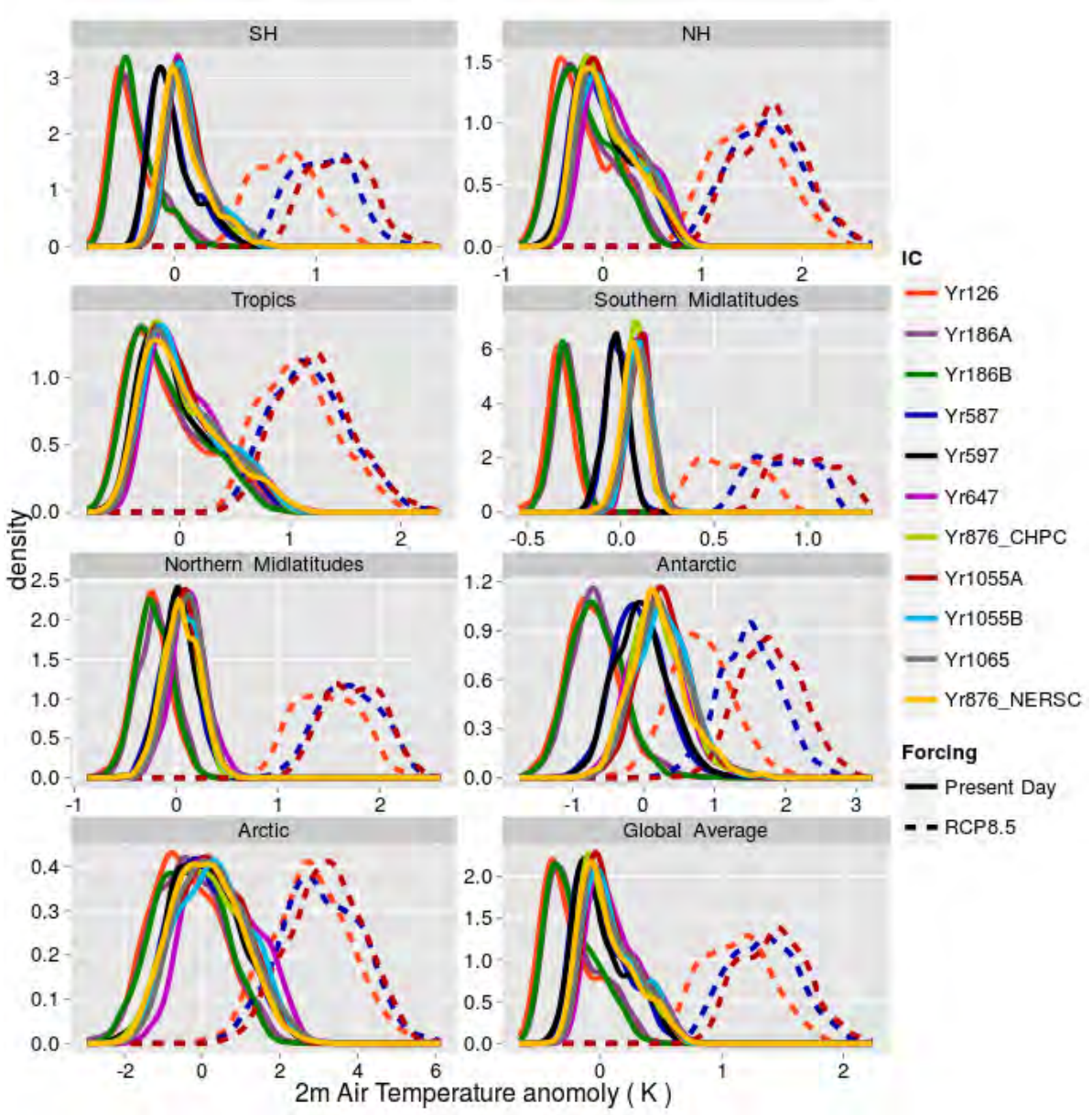

Figure 5.1: As in Figure 4.6, but showing TAS, considering only the last 20 years of each ensemble (the 5$^{\text{th}}$ and 6$^{\text{th}}$ ensemble decades) and showing "latitudinal band" domains; see Table 3.4 for details.

It would appear that, under fixed external forcing conditions, over a given range of model years (see section 3.3), there is a tendency for atmospheric variable PDFs of

different ensembles to converge towards a single "climatic" distribution. This is illustrated in Figures 4.2 and 4.7. Presumably this distribution is what one attempts to capture as a "variable climatology".

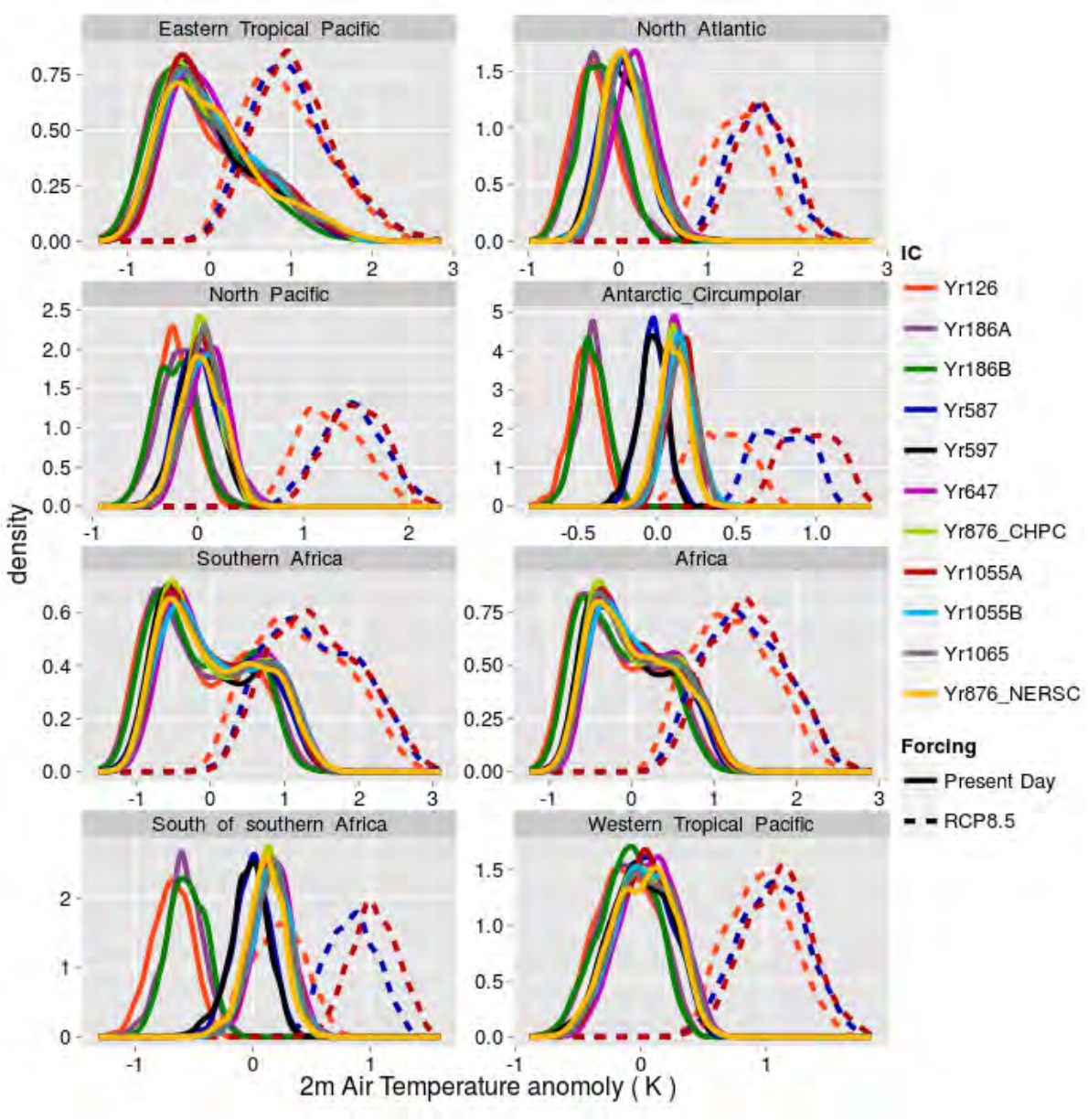

Figure 5.2: As in Figure 5.1, but for the regional domains; see Table 3.3 for the domain bounds used.

The mean value of the climatological distribution for a time-dependent model system variable $v(t)$, will be denoted by $v_p(t)$ (the variable's preferred state), where t is model time in years. Unless otherwise indicated, $v_p(t)$ is understood to be the steady state under

present day forcing conditions. The PDF of v will be denoted by f_v. Its cumulative density function (CDF) will be denoted by F_v. The dependence of these distributions on t will be made explicit by referring to $(f_v(t))(v)$ and $(F_v(t))(v)$, respectively. Because the width and shape of variable distributions tend to change little as a function of model year (under constant forcing), the evolution of $v_p(t)$ usually characterises changes in $F_v(t)$ sufficiently.

In the context of $v_p(t)$, t is approximate; $v_p(t)$ and $f_v(t)$ should be thought of as values for a period of time around model year t. It is essentially assumed that $t_1 - t_2 \lesssim 50 \Rightarrow f_v(t_1) \approx f_v(t_2)$. For example, if the spatial mean time series of TAS over a given region is denoted by $T(t)$, then the mean value of the preferred state distribution of T during roughly the 7^{th} model century (model years 601-700) would be denoted by $T_p(650)$. The corresponding distribution of T would be denoted as $(f_T(650))$. It should be noted that these are functions of T, so that, for example $(F_T(650))(T_0)$ would represent the the probability of the event $T < T_0$ occurring during a given year in the 7^{th} model century. In quantifying variable climatologies thus, an ensemble-temporal definition of climate (see subsubsection 2.1.3.2 and subsubsection 2.1.5.1) is being applied. The tendency of variable distributions to converge towards an apparent preferred state distribution is discussed at greater length in section 5.3.

5.1.2 Levels of IC Influence

In this section different types of IC influence are considered. One way to conceptualise differences in IC influence scale is in terms of the characteristic time scales of decay of corresponding IC perturbations (see also section 1.3 and subsubsection 2.2.3.3). In other words, after how long a model integration time Δt does particular knowledge about the location of the model trajectory in its state space at model time t_0, no longer provide meaningful knowledge about the model system state at $t_0 + \Delta t$?

The smallest scale of perturbations considered in this study—changes to atmospheric variable fields only slightly larger than round-off error (see Equation 3.1)—decay within a couple of days. Round-off error necessarily occurs at every time step and, subsequently, grow rapidly. Hence, the effects of round-off errors and IC perturbations of this kind are almost immediately indistinguishable, implying that knowledge of the exact perturbation introduced has no predictive value.

Larger perturbations (up to $\sim$ 30K) to the atmospheric temperature fields usually decay on weather time scales—i.e. within a month (not shown). However, this is not always the case. In Figure 5.3 it is shown that, initially, some members of Yr1055B—which was produced by perturbing atmospheric temperature ICs according to Equation 3.2—have much higher global mean temperatures than the other members of Yr1055B and ensemble Yr1055A—which was produced by perturbing atmospheric temperature ICs according to Equation 3.1. These anomalous members are Run29, Run30, Run33 and Run35; to a lesser degree this also applies to Run31, Run32 and Run34. The temperature series of

the four most anomalous members are distinguishable from the rest of the ensemble until ensemble year 3 or 4. It is notable that all 7 anomalous members had IC perturbations between $a_{29} = 0.1364$ and $a_{35} = 0.146$ (see Equation 3.2) applied to the atmospheric temperature; larger perturbations (up to $a_{50} = 0.17$) did not result in unusually anomalous atmospheric variable time series. It is also noteworthy that all anomalously behaving ensemble members were warmer than the members of Yr1055A. This is possibly due to the unusually cold ICs present at initialisation (see subsubsection 3.5.3.1).

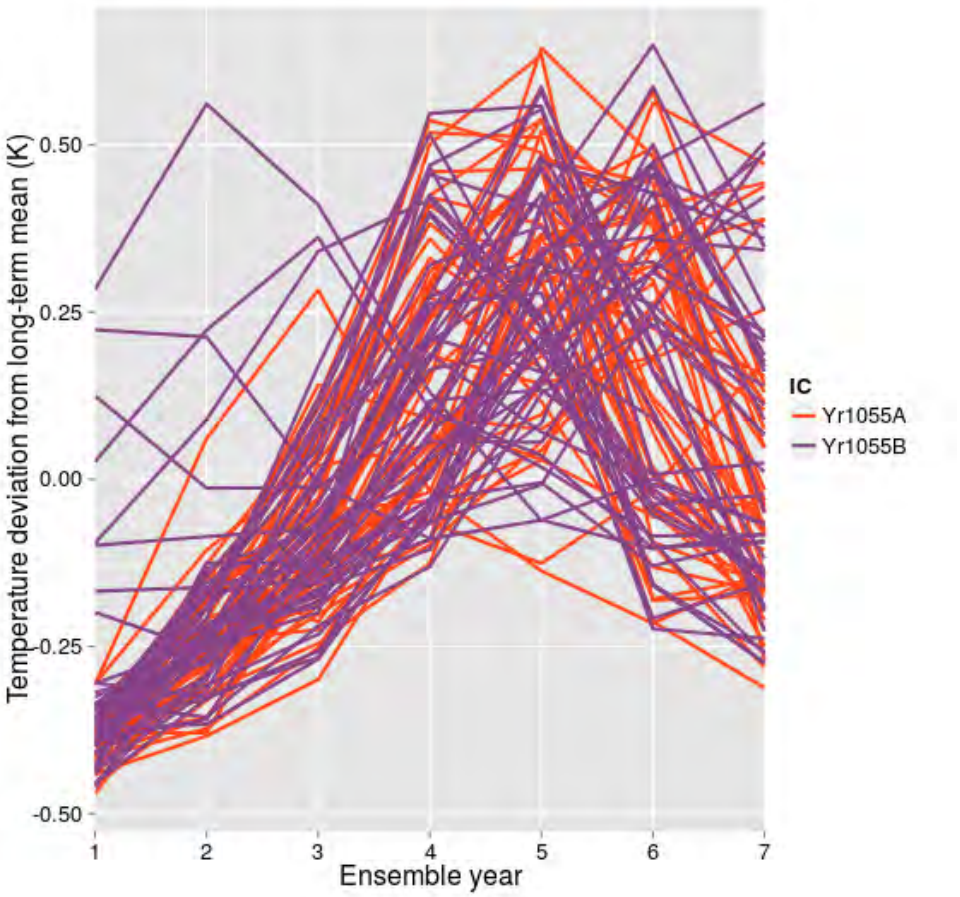

Figure 5.3: Gl TAS ensemble time series for Yr1055A and Yr1055B over the first 7 ensemble years

Although the distinction between the seven anomalous members is prominent in Gl, the difference is barely detectable over the Southern Hemispheric extratropics and is most apparent in the Northern Hemispheric extratropics (not shown). As noted, Yr1055 ICs were particularly cold, especially over NP. Furthermore, the ensemble was initialised during the boreal winter. In those ensemble members exhibiting anomalous behaviour, it is possible that atmospheric IC perturbations were sufficient to result in ice melt, thus destroying the "memory" of model system state captured by the Arctic sea ice. Testing

this hypothesis would require further analysis and perhaps additional ensembles with larger perturbations.

Atmospheric variable distributions across Yr1055B—disregarding the seven anomalous members—are indistinguishable from equivalent ensembles over Yr1055A, within a month. This implies that after a month, in these cases, knowledge of the size of the atmospheric perturbation applied is no longer predictively useful; the observed trajectory could as well have resulted from a much smaller perturbation. This behaviour is consistent with well-established findings by Lorenz (1965, 1969a,b, 1982, see also subsubsection 2.1.3.2).

The IC influence of IC differences that decay within a month are clearly "microscopic", in the sense that the term is used by Stainforth et al. (2007a). A model trajectory with a particular microscopic IC perturbation imposed might better approximate, in some sense, the "true" climatic trajectory, than model trajectories with other microscopic IC perturbations imposed. However, no finite improvement in knowledge of "true" microscopic state of the system would allow one determine, beforehand, which microscopic IC perturbations would provide more accurate information about the evolution of the true climatic trajectory. In the context of climate investigation, therefore, microscopic IC influence is reflected in within-ensemble differences. The extent to which IC ensembles are required to quantify this influence in this model configuration is explored in subsection 5.1.3.

In this study, larger scales of IC influence are investigated using ensembles with ICs for all climate system components from a particular model year (see subsection 3.5.3). The influence of ICs from nearby years—to be referred to as "interannual-scale IC influence"—is considered first. This influence is found to generally take the form of a difference between the ensemble PDF and $f_v(t)$ (see subsection 5.1.1). This involves both differences in the location and spread of the ensemble distributions and, at times, differences in their "shape". It is thus closely associated with decadal climate predictability (see subsubsection 2.2.2.4).

CFE member variable evolution, for selected variables, ensembles and regions is depicted in Figures 5.4–5.7. Interannual-scale IC variability is discussed primarily in reference to these figures. Corresponding PDC state over the ensemble period is also shown. The initial difference between the PDC and ensemble members is of round-off error-order. Its behaviour can therefore be thought of as that of an example ensemble member.

The extent of interannual-scale IC influence is highly dependent on the year of initialisation. Differences between ensemble PDFs and the corresponding $f_v(t)$ are generally much larger for Yr587 and Yr1065 variables than other variables. Considerable regional variation is also observed. Interannual-scale IC influence is most pronounced over the first decade of ensemble output (as illustrated, for example, in Figure 5.10), but may extend for as long as three decades in some regions. More extended influence is confined to distributional location (measured here by ensemble mean) as has previously been found in decadal predictability studies (see subsubsection 2.2.2.4). Extended IC influence is seen in Yr587 ACC, NPa and NPI TS ensemble member time series, depicted in Figure 5.4.

It is postulated that interannual-scale IC influence is related primarily to two factors:

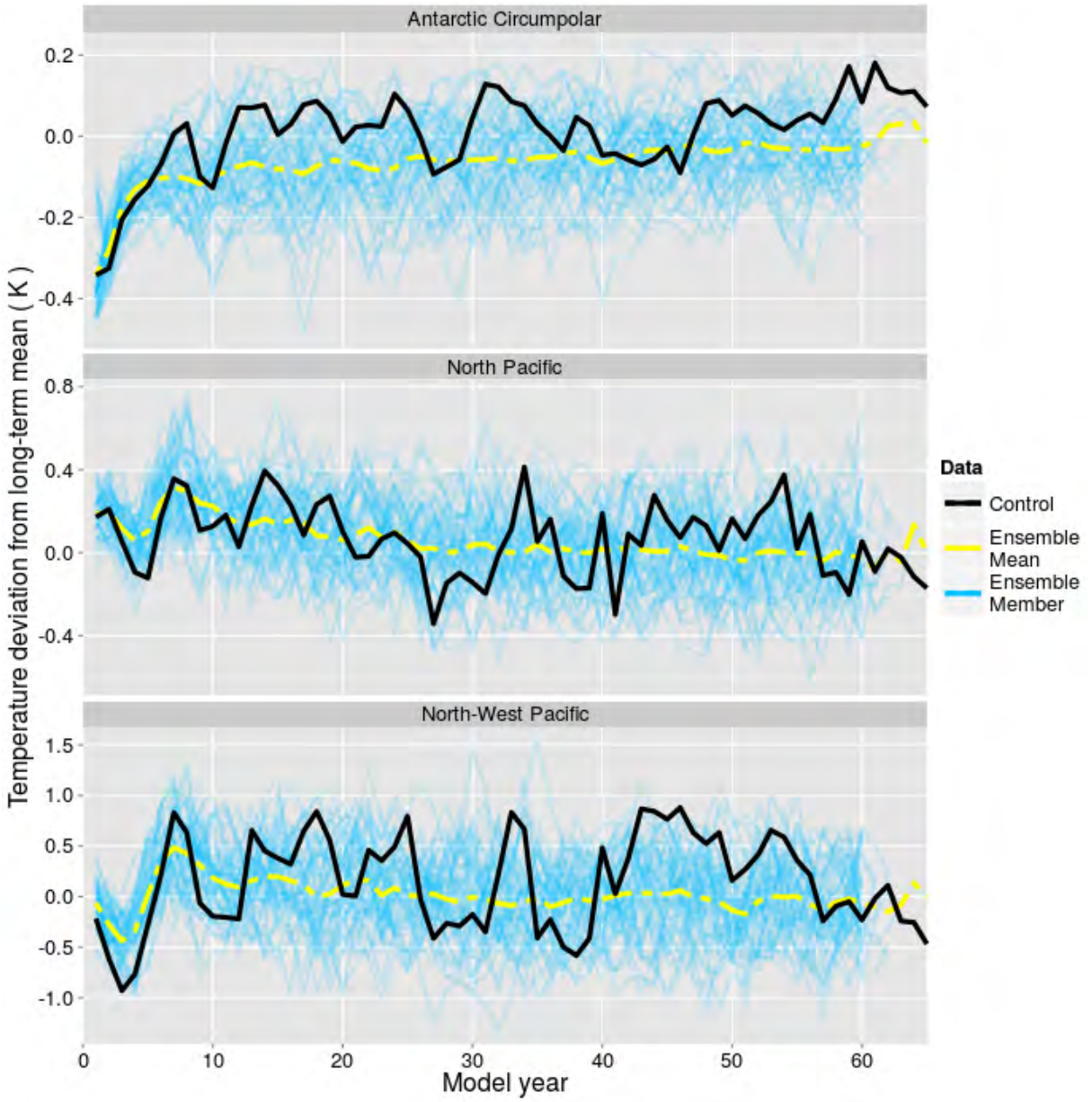

Figure 5.4: Time series of Yr587 TS over ACC, NPa and NPI. The "Control" shown is the CHPC Control, from which Yr587 was initialised. See section 3.6 for domain bounds used.

Factors

(F1) Evolution of interannual- to interdecadal-scale quasi-oscillatory modes of variability (such as ENSO or NAO; see also subsubsection 2.2.2.1), dictated by their phases at the time of initialisation; and

(F2) "Memory" of earlier system states, resulting in high autocorrelation and aperiodic variability, potentially due to thermal inertia of the oceans, and possibly associated with long-term persistence (see subsubsection 2.1.4.4 and subsubsection 2.2.2.5).

There may be a case for regarding these two phenomena as responsible for distinct levels of IC influence. Both Factors can contribute to decadal and multidecadal predictability. Under the influence of (F1), probabilities of particular modes of variability may be significantly enhanced. This is, in turn, reflected as a near-sinusoidal oscillation, with modulated amplitude, in the ensemble mean. Ensemble spread around this preferred mode may be reduced relative to climatology. These tendencies are illustrated by NAO PSL during the first two decades of ensemble Yr587 in Figure 5.5. Under the influence of (F2), a gradual decay of perturbed fields is likely, as, for example, for ACC TS in Figure 5.4.

In the present model configuration, (F1) is associated primarily with the model ENSO (see subsection 4.2.1). Its IC influence is evident especially over ETP and the central Pacific Niño index domains, but also across the tropics, subtropics, northern Atlantic and in the global mean. In some ENSO-related ensemble time series, the oscillation in the mean can maintain an amplitude of greater than 10% of the ensemble spread for most of the ensemble duration (60 years). This is reflected in the behaviour of numerous variables (especially temperature, wind, vertically integrated cloud cover (CLD) and PSL) across the tropical Pacific (see Niño-3.4 PSL in Figures 5.5 and 5.6.

How much (F1) influences ensemble behaviour over the Niño domains and—particularly—the NAO PSL index, is greatly dependent on the ICs used. Compare, for example, ensemble time series of Yr587 with Yr876_CHPC NAO PSL in Figure 5.5. This concurs with results of Tang and Deng (2010), suggesting interdecadal variability in the predictability of ENSO, related to the degree of nonlinearity in the system dynamics. Previous evidence of state dependence of IC influence is discussed in subsubsection 2.2.2.4.

It is postulated that the observed differences in predictability between ensembles may be due—at least in part—to quasi-oscillatory modes (such as the model ENSO and NAO) being driven by feedback processes acting on different time scales. The precursors of these processes are present in the ICs to varying degrees. For example, extreme ENSO anomalies often occur during ENSO EP events, such as at the initialisation of ensembles Yr587 and Yr1065 (see subsection 4.2.2 and Figure 4.8). These events are likely to result in unstable climate states which may set in motion processes acting to dampen them. This could explain the narrower spread in variable states observed over the tropical domains and the NAO PSL index for these ensembles (see Figure 5.5 and Figure 5.6).

The influence of (F1) is most often particularly prominent in the first two decades (2-3 cycles of the oscillation), before decaying in amplitude in the middle decades and then recovering somewhat towards the end. This is best illustrated by Yr587 NAO PSL in Figure 5.5. It is possible that this modulation of amplitude—which occurs in a number of ensembles—may be indicative of a weaker, longer-period oscillation which influences the propensity of the model to assume a particular mode of an oscillation. In observational

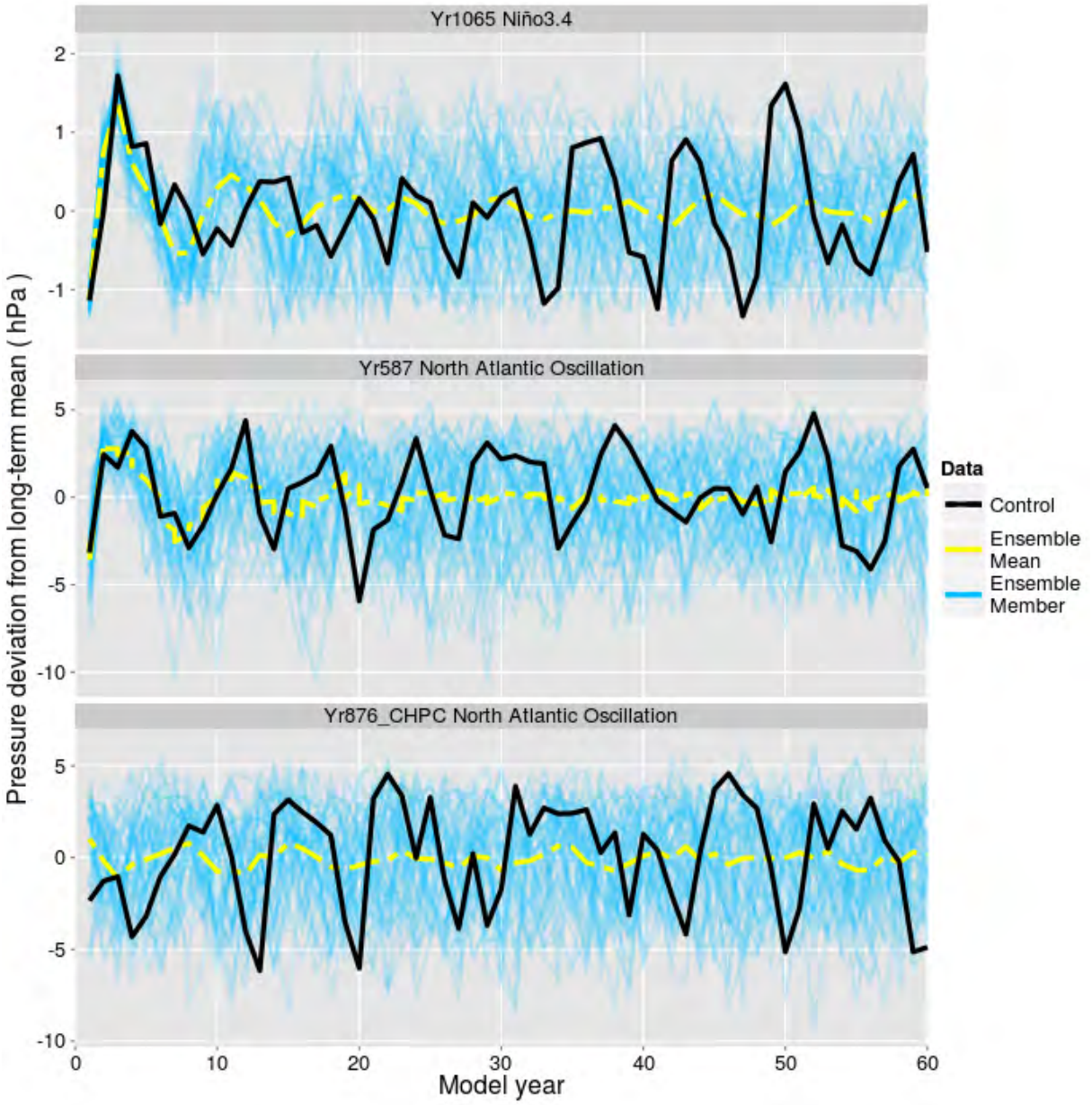

Figure 5.5: As in Figure 5.4, but for PSL and showing Yr1065 Niño-3.4 and Yr587 and Yr876_CHPC NAO, as indicated.

and theoretical studies, decadal and interdecadal variability has been observed in ENSO amplitude (see subsubsection 2.1.4.4). These have been associated with modes of variability acting predominantly in the northern Pacific. Similar results are also found in this study (see section C.1).

As discussed in subsubsection 2.1.4.4, PDV in the real climate system has both

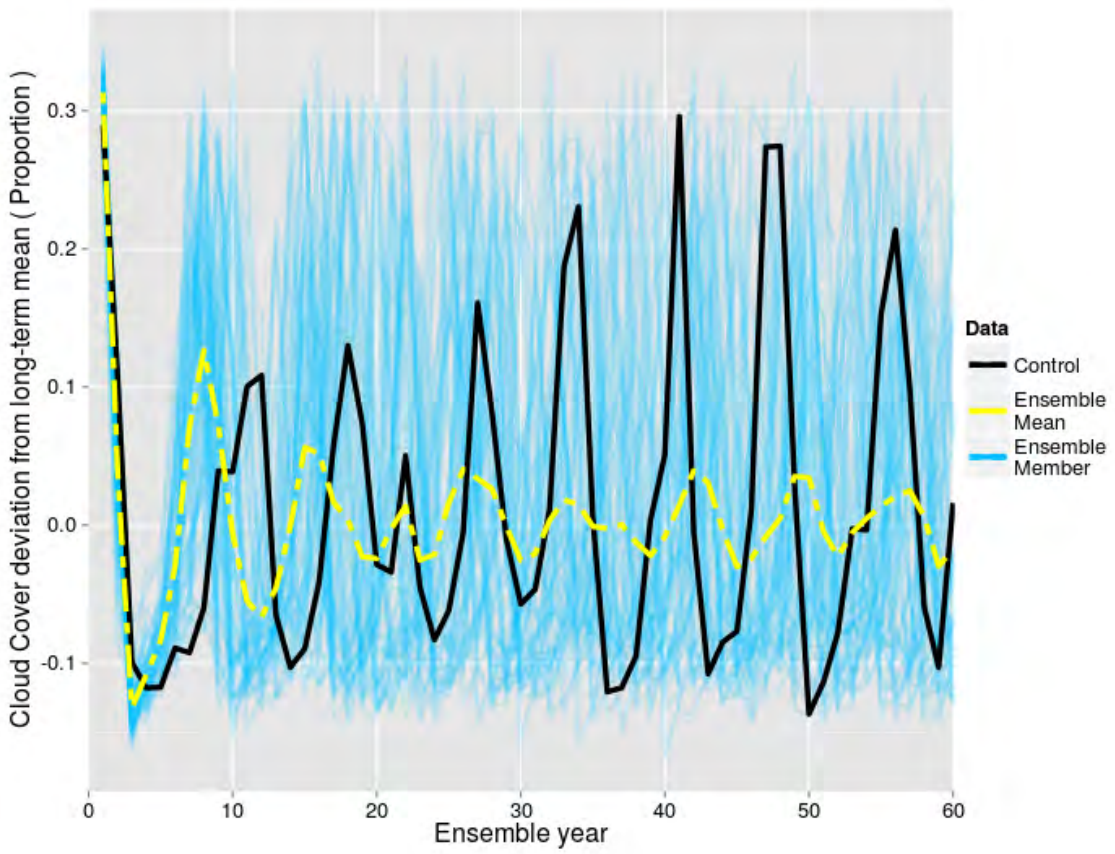

Figure 5.6: As in Figure 5.4, but for CLD for Ensemble Yr1065 over the Niño-4 index domain.

important quasi-periodic and aperiodic components. In this study, ensemble time series of temperature for NPI and NPa often initially appear to have a preferred behaviour, which is reflected in reduced model spread and largely similar trend patterns. These sometimes involve starting near $T_p(t_E)$ (where t_E is the approximate model time for the ensemble) and then evolving away from $T_p(t_E)$. Thereafter, however, the oscillatory behaviour appears to be approximately critically damped, with very little overshoot, as the ensemble distribution slowly evolves back towards $f_T(t)$. There do appear to be times when relatively abrupt changes in the probabilities of large positive and negative anomalies occur, as at approximately ensemble years 30 and 45 for Yr186B (see NPI TS in Figure 5.7). As discussed at greater length in subsection 5.1.3, the length of time for which individual ensemble members maintain an initial anomaly of a given sign varies greatly, implying that temporal distributions of individual members may differ significantly.

The Southern Hemisphere midlatitude domains are almost entirely covered by ocean. Much of it has an unusually deep mixed layer and shows signs of active deep convection (Orsi et al., 1995, also observed in the present model, but not shown). The temperature

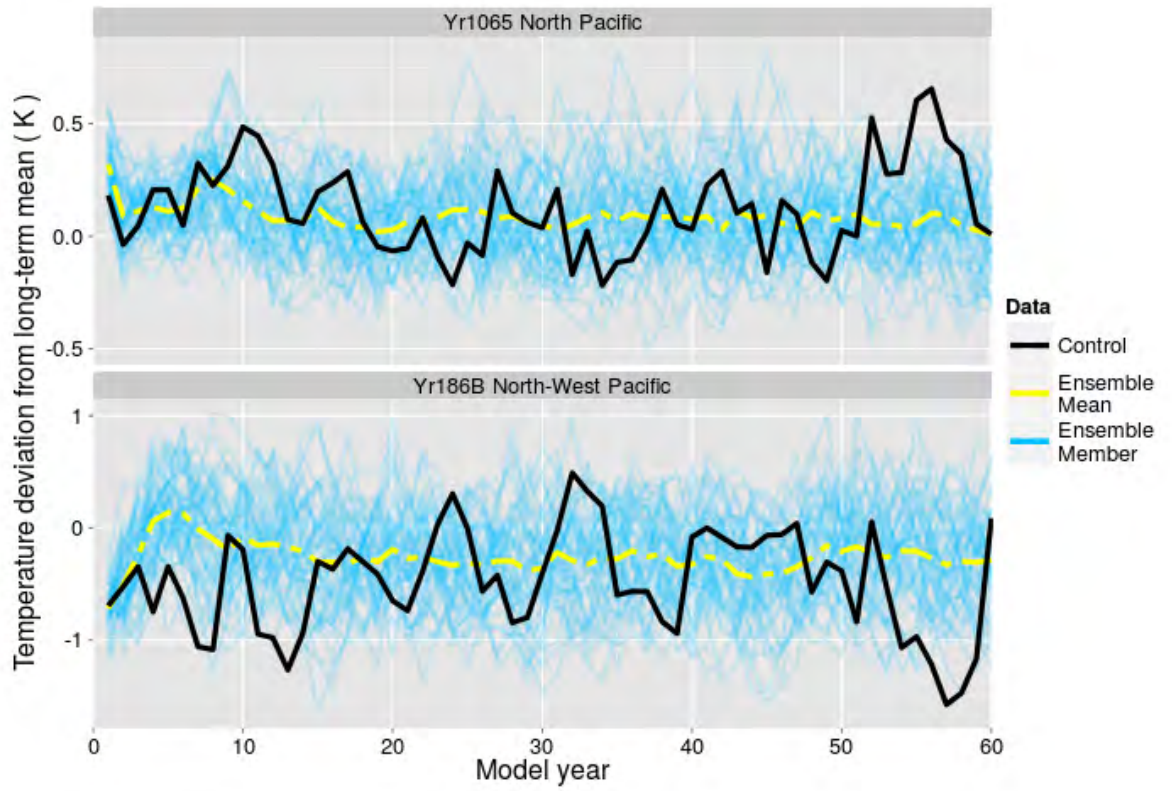

Figure 5.7: As in Figure 5.4, but for Yr1065 NPa and Yr186B NPI TS, as indicated.

variance spectrum shows little deviation from red noise in this model (see subsection 4.2.4). Consequently, the response to IC perturbation over these domains resemble overdamped oscillations, exhibiting behaviour somewhat like exponential decay in the ensemble mean (see ACC TS in Figure 5.4). This is indicative of (F2) being at play.

Beyond the interannual-scale IC influence, model drift (see section 4.1) plays the dominant role in establishing the distributions $f_v(t)$, towards which ensemble variable PDFs evolve (see subsection 5.1.1). This is evidenced by the distinct "clusters" of CFE climatic TAS distributions seen for numerous domains in Figures 5.1 and 5.2. These clusters appear to be determined essentially by the model century at initialisation. They are especially apparent over SML, the Antarctic (SP), ACC and SSA. The generally slow evolution of $v_p(t)$ with model time suggests that intercentennial-scale IC influence is linked to centennial- to millennial-scale adjustments in the deep to intermediate level ocean circulation, as well as other slowly varying components of the model system. This hypothesis is supported by the observation that the influence is most pronounced over the northern Atlantic and—especially—the Southern Hemishperic extratropics.

The IC influence evident in Yr647 variable evolution is, in many ways, fundamentally different from that seen with the other CFEs. Its setup is discussed in subsubsection 3.5.3.3.

Although it is a CFE, it was initialised from the output of a TFE member. Hence, two types of adjustment are likely to be taking place:

1. readjustment to the present day external forcing; and
2. internal adjustment to, and redistribution—between regions and model system components—of the excess heat in to the model system.

The former is most apparent and is the focus of subsection 5.1.4. The latter may explain why, after six decades of relaxation behaviour has taken place—almost all of which appears to occur in the first three decades—the ensemble temperature PDFs for most regions appear to tend towards a warmer state than even $f_T(900)$ (as deduced from ensembles Yr876_NERSC and Yr876_CHPC). This is especially apparent over NP, NPa and NPI (see Figures 5.1 and 5.2). It is possible that this is related to Arctic sea ice loss, which might not recover when radiative forcing is reduced. This could be responsible for hysteresis in the model system. This possibility warrants further investigation, which is, however, beyond the scope of the present study.

The qualitatively more prominent difference between the IC influence evident in Yr647 and the other CFEs is that the ensemble climate after relaxation displays distinctly different spatial patterns, due possibly to the above mentioned sea ice loss. Figure 5.8 shows the PDF of the SST gradient across the North Atlantic (measured by NAO TS index), sampling the last three decades of each ensemble member. It shows that the NAO TS PDFs for Yr647 is significantly different to that of each of the other CFEs ($D > 0.1, p < 0.001$, where D is the KS D-statistic; see subsection 3.6.6). The Yr647 NAO TS state is between those assumed by all other CFEs, and the state assumed by the TFEs.

Not all Yr647 distributions represent an intermediate state between CFEs and TFEs, however. For example, PDFs of NAt and WTP PPT over the sixth decade of collections of ensembles—grouped by model year at initialisation—are shown in Figure 5.9. Considering Yr647 NAt PPT relative to the other CFEs, the shift in the positive tail PPT PDFs is opposite to that seen when comparing TFEs to CFEs. Different modes of the WTP PPT PDF are favoured by Yr647 than by both the CFEs and TFEs.

Comparing the initial Yr587 ETP TAS perturbation (relative to $T_p(587)$) to the difference between the Yr186A and Yr587 ETP TAS ICs, shows that former is substantially larger. This is evident in the TAS PDFs over the first decade of the ensembles, shown in Figure 5.10. The D-statistic obtained by comparing the first decades of Yr186A and Yr587 TAS is approximately 0.05; the corresponding value for comparison between the first and other (second to sixth) decades of Yr587 TAS is 0.12. However, it takes many centuries of model integration before the TAS climatological distribution—determined by the largest scale of IC influence found in this study—shifts from $(F_T(186))$ to $(F_T(587))$, whereas the corresponding interannual-scale ensemble CDF shift clearly occurs within a decade or two. This is illustrated by the difference between clusters of ensemble distributions in Figure 5.2, alluded to previously.

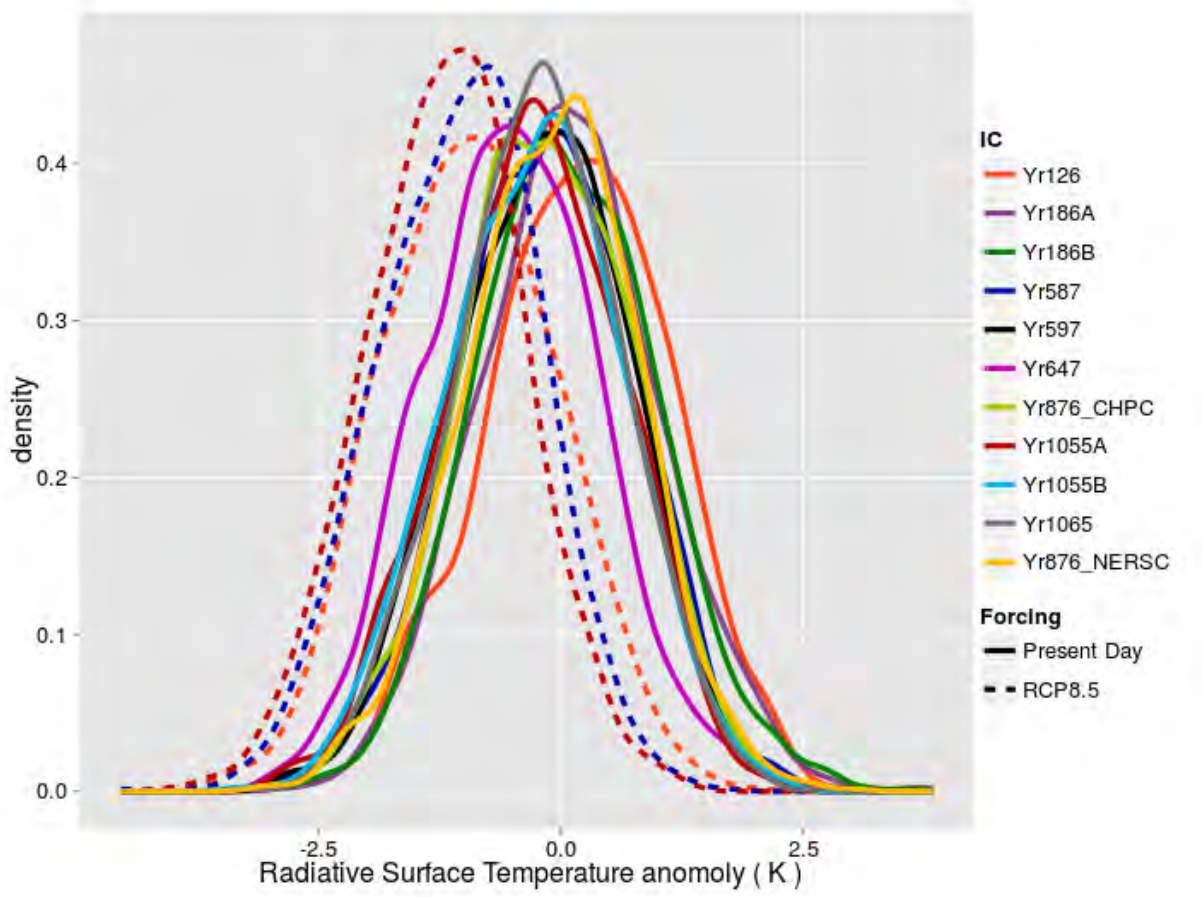

Figure 5.8: As in Figure 4.6, but for TS difference across the North Atlantic, as defined by the NAO index latitudes (see Table 3.6), considering ensemble years 31 and 60.

Similarly, a very large perturbation is apparent in the first decade TAS distribution over Tr for Yr647 (see Figure 5.10 and subsection 5.1.4). However, by the final decade of the ensemble run, it has decayed sufficiently that the decade 6 Yr647 TAS distribution is more similar to the decade 6 Yr597 TAS distribution ($D \approx 0.15$) than the decade 6 Yr597 TAS distribution is to the decade 6 Yr126 distribution ($D \approx 0.17$). This despite the corresponding D-statistics for the first decades being approximately 0.57 and 0.26, respectively.

These comparisons demonstrate that the scale of IC influence evident in the ensemble time series of a particular variable (e.g. ETP TAS) is not equivalent to, or even in direct correspondence with, the amplitude of IC perturbation applied (directly or indirectly) to that variable at initialisation. This is probably due to both:

- the large range of time scales on which the different mechanisms responsible for different scales of IC influence act; and

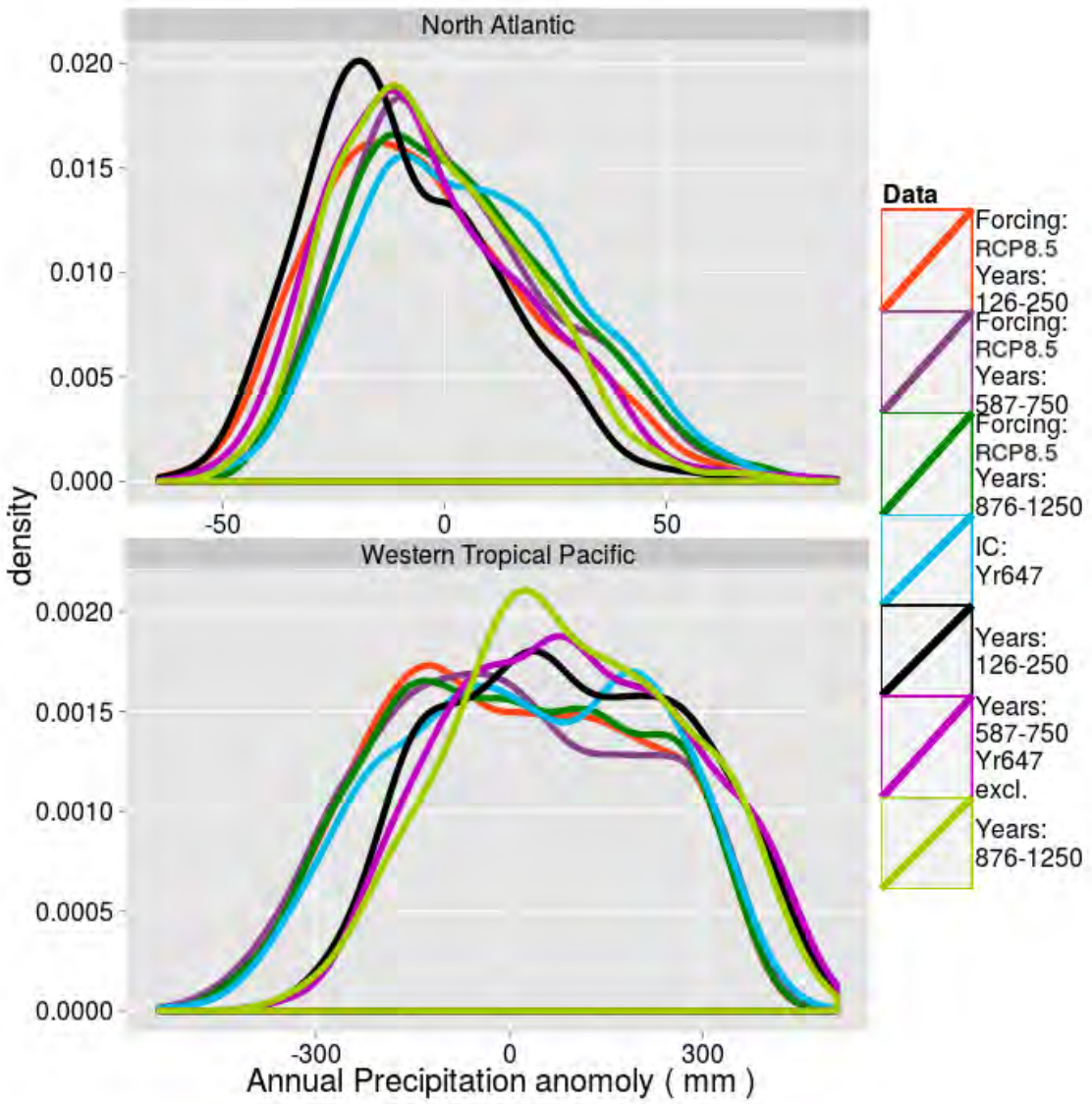

Figure 5.9: Probability density estimates (as in Figure 4.6), using data from only the sixth decade of each ensemble and showing CFE and TFE NAt annual precipitation (PPT) distributions. Data are grouped and plotted by model year period (four periods are used here; model years are denoted by "Years" in the legend). Unless otherwise indicated, forcing is present day (i.e. data is from CFEs).

- the influence of the rest of the model system on the variable and region of interest.

Teng and Branstator (2011) demonstrate that, through a propagating mode of variability, the latter can result in decadal-scale predictability.

Admittedly, given that no ensembles were initialised between model years 250 and 550,

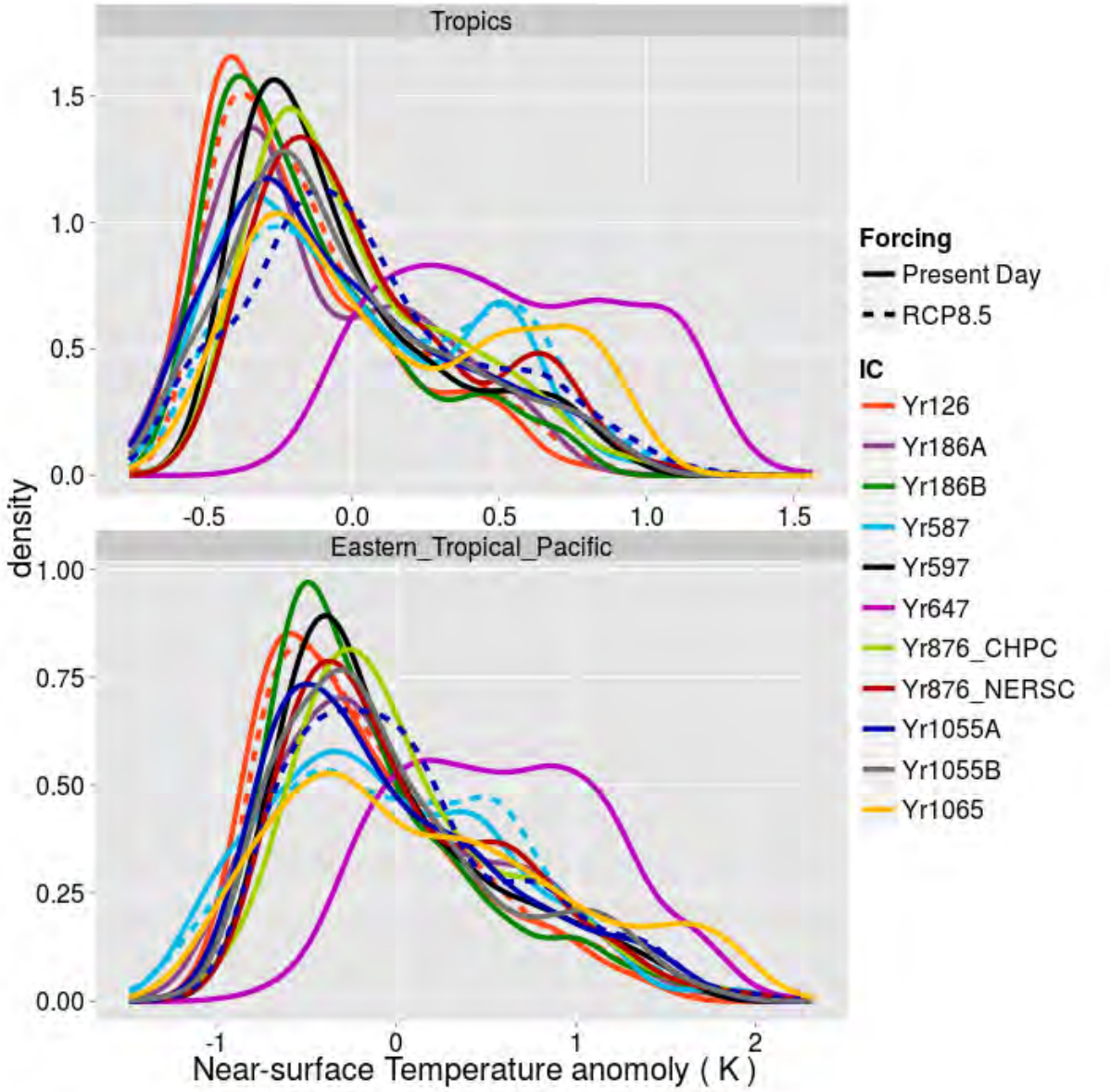

Figure 5.10: As in Figure 4.6, but including data from the first decade of each ensemble only and showing ETP and Tr TAS.

it cannot be concluded with certainty that the change in climatological distribution evident between ensembles Yr186A and Yr587 did not occur rapidly. More generally, the ability to distinguish the consequences of different levels of IC influence is limited in this study, as the mechanisms responsible for them are not investigated in any detail. There are also no multicentennial ensemble simulations from which it can be established whether $F_T(t)$, for any given variable, is well-defined, and if so, what form it takes. However, the nature

of observed model drift (section 4.1) and the small, progressive changes in climatological distribution with model year apparent in, for example, Figures 5.1 and 5.2, suggest a smooth, slow evolution of a well-defined $F_T(t)$.

The discussion in this section is suggestive of three distinct levels of IC influence, discussed further in section 6.1:

Scales of IC Influence

Microscopic "weather"-scale influence;

Interannual-scale influence which determines the evolution of ensemble distributions around their climatological distribution; and

Intercentennial-scale influence on the background climatological distributions of model variables.

5.1.3 The Kairodic Assumption

In this section, ensemble member variable probability distributions are compared. The assumption being tested is discussed at greater length in subsubsection 2.1.5.1. Essentially, it states that temporal distributions of a single ensemble member—or a small ensemble of, say, five or fewer members—taken over a period of time, should be indistinguishable from distributions obtained from multiple ensemble members at a given instant. However, instantaneous data are not considered in this study. Furthermore, diurnal and annual cycles make the general assumption difficult to interpret precisely and test comprehensively. Hence, here, this assumption is investigated by comparing probability distributions of regional variables from individual ensemble members over the entire ensemble duration (equal to two periods of standard climatology; see subsubsection 2.1.3.1) to:

Kairodic Comparison Types

1. One another;
2. Distributions over all ensemble members for individual ensemble years;
3. Distributions over all ensemble members and all years during a given ensemble decade; and
4. The complete ensemble distribution over all years.

Additionally, distributions for individual years and decades are also compared to the overall distribution and the climatological distribution (see subsection 5.1.1) over the second

half of the ensemble duration. The decision to consider decadal—rather than shorter—periods for comparisons, is taken primarily because of the lower frequency of the dominant mode of variability observed in the present model configuration (see subsection 4.2.1). KS D-statistics (see subsection 3.6.6) are used as the primary measure of difference in distribution. Unless otherwise indicated, a 1% level of significance is used. Violation of the kairodic assumption is equated with a sizeable collection of ensemble members behaving qualitatively differently from the other members, thus producing probability distributions significantly different from the climatological distribution.

We observe that the validity of the kairodic assumption depends largely on the region and variable considered. Temperature variables appear most likely to violate the assumption. The likelihood of significant differences between ensemble member distributions is strongly dependent on the interannual-scale IC state (see subsection 5.1.2). For example, as shown in Table 5.1, for NAt TS the overall Yr186B, Yr876_CHPC and Yr1055A ensemble distributions are significantly different from the temporal distributions of eight of their individual members; however, the corresponding number for ensembles Yr597 and Yr1065 is only two, for Yr587 it is three (type 4 comparisons are used here—as defined on page 91). Thus, for NAt TS, the likelihood of ensemble member distributions differing significantly from the overall ensemble distribution appears to be anti-correlated with the degree of "memory"—and consequent predictability—apparent in NAO PSL time series (cf. Figure 5.5).

Two regions stand out as showing greater distributional differences between members (type 1 comparisons): the northern mid-latitudinal domains and southern mid-latitudinal and subpolar domains. For TS distribution comparisons over the ACC and SML domains respectively, 4360 and 4638 of the 13475 type 1 comparisons were statistically significant. Over these domains, significant type 4 comparisons are also more likely (see Table 5.1); of the 550 type 4 comparisons conducted, respectively 162 and 181 were significant.

The largest D-statistic observed for a type 1 comparison on any of the Niño index domains, for any variable, is relatively large at 0.402 ($p < 10^{-4}$). This was for comparison of two ensemble member Niño-4 TS distributions from the Yr876_NERSC ensemble. However, the largest D-statistics for NPa and ACC TS type 1 comparisons are much larger: respectively, they are approximately 0.7 ($p < 10^{-13}$; from Yr186A) and 0.82 ($p < 10^{-15}$; from Yr876_CHPC).

Hence, it would appear that strong internal feedbacks associated with quasi-periodic modes of variability, driving the ensemble member responses to ICs, exert sufficient control over the ensemble member evolution to dominate the influences of aperiodic variability and almost-intransitivity. Conversely, aperiodic variability and almost-intransitivity (see subsection 3.5.2) are more apparent over NPa and ACC (see Figure 5.4), for example. This appears to lead to violations of the kairodic assumption. Hence, where interannual-scale IC influence is related primarily to Factor (F1) (introduced on page 82), the kairodic assumption usually holds; conversely where Factor (F2) dominates, the kairodic assumption is often violated.

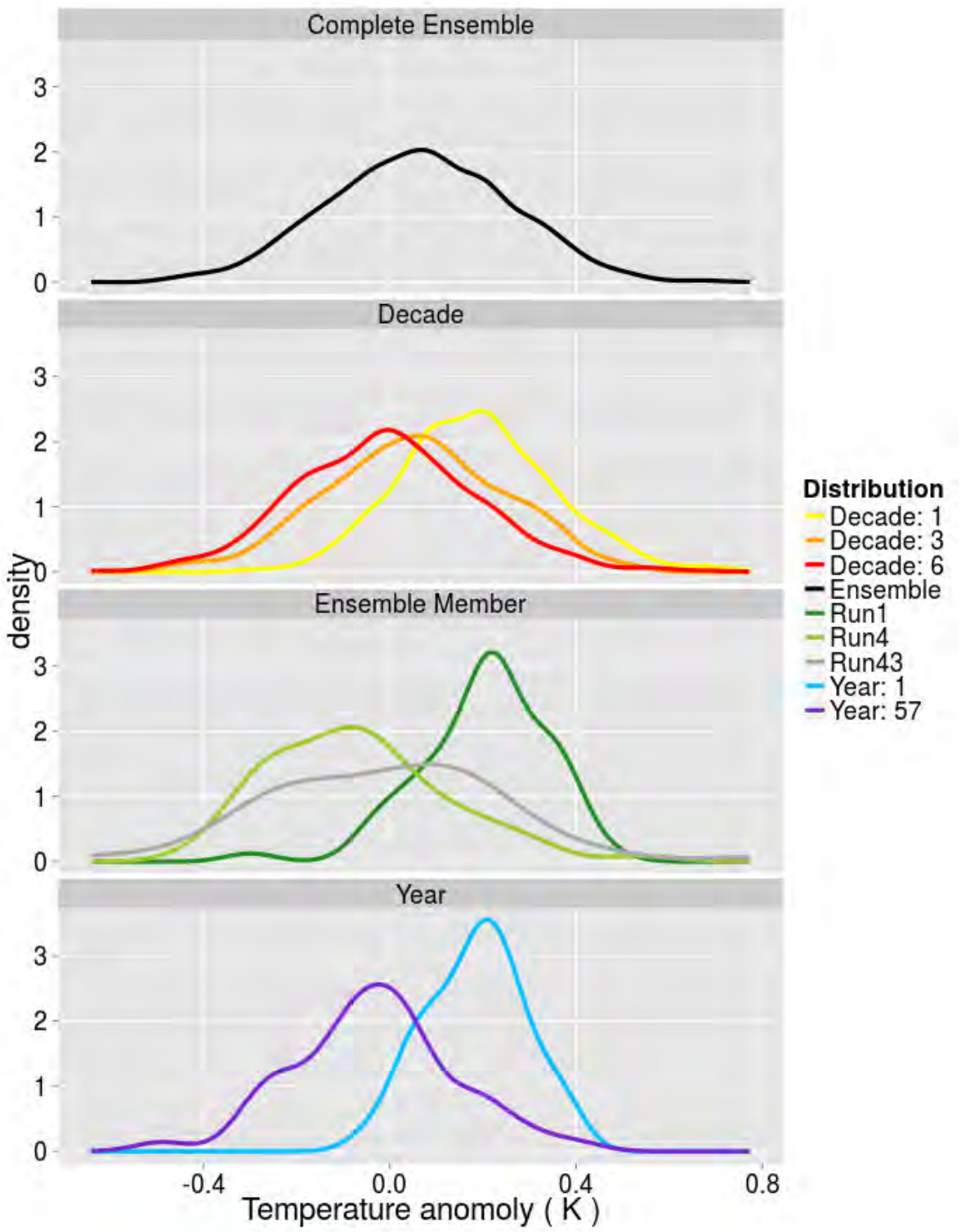

Figure 5.11: Plots of Gaussian kernel density estimates—as in Figure 4.6—of NPa TAS for selected ensemble members, years and decades of Yr587

Furthermore, over regions where the system behaviour is strongly determined by quasi-periodic behaviour—especially the tropics and subtropics in this model configuration (see, for example, SA in Table 5.1)—there is little tendency for ensemble member distributions to differ significantly from one another (type 1 comparisons), decadal periods (type 2 comparisons) or the overall ensemble distribution (type 4 comparisons). For example, none of the type 4 Niño TS comparisons are significant (and hence are not shown in Table 5.1). Over the 5 Niño domains and 11 ensembles considered, the 67375 type 1 comparisons yielded only 21 significant results. However, especially during the first decade of ensembles displaying high predictability, distributions of individual years can deviate significantly from ensemble member distributions over the Niño domains (type 2 comparison). For example, comparing Niño-4 PSL distributions of year 7 and Run21 of Yr587, yields a D-statistic of 0.447 ($p < 10^{-4}$). The year 7 distribution is significantly different from the overall ensemble distribution at the 0.1% level.

The above suggestions are also supported by fact that, generally, ensemble member distributions appear to differ less from one another and the overall ensemble in Yr647 (see Table 5.1). This is the case despite the unusual evolution of Run3 (see subsection 5.1.2). For Yr647, the strong external influence of reduced radiative forcing, appears to dominate the influence of aperiodic internal variability in shaping temporal distributions. For example, the number of significant Yr647 SML TS type 1 comparisons is 171, whereas for other ensembles the number varies between 390 and 519 out of 1275. For comparison, at random, the average number comparisons that would yield a significant result is $0.01 \sum_{i=1}^{50} i \approx 13$. Without an extension of the Yr647 ensemble duration beyond 60 years, it is not possible to tell directly whether the resulting pseudo-steady climate is less likely to display almost-intransitivity.

Among the ensembles, Yr126, Yr876_CHPC, Yr186A and Yr186B appear to show the greatest tendency to produce ensemble members whose distributions differ significantly from one another (significant type 1 differences). It is postulated that this is partially due to large IC perturbations which do not project strongly onto prominent quasi-oscillatory modes of variability being in place at initialisation, over domains susceptible to displaying almost-intransitive behaviour. Dynamically important variables such as the 500-hPa zonal and meridional wind speeds in the extratropics, are substantially different from their preferred states in the ICs of these ensembles. Subsequently, different ensemble member distributions vary in how long they take to return towards the climatological state. This is illustrated in Figure 5.11, which shows ensemble member, year and decade NPa TS PDFs, selected to indicate the extent of difference in distribution that is possible. This behaviour is also discussed in relation to Figures 5.4 in subsection 5.1.2.

Another possible cause of significant differences in ensemble member distributions is different rates of variable trends, related to model drift. It is particularly relevant to southern mid- to subpolar latitudes, because, in this model configuration, the interannual temperature variability over this region is comparatively small. This is illustrated in the very narrow ensemble temperature distributions produced over these domains; see, for

Domain	Yr126	Yr186A	Yr186B	Yr587	Yr597	Yr647	Yr876_CHPC	Yr876_NERSC	Yr1055A	Yr1055B	Yr1065
ACC	19	14	25	12	12	7	11	14	18	14	16
SML	20	16	22	15	18	6	15	17	17	16	16
SO	12	7	10	6	9	2	5	7	10	8	7
SP	3	0	0	1	3	0	2	3	1	1	0
NPa	5	11	5	9	11	13	9	8	7	13	6
NAt	7	7	8	3	2	6	8	6	8	4	2
NPI	1	3	1	4	5	3	3	3	2	5	0
NAO	5	1	2	5	3	2	5	0	2	2	2
NML	13	18	11	9	10	13	18	14	15	15	10
NP	0	0	0	0	0	0	0	0	1	0	0
SA	0	0	0	1	0	0	0	0	0	0	0

Table 5.1: Number of significant differences obtained from type 4 comparisons (between ensemble distributions and individual member distributions) for TS, for each CFE and a selection of domains (see subsection 3.6.2 for details about domain names and bounds used).

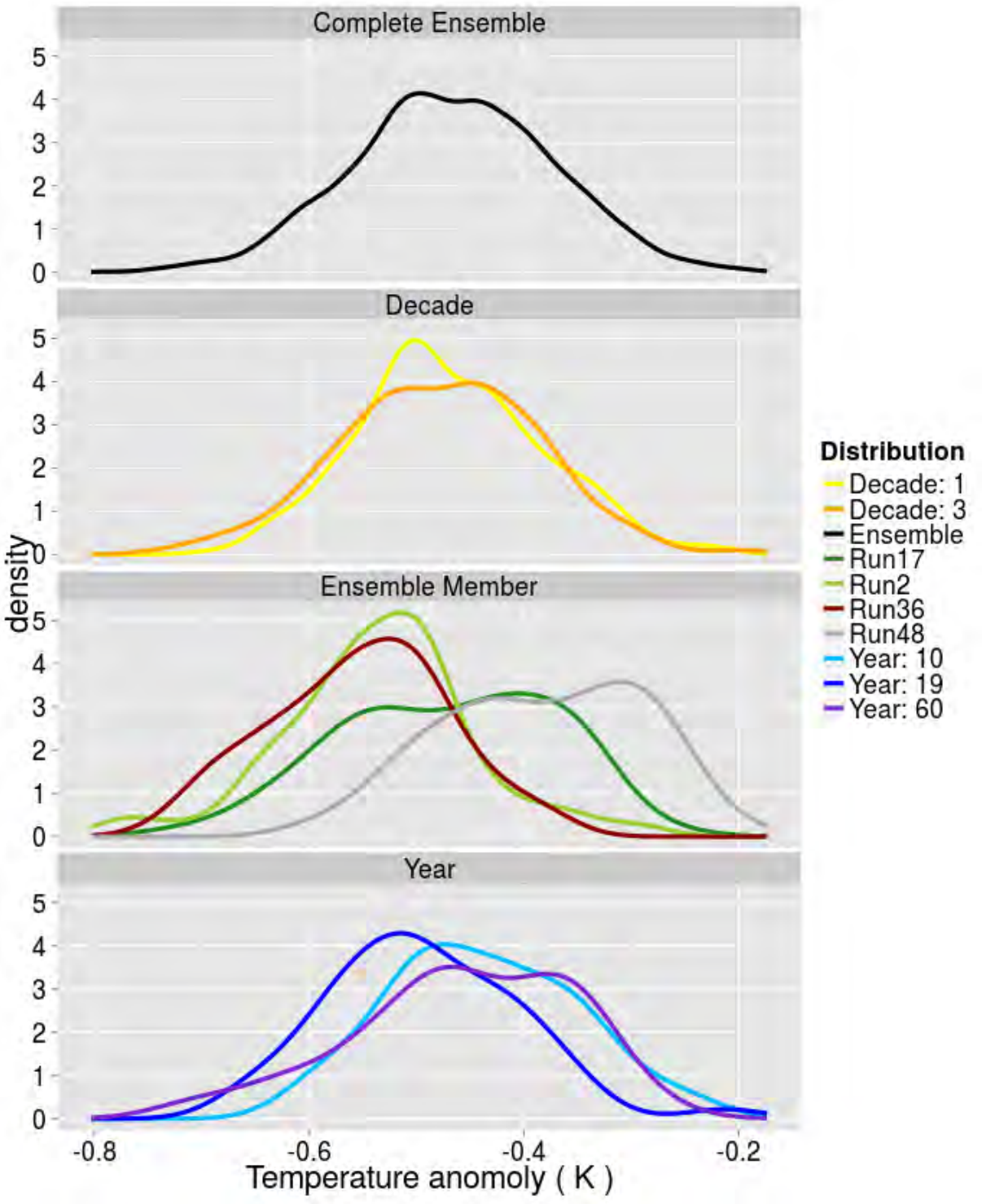

Figure 5.12: As in Figure 5.11, but for Yr126 ACC TAS

example, Figures 5.1 and 5.2). This holds even if the variable ICs imposed are relatively close to their respective preferred state values. When substantial changes in slowly evolving model components occur, to which the model atmosphere responds primarily through incremental "jumps" between states (see chapter 4), differences in the timing of such jumps for individual ensemble members could significantly alter their temporal distributions. This may be responsible for the very large differences between ensemble member Yr126 TAS distributions (type 1 comparisons) displayed in Figure 5.12.

For type 2 comparisons—when years from the first decade of substantial interannual-scale IC influence are not considered (see subsection 5.1.2)—the largest D-statistic obtained is 0.78, for NML TS year 51 of Yr597.

It is notable that Yr186A Run46 appears to behave particularly unusually over NML. The D-statistic for comparison between its TS distribution and that of Run39 is 0.82 ($p < 10^{-15}$). Temperature states for Run46 deviate little from the particularly cold Yr186A NML ICs. Consequently, its TS distribution is significantly different ($D \approx 0.57; p < 10^{-15}$) from the overall ensemble distribution, as illustrated in Figure 5.13. Whereas the Run46 TS distribution remained similar to that of ensemble year 1 (type 2 comparison, $D = 0.13, p > 0.7$), the Run46 500hPa-level zonal and meridional squared wind speed (UU and VV, respectively) distributions are centred around much higher speeds than the overall ensemble (not shown). Type 4 comparisons of Run46 UU and VV distributions yield $D \approx 0.25$, $p < 0.005$ and $D \approx 0.22$, $p < 0.01$, respectively—both the largest Yr186A NML type 4 D-statistics. However, the corresponding 500-hPa zonal wind component (U) shift was relatively less marked: type 4 comparison yields $D \approx 0.15$, $p > 0.1$. In contrast, Run5, for which a type 4 NML UU comparison yields $D < 0.15$ ($p > 0.15$), gives a much larger type 4 NML U D-statistic of 0.24, ($p < 0.005$). This suggests that the unusual behaviour of Run46 may be driven by continued instability in the mid-tropospheric westerly wave—the similarity between the year 1 and Run46 VV distributions ($D \approx 0.07; p > 0.9$) suggests that such an anomalous configuration was present in the ICs. Hence, it appears that chaotic behaviour in the large scale mid-latitude dynamics (to the extent that it can be captured by annual spatial mean statistics) can persist for much of the 60-year ensemble duration.

5.1.4 Decay Behaviour of a Large IC Perturbation

The focus of this section is ensemble Yr647 and its relaxation behaviour behaviour (see subsubsection 2.2.3.3). It is a CFE, but was initialised from output of an ensemble run under rapidly evolving external forcing conditions. See subsubsection 3.5.3.3 for a more detailed discussion of the Yr647 ensemble set-up. Because transient radiative forcing had been applied to the model system for only 60 years, the full system circulation had not yet adjusted fully to the external forcing; i.e. the model system is "committed" (e.g., Meehl et al., 2005) to additional warming.

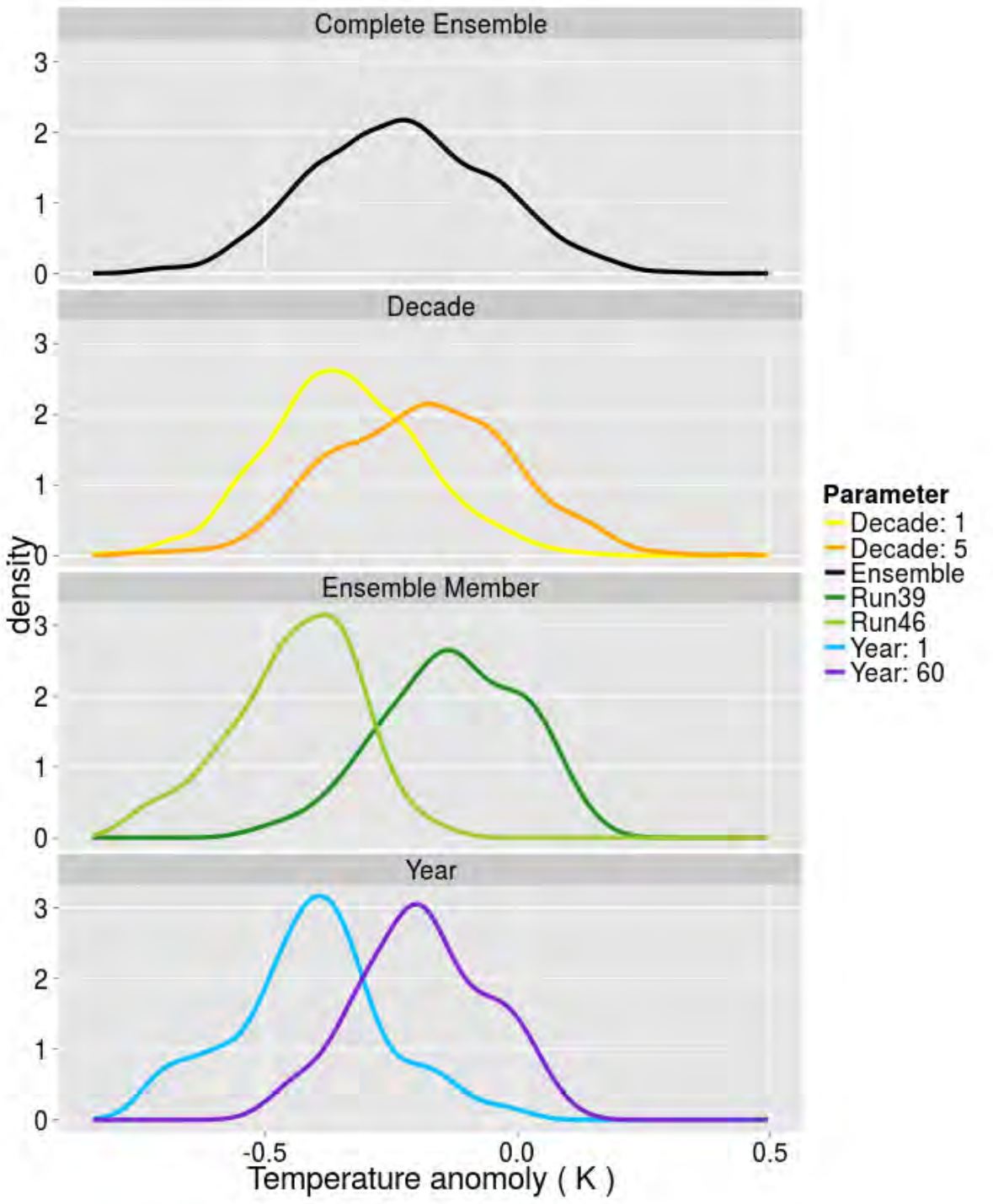

Figure 5.13: As in Figure 5.11, but for Yr186A NML TS

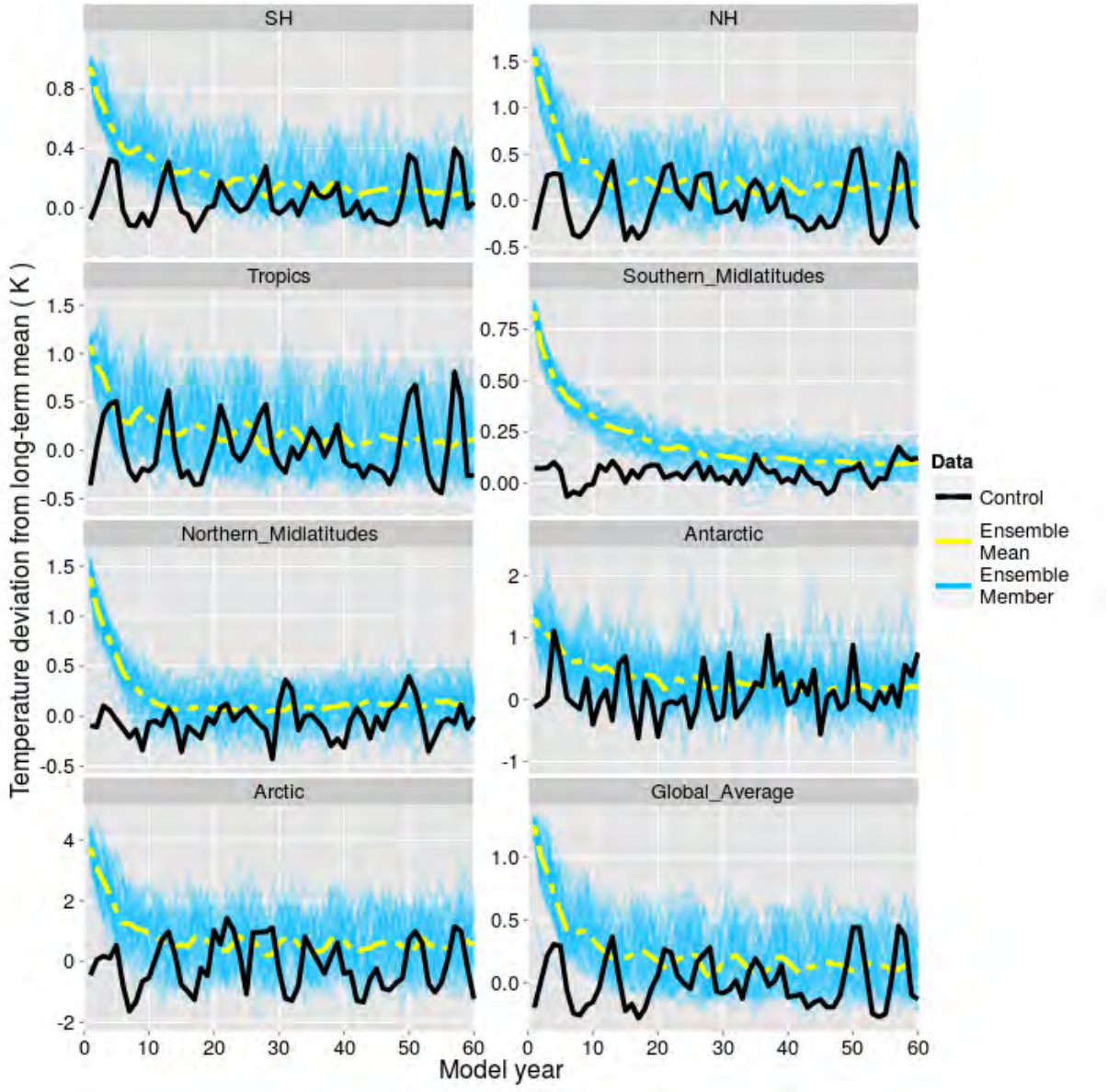

Figure 5.14: Time series plot of Yr647 TAS over latitudinal bands (see Table 3.4). The CHPC Control is also shown.

Let regional TAS be denoted as $T(t)$. In the present discussion, it will be assumed that $(\forall t_0, t_1 \in \{t \in \mathbb{Z} | 647 \leq t \leq 706\})(T_p(t_0) \approx T_p(t_1))$ so that T_p is understood to refer to a single common value for the duration of Yr647. Let $\Delta T = T(646) - T_p$ be the initial temperature perturbation away from T_p (noting that the ensemble was initialised at the end of model year 646), produced by the applied transient forcing. Let C be the effective regional climate system specific heat capacity and λ the equilibrium regional climate

sensitivity (as defined in subsubsection 2.2.3.3). Then the characteristic decay rate r of ΔT is given by Equation 2.1 and (see subsubsection 2.2.3.3):

$$T(t) \approx T_p + \Delta T e^{-rt} \tag{5.1}$$

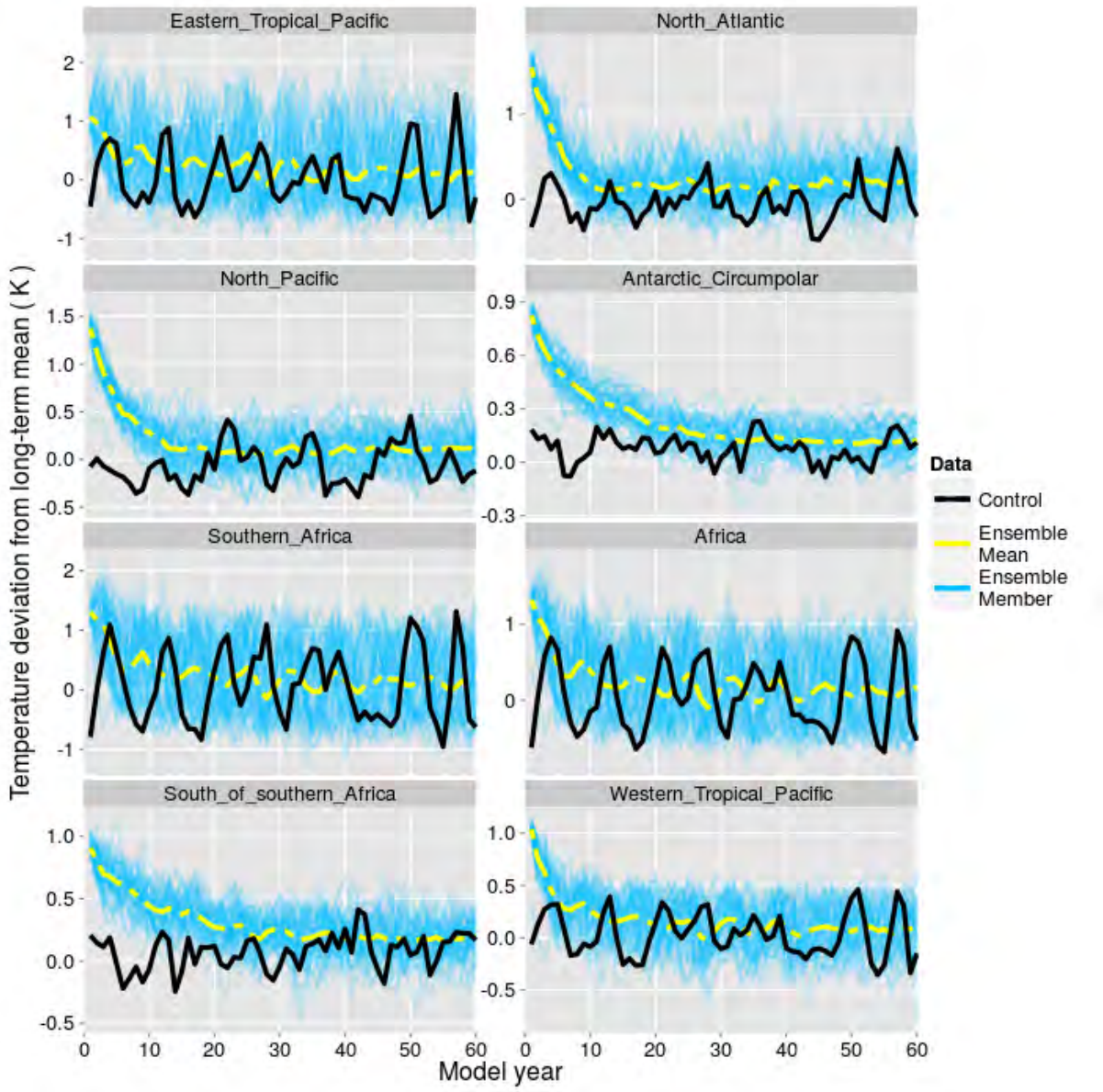

Figure 5.15: As in Figure 5.14, but for regional domains (see Table 3.3)

Qualitatively, the relaxation behaviour behaviour of the ensemble mean regional temperatures shown in Figures 5.14 and 5.15, seem to all be consistent with Equation 5.1.

However, the characteristic time scales of decay, $\tau = \frac{1}{r}$, vary regionally. In particular, whereas in most regions the ensemble trajectory appears to flatten after about fifteen years, over Southern Hemispheric extratropics, appreciable decay continues for at least three decades. These extended decay times are also reflected, to a lesser degree, in SH and global averages. This apparent regional difference in the value of λ is likely the result of different values of C. It is probably a consequence of the extent to which the Southern Hemispheric extratropics are covered by ocean, but it is notable that the ocean-dominated ETP, WTP, NPa and NAt domains display comparatively much more rapid temperature decay rates.

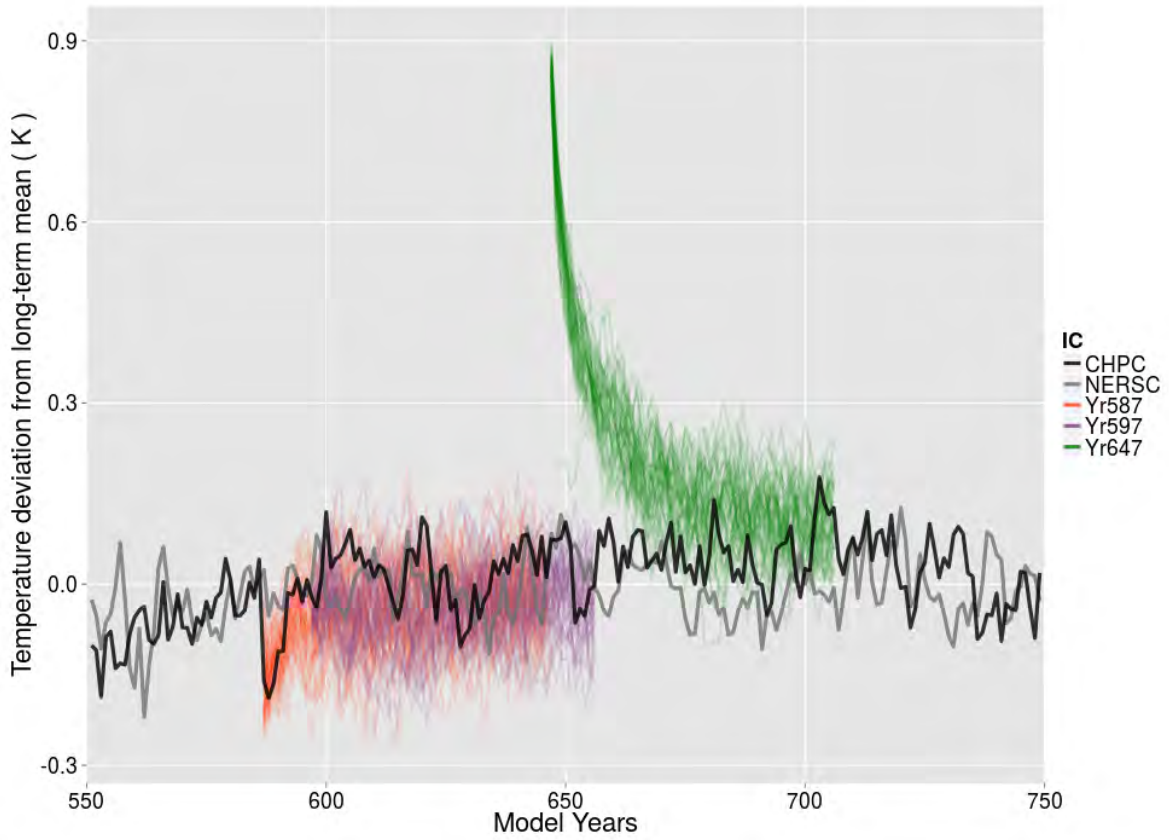

Figure 5.16: Time series of SML TAS for PDCs and CFEs, between model years 550 and 750.

Regional ensemble mean temperatures do not decay back to their respective $T_p(650)$ values (as determined from the PDCs and ensembles Yr587 and Yr597). This is most clearly illustrated for SML TAS in Figure 5.16, which shows time series of the PDCs and ensembles Yr587, Yr597 and Yr647, as a function of model year. Ensemble PDF estimates in Figures 5.1, and 5.2 also illustrate the difference. Generally, regional ensemble mean temperatures over the last 3 decades of Yr647 are $\Delta T_p \approx 0.2$K larger than the corresponding $T_p(650)$ values. However, there is considerable regional variation in ΔT_p: over NP $\Delta T_p \approx 0.5$K;

over the Northern Hemisphere mid-latitude domains (NML, NPa and NAt) $\Delta T_P \approx 0.1$ or smaller. The changes in spatial temperature distribution suggested by these differences and a potential link to changes in ice cover are discussed in subsection 5.1.2). For most domains $0.05\Delta T \leq \Delta T_p \leq 0.1\Delta T$. Gl ΔT_p is comparable to the ensemble standard deviation.

This suggests that, although it may appear that ensemble mean temperatures in most regions converge to a pseudo-steady state value by the end of the ensemble period (not equal to $T_p(650)$), not all the excess heat trapped in the model system is lost over the 60 year ensemble duration. This may indicate the existence of a second, much longer, characteristic time scale of temperature decay in the model, corresponding perhaps to a release of OHC, primarily from intermediate depths.

One Yr647 member (Run3) initially exhibits particularly unusual behaviour over all domains, other than the poles. Its temperature evolution (and that of other atmospheric variables, including PPT and CLD) deviates substantially from that of the ensemble mean and all other ensemble members during the first 5 years of the relaxation behaviour period. In particular, ΔT decays much more quickly in Run3 than in other ensemble members; whereas most other members lose roughly 25% of the initial perturbation in the first year, Run3 loses about 90%. It exhibits temperatures much lower than those of other members within the first three months of the ensemble run (not shown).

Run3 continues to display unusual behaviour, especially over SML and ACC, throughout its 60 year duration. It is not clear whether this behaviour is indicative of a true fine-scale sensitivity to ICs in the model's response to particularly large IC perturbations, or whether it is purely a consequence of numerical instability resulting from applied forcing and variable fields being too far out of balance. However, the possibility of "rogue" ensemble members is noteworthy and warrants further investigation, although this is beyond the scope of the present study.

Figures 5.1 and 5.2 show that the IC perturbation applied to Yr647 produces ensemble behaviour and regional relaxation behaviour time scales distinct to that observed with other ensembles. The nature of the IC perturbation applied is fundamentally different, in that the model state from which Yr647 ICs are derived were not produced—and can presumably not be produced—by the model run, when run under the forcing conditions applied during the ensemble. If TAS is conceptualised as a variable in a low-dimensional dynamical system (see subsubsection 2.1.4.2), of which the net radiative forcing and degree of model drift having occurred are control parameters, the Yr647 ICs can be thought of as lying some distance away from the system's attractor in its state space. Using the same (not necessarily strictly valid) conceptualisation, ICs for other ensembles lie on—or near—the system's attractor for the appropriate control parameter values.

5.2 Transient Forcing Runs

5.2.1 Transient vs Constant Forcing Ensemble Distributions

In this section some attributes of probability distributions which change in TFEs, relative to CFEs, are discussed. In subsubsection 5.2.1.1, changes in predictability under RCP8.5 forcing are discussed. In subsubsection 5.2.1.2, distributional changes that are suggestive of nonlinear climate change, as conceptualised in Palmer (1999), are considered.

Predictability, as noted in section 1.3, is assessed through conditional probability distributions. Differences between conditional and unconditional distributions may take the form of a change in:

- "location" (measured by, for example, the mean or median); or
- "spread" (often measured by standard deviation, or—particularly for non-normal data—interquartile range)
- "shape" (characterised by, for example, skewness and modality).

In comparing IC and forcing influence during ensemble evolution, the ensemble mean is used as the primary measure of comparative predictability in subsubsection 5.2.1.1. The influence of forcing on ensemble spread is also addressed. Changes in shape resulting from changed forcings are discussed primarily in subsubsection 5.2.1.2. A discussion of IC influence on CFE behaviour, closely tied to predictability, is given in subsection 5.1.2.

5.2.1.1 Forced and IC Predictability

How long it takes before forced predictability exceeds ICP (the use of the terms here follows that of Branstator and Teng (2010) and Teng and Branstator (2011)) for temperature is largely dependent on the relative magnitudes of regional internal temperature variation and response to increased radiative forcing. As distributional spread in temperature is initially relatively similar between TFEs and CFEs (discussed below), and IC influence is usually detectable in the distributional location for longer than for spread (see subsection 5.1.2 and section 5.3), the evolution of the ensemble mean is used to assess the relative contributions of ICs and forcings to predictability. The case for SO TAS, which exhibits relatively small internal variability—somewhat larger than SML or ACC TAS—is illustrated in Figure 5.17.

Generally, temperature ICP appears to exceed forced predictability for about 5 ensemble years. Thereafter, IC and forced predictability are similar in magnitude until about ensemble year 10 or 15—depending on the domain. Subsequently, forced predictability

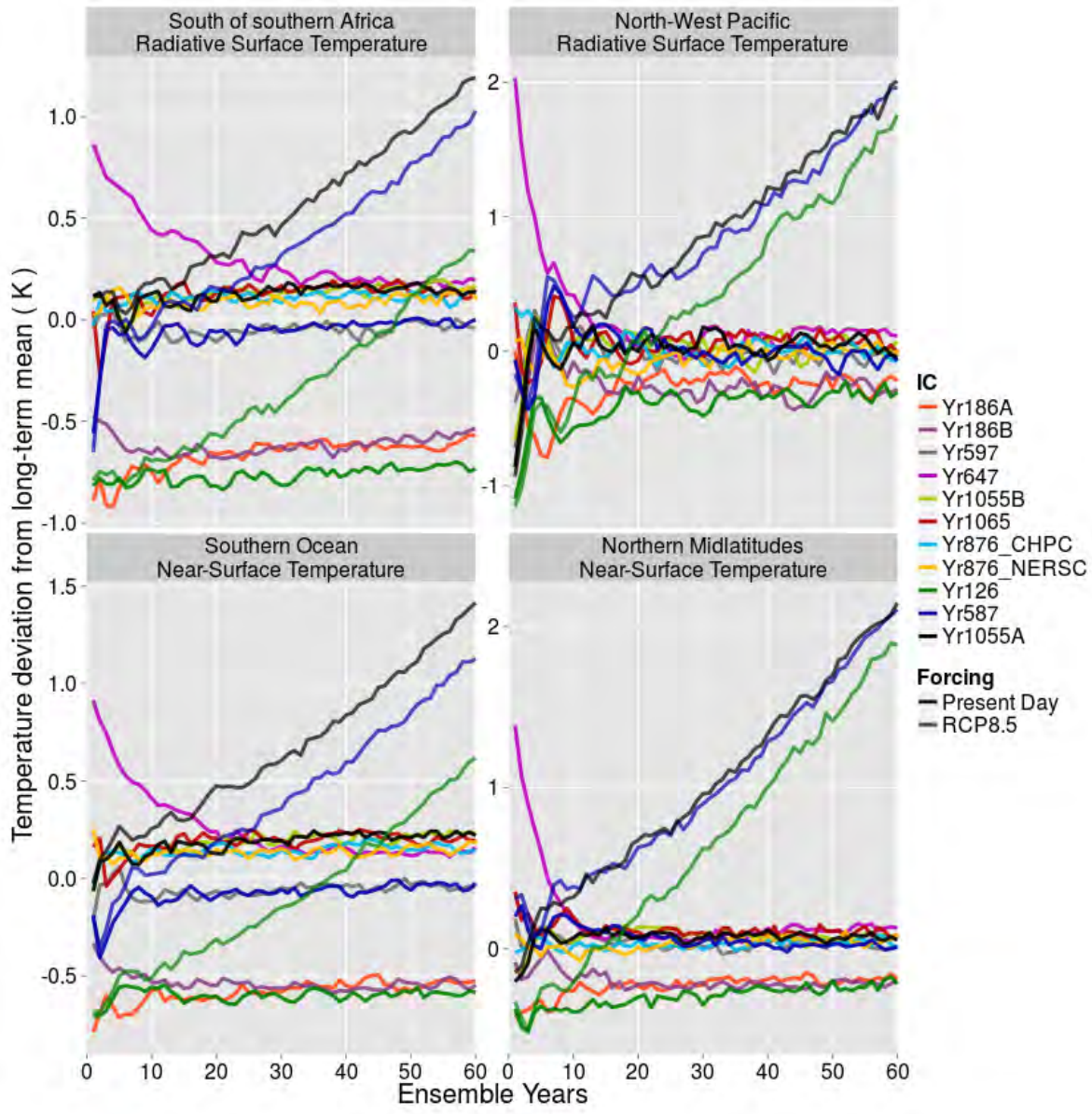

Figure 5.17: Ensemble mean SSA and NPI TS (top row) and SSA and NML TAS (bottom row), as a function of ensemble year. Both CFEs (less transparent lines) and TFEs (more transparent lines) are shown.

is much greater, as it continues to increase, while ICP decreases, as interannual-scale IC influence decays (see subsection 5.1.2).

Two regions where IC temperature predictability extends for a longer duration are SSA and NPI (illustrated in Figure 5.17). SSA ensemble mean TAS for TFEs initially reflect IC perturbation decay (see subsubsection 2.2.3.3), whereas NPI TS ensemble mean evolution

also exhibits a contribution from memory of the approximate initial phase of modes of variability. This is consistent with the finding in subsection 5.1.2 that SSA variability is driven mainly be Factor (F2) (page 82), whereas NPI exhibits variability driven by both Factors (F1) and (F2). Note that the influence of the model ENSO variability (see subsection 4.2.1) is more prominent over NPI than NPa.

The time of "emergence" of a variable is considered here to be the length of time before TFE mean and lower quartile values for that variable consistently fall outside the range of corresponding CFE time series. This definition differs from that used in IPCC (2013b), but should be qualitatively similar. For the purposes of this study, it is not necessary to make the ensemble-based definition precise, as it is not used to come to quantitative conclusions. The potential value of using an ensemble-based emergence definition is discussed further in section 6.4.

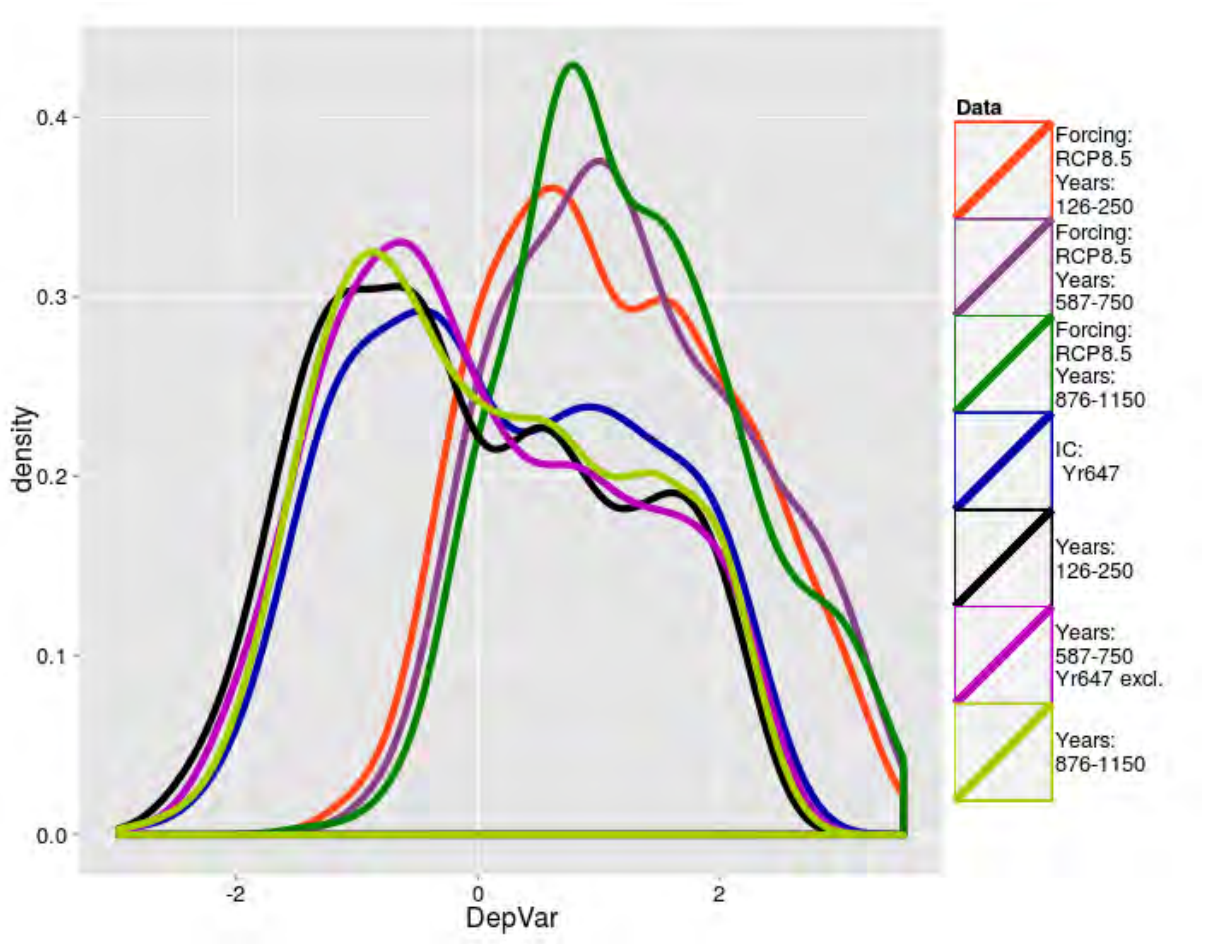

Figure 5.18: As in Figure 5.9, but for the Niño4 TS index.

Time scales to emergence are determined by the same two factors (magnitude of internal variability and forced response) as the transition from an IC to a forced predictability

regime. Over ETP, the emergence time scale is longer than 20 years for the Yr587 ensemble, whereas over the the Southern Hemispheric extratropical domains, emergence always occurs within the first ensemble decade. Over tropical and subtropical domains, where model interannual variability is comparatively large, temperature distributions do not—during the 60-year ensemble periods considered—shift sufficiently away from CFE distributions that no overlap occurs. This is illustrated, for example, in Figure 5.18, which shows Niño-4 TS distributions for ensembles from different model year periods, for CFEs and TFEs separately, over only the final ensemble decade. However, for SML TAS, for example, non-overlap between TFE and CFE PDFs with equivalent ICs occurs within 30 ensemble years (i.e. when 2035AD RCP8.5 forcing applies). This is illustrated in Figure 5.19.

These findings appear to disagree with most other studies of regional time to emergence (e.g., Mahlstein et al., 2011; Hawkins and Sutton, 2012). However, it is likely that this is entirely the consequence of the unrealistically high (low) interannual temperature variability over the tropics (mid-latitudes) in the present model configuration (see subsection 4.2.1, subsection 5.1.3 and section C.1).

There appears to be a tendency for ensemble spread to be reduced in the last decades of TFEs, compared to the corresponding CFEs. Establishing whether this is representative of a more confined model possibility space is complicated by an apparent tendency for ensemble spread to increase until around the middle of the ensemble duration, before decreasing somewhat again towards the end (see also section 5.3 and subsection 5.1.2). Significant regional variations also occur.

However, for cases such as TAS over Af, illustrated in Figure 5.20, it is relatively clear that TFEs show smaller spread after about ensemble year 50 (corresponding to 2054AD RCP8.5 forcing). After this time, Af TAS in Figure 5.20 exhibits a sharp decrease in interquartile range for TFEs, to values substantially lower than those in the corresponding CFEs. This would contribute further to forced predictability increasing as function of ensemble time.

It is notable in Figure 5.20 that for approximately the first ten ensemble years, there is close correspondence between the interquartile ranges of equivalent CFEs and TFEs, a feature observed for numerous variable-region combinations. This is suggestive of interquartile range over this period being strongly determined by ICP. Additionally, it suggests relatively little impact from the discontinuity in applied external forcing (see subsection 3.5.5).

5.2.1.2 Linear and Nonlinear Change

In this section, the tendency for variable probability distributions to exhibit changes consistent with Palmer's (1999) low-dimensional nonlinear system conceptualisation of climate change (see subsubsection 2.2.1.2), is investigated. The variables considered in Palmer (1999) are "principal components", but to the extent that the variables considered

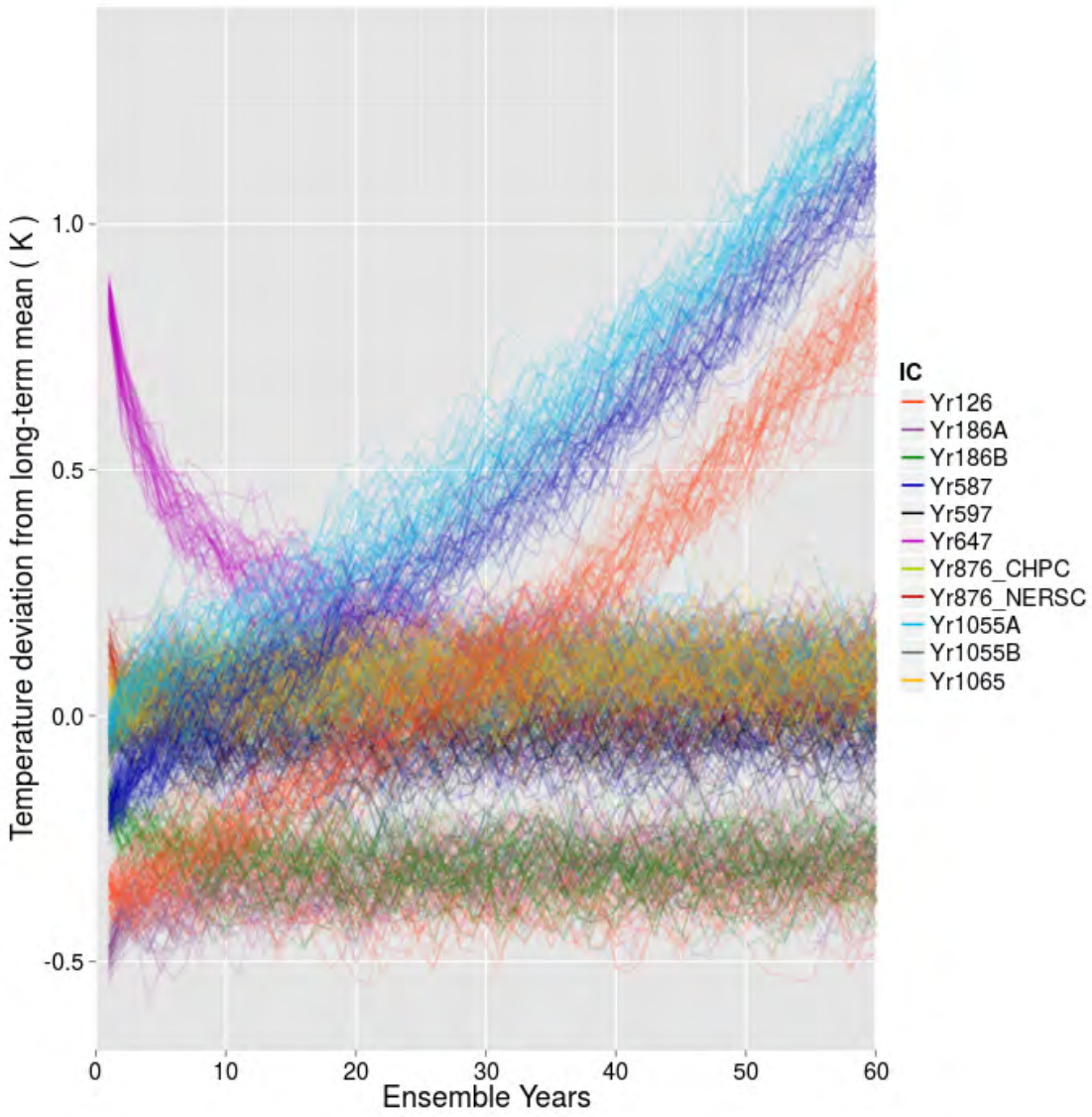

Figure 5.19: TAS over SML as a function of ensemble year, for each member of each ensemble. Both CFEs and TFEs are shown.

here are representative of multimodal patterns of internal variability of the model system, evidence of such changes should be observable, if indeed they occur.

Linear translational shifts (see subsubsection 2.2.1.2) dominate changes in temperature distributions. This is illustrated by, for example, Figures 5.1, 5.2 and 5.8. This is not, however, necessarily meaningful, as there is no reason to expect the distributions depicted in these figures to represent important modes of variability in the model.

Some variable-region combinations do, however, reflect a distributional shift charac-

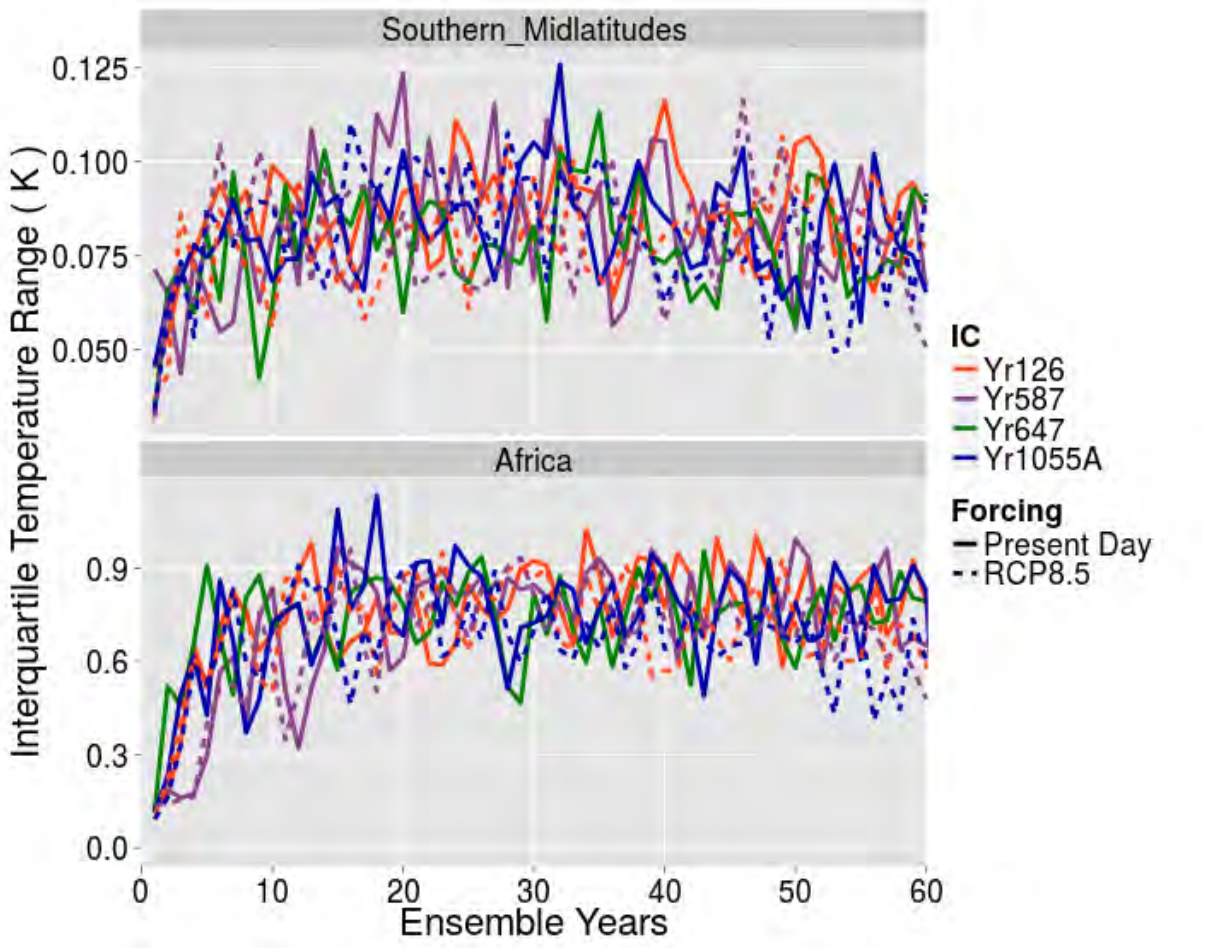

Figure 5.20: Time series of ensemble interquartile range of Af and SML TAS, as a function of ensemble year, for selected ensembles. Both CFEs and TFEs are shown.

terised by only a small translation of a particular distributional mode, accompanied by a substantial shift in the frequency of years clustering around that mode. The most prominent such examples occur over the western to central tropical and equatorial Pacific. In general, distributional changes indicate only a slight strengthening of El Niño events: shifts in the positive tails of TS distributions are relatively small, even in the final decade of the TFEs. However, El Niño-like events become much more common; by the final decade of TFEs, La Niña events have all but ceased to occur. This is illustrated in Figure 5.18.

Especially, during earlier model year periods (126-250), there are indications of trimodality in Figure 5.18: three separate peaks that may be considered representative of La Niña, ENSO-neutral and El Niño years. For the corresponding TFE, two of these peaks remain prominent—the ENSO-neutral and El Niño peaks, the former showing the greatest increase in frequency of occurrence—whereas the La Niña peak is no longer apparent. It

is notable that the distributional shifts in TAS (not shown) involve a much larger linear translational component than the TS distributions.

Shifts in other ENSO TS indices follow a somewhat similar pattern, especially thee SOI TS index, which serves as a measure of the zonal TS gradient across the southern tropical Pacific. This is illustrated in Figure 4.6, in which all ensemble decades are considered.

Regions where variability is strongly coupled to tropical Pacific variability, such as Af and SA, also show prominent shifts in distributional characteristics, often from bimodal towards unimodal. Such distributional changes may also explain the reduced interquartile range in TFEs, discussed in subsubsection 5.2.1.1.

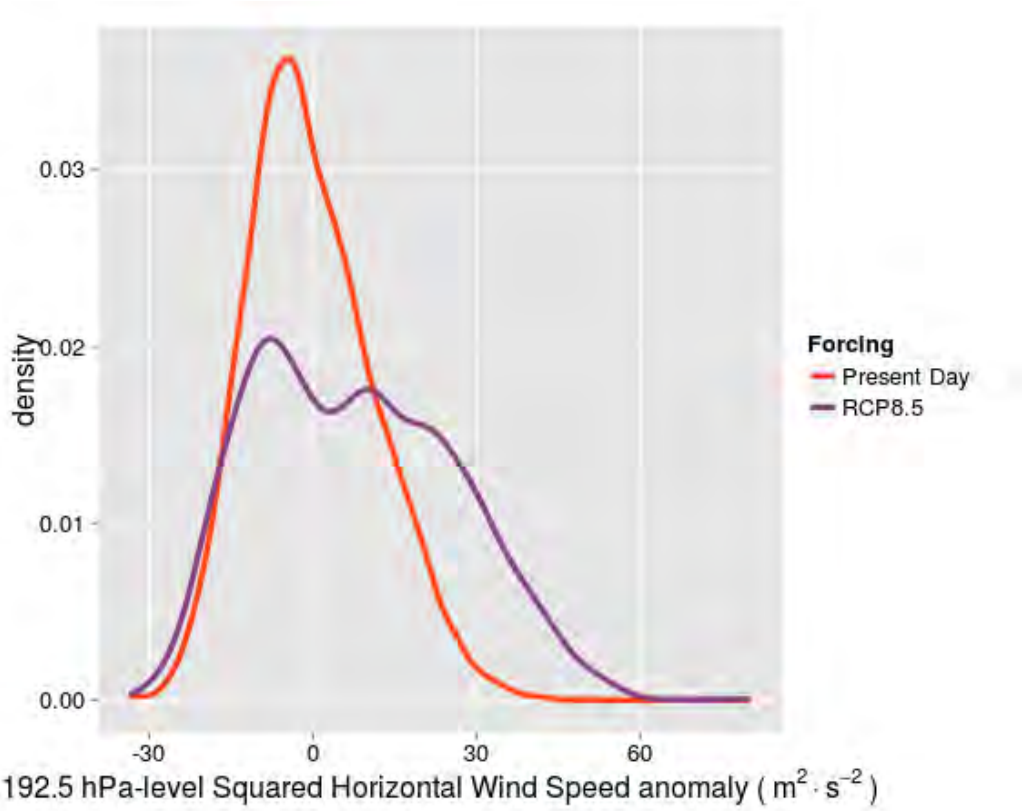

Figure 5.21: Comparison of probability density estimates (as in Figure 5.1) for WTP 192.5hPa-level squared horizontal wind speed, between CFEs and TFEs. Only the last ten ensemble years (51-60) are considered.

In contrast, over WTP, squared horizontal wind speed distributions at various pressure levels show a mode which is rarely visited in CFEs becoming much more common during the final decade of the TFEs. Figure 5.21 shows that, at approximately 200hPa, a mode involving stronger wind speeds becomes much more common under RCP8.5 forcing. Additionally, the distribution becomes somewhat wider to the left and the right, suggestive

of lower predictability of these modes underRCP8.5 forcing. Similar shifts (not shown) are also seen at lower levels.

Hence, a nonlinear dynamical systems approach, coupled with assessment of probability distribution comparisons, provides additional understanding regarding the nature of climate change experienced under RCP8.5 forcing in this model, even when considering untransformed atmospheric model output.

5.2.2 Interaction between Internal Variability and External Forcing: Influence of Macroscopic IC Differences on Trends

Generally, as might be expected, temperature trend resulting from RCP8.5 forcing for the 2005–2064AD period, proceeds at approximately the same rate in the three TFEs. Hence, ensemble mean temperature evolution curves for the TFEs appear to be locally parallel. This is illustrated in Figures 5.17 (for SSA TS and SO TAS) and 5.19 (for SML TAS). However, this is not the case for all regions. The rate of temperature increase over the Northern midlatitude ocean basin domains (NAt, NPa, NPI and NAO) and NP, is clearly greater for Yr126_RCP than for the other two TFEs. This is illustrated by NPI TS ensemble mean evolution in Figure 5.17. For SP TAS, the trend appears to increase for TFEs initialised during a later model year.

The influence of ICs on temperature trends is investigated by considering the difference between the mean temperature (TS or TAS) during the final ensemble decade (ensemble years 51–60) and the first ensemble decade (ensemble years 1–10), for each ensemble member. Differences between the sixth and second ensemble decades (ensemble years 11–20), are also computed. In other words, for each ensemble member i of each TFE, over each considered region, the following two quantities are computed:

$$\Delta T_{i,1} = \overline{T_i(51,60)} - \overline{T_i(1,10)} \tag{5.2}$$

$$\Delta T_{i,2} = \overline{T_i(51,60)} - \overline{T_i(11,20)} \tag{5.3}$$

where $\overline{T_i(t_0,t_1)}$ is the mean temperature between ensemble year t_1 and t_0, in ensemble member i. The corresponding ensemble mean quantities $\overline{\Delta T_1}$ and $\overline{\Delta T_2}$ are computed as the ensemble mean of all 50 $\Delta T_{i,1}$ and $\Delta T_{i,2}$ values for each ensemble. Tests for differences in distribution (KS tests; see subsection 3.6.6) and mean (Student's t-tests) are then conducted to assess whether there is evidence for differences in ensemble trend, due to ICs.

A number of regions show significant difference in ΔT_1 distribution between two TFEs (for example, Af and SML TAS between Yr126_RCP and Yr587_RCP: $p < 0.05$; NML, NAt, NP, NPI and NPa TAS between Yr1055A_RCP and Yr587_RCP: $p < 0.005$), where the corresponding ΔT_2 D-statistic is not significant ($p > 0.1$). This suggests that interannual-scale IC influence (see subsection 5.1.2) contributes appreciably to decadal mean regional

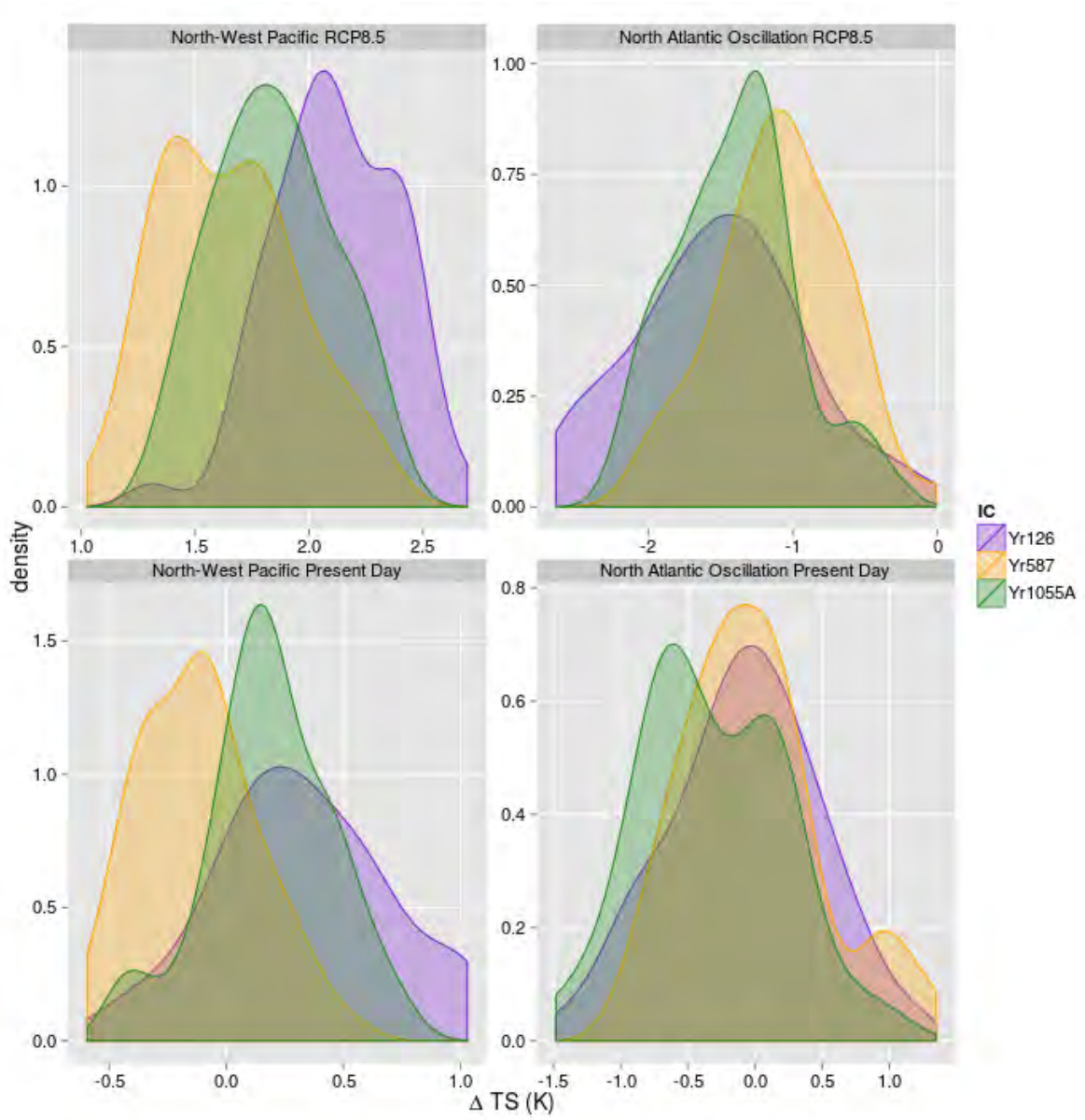

Figure 5.22: Probability density estimates (as in Figure 5.1) of ensemble member TS difference between the 6th and 1st ensemble decades, for the NPI and NAO TS indices. Distributions for the three TFEs are shown (top row), together with estimates for the corresponding CFE distributions (bottom row). Note that the scales on the horizontal and vertical axes differ

temperature changes for certain ICs. This effect is illustrated for NPI TS in Figure 5.17. The Yr1055A_RCP ensemble TS mean takes approximately 15 years before it overtakes the Yr587_RCP ensemble TS mean, which had warmer NPI ICs. PDF estimates of ΔTS_1

values for NPI and NAO TS are presented in Figure 5.22, with CFE changes also shown to illustrate the ensemble relaxation behaviour response to the imposed ICs (note the difference in axis scales and limits).

This influence of interannual-scale IC differences can mostly be corrected for by averaging over longer periods than decades, although the potential for ICs to influence statistics of change obtained in such a manner should probably be noted when considering regional climate change projections. Of greater interest, however, are the instances of large-scale IC differences apparently influencing rates of temperature change over multidecadal periods. There are two sets of regions where such IC influence is detected, in both cases when the Yr126_RCP ΔTS_2 distribution is compared to the Yr1055A_RCP ΔTS_2 distribution. The most significant differences are observed in NAO, NAt, NPI and NPa TS. To illustrate this, PDF estimates of NPI and NAO ΔTS_2 are shown in Figure 5.23.

These higher trend rates occur during a period when the Northern Hemispheric extratropics were experiencing appreciable model drift, while, over other regions of the globe, temperature trends were relatively low (see section 4.1). This is reflected in the trends observed in the CFEs over these regions (see, for example, Figures 5.17 (NPI TS), 5.22 and 5.23). It should be noted that without corresponding CFE runs, it would be difficult to correct for the additional drift-contributed trend. For example, 16% of Yr126 ensemble members show negative temperature change between the second and final decades for NPI TS. There is also a marked difference in the temperature evolution of the two PDCs over the corresponding period.

After correcting for model drift observed in the CFEs, over most regions where significant differences were previously observed, ΔT_2 is no longer significantly different between the Yr126_RCP and Yr1055A_RCP ensembles. The exception is the NAO TS index, which still shows highly significant ($p < 0.0001$) differences in ΔTS_2 between Yr126_RCP and Yr1055A_RCP. This may be indicative of low-frequency variability captured in NAO TS (see Figure 4.9 and the discussion in subsection 4.2.3), which interacts nonlinearly with applied external forcing. Whether or not such nonlinear interaction between ICs and forcing response occurs in this model—or in CSMs more broadly—this result indicates state dependence of the model system response to forcing, albeit in a rather artificially defined and not commonly used climate "index".

In contrast to the Northern Hemispheric cases, ΔTAS_2 over SP is significantly lower ($p < 0.05$, for both Kolmogorov-Smirnov and t-tests) for the Yr126_RCP ensemble than the Yr1055A_RCP ensemble. It is notable that over SP virtually no interannual-scale IC influence beyond the first ensemble year is observed in any ensemble. Interquartile range is essentially constant throughout all ensemble periods (not shown). Also, little significant temperature variability occurs in this domain. Accordingly, observed differences are unlikely to reflect interaction between internal modes of variability and forcing; rather it suggests a relatively weak, but detectable state dependence in model response to forcing. This conjecture is supported by the ΔTAS_2 values being lower for Yr126_RCP than Yr587_-RCP, for which the value is, in turn, lower than for Yr1055A_RCP. Possibly an ice-albedo

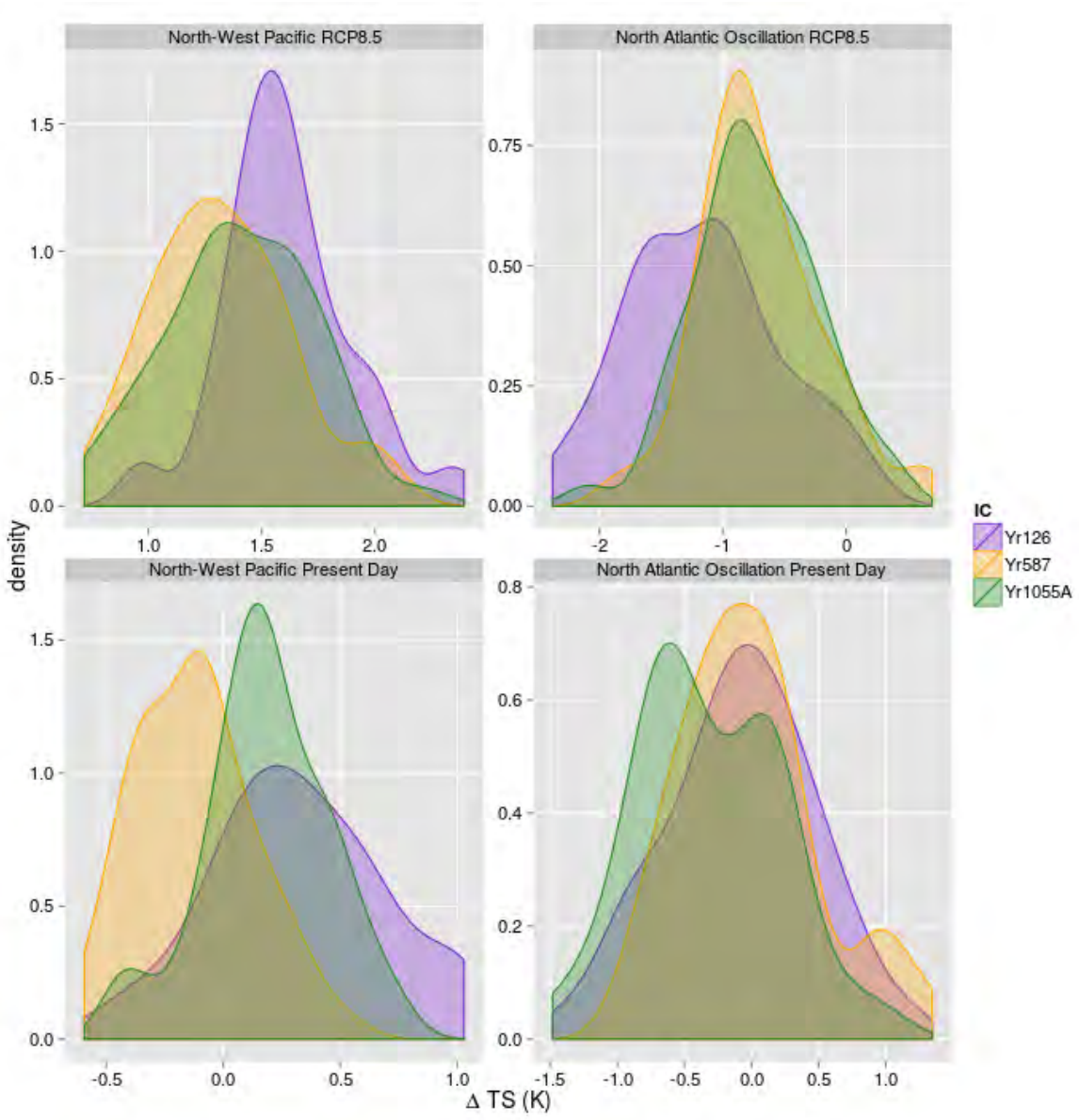

Figure 5.23: As in Figure 5.22, but showing differences between the 6th and 2nd ensemble decades.

feedback is at play, leading to slightly earlier accelerated warming over regions of the Antarctic covered in sea ice. More TFEs would be required to make robust conclusions.

It should be noted that multiple comparisons have been conducted in this section, so that it is to be expected that on average 1 in 20 comparisons will be significant at the 5% level. Hence, only results that are highly significant, or results from a selection of tests that produced significant results appreciably more often, are commented on.

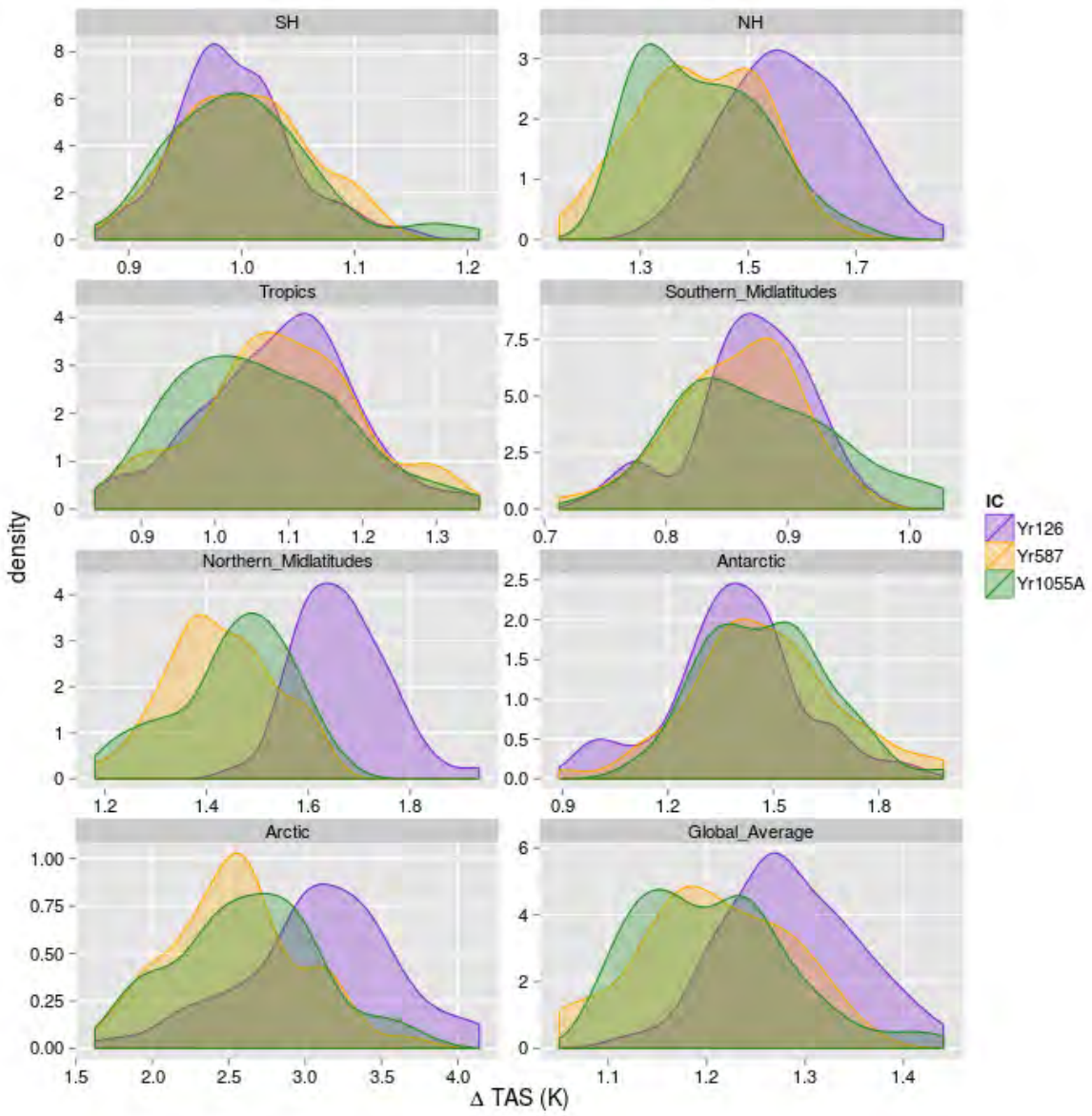

Figure 5.24: As in Figure 5.23, but for Latitudinal Bands and showing RCP ensembles only.

It is also notable that there is considerable spread ($\sim 15-50\%$ of the mean) in the 40-year change in decadal mean temperatures between ensemble members over all regions, including GI. This further underscores the value of using IC ensembles in climate change projections, as also noted in Kay et al. (2014). Decadal averages sample shorter periods than are usually used to compute temperature change, but, due to the rapid trends in the TFEs, averages and other distributional statistics computed over longer periods are unlikely to be representative of the variable possibility space for a given year. Compare,

for example, the rapid change in ensemble TAS TFE distributions for years a decade apart in Figure 5.19).

5.3 Comparison of Ensemble Results

In this section, a comparison between results of different ensembles is presented, together with a discussion of the evolution of ensemble distributions across ensemble time.

As noted in subsection 5.1.1, there appears to be a model time-dependent "climatological distribution", towards which ensemble variable distributions tend to converge, as they evolve away from distributions centred around their ICs. Comparing the CFE and TFE distributions for ensemble years 41-60 (Figures 5.1 and 5.2), regional differences in the drivers of the most significant differences in climatological distributions are apparent. Over each domain, different ensemble distributions appear to cluster into groups of similar states (discussed in relation to CFEs in subsection 5.1.2). Depending on the region, the number of such "distribution clusters" varies between 2 and 6. Broadly, differences in distribution clusters arise as a result of: (a) intercentennial-scale IC influence (see subsection 5.1.2); or (b) differences in forcing scenarios. The relative importance of these drivers also varies substantially by region; IC influence is relatively unimportant in lower latitudes, especially in the Northern Hemisphere. However, in the Southern Hemispheric extratropics IC influence is much greater. For example, over SSA, intercentennial-scale IC influence is even comparable in magnitude to the effects of about 50 years of strong external forcing (RCP8.5).

In the Southern Hemispheric extratropical domains, there generally exist three distinct distribution clusters for each of the two forcings used: a colder state, further removed from the other two, corresponding to an early, quasi-stable state (see section 4.1); a warmer intermediate state to which the ensembles initialised at the end of the 6^{th} model century converge; and a third state that ensembles initialised later appear to cluster around. In the Northern Hemispheric extratropical domains, the first of these clusters is easily distinguishable from the other distributions, but further distinctions among CFEs are difficult to discern. In fact, only Yr647 distributions are generally distinguishable from the other "warm" ensemble distributions. The nature of the shift in location of distributions observed with this ensemble is discussed further in subsection 5.1.2 and other aspects of the ensemble behaviour in subsection 5.1.4.

Because two decades of data are used for Figures 5.1 and 5.2, there is an apparent widening and flattening of most of the regional TAS distributions of TFEs. This occurs as a result of shifts in the position of the TAS distributions occurring during the sampling period, due to strong trends (see section 5.2). This effect is greatest where the trend is most pronounced when compared to internal variability; over SSA for example, the flattening remains pronounced even when only a single decade (such as the fifth or sixth) is considered (not shown). A shift is already apparent when looking even at distributions

over only the first decade (not shown).

The widening and flattening of distribution does not occur in ETP TAS; in fact, there is even an apparent narrowing of the distribution over this domain, as a result of a shift from a bi- to a more unimodal distribution of certain ENSO-related indices, in response to the changing external forcing (see subsection 5.2.1). This "merging" of modes in the distribution is clearly illustrated in both the SA and Af TAS distributions (Figure 5.2).

Distributions over the first ensemble decade tend to vary considerably between ensembles and are strongly determined by ICs. CFEs and TFEs with equivalent ICs tend to have similar distributions. Often interannual-level IC influence is greater than intercentennial-scale IC influence. This is illustrated in Figure 5.10.

Some sets of ensemble distributions, initialised from similar or equivalent model years are substantially different until some time in the third ensemble decade. Corresponding differences in ensemble mean are illustrated for SO TAS, NPI TS and SSA TS between ensembles Yr186A and Yr186B; and for NPI TS between ensembles Yr876_CHPC and Yr876_NERSC, in Figure 5.17. Accordingly, interannual-scale IC influence is, for certain ICs over certain domains, detectable in the mean for much longer than in the inter-quartile range. This finding is consistent with Teng and Branstator (2011).

Over the ensemble duration, ensemble spread generally increases, roughly as $R_0 e^{-kt} + R(1 - e^{-kt})$, where R_0 represents the initial spread, R the spread when interannual-scale IC influence has decayed to 0 and k some characteristic time decay rate. This is illustrated, for example, by Af TAS in Figure 5.20. The ensemble width tends thus to broaden around a decaying ensemble mean anomaly "signal". For certain ensembles, notably Yr587 and Yr1065, years with considerably lower spread occur as far into the ensemble duration as year 15, especially over the tropics.

For certain regional variables, the ensemble interquartile range, considered as a function of time, appears to evolve as an inverted "u" shape. SML TAS in Figure 5.20 shows this pattern for both CFEs and TFEs. This would suggest that ensemble spread initially increases, for approximately 20 years, before decreasing again until the end of the ensemble length. This occurs with various CFEs and TFEs. It is noted in subsection 5.1.2 (illustrated in Figure 5.5) that the amplitude of oscillation of the ensemble mean often decreases around the middle of the ensemble period, before increasing again, somewhat. Together, these factors suggest an increase in predictability related to modes of variability, towards the end of the ensemble period, even in the absence of external forcing. However, numerous other factors may be at play.

One factor that may relate to this apparent increase in predictability is distributional skewness, which is exhibited by numerous variable-region combinations (see subsection 4.2.2). In these cases, interquartile range will be dependent on ensemble mean state. Accordingly, if the evolution of the ensemble mean has a component which is predictable throughout the ensemble duration, it may appear to modulate the ensemble spread. If the ensemble starting times, which were generally chosen to represent unusual

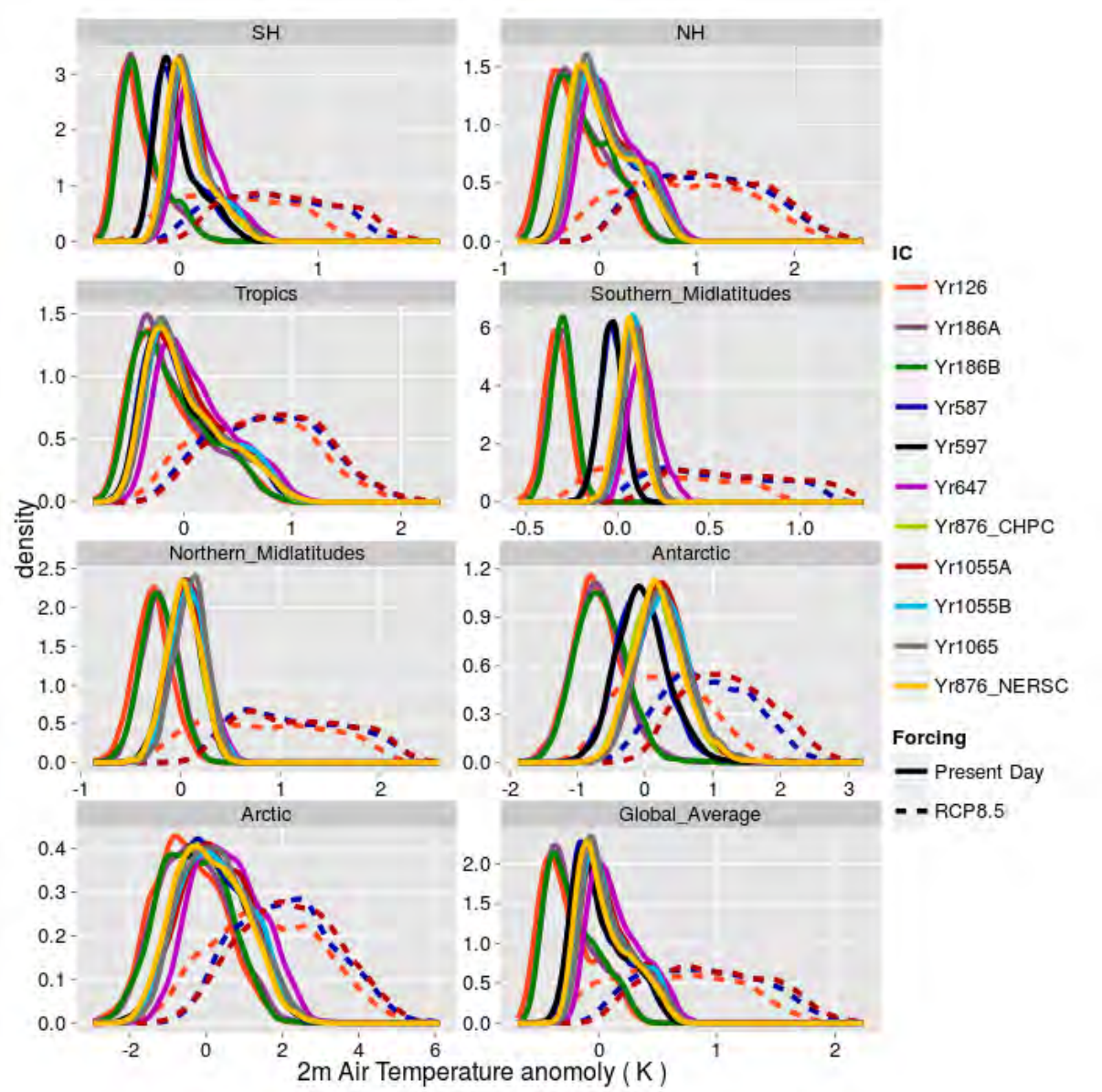

Figure 5.25: As in Figure 5.1, but including data for all but the first decade of each ensemble.

or anomalous years (see subsection 3.5.3), tend to coincide with a particular state of a low frequency mode of variability, with a high degree of skewness associated with its regional expression in atmospheric variable time series, this could explain the above discussed feature. Support for this hypothesis is gained from the observation that inter-ensemble variation in interquartile range tends to peak between ensemble years 15-30. This is illustrated by Af and SML TAS interquartile ranges in Figure 5.20.

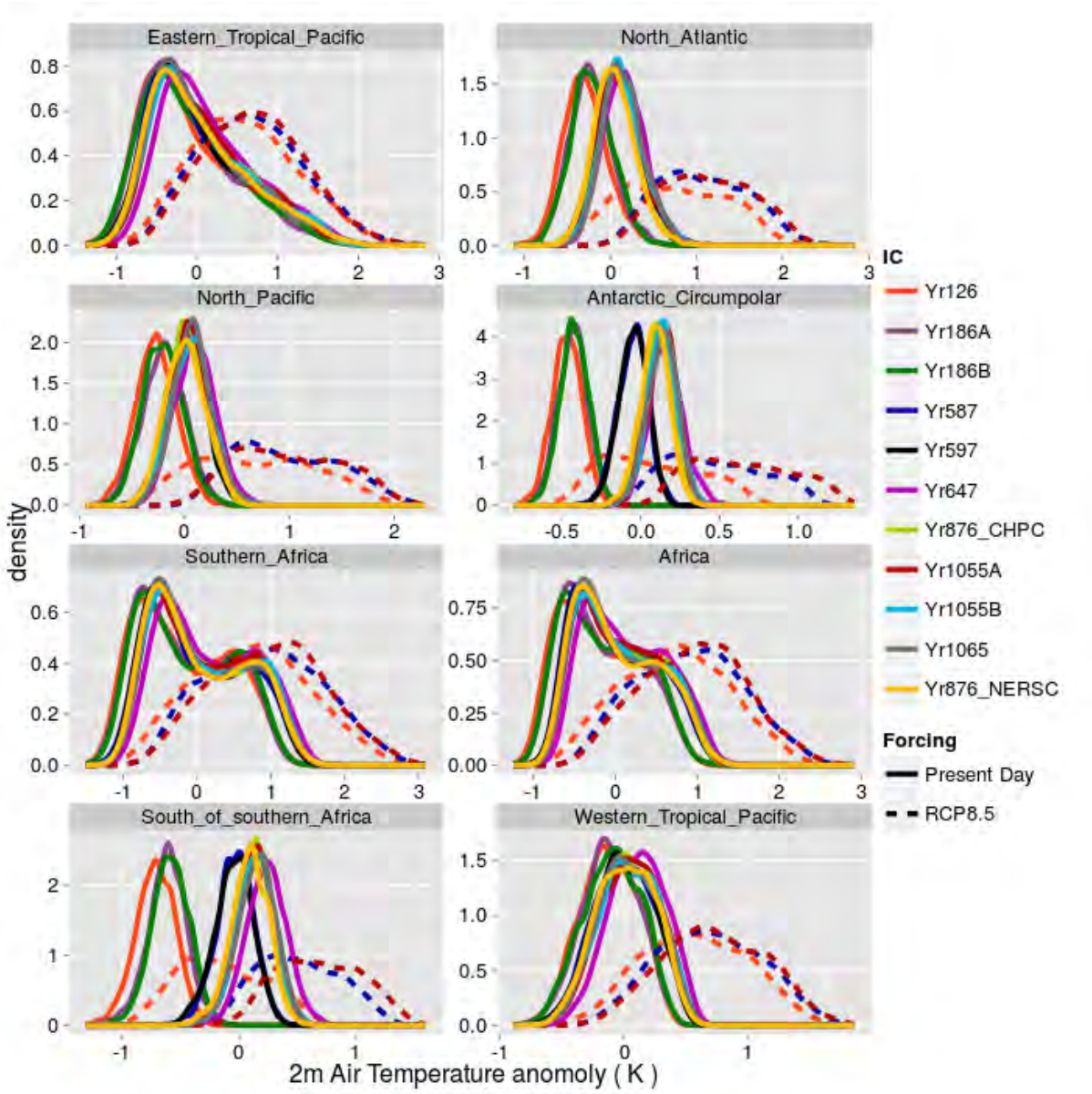

Figure 5.26: As in Figure 5.2, but including data for all but the first decade of each ensemble.

In the final ensemble decades, differences between distributions of two different ensembles, initialised at a similar (for example, ensembles Yr587 and Yr597 and ensembles Yr1055A and Yr1065) or equivalent (for example, ensembles Yr186A and Yr186B, ensembles Yr876_CHPC and Yr876_NERSC and ensembles Yr1055A and Yr1055B) model time, distributional differences are minor ($D \approx 0$). Even when considering distributions over all ensemble decades other than the first (see Figures 5.25 and 5.26), deviations from this

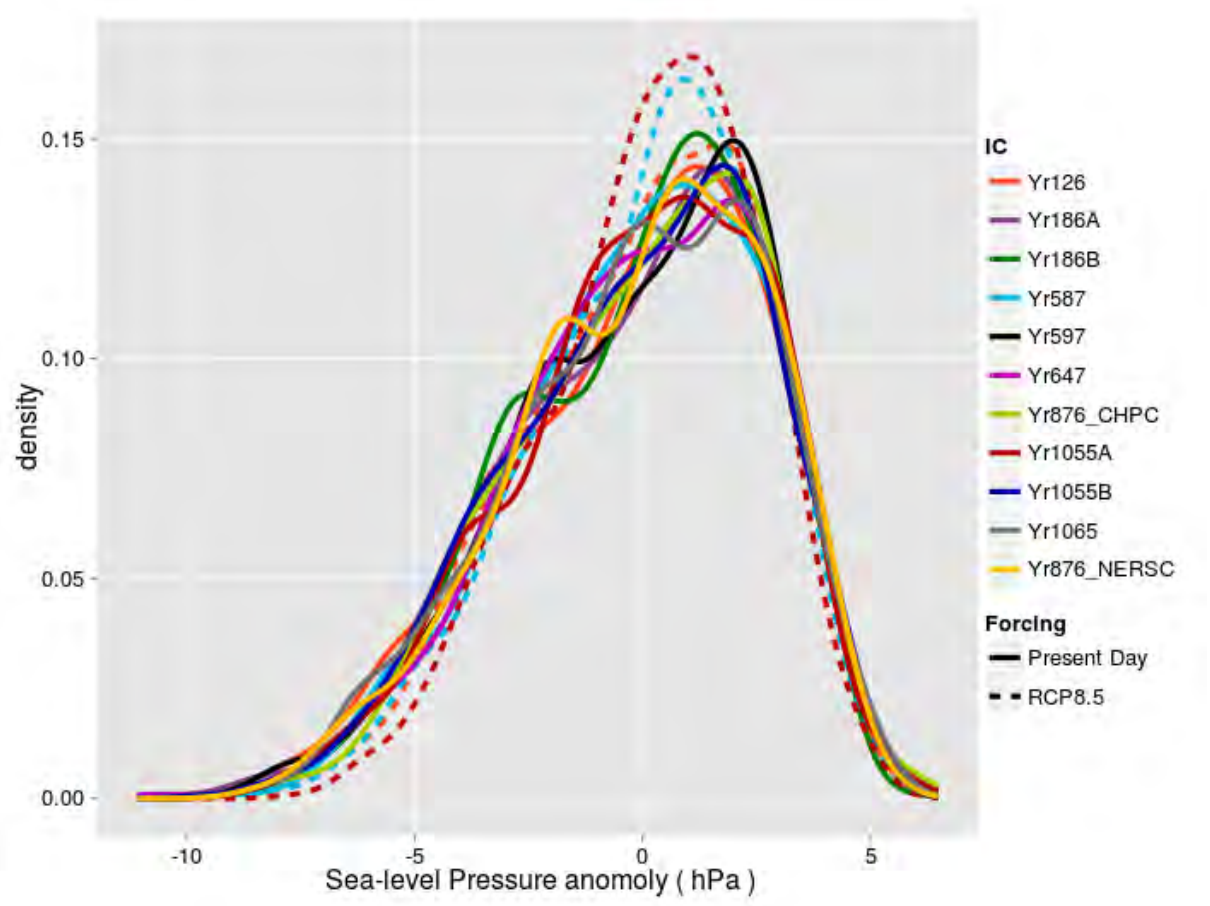

Figure 5.27: As in Figure 5.1, but for PSL difference across the North Atlantic, as defined by the NAO index latitudes.

apparent climatological distribution are relatively small for CFEs.

For TFEs, in considering 50-year TAS distributions, almost all distributional attributes are indiscernible. Trend in mean and median values over the period of consideration lead to a flattening and smoothing of ensemble-temporal distributions, hiding bimodality (for example, see the Northern Hemishpere (NH) and SH panes in Figure 5.25) and skewness (for example, see the ETP pane in Figure 5.26). Generally, TFE ensemble temporal distributions taken over multidecadal periods produce broad, "flat" sections in distributions for which temporally local temperature is roughly normally distributed (as in the SML and NML TAS panes in Figure 5.25). Thus, it would appear that TFE distributions have become broader, when, in fact, as shown in subsubsection 5.2.1.1, a number of distributions become narrower in response to imposed forcing.

Certain variables (although this is never the case for temperature) show little change in distribution between CFEs and TFEs. This is the case for the (influential, see section 4.2)

NAO PSL index, especially for the Yr126 ensembles. In the other two TFEs, it appears that the ensemble distribution becomes somewhat narrower towards the end of the period, when only the final two ensemble decades are considered (as shown in Figure 5.27). However, compared to within-ensemble (between ensemble member) differences, between-ensemble differences are still slight; qualitatively there is little change.

The difference, between Yr126_RCP and the other TFEs, in distributional shape change, suggests a possible state-dependence in the influence of the external forcing on the NAO PSL index distribution (i.e. an IC influence on TFE distributional change). The difference in distributional shape change appears to be larger than differences between CFEs (see Figure 5.27). However, the change is relatively minor.

Chapter 6

Implications for Climate Prediction and Model Experimental Design

In this chapter, implications of results from chapter 5 are discussed, in the context of ideas presented in sections 1.3, 1.4, 2.1 and 2.2.

In section 6.1, results are discussed in the context of IC influence and predictability. In section 6.2, matters explored in section 2.1 are re-examined in light of results described in chapter 5. Limitations and recommendations for furthering the investigation conducted here is presented in section 6.3. Some of the advantages of ensemble simulations in climate modelling studies, which come to light in this study, are highlighted in section 6.4. A brief assessment of the outcomes of the conceptual component of the work is given in section 6.5.

6.1 Levels of IC Influence

IC influence in CFEs is explored in depth in subsection 5.1.2. The influence of ICs on subsequent temperature changes in TFEs is described in subsection 5.2.2.

The nature of the differences in distribution produced by the different ICs used in CFEs, suggests that meaningful distinctions exist between at least three levels of IC influence. On the smallest scale, there are IC differences that could be considered microscopic: no finite improvement in knowledge of the (initial) system state could meaningfully reduce related uncertainties about the subsequent evolution of climate system trajectories, beyond weather time scales. After a month, the "distance" in state space between two ensemble members is essentially independent of their initial separation—the only relative IC information maintained is the fact that the initial separation was microscopic. The precise nature of microscopic IC differences—small atmospheric field perturbations, in this study—appear to have negligible influence on variable climatological distributions. Here, variable

climatological distributions are defined as decadal-scale or longer ensemble-temporal distributions, using sufficiently large ensembles—the approach taken in subsection 5.1.1. However, as a result of almost-intransitivity, significant differences between temporal distributions over a single run—or small ensemble—and the climatological distribution, may occur (see subsection 5.1.3).

Intermediately, there is IC influence referred to as being of interannual scale. IC differences at this scale influence the evolution of ensemble distributions on time scales up to a couple of decades. Such differences can be obtained by selecting different model years to use as model system ICs. The resulting interannual-scale IC influence may result from aperiodic and/or quasi-periodic modes of variability, memory of the state or phase of which is captured in the ICs. These two Factors (see page 82) are postulated to produce distinct "footprints" on ensemble evolution. Potentially, one could consider the resulting IC influences as distinct scales of influence. However, further investigation into the relationship between underlying mechanisms of variability and ensemble evolution, would be required to justify such a distinction and make it precise.

Potential predictability, as defined in section 1.3, when considered on decadal scales, is strongly associated with interannual-scale IC influence. In particular, IC influence is also expressed through the three changes in variable probability distribution character described in subsection 5.2.1. As was found by Branstator and Teng (2010) and Teng and Branstator (2011), when predictability—or interannual-scale IC influence—persists for longer than a decade, it is reflected primarily in the location of ensemble distributions, as quantified by the ensemble mean. The temporal range of interannual-scale IC influence on ensemble mean is dependent not only on the regions and variables considered, but also on the model system ICs applied (see, for example, Figure 5.5). Reduced ensemble spread—quantified by variance or a specified percentile range—is rarely detectable beyond six or seven years. This is particularly relevant because, as pointed out by Teng and Branstator (2011), ICP is commonly conceptualised in terms of reductions in ensemble spread.

Changes in regional-scale temperature in response to RCP8.5 forcing applied over a number of decades, when considered relative to the first ensemble decade, can also be significantly affected by interannual-scale IC influence (see subsection 5.2.2).

Stainforth et al. (2007a) distinguish between microscopic and macroscopic ICU, based on the "mixing scales" of particular climate system variables. Implicitly, one might consequently expect that changes to a given variable should result in IC influence at a well-defined scale. However, two results obtained here—admittedly both derived from rather extreme and unrealistic scenarios—suggest otherwise. Most Yr1055B ensemble members—to which a much larger atmospheric temperature perturbations were applied (see Equation 3.2)—behave, as far as can be deduced from monthly- and annual-mean atmospheric variable evolution, essentially as the members of Yr1055A. However, 4 of the ensemble members are much warmer than the rest of the ensemble for 3–4 years; "memory" of the particularly cold ICs at initialisation appears to have been lost, in these cases,

within a month (see Figure 5.3). In Yr647, one of the ensemble members cools down much more rapidly than the other 49 (see subsection 5.1.4).

Together, these two results suggest that atmospheric variable perturbations can, under certain circumstances, lead to effective destruction of interannual-scale IC influence. In effect, then, one cannot determine with certainty the scale of IC influence a particular IC perturbation will result in, prior to running the corresponding model simulation. One could, however, determine probabilities that particular scales of IC influence would result from a given perturbation. Such estimates could be based on the nature of the perturbation imposed, the "stability" of the state relative to which the perturbation is imposed and perhaps other factors. Based on the evidence considered, in the case of small atmospheric IC perturbations, the probability that the corresponding IC influence would be microscopic is very large ($\gtrsim 0.99$). The prior uncertainty would appear to be greater when the perturbations tend to impose unstable atmospheric states.

At the largest scale investigated in this study, there is IC influence that dictates the model's (multivariate) climatological distribution. Corresponding IC differences—obtained by using ICs from different model centuries, for example—can result in profoundly different ensemble variable distributions, although primarily because of differences in distributional location (as measured by ensemble mean). This level of IC influence is referred to as being of intercentennial scale. It can be influential in determining multidecadal-scale rates of regional-scale ensemble mean temperature change in response to external forcing (see subsection 5.2.2).

It could be argued that such IC influence is primarily the consequence of model drift (see subsubsection 2.2.3.2 and section 4.1) and that it is therefore of little relevance in a theoretical or observational context; in other words, that intercentennial-scale IC influence is simply an artefact of model inadequacies. However, Yr647 output suggests that (see subsection 5.1.2 and subsection 5.1.4) intercentennial-scale IC influence could also result from distinct forcing trajectories, i.e. some "memory" of the evolution of past states. Uncertainties regarding the state and nature of slowly evolving components of the climate system could potentially also result in IC influence of this kind. Additionally, it is usually not trivial to distinguish between model system behaviour resulting from drift (for which no universally accepted definition appears to exist), and that resulting from slowly evolving components of the system.

Lovejoy et al. (2013) claim that presently used CSMs do not capture the regime of climate system variability referred to as "macroclimate" (see subsubsection 2.1.3.3). It is thus unlikely that intercentennial-scale IC influence found here is a consequence of the same processes. However, given that macroclimate evolution is likely related to internal variability in climate system states (Lovejoy, 2014), if a model were capable of reproducing this regime of climate system behaviour, it would likely exhibit characteristics of intercentennial-scale IC influence.

6.2 Implications for Defining Climate

In this section, different approaches to conceptualising and quantifying climate (see section 2.1) are reconsidered, in the light of results of this study. The focus is on a modelling context. In subsection 6.2.1 broader questions regarding definitions of climate are addressed, whereas subsection 6.2.2 considers numerous parameters, the values of which need to be fixed in order to make definitions of climate precise.

6.2.1 Approaches to Quantifying Model Climate

As noted in section 6.1, effectively, an ensemble-temporal definition of variable climatologies is applied in assessments made about the model climate in subsection 5.1.1. Following arguments presented by Werndl (2015), discussed in subsubsection 2.1.3.1, the use of distributions to characterise the climate is preferred. In a—necessarily theoretical—constant forcing context, an ensemble-temporal definition is found in this study to provide the most useful characterisation of model climate, for both theoretical and practical reasons. Relative to a definition considering an IC ensemble at a particular time (an ensemble definition), it has the advantages that it allows:

1. the distribution to be taken over a larger sample of data, which is particularly useful when only relatively small IC ensembles are available; and
2. the varying influence of at least partially predictable decadal- to interdecadal-scale quasi-periodic modes of variability to be sampled for the definition, as Lorenz (1995) suggests should be done (see subsubsection 2.1.4.4).

There are also advantages compared to using temporal definition (i.e. considering single model runs in isolation) distributions. These include computational advantages (Wittenberg et al., 2014, as discussed in subsubsection 2.2.1.3). Additionally, the potential, unpredictable influences of almost-intransitivity and long-term persistence (see subsubsection 2.1.5.1 and subsubsection 2.1.4.4) are reduced, especially with larger ensembles. Long-term, predictable IC influence, if it is found to occur in a particular model set-up, can also be better isolated temporally, at relevant lead times.

Under more realistic, transient forcing conditions, ensemble distributions at a single point have the advantage that trends do not distort their shape, as occurs when temporal or ensemble-temporal distributions are used. Examples of this are discussed in section 5.3. If ensemble-temporal distributions are taken over sufficiently short periods, however, it should be possible, in most circumstances, to approximate long-term trends as being locally linear. Consequent detrending could thus be applied to time series prior to constructing distributions. A climatological distribution thus produced can then be adjusted for the

influence of trend, if a distribution for a particular time is desired. On more local scales—which are the most relevant for decision-making (e.g., Oreskes et al., 2010; Frigg et al., 2015)—internal variability is likely to dominate forcing signals on decadal time scales (Deser et al., 2012a).

In subsubsection 2.1.5.3, it is noted that correlation between variable states is an important aspect of climate characterisation. As a definition of a model system or subsystem (see subsubsection 2.1.4.1) climate, a multivariate distribution of the relevant variables (see also subsection 6.2.2) has the advantage of allowing quantification of associations between variables. Such joint probability distributions can be derived from temporal, ensemble or ensemble-temporal data. Quantifying associations is particularly important when considering climate indices, modes of variability and teleconnections (e.g., Alexander et al., 2014; Dong and Dai, 2015). In addition to statistical information derivable from multivariate distributions, autocorrelation is also sometimes valuable for climate characterisations (see subsubsection 2.1.5.2). However, this requires time series data to be available (i.e. it is not derivable from ensemble-only distributions).

Hence, it is suggested that ensemble-temporal multivariate distributions together with measures of autocorrelation, be used as quantification of model climates. This definition is by no means precise. Some of the factors that would need to be taken into account in fixing various parameter values required to do so, are considered in subsection 6.2.2. Such decisions are likely to vary depending on the context and aims towards which the definition is to be applied.

Ensemble-only distributions may be predictively valuable with lead times up to decades hence, even in the absence of varying external forcing. Even if an ensemble-temporal definition is preferred (see subsection 6.2.1), an ensemble-only multivariate distribution could provide additional value in a prediction context (see also Werndl (2014a, 2015)).

It should be noted that multi-model ensemble distributions (see subsubsection 2.2.1.3) do not translate directly to quantification of model climates (Daron and Stainforth, 2013), in part because data obtained thus cannot be considered to have been sampled from the same distribution. In other words, one is not capturing the same "climate". In addition, statistical difficulties arise, because the nature and extent of internal variability differs substantially between models (e.g., Brown et al., 2012). However, multiple models and/or a range of parameterisations, are required to adequately sample uncertainty in climate projections (Stainforth et al., 2005, 2007a; Haughton et al., 2014).

All ensemble-based definitions have the disadvantage that they are not directly applicable to—or comparable with—observed climate quantifications, which necessarily take the form of temporal distributions and associated statistics (e.g., Werndl, 2015, see also, subsubsection 2.1.5.1). This incomparability is due to the likelihood of failure of the kairodic assumption (see subsection 5.1.3) and the likely nonlinear—and hence not easily detectable—transient forcing signal in observed data.

6.2.2 Determining Precise Definitions for Climate

In subsection 5.1.3 it is shown that round-off order changes in ICs can produce regional annual-mean climate trajectories differing significantly from one another, under constant forcing. Where quasi-periodic variability (see subsubsection 2.2.2.1) is dominant, such as over the tropics and subtropics in the present model (see subsection 4.2.1 and subsection 5.1.2), this occurs rarely. However, where variability is essentially aperiodic, such as over the Southern Hemispheric extratropics, 60-year climate variable distributions often (in up to $\sim 30\%$ of cases for TS) are detectably different from one another and the overall ensemble distribution (see Table 5.1). Over NML and NH ocean basins, where aperiodic and quasi-periodic variability are both apparent, ensemble member distributions also frequently (in up to $\sim 20\%$ of cases for TS) differ significantly. Furthermore, ensemble distributions for a particular ensemble year or decade sometimes differ significantly from ensemble member temporal distributions. This is particularly true for years in the first ensemble decade, when predictability related to interannual-scale IC influence is present. The tendency for such differences to occur also varies between variables and ensembles.

Based on these findings it is concluded that:

- The time period required to capture a predictively useful temporal climate distribution may vary spatially, and depend on the spatial-scale of aggregation.
- Centennial-order periods may, for certain regional variables, be required to adequately characterise the variable probability distribution from a single time series, in a system with similar characteristics to the one investigated here. Similar findings are reported by Daron and Stainforth (2013).

It should be noted that the above applies primarily in the context of fixed forcings.

When deciding on lead times (see subsubsection 2.1.3.2) to use in ensemble studies, or temporal sampling and averaging periods to use in temporal definition, the above and numerous other context-specific factors would likely need to be taken into account. The order to which autocorrelation values need to be computed also warrants consideration, but is beyond the scope of this work.

How large an ensemble is required for quantification depends on a number of factors. These include the temporal sample size to be used, the region and variables of interest, the nature of climate variability in the model considered and the attributes of the distribution that are of primary interest. However, the results presented in subsection 5.1.3, subsection 5.2.2 and section 5.3 indicate that, under rapidly evolving external forcing, quantifications based on small ensembles ($\lesssim 5$) could, with non-negligible probability, lead to substantial misrepresentation of the climatic possibility space (see subsubsection 2.1.4.2).

Subsystems of the climate system might act, at least at times, as relatively isolated low-dimensional systems (see subsubsection 2.2.1.4). Hence, characterising regional climates

using a multivariate distribution of indices known to be important drivers of climate, may be a valuable avenue to explore. At local scales, variables relevant to human activity in the area are perhaps best considered in producing climatological distributions. On global scales, in certain contexts, a low-dimensional characterisation in terms of the most important predictable determinants of future global climate possibility space, could serve as a quantification of climate, when conceptualised as in Notion (N4) (see page 17).

However, as discussed in subsubsection 2.1.5.3 and subsubsection 2.2.1.4, it is not clear which—or even how many—variables are required to characterise climate, at local, regional or global scales. This is true even for low-resolution climate models, as the dimensionality is still very high (e.g., Daron and Stainforth, 2013). Consequently, it is highly nontrivial to determine which variables are required for a sufficient characterisation of a model or subsystem climate, for example. Whilst outside scope for this work, exploring this question further would be a worthwhile endeavour for improving approaches to quantifying model climates (see also the Recommendations on page 128).

6.3 Limitations and Future Directions

The primary limitations of this study, of which the authors are aware, are summarised by the following key points:

Limitations

1. To limit computational expense, a very coarse resolution finite volume dynamical core is used—a numerical approach which is very rarely applied, for reasons discussed in subsection 3.2.2.

2. The analysis involves the model's atmospheric output only. More slowly varying components of the model climate system, such as the ocean and sea ice, could likely provide more information regarding low-frequency variability, longer-term predictability, IC influence and their associated mechanisms.

3. Only annual-mean regional-mean quantities are considered.

4. The analysis methodologies applied are exploratory, limiting the scope for robust conclusions to be drawn.

These numerical and analysis approaches taken, make it difficult to discern the influence of model inadequacies from factors of central theoretical importance in exploring conceptualisations and quantifications of the climate system state. This is discussed briefly in relation to intercentennial-scale IC influence in section 6.1.

In relation to Limitation (1), it is noted briefly in section 4.2 that the extent to which model variability is dominated by its ENSO variability is unrealistic. Again it should be emphasised that this study is performed under the perfect model assumption (see subsubsection 2.2.2.4). Hence, extensive model validation is not conducted in this study and in particular, direct comparison to observations is not done. However, it should be noted that the model ENSO is qualitatively distinct from observed ENSO; for example, variance (s^2) is much too large for all Niño TS indices and frequency (ν) too low (compared to, for example, An and Wang (2000); An (2009)). The analysis of variability here is performed in the perfect model scenario (see subsubsection 2.2.2.4) and hence these differences are ignored. However, they do limit the extent to which one can infer from the ensemble behaviour documented in section 5.1, likely characteristics of (a) CSMs/ESMs used for predictive purposes; and (b) the real climate system.

In relation to Limitation (2), analysis of OHC to various depths could contribute valuable understanding of the nature and rate of model drift, as distinct from internal processes that could have counterparts in the real climate system. In this regard, analysis of radiative energy budgets could also be useful. Understanding of the model state at ensemble initialisation that gives rise to different degrees and types of ICP, would also benefit from assessment of spatial patterns of (near-surface) ocean state. Knowledge of sea-ice state at initialisation and evolution of sea-ice patterns—particularly for Yr647 (see subsection 5.1.4)—could allow for more robust attribution of ensemble behaviour to underlying mechanisms.

To address the above limitations, it is recommended that the following approaches be attempted:

Recommendations

1. Perhaps most crucially, a similar experimental design should be tested on a low-resolution spectral element model configuration, which has been more widely validated. Thus it could be determined whether the system behaviour found in this study is an artefact of a potentially inconsistent or unbalanced (e.g., Dijkstra, 2013, chapter 6) discretised model formulation.

2. Employ alternative IC sampling approaches to explore potential additional scales of IC influence and begin to better understand delineations between them.

3. Apply the exploratory analysis techniques from this study to the high resolution earth system ensemble output of Kay et al. (2014), much of which is freely available (see subsubsection 2.2.1.3).

4. Perform analysis on data with higher temporal resolution. This would require approaches to be used to remove the seasonal signal, or alternatively, for separate analyses to be conducted by season or month (as in, for example Deser et al. (2004)

or Thompson et al. (2011)). This would allow for consideration of implications of periodically varying forcing on the conceptualisation of the climate system as an attractor-like entity in some state space.

5. Explore IC influence on ocean and sea ice ensemble evolution.

6. Run control simulations for sufficiently long that model drift becomes negligible and then determine the most different (a) atmospheric, (b) ocean boudary-layer, (c) deep ocean and (d) sea ice states of the system, at regional and global scales. CFEs and TFEs can then be run from the corresponding ICs. One can also test whether interactions between ICs and forcing are still detected.

7. Conduct spatial analysis. The exploratory statistical techniques used could then be applied to series which reflect prominent modes of variability of various components of the model system.

8. Apply more rigorous nonlinear statistical analysis techniques. For example, in an attempt to detect potential signs of chaos bred vector (BV) analysis could be applied, such as in Tang and Deng (2010), and originally in Toth and Kalnay (1993, 1997). More advanced measures of predictability, such as the measure of Kleeman (2002), applied in, for example, Branstator and Teng (2010), could also be employed. This could also be useful in detecting different levels of IC influence. Network-related approaches (e.g., Tsonis and Swanson, 2012; Tantet and Dijkstra, 2014) to studying interactions and evolution of the climate system, could potentially also be studied in an ensemble context.

9. Use different forcing pathways and subsequent constant forcing runs to assess the path independence assumption for forcings, as in Daron and Stainforth (2015). This would complement the work of, for example, Andrews et al. (2015) in a large ensemble context, at lower resolution.

10. Extend the conceptual component of the study by considering the role of multi-model and varied-parameter ensembles (e.g., Haughton et al., 2014) in quantification and conceptualisation of climate in a broader context.

6.4 Implications for Model Experimental Design and Interpretation

Numerous advantages of IC ensemble simulations, illustrated by results of this study, are discussed in this section. The intention is to support the position that, in a transient forcing context, in addition to the numerous other avenues being investigated to quantify and explore uncertainty in climate projections, large IC ensemble experiments could be a valuable tool to advancing our understanding of the climate system. This is particularly

true in the context of quantifying climate (as discussed in section 6.2) and understanding evolving climate model possibility space. Another important application of IC ensembles in climate science is in climate change attribution (e.g., Stone et al., 2007), the study of which can be made more robust through the use of IC ensembles (Stone et al., 2009).

A precise ensemble-based definition of time to "emergence" (e.g., Mahlstein et al., 2011; Hawkins and Sutton, 2012, see also subsubsection 5.2.1.1) should allow one to detect critical climate changes more robustly. Because statistics sensitive to non-normality, such as variance, need not be employed, this approach should also be less sensitive to the nature of local variable distribution characteristics. An approach similar to Mahlstein et al. (2011) could also be used, in which distributions from a base period and a transient run are compared using KS D statistics (as in subsection 5.1.2). Using ensemble statistics considered over—perhaps—a decade, would allow for larger sample sizes and suffer lesser influence from almost-intransitivity and nonlinear variable responses to external change.

Ensembles are also shown in section 4.1 and subsection 5.2.2 to be useful in quantifying the role of model drift in the variable evolution. In the present study, there is little evidence of predictable internal modes of variability on centennial-order ($\sim 60 - 200$yr) time scales. In this context, a pronounced ensemble mean signal of a sufficiently large ensemble—persisting well beyond three ensemble decades—is presumably a consequence primarily of model drift. More generally, quantifying a signal using the ensemble mean—or a histogram of ensemble member responses—of a large IC ensemble could prove to be valuable, for example in regional climate change projections (O'Brien et al., 2011). This is particularly true for model variables which display almost-intransitivity (Lorenz, 1968).

Ensemble results from this study also suggest that at local to regional spatial scales, significant—relative to interdecadal- to multidecadal-scale internal variability—drift can continue to occur, even when global mean temperatures stabilise. This could have important implications for attributing and interpreting regional-scale changes in longer-duration transient forcing simulations, initialised from a control run. This is especially true if this is done soon after approximate energy balance is achieved.

Wittenberg et al. (2014) propose that in studies of essentially unpredictable model attributes, ensemble simulations could be employed for model validation—an essential components of climate modelling (e.g., Dijkstra, 2013, chapter 6). Given that computational advantages are provided by short-duration ensemble simulations (Wittenberg et al., 2014), compared to single runs of longer duration (see subsubsection 2.2.1.3), ensemble validation approaches could allow either (a) more data and thus larger samples to be used for model validation; or (b) a reduction in the associated computational cost. Furthermore, the comparatively short observational record (Dijkstra, 2013) makes it difficult to establish whether differences between model and observed fields are the result of model shortcomings or long-term persistence (e.g., Wittenberg, 2009), potentially associated with almost-intransitivity. In this study it is also found that single model run trajectories may, as a result of small atmospheric IC differences, deviate for significant periods of time—relative to length of acceptable climate records in many locations—from the states which ensemble

simulations suggest are more likely (subsection 5.1.3). This would suggest that comparison to ensemble probability distributions, especially under transient forcings, may be required to establish whether observations are compatible with the model possibility space.

6.5 How Well Can We Define "The Climate"?

The proposed quantification of model climates is not applicable to observational contexts (see subsection 6.2.1). There is a non-negligible likelihood that the kairodic assumption will fail (see subsubsection 2.1.5.1 and subsection 5.1.3). Furthermore, there exist inherent difficulties in detecting a signal response to a specified external driver in a system exhibiting an uncertain degree of nonlinear interactions, among internal subsystems, and with forcing trajectories (e.g., Smith, 2000b; Katzav et al., 2012; Daron and Stainforth, 2015, see also subsubsection 2.1.3.2 and subsubsection 2.2.2.3). Hence it is not clear how to compare ensemble definition and temporal definition or how to detect the likely trajectory of the climate possibility space on scales of relevance (Daron, 2012; Daron and Stainforth, 2013, 2015).

Different conceptualisations of climate will also necessarily lead to different approaches being taken to quantifying climate (see subsection 6.2.2). Even for a given conceptualisation of climate, uncertainties regarding the nature of processes acting in the relevant subset of the climate system and their influence on observable quantities, finding a suitable precise definition for a particular context remains highly nontrivial.

Together, this implies that a widely applicable definition—or even a collection of intercomparable definitions—for use in climate science, is unlikely to be established in the foreseeable future. However, this does not imply that investigations into different approaches to quantification of climate, together with innovative attempts to develop techniques for robust comparison between model and observational climate characterisations at regional scales, could not yield valuable progress in this regard. In addition, as also argued by Daron (2012) and Werndl (2015), more careful and explicit consideration of the quantifications and conceptualisations of climate effectively being applied in a given study, is necessary in various climate science contexts. This could help clarify the extent of existing uncertainties in the discourse, while advancing our understanding of the mechanisms driving climate variability.

Chapter 7

Conclusion

In this chapter, the key study findings are summarised in relation to the stated aim and objectives (section 1.5). The research question posed in subsection 1.5.1 leads to the aim, stated in subsection 1.5.2 as being "[t]o explore different possible influences of ICs on climate variable distributions, employing a nonlinear dynamical systems perspective." In order to address this aim, seven research objectives (subsection 1.5.3) were formulated. The extent to which these objectives have been fulfilled is addressed in section 7.1. Thereafter, progress made towards answering the study research question is discussed in section 7.2.

7.1 Assessing the Achievement of Research Objectives

The first objective is to "**[d]evelop a comprehensive overview of definitions of climate that have been—and continue to be—applied in the climate discourse and review the literature on their utility**". This objective is addressed primarily in section 2.1. A key insight gained is that the term "climate" is applied to distinct, but related concepts (see subsection 2.1.4). These differences arise, in part, as a result of answers provided—often implicitly—to questions introduced in section 1.3. Approaches to understanding the nature—and characterising the state—of climate thus conceptualised, lead to differences in the precise definitions proposed for climate (see subsection 2.1.5). The value and limitations of these approaches are carefully considered. Assessment of the results of this study in the context of section 2.1 lead to the proposal in section 6.2 that "ensemble-temporal multivariate distributions together with measures of autocorrelation" be used as an approach to quantifying model climates.

The second objective is to "**[c]onsider aspects of the current state of understanding of variability and uncertainty in the climate system, which have implications for conceptualisations and quantification of climate.** " This objective

is addressed primarily chapter 2. Key points arising from reviewing relevant literature, are that:

1. Climate variability may take on distinct periodic, quasi-periodic and aperiodic characteristics (see subsubsection 2.2.2.1).

2. There is substantial evidence that currently used climate system models do not meaningfully resolve certain types of such behaviour, especially lower-frequency variability (see subsubsection 2.2.2.3).

3. There is insufficient understanding of uncertainties in climate projections on various time scales, related to climate system state—and particularly large-scale modes of variability—at model initialisation (see subsubsection 2.2.1.3, subsubsection 2.2.2.4 and subsection 2.2.4).

4. Components and subsets of the climate system appear to exhibit variable degrees of predictability in their internal variability (see subsubsection 2.2.2.4).

5. The degree of ICP present at regional scales, can vary considerably depending on the ICs specified (Teng and Branstator, 2011, see also subsubsection 2.2.2.4).

6. Variability in the Southern Hemispheric extratropics is generally understudied, but might exert considerable influence on the global climate system state (see subsubsection 2.2.2.5).

These points inform the analysis approaches used in addressing objectives four to seven, as discussed below.

The third objective is to "**[r]un a set of large IC ensemble simulations of a coupled [climate system model (CSM)], with the intention of sampling a range of possible IC influences on the model climate, under stationary and transient forcing conditions**." This objective is addressed through the modelling experiment conducted in this study, described in chapter 3. To limit the necessarily considerable computational cost involved, the experiment was conducted using CESM1.2 in CCSM4 mode, at $4 \times 5^{\circ}$ resolution, using a finite volume dynamical core. Subsequently it has been ascertained that the configuration used was probably not optimal for the exploring the study aims (see subsection 3.2.2). However, whereas it is suggested that work aiming to extend the ideas of this work employ a coarse resolution spectral set-up, the output of the experiment as run should still provide valuable insights into the research question.

As part of the experiment, two millennial scale present day forcing control simulations were run. Using these as a basis for ensemble simulations, eleven CFEs and three RCP8.5 (van Vuuren et al., 2011) TFEs were run. Each ensemble consists of fifty members, run for sixty years (with a few minor exceptions; see section 3.5). The experimental set-up is summarised in Figure 3.1. Optimally, more TFEs would have been run, but due to

computational constraints this was not possible. However, the 14 50-member ensembles run provide ample opportunity to explore different influences of ICs on climate evolution, as per the study aim.

The fourth objective is to "**[e]xplore the nature of the atmospheric variability produced by the model control runs, to inform assessment of the likely connections between IC influence and modes of variability**". This objective is addressed in chapter 4, using wavelet decomposition of atmospheric component variable time series. It was found that model atmospheric variability over most regions and in the global average is dominated by a quasi-periodic mode, which appears to be the model's ENSO. Highly persistent in-phase connections between the Southern Oscillation and North Atlantic Oscillation are observed. Southern Hemispheric extratropical variability appears to be essentially independent of the quasi-periodic mode and is mainly aperiodic in character. However, during rare years when an apparently distinct type of ENSO event occurs (referred to as EP events; see Figure 4.8), teleconnections to the extratropical Southern Hemisphere are apparent. Evidence is presented for both quasi-periodic and aperiodic lower-frequency modes of variability in the ocean basins of the Northern Hemisphere. There is some evidence that model drift (see section 4.1) influences the nature of variability which occurs.

Addressing objective four—and consequently the three that follow—would have benefited from assessment of ocean and sea ice variability, as discussed in section 6.3. However, doing so would extend the work beyond its exploratory scope and was not feasible in the available time frame. Considering more slowly varying climate system components may prove to be a fruitful avenue for development of the present work.

The fifth objective is to "**[i]nvestigate the nature of IC influence apparent in atmospheric variable time series**." This objective is addressed primarily in subsection 5.1.2 and section 6.1. At least three distinct levels of IC influence are identified: (a) microscopic-scale IC influence, which decays on weather time scales; (b) interannual-scale IC influence, which can significantly alter ensemble variable distributions on time scales up to a couple of decades; and (c) intercentennial-scale IC influence, which determines the "climatological" distribution towards which variable ensemble distributions converge. Distinct patterns of interannual-scale IC influence are found to be attributable to aperiodic and quasi-periodic modes of variability. The extent of interannual-scale influence depends strongly on the ICs employed and is often greater when the ICs are from an EP event. Decadal-scale ICP is found to be strongly associated with this scale of IC influence.

A limitation resulting from the analysis methodologies applied here is that it is difficult to discern the influence of model short-comings and unrealistic slow adjustment processes, from those of slowly evolving components of the model climate system which are of great theoretical significance. However, in section 6.1 it is concluded that there is sufficient evidence to suggest that intercentennial-scale IC influence should be discernible in systems similar to that of the present model configuration.

The sixth objective is to "**[a]nalyse regional-mean atmospheric data to assess the validity of the kairodic assumption in this model**." This objective is addressed primarily in subsection 5.1.3. It is found that over regions and in variables that exhibit dominantly aperiodic variability—especially over the midlatitudes of the Southern Hemisphere—there is ample evidence that the kairodic assumption does not hold, even under constant external forcing. Significant differences ($p < 0.01$) are frequently (in up to a third of cases considered) detected between 60-year ensemble member variable distributions and (a) ensemble distributions for years throughout the ensemble duration; (b) ensemble-temporal distributions over decadal periods; (c) the overall ensemble distribution; and (d) each other. Over the tropics and subtropics, the assumption is generally valid in this model under constant forcing, but violations appear to occur relatively frequently over the midlatitudes of the Northern Hemisphere. Studies building on the present work, would be strengthened by a more robust extension of this analysis to the more realistic setting of evolving external forcing conditions.

The seventh objective is to "**[c]onsider possible evidence of interaction between IC influence and transient climate change response**." It is addressed primarily in section 5.2. It is found that ICP up to decadal scales is clearly distinguishable and relatively unaffected by rapidly changing external forcings (see subsubsection 5.2.1.1). This influence is detectable in computed changes in ensemble decadal mean temperature response (see subsection 5.2.2). Centennial-scale IC differences can also alter multidecadal scale trend response to external forcings, but it is not clear whether this would occur in the absence of model drift (subsection 5.2.2).

Additionally, it is found that the value of ensemble-based quantifications of climatic state hold substantial advantages over temporal distributions in quantifying the evolving climatic possibility space (see section 5.3). Future work could extend this analysis by assessing the extent to which this difficulty can be ameliorated by detrending time series prior to taking distributional statistics. However, evidence presented in this study suggests that the nonlinear nature of the system response implies that a relatively large IC ensemble would be required to ascertain the nature of the forcing signal.

7.2 Concluding Remarks

A brief discussion is now presented of progress made towards answering the study research question: "[w]hat role, if any, should ICs play in our conceptualisation and approaches to quantifying climate?". The discussion in section 2.1 and chapter 6, together with the experimental component of the study, provide evidence that ICs have a key role to play in climate studies, both experimental and theoretical in nature.

It is suggested that CSMs such as the one investigated presently, exhibit a range of behaviours that can be most meaningfully explored and quantified using IC ensembles, such as those employed in the experiment conducted here. The ability to detect signals of

particular influences on the climate of the model system is greatly enhanced through the use of IC ensembles (see section 6.4).

Uncertainty in climate projection has been divided into three primary components or "sources of uncertainty" (Hawkins and Sutton, 2009): (a) ICU, related to "internal variability", (b) forcing uncertainty, and (c) model uncertainty (Stainforth et al., 2007a). Understanding the priority warranted by each of these sources of uncertainty, requires insight into the different roles ICs can play in climate model simulations. It is also essential to understand the nature of IC differences which can be expected to produce such differences in IC influence. For example, which system components should be considered, which quantities of those components are most important and what magnitudes of difference should be assessed, and which spatial and temporal scales should they be considered at?

To this end, this study suggests at least three scales of influence that are relevant. The microscopic scale is of little value in attempting to reduce ICU in climate projections, but the interface between this level of IC influence and macroscopic IC influences warrants particular attention. This study indicates that it is not fixed and itself depends on nonlinear intricacies of the model system. Exploring whether there are uncertainties regarding climate system state which may reflect as intercentennial-scale IC influence in CSM simulations, would also appear to be important. This is especially true given evidence that is presented in subsection 5.2.2 (see also subsubsection 2.2.2.3) suggesting that IC differences at larger scales can influence ensemble response to external forcings.

This study suggests that, in the prominent fields of climate investigation and climate change projection, being cognisant of ICs is important—both in quantifying climate and in designing and interpreting climate model experiments.

Bibliography

Abram, N. J., R. Mulvaney, F. Vimeux, S. J. Phipps, J. Turner, and M. H. England, 2014: Evolution of the Southern Annular Mode during the past millennium. *Nat. Clim. Chang.*, **4 (7)**, 564–569, doi:10.1038/nclimate2235.

Alexander, M. A., K. Halimeda Kilbourne, and J. A. Nye, 2014: Climate variability during warm and cold phases of the Atlantic Multidecadal Oscillation (AMO) 1871–2008. *J. Mar. Syst.*, **133**, 14–26, doi:10.1016/j.jmarsys.2013.07.017.

Allen, M., 2003: Liability for climate change. *Nature*, **421 (6926)**, 891–892, doi:10.1038/421891a.

Allison, L. C., H. L. Johnson, and D. P. Marshall, 2011: Spin-up and adjustment of the Antarctic Circumpolar Current and global pycnocline. *J. Mar. Res.*, **69**, 167–189, doi:10.1357/002224011798765330.

AMS, 2013: Glossary of Meteorology. URL: http://glossary.ametsoc.org/wiki/Main_Page, [online 1 June 2013].

An, S.-I., 2009: A review of interdecadal changes in the nonlinearity of the El Niño-Southern Oscillation. *Theor. Appl. Climatol.*, **97 (1–2)**, 29–40, doi:10.1007/s00704-008-0071-z.

An, S.-I., and F.-F. Jin, 2004: Nonlinearity and Asymmetry of ENSO. *J. Clim.*, **17 (12)**, 2399–2412.

An, S.-I., and B. Wang, 2000: Interdecadal Change of the Structure of the ENSO Mode and Its Impact on the ENSO Frequency. *J. Clim.*, **13 (12)**, 2044–2055.

Andrews, T., J. M. Gregory, and M. J. Webb, 2015: The dependence of radiative forcing and feedback on evolving patterns of surface temperature change in climate models. *J. Clim.*, **28 (4)**, 1630–1648, doi:10.1175/jcli-d-14-00545.1.

Angel, J., W. Easterling, and S. Kirtsch, 1993: Towards defining appropriate averaging periods for climate normals. *Clim. Bull.*, **27 (2)**, 29–44.

Arguez, A., and R. S. Vose, 2011: The definition of the standard WMO climate normal: The key to deriving alternative climate normals. *Bull. Am. Meteorol. Soc*, **92 (6)**, 699 –704.

Balmaseda, M. A., K. E. Trenberth, and E. Källén, 2013: Distinctive climate signals in reanalysis of global ocean heat content. *Geophys. Res. Lett.*, **40 (9)**, 1754–1759, doi:10.1002/grl.50382.

Bellucci, A., and Coauthors, 2015: An assessment of a multi-model ensemble of decadal climate predictions. *Clim. Dyn.*, **44 (9–10)**, 2787–2806, doi:10.1007/s00382-014-2164-y.

Bódai, T., and T. Tél, 2012: Annual variability in a conceptual climate model: Snapshot attractors, hysteresis in extreme events, and climate sensitivity. *Chaos*, **22 (2)**, 023 110, doi:10.1063/1.3697984.

Boer, G. J., and S. J. Lambert, 2008: Multi-model decadal potential predictability of precipitation and temperature. *Geophys. Res. Lett.*, **35 (5)**, doi:10.1029/2008GL033234.

Boulton, C. A., L. C. Allison, and T. M. Lenton, 2014: Early warning signals of atlantic meridional overturning circulation collapse in a fully coupled climate model. *Nat. Commun.*, **5**, doi:http://dx.doi.org/10.1038/ncomms6752 10.1038/ncomms6752.

Box, G. E. P., 1953: Non-Normality and Tests on Variances. *Biometrika*, **40 (3–4)**, pp–318–335, URL: http://www.jstor.org/stable/2333350.

Branstator, G., and H. Teng, 2010: Two Limits of Initial-Value Decadal Predictability in a CGCM. *J. Clim.*, **23 (23)**, 6292–6311, doi:10.1175/2010jcli3678.1.

Branstator, G., and H. Teng, 2012: Potential impact of initialization on decadal predictions as assessed for CMIP5 models. *Geophys. Res. Lett.*, **39 (12)**, doi:10.1029/2012GL051974.

Branstator, G., H. Teng, G. A. Meehl, M. Kimoto, J. R. Knight, M. Latif, and A. Rosati, 2012: Systematic Estimates of Initial-Value Decadal Predictability for Six AOGCMs. *J. Clim.*, **25 (6)**, 1827–1846, doi:10.1175/jcli-d-11-00227.1.

Broer, H., C. Simó, and R. Vitolo, 2002: Bifurcations and strange attractors in the Lorenz-84 climate model with seasonal forcing. *Nonlinearity*, **15 (4)**, 1205.

Broer, H., and R. Vitolo, 2008: Dynamical systems modeling of low-frequency variability in low-order atmospheric models. *Discrete Cont. Dyn. B*, **10**, 401–419.

Brönnimann, S., 2007: Impact of El Niño–Southern Oscillation on European climate. *Rev. Geophys.*, **45 (3)**, doi:10.1029/2006RG000199.

Brown, P. T., E. C. Cordero, and S. A. Mauget, 2012: Reproduction of twentieth century intradecadal to multidecadal surface temperature variability in radiatively forced coupled climate models. *J. Geophys. Res.*, **117**, D11 116, doi:10.1029/2011jd016864.

Brown, P. T., W. Li, L. Li, and Y. Ming, 2014: Top-of-atmosphere radiative contribution to unforced decadal global temperature variability in climate models. *Geophys. Res. Lett.*, **41 (14)**, 5175–5183, doi:10.1002/2014gl060625.

Brown, P. T., W. Li, and S.-P. Xie, 2015: Regions of significant influence on unforced global mean surface air temperature variability in climate models. *J. Geophys. Res. Atmos.*, **120 (2)**, 480–494, doi:10.1002/2014JD022576.

Bryan, F., G. Danabasoglu, N. Nakashiki, Y. Yoshida, D.-H. Kim, J. Tsutsui, and S. Doney, 2006: Response of the North Atlantic thermohaline circulation and ventilation to increasing carbon dioxide in CCSM3. *J. Clim.*, **19 (11)**, 2382–2397.

Bryson, R. A., 1997: The Paradigm of Climatology: An Essay. *Bull. Am. Meteorol. Soc.*, **78 (3)**, 449–455.

Budyko, M. I., 1969: The effect of solar radiation variations on the climate of the Earth. *Tellus*, **21 (5)**, 611–619, doi:10.1111/j.2153-3490.1969.tb00466.x.

Burgers, G., and D. B. Stephenson, 1999: The "normality" of El Niño. *Geophys. Res. Lett.*, **26 (8)**, 1027–1030, doi:10.1029/1999GL900161.

Cazelles, B., M. Chavez, D. Berteaux, F. Ménard, J. Vik, S. Jenouvrier, and N. Stenseth, 2008: Wavelet analysis of ecological time series. *Oecologia*, **156 (2)**, 287–304, doi:10.1007/s00442-008-0993-2.

Changnon Jr, S. A., 1985: Climate fluctuations and impacts: The Illinois case. *Bull. Am. Meteorol. Soc*, **66 (2)**, 142–151.

Chylek, P., J. D. Klett, G. Lesins, M. K. Dubey, and N. Hengartner, 2014: The Atlantic Multidecadal Oscillation as a dominant factor of oceanic influence on climate. *Geophys. Res. Lett.*, **41 (5)**, 1689–1697, doi:10.1002/2014gl059274.

Claussen, M., and Coauthors, 2002: Earth system models of intermediate complexity: closing the gap in the spectrum of climate system models. *Clim. Dyn.*, **18 (7)**, 579–586.

Clement, A., P. DiNezio, and C. Deser, 2011: Rethinking the ocean's role in the Southern Oscillation. *J. Clim.*, **24 (15)**, 4056–4072.

Collins, M., B. B. B. Booth, G. R. Harris, J. M. Murphy, D. M. H. Sexton, and M. J. Webb, 2006a: Towards quantifying uncertainty in transient climate change. *Clim. Dyn.*, **27 (2)**, 127–147, doi:10.1007/s00382-006-0121-0.

Collins, M., and Coauthors, 2006b: Interannual to decadal climate predictability in the North Atlantic: A multimodel-ensemble study. *J. Clim.*, **19 (7)**, 1195–1203.

Collins, M., and Coauthors, 2013: *Long-term Climate Change: Projections, Commitments and Irreversibility*, chap. 12, 1029 – 1136. Cambridge University Press, Cambridge, United Kingdom and New York, NY, USA, doi:10.1017/CBO9781107415324.024.

Cornell, S. E., I. C. Prentice, J. I. House, and C. J. Downy, 2012: *Understanding the Earth System: Global Change Science for Application*. Cambridge University Press.

Corti, S., F. Molteni, and T. N. Palmer, 1999: Signature of recent climate change in frequencies of natural atmospheric circulation regimes. *Nature*, **398 (6730)**, 799–802, doi:10.1038/19745.

Corti, S., A. Weisheimer, T. N. Palmer, F. J. Doblas-Reyes, and L. Magnusson, 2012: Reliability of decadal predictions. *Geophys. Res. Lett.*, **39 (21)**, doi:10.1029/2012GL053354.

Cowtan, K., and R. G. Way, 2014: Coverage bias in the HadCRUT4 temperature series and its impact on recent temperature trends. *Q. J. R. Meteorol. Soc.*, **140 (683)**, 1935–1944, doi:10.1002/qj.2297.

Craig, A. P., M. Vertenstein, and R. Jacob, 2012: A new flexible coupler for earth system modeling developed for CCSM4 and CESM1. *Int. J. High Perform. Comput. Appl.*, **26 (1)**, 31–42, doi:10.1177/1094342011428141.

Crowley, T. J., S. P. Obrochta, and J. Liu, 2014: Recent global temperature "plateau" in the context of a new proxy reconstruction. *Earth's Future*, **2 (5)**, 281–294, doi:10.1002/2013ef000216.

Dai, A., J. C. Fyfe, S.-P. Xie, and X. Dai, 2015: Decadal modulation of global surface temperature by internal climate variability. *Nat. Clim. Chang.*

Danabasoglu, G., S. C. Bates, B. P. Briegleb, S. R. Jayne, M. Jochum, W. G. Large, S. Peacock, and S. G. Yeager, 2012: The CCSM4 ocean component. *J. Clim.*, **25 (5)**, 1361–1389.

Daron, J. D., 2012: Examining the decision-relevance of climate model information for the insurance industry. Ph.D. thesis, The London School of Economics and Political Science.

Daron, J. D., and D. A. Stainforth, 2013: On predicting climate under climate change. *Environ. Res. Lett.*, **8 (3)**, 034 021, doi:10.1088/1748-9326/8/3/034021.

Daron, J. D., and D. A. Stainforth, 2014: How big should a climate model ensemble be? Lessons from a low dimensional system. *EGU General Assembly Conference Abstracts*, Vol. 16, 11645.

Daron, J. D., and D. A. Stainforth, 2015: On quantifying the climate of the nonautonomous Lorenz-63 model. *Chaos*, **25 (4)**, doi:10.1063/1.4916789.

DelSole, T., L. Jia, and M. K. Tippett, 2013a: Decadal prediction of observed and simulated sea surface temperatures. *Geophys. Res. Lett.*, **40 (11)**, 2773–2778, doi:10.1002/grl.50185.

DelSole, T., M. K. Tippett, and L. Jia, 2013b: Multi-year Prediction and Predictability. *Climate Change: Multidecadal and Beyond*, C.-P. Chang, M. Latif, and M. Ghil, Eds., Asia-Pacific Weather and Climate, Vol. 6, World Scientific, Singapore, chap. 1, 1–17.

DelSole, T., M. K. Tippett, and J. Shukla, 2011: A Significant Component of Unforced Multidecadal Variability in the Recent Acceleration of Global Warming. *J. Clim.*, **24 (3)**, 909–926, doi:10.1175/2010jcli3659.1.

Delworth, T. L., and M. E. Mann, 2000: Observed and simulated multidecadal variability in the Northern Hemisphere. *Clim. Dyn.*, **16 (9)**, 661–676, doi:10.1007/s003820000075.

Delworth, T. L., and Coauthors, 2012: Simulated climate and climate change in the GFDL CM2. 5 high-resolution coupled climate model. *J. Clim.*, **25 (8)**, 2755–2781.

Dennis, J. M., and Coauthors, 2012: CAM-SE: A scalable spectral element dynamical core for the Community Atmosphere Model. *Int. J. High Perform. Comput. Appl.*, **26 (1)**, 74–89, doi:10.1177/1094342011428142.

Deser, C., R. Knutti, S. Solomon, and A. S. Phillips, 2012a: Communication of the role of natural variability in future North American climate. *Nat. Clim. Chang.*, **2 (11)**, 775–779, doi:10.1038/nclimate1562.

Deser, C., A. S. Phillips, and J. W. Hurrell, 2004: Pacific interdecadal climate variability: Linkages between the tropics and the North Pacific during boreal winter since 1900. *J. Clim.*, **17 (16)**, 3109–3124.

Deser, C., and Coauthors, 2012b: ENSO and Pacific Decadal Variability in the Community Climate System Model Version 4. *J. Clim.*, **25 (8)**, 2622–2651, doi:10.1175/jcli-d-11-00301.1.

Dijkstra, H. A., 2013: *Nonlinear Climate Dynamics*. Cambridge University Press.

Dijkstra, H. A., and M. Ghil, 2005: Low-frequency variability of the large-scale ocean circulation: A dynamical systems approach. *Rev. Geophys.*, **43 (3)**, doi:10.1029/2002RG000122.

Dijkstra, H. A., and J. P. Viebahn, 2015: Sensitivity and resilience of the climate system: A conditional nonlinear optimization approach. *Comm. Nonlinear Sci. Numer. Simulat.*, **22 (1 - 3)**, 13–22, doi:10.1016/j.cnsns.2014.09.015.

Doblas-Reyes, F. J., and Coauthors, 2013: Initialized near-term regional climate change prediction. *Nat. Commun.*, **4**, 1715, doi:10.1038/ncomms2704.

Dommenget, D., and M. Latif, 2008: Generation of hyper climate modes. *Geophys. Res. Lett.*, **35 (2)**, doi:10.1029/2007GL031087.

Dong, B., and A. Dai, 2015: The influence of the Interdecadal Pacific Oscillation on Temperature and Precipitation over the Globe. *Clim. Dyn.*, 1–15, doi:10.1007/s00382-015-2500-x.

Douglass, D. H., 2011: Separation of a Signal of Interest from a Seasonal Effect in Geophysical Data: I. El Niño/La Niña Phenomenon. *Int. J. Geosci.*, **2 (04)**, 414.

Drijfhout, S. S., 2014: Global radiative adjustment after a collapse of the Atlantic meridional overturning circulation. *Clim. Dyn.*, doi:10.1007/s00382-014-2433-9.

Eckmann, J.-P., and D. Ruelle, 1985: Ergodic theory of chaos and strange attractors. *Rev. Mod. Phys.*, **57**, 617–656, doi:10.1103/RevModPhys.57.617.

Estrada, F., P. Perron, and B. Martínez-López, 2013: Statistically derived contributions of diverse human influences to twentieth-century temperature changes. *Nat. Geosci.*, **6 (12)**, 1050–1055, doi:10.1038/ngeo1999.

Fanning, A. F., and A. J. Weaver, 1997: On the role of flux adjustments in an idealized coupled climate model. *Clim. Dyn.*, **13 (10)**, 691–701, doi:10.1007/s003820050191.

Fedorov, A. V., and S. G. Philander, 2000: Is El Niño Changing? *Science*, **288 (5473)**, 1997–2002, doi:10.1126/science.288.5473.1997.

Flato, G. M., 2011: Earth system models: an overview. *WIREs Clim Chang.*, **2 (6)**, 783–800, doi:10.1002/wcc.148.

Fogt, R. L., J. Perlwitz, A. J. Monaghan, D. H. Bromwich, J. M. Jones, and G. J. Marshall, 2009: Historical SAM Variability. Part II: Twentieth-Century Variability and Trends from Reconstructions, Observations, and the IPCC AR4 Models. *J. Clim.*, **22 (20)**, 5346–5365, doi:10.1175/2009jcli2786.1.

Fraedrich, K., 1986: Estimating the dimensions of weather and climate attractors. *J. Atmos. Sci.*, **43 (5)**, 419–432.

Fraedrich, K., and R. Wang, 1993: Estimating the correlation dimension of an attractor from noisy and small datasets based on re-embedding. *Physica D*, **65 (4)**, 373–398.

Franzke, C. L. E., S. M. Osprey, P. Davini, and N. W. Watkins, 2015: A dynamical systems explanation of the Hurst effect and atmospheric low-frequency variability. *Sci. Rep.*, **5**.

Frigg, R., L. Smith, and D. Stainforth, 2015: An assessment of the foundational assumptions in high-resolution climate projections: The case of UKCP09. *Synthese*, 1–30, doi:10.1007/s11229-015-0739-8.

Gedalof, Z. E., and D. J. Smith, 2001: Interdecadal climate variability and regime-scale shifts in Pacific North America. *Geophys. Res. Lett.*, **28 (8)**, 1515–1518, doi:10.1029/2000GL011779.

Gent, P. R., and Coauthors, 2011: The Community Climate System Model Version 4. *J. Clim.*, **24 (19)**, 4973–4991, doi:10.1175/2011jcli4083.1.

Ghil, M., 2001: Hilbert problems for the geosciences in the 21st century. *Nonlin. Processes Geophys.*, **8 (4 - 5)**, 211–211, doi:10.5194/npg-8-211-2001.

Ghil, M., 2002: Natural Climate Variability. *Encyclopedia of Global Environmental Change Volume 1: The Earth system: physical and chemical dimensions of global environmental change*, T. Munn, and J. S. P. M. C. MacCracken, Eds., Encyclopedia of Global Environmental Change, Vol. 1, John Wiley & Sons, Chichester, 544–549.

Ghil, M., in press, 2015: A mathematical theory of climates sensitivity or, How to deal with both anthropogenic forcing and natural variability? *Climate Change: Multidecadal and Beyond*, C. P. Chang, M. Ghil, M. Latif, and J. Wallace, Eds., World Scientific Review Volume, World Scientific Pub Co./Impress College Press, Singapore and London, UK, chap. 2, 21.

Gong, D., and S. Wang, 1999: Definition of Antarctic oscillation index. *Geophys. Res. Lett.*, **26 (4)**, 459–462, doi:10.1029/1999GL900003.

Goosse, H., P. Barriat, W. Lefebvre, M. Loutre, and V. Zunz, 2013: *Introduction to climate dynamics and climate modeling*. Online textbook available at http://www.climate.be/textbook.

Gordon, C., C. Cooper, C. A. Senior, H. Banks, J. M. Gregory, T. C. Johns, J. F. Mitchell, and R. A. Wood, 2000: The simulation of SST, sea ice extents and ocean heat transports in a version of the Hadley Centre coupled model without flux adjustments. *Clim. Dyn.*, **16 (2-3)**, 147–168.

Grassberger, P., 1986: Do climatic attractors exist? *Nature*, **323 (6089)**, 609–612.

Grassberger, P., and I. Procaccia, 1983: Characterization of Strange Attractors. *Phys. Rev. Lett.*, **50**, 346–349, doi:10.1103/PhysRevLett.50.346.

Griffies, S. M., and Coauthors, 2014: Impacts on Ocean Heat from Transient Mesoscale Eddies in a Hierarchy of Climate Models. *J. Clim.*, **28 (3)**, 952–977, doi:10.1175/JCLI-D-14-00353.1.

Grinsted, A., J. C. Moore, and S. Jevrejeva, 2004: Application of the cross wavelet transform and wavelet coherence to geophysical time series. *Nonlin. Processes Geophys.*, **11 (5 - 6)**, 561–566, doi:10.5194/npg-11-561-2004.

Gu, D., and S. G. H. Philander, 1997: Interdecadal climate fluctuations that depend on exchanges between the tropics and extratropics. *Science*, **275 (5301)**, 805–807.

Guttman, N., 1989: Statistical Descriptors of Climate. *Bull. Am. Meteorol. Soc.*, **70 (6)**, 602–607.

Guttorp, P., 2014: Statistics and Climate. *Annu. Rev. Stat. Appl.*, **1 (1)**, 87–101, doi:10.1146/annurev-statistics-022513-115648.

Hansen, J., and Coauthors, 1997: Forcings and chaos in interannual to decadal climate change. *J. Geophys. Res.*, **102 (D22)**, 25 679–25 720, doi:10.1029/97JD01495.

Harmel, R. D., C. W. Richardson, C. L. Hanson, and G. L. Johnson, 2002: Evaluating the adequacy of simulating maximum and minimum daily air temperature with the normal distribution. *J. Appl. Meteorol.*, **41 (7)**, 744–753.

Hasselmann, K., 1976: Stochastic climate models Part I. Theory. *Tellus*, **28 (6)**, 473–485, doi:10.1111/j.2153-3490.1976.tb00696.x.

Haughton, N., G. Abramowitz, A. Pitman, and S. Phipps, 2014: On the generation of climate model ensembles. *Clim. Dyn.*, **43 (7–8)**, 2297–2308, doi:10.1007/s00382-014-2054-3.

Hauser, T., E. Demirov, J. Zhu, and I. Yashayaev, 2015: North Atlantic atmospheric and ocean inter-annual variability over the past fifty years– Dominant patterns and decadal shifts. *Prog. Oceanogr.*, **132 (0)**, 197–219, doi:10.1016/j.pocean.2014.10.008.

Hawkins, E., T. Edwards, and D. McNeall, 2014: Pause for thought. *Nat. Clim. Chang.*, **4 (3)**, 154–156, doi:10.1038/nclimate2150.

Hawkins, E., R. S. Smith, L. C. Allison, J. M. Gregory, T. J. Woollings, H. Pohlmann, and B. de Cuevas, 2011: Bistability of the Atlantic overturning circulation in a global climate model and links to ocean freshwater transport. *Geophys. Res. Lett.*, **38 (10)**, doi:10.1029/2011GL047208.

Hawkins, E., and R. Sutton, 2009: The potential to narrow uncertainty in regional climate predictions. *Bull. Am. Meteorol. Soc*, **90 (8)**, 1095 – 1107.

Hawkins, E., and R. Sutton, 2012: Time of emergence of climate signals. *Geophys. Res. Lett.*, **39 (1)**, doi:10.1029/2011GL050087.

Held, I. M., 2005: The Gap between Simulation and Understanding in Climate Modeling. *Bull. Am. Meteorol. Soc.*, **86 (11)**, 1609–1614, doi:10.1175/bams-86-11-1609.

Hirst, A. C., S. P. O'Farrell, and H. B. Gordon, 2000: Comparison of a coupled ocean-atmosphere model with and without oceanic eddy-induced advection. Part I: Ocean spinup and control integrations. *J. Clim.*, **13 (1)**, 139–163.

Hsu, C. J., and F. Zwiers, 2001: Climate change in recurrent regimes and modes of northern hemisphere atmospheric variability. *J. Geophys. Res.*, **106 (D17)**, 20 145–20 159, doi:10.1029/2001JD900229.

Huang, J., K. Higuchi, and A. Shabbar, 1998: The relationship between the North Atlantic Oscillation and El Niño-Southern Oscillation. *Geophys. Res. Lett.*, **25 (14)**, 2707–2710, doi:10.1029/98GL01936.

Huang, J., H. van den Dool, and A. Barnston, 1996: Long-lead seasonal temperature prediction using optimal climate normals. *J. Clim.*, **9 (4)**, 809–817.

Hunke, E., and W. Lipscomb, 2008: CICE: The Los Alamos sea ice model, documentation and software, version 4.0, Los Alamos National Laboratory Tech. Rep. LA-CC-06-012. 76pp.

Hunt, B., and T. Elliott, 2004: Interaction of climatic variability with climatic change. *Atmos.-Ocean*, **42 (3)**, 145–172, doi:10.3137/ao.420301.

Hurrell, J. W., and Coauthors, 2013: The Community Earth System Model: A framework for collaborative research. *Bull. Am. Meteorol. Soc*, **94 (9)**, 1339–1360.

IPCC, 2007: Annex I: Glossary. *Climate Change 2007: The Physical Science Basis. Contribution of Working Group I to the Fourth Assessment Report of the Intergovernmental Panel on Climate Change*, A. Baende, Ed., Cambridge University Press, Cambridge, UK.

IPCC, 2013a: Annex III: Glossary. *Climate Change 2013: The Physical Science Basis. Contribution of Working Group I to the Fifth Assessment Report of the Intergovernmental Panel on Climate Change* [Stocker, T.F., D. Qin, G.-K. Plattner, M. Tignor, S.K. Allen, J. Boschung, A. Nauels, Y. Xia, V. Bex and P.M. Midgley (eds.)], S. Planton, Ed., Cambridge University Press, Cambridge, UK.

IPCC, 2013b: *Climate Change 2013: The Physical Science Basis. Contribution of Working Group I to the Fifth Assessment Report of the Intergovernmental Panel on Climate Change*. Cambridge University Pres, Cambridge, United Kingdom and New York, NY, USA.

IPCC, 2014: *Climate Change 2014: Impacts, Adaptation and Vulnerability. Part A: Global and Sectoral Aspects. Contribution of Working Group II to the Fourth Assessment Report of the Intergovernmental Panel on Climate Change: Summary for Policymakers.* Cambridge University Press, Cambridge, UK and New York, NY, USA.

Ivchenko, V. O., V. B. Zalesny, and M. R. Drinkwater, 2004: Can the equatorial ocean quickly respond to Antarctic sea ice/salinity anomalies? *Geophys. Res. Lett.*, **31 (15)**, doi:10.1029/2004GL020472.

Ivchenko, V. O., V. B. Zalesny, M. R. Drinkwater, and J. Schröter, 2006: A quick response of the equatorial ocean to Antarctic sea ice/salinity anomalies. *J. Geophys. Res.*, **111**, C10 018, doi:10.1029/2005JC003061.

Jablonowski, C., and D. L. Williamson, 2006: A baroclinic instability test case for atmospheric model dynamical cores. *Q. J. R. Meteorol. Soc.*, **132 (621C)**, 2943–2975, doi:10.1256/qj.06.12.

Jevrejeva, S., J. C. Moore, and A. Grinsted, 2003: Influence of the Arctic Oscillation and El Niño-Southern Oscillation (ENSO) on ice conditions in the Baltic Sea: The wavelet approach. *J. Geophys. Res.*, **108 (D21)**, 4677.

Jin, F.-F., S.-I. An, A. Timmermann, and J. Zhao, 2003: Strong El Niño events and nonlinear dynamical heating. *Geophys. Res. Lett.*, **30 (3)**, 20–1–20–1, doi:10.1029/2002GL016356.

Kabat, P., and Coauthors, Eds., 2004: *Vegetation, Water, Humans and the Climate: A New Perspective on an Internactive System*. Global change, Springer.

Kalognomou, E.-A., and Coauthors, 2013: A Diagnostic Evaluation of Precipitation in CORDEX Models over Southern Africa. *J. Clim.*, **26 (23)**, 9477–9506, doi:10.1175/jcli-d-12-00703.1.

Katzav, J., H. A. Dijkstra, and A. T. J. de Laat, 2012: Assessing climate model projections: State of the art and philosophical reflections. *Stud. Hist. Philos. Modern Phys.*, **43 (4)**, 258–276, doi:10.1016/j.shpsb.2012.07.002.

Kay, J. E., and Coauthors, 2014: The Community Earth System Model (CESM) Large Ensemble Project: A community resource for studying climate change in the presence of internal climate variability. *Bull. Am. Meteorol. Soc*, doi:10.1175/BAMS-D-13-00255.1.

Kirtman, B., and Coauthors, 2012: Impact of ocean model resolution on CCSM climate simulations. *Clim. Dyn.*, **39 (6)**, 1303–1328, doi:10.1007/s00382-012-1500-3.

Kirtman, B., and Coauthors, 2013: *Near-term Climate Change: Projections and Predictability*, chap. 11, 953 – 1028. Cambridge University Press, Cambridge, United Kingdom and New York, NY, USA, doi:10.1017/CBO9781107415324.023.

Kleeman, R., 2002: Measuring dynamical prediction utility using relative entropy. *J. Am. Stat. Assoc.*, **59 (13)**, 2057–2072.

Knutti, R., and G. C. Hegerl, 2008: The equilibrium sensitivity of the Earth's temperature to radiation changes. *Nat. Geosci.*, **1 (11)**, 735–743, doi:10.1038/ngeo337.

Knutti, R., S. Krähenmann, D. J. Frame, and M. R. Allen, 2008: Comment on "Heat capacity, time constant, and sensitivity of Earth's climate system" by S.E. Schwartz. *J. Geophys. Res.*, **113**, D15 103.

Köppen, W., 1900: Versuch einer Klassifikation der Klimate, vorzugsweise nach ihren Beziehungen zur Pflanzenwelt. *Geographische Zeitschrift*, **6 (11)**, 593–611, URL: http://www.jstor.org/stable/27803924.

Kraus, H., 1984: Was Ist Klima? *Erdkunde*, 249–258.

Kravtsov, S., W. K. Dewar, M. Ghil, J. C. McWilliams, and P. Berloff, 2008: A mechanistic model of mid-latitude decadal climate variability. *Physica D*, **237 (5)**, 584–599, doi:10.1016/j.physd.2007.09.025.

Kravtsov, S., M. G. Wyatt, J. A. Curry, and A. A. Tsonis, 2014: Two contrasting views of multidecadal climate variability in the twentieth century. *Geophys. Res. Lett.*, **41 (19)**, 6881–6888, doi:10.1002/2014GL061416.

Kutzbach, J. E., 1976: The nature of climate and climatic variations. *Quat. Res.*, **6 (4)**, 471–480, doi:10.1016/0033-5894(76)90020-X.

Lamb, H. H., 1972: *Climate: Present, past and future. Vol. 1, Fundamentals and climate now*. Methuen and Co., London.

Lamb, P., and S. Changnon Jr, 1981: On the "Best" Temperature and Precipitation Normals: The Illinois Situation. *J. Appl. Meteorol.*, **20**, 1383–1390.

Lance, G. N., and W. T. Williams, 1967: A General Theory of Classificatory Sorting Strategies: 1. Hierarchical Systems. *Comput. J.*, **9 (4)**, 373–380, URL: http://comjnl.oxfordjournals.org/content/9/4/373.abstract.

Larson, J., 2010: Can we define climate using information theory? *IOP Conference Series: Earth and Environmental Science*, IOP Publishing, Vol. 11, 012028.

Larson, J. W., 2012: Visualizing Climate Variability with Time-Dependent Probability Density Functions, Detecting It Using Information Theory. *Procedia Comput. Sci.*, **9 (0)**, 917 –926, doi:10.1016/j.procs.2012.04.098.

Latif, M., and N. S. Keenlyside, 2011: A perspective on decadal climate variability and predictability. *Deep Sea Res. II*, **58 (17 - 18)**, 1880–1894, doi:10.1016/j.dsr2.2010.10.066.

Latif, M., T. Martin, and W. Park, 2013: Southern Ocean Sector Centennial Climate Variability and Recent Decadal Trends. *J. Clim.*, **26 (19)**, 7767–7782, doi:10.1175/jcli-d-12-00281.1.

Latif, M., and Coauthors, 2004: Reconstructing, monitoring, and predicting multidecadal-scale changes in the North Atlantic thermohaline circulation with sea surface temperature. *J. Clim.*, **17 (7)**, 1605–1614.

Lawrence, D. M., K. W. Oleson, M. G. Flanner, C. G. Fletcher, P. J. Lawrence, S. Levis, S. C. Swenson, and G. B. Bonan, 2012: The CCSM4 land simulation, 1850-2005: Assessment of surface climate and new capabilities. *J. Clim.*, **25 (7)**, 2240–2260.

Leith, C. E., 1978: Predictability of climate. *Nature*, **276**, 352–355, doi:10.1038/276352a0.

Leith, C. E., 1985: Global Climate Research. *The Global Climate*, J. Houghton, Ed., Cambridge University Press.

Lenhard, R. W., and W. A. Baum, 1954: Some considerations on normal monthly temperatures. *J. Meteor.*, **11 (5)**, 392–398.

Lenton, T., H. Held, E. Kriegler, J. Hall, W. Lucht, S. Rahmstorf, and H. Schellnhuber, 2008: Tipping elements in the Earth's climate system. *Proc. Natl. Acad. Sci. U.S.A.*, **105 (6)**, 1786–1793.

Lenton, T. M., R. J. Myerscough, R. Marsh, V. N. Livina, A. R. Price, and S. J. Cox, 2009: Using GENIE to study a tipping point in the climate system. *Phil. Trans. R. Soc. A*, **367 (1890)**, 871–884, doi:10.1098/rsta.2008.0171.

Levitus, S., and Coauthors, 1998: NOAA Atlas NESDIS 18, World Ocean Database 1998: Vol. 1: Introduction. U.S. Dept. of Commerce, National Oceanic and Atmospheric Administration, National Environmental Satellite, Data, and Information Service, Washington, D.C., 346 pp.

Li, J. P., and J. X. L. Wang, 2003: A new North Atlantic Oscillation index and its variability. *Adv. Atmos. Sci.*, **20 (5)**, 661–676, doi:10.1007/BF02915394.

Limpasuvan, V., and D. L. Hartmann, 1999: Eddies and the annular modes of climate variability. *Geophys. Res. Lett.*, **26 (20)**, 3133–3136, doi:10.1029/1999GL010478.

Lin, S.-J., 2004: A "vertically Lagrangian" finite-volume dynamical core for global models. *Mon. Weather Rev.*, **132 (10)**, 2293–2307.

Liu, Y., X. San Liang, and R. H. Weisberg, 2007: Rectification of the bias in the wavelet power spectrum. *J. Atmos. Ocean. Tech.*, **24 (12)**, 2093–2102.

Livezey, R. E., K. Y. Vinnikov, M. M. Timofeyeva, R. Tinker, and H. M. van den Dool, 2007: Estimation and Extrapolation of Climate Normals and Climatic Trends. *J. Appl. Meteorol. Climatol.*, **46 (11)**, 1759–1776, doi:10.1175/2007jamc1666.1.

Lorenz, E. N., 1963: Deterministic Nonperiodic Flow. *J. Atmos. Sci.*, **20 (2)**, 130–141.

Lorenz, E. N., 1964: The problem of deducing the climate from the governing equations. *Tellus*, **16 (1)**, 1–11.

Lorenz, E. N., 1965: A study of the predictability of a 28-variable atmospheric model. *Tellus*, **17 (3)**, 321–333.

Lorenz, E. N., 1968: Climatic Determinism. *Meteor. Monogr.*, **8 (30)**, 1–3.

Lorenz, E. N., 1969a: Atmospheric predictability as revealed by naturally occurring analogues. *J. Atmos. Sci.*, **26 (4)**, 636–646.

Lorenz, E. N., 1969b: The predictability of a flow which possesses many scales of motion. *Tellus*, **21 (3)**, 289–307.

Lorenz, E. N., 1970: Climatic change as a mathematical problem. *J. Appl. Meteorol.*, **9 (3)**, 325–329.

Lorenz, E. N., 1976: Nondeterministic theories of climatic change. *Quat. Res.*, **6 (4)**, 495–506, doi:10.1016/0033-5894(76)90022-3.

Lorenz, E. N., 1980: Attractor sets and quasi-geostrophic equilibrium. *J. Am. Stat. Assoc.*, **37 (8)**, 1685–1699.

Lorenz, E. N., 1982: Atmospheric predictability experiments with a large numerical model. *Tellus*, **34 (6)**, 505–513.

Lorenz, E. N., 1984: Irregularity: a fundamental property of the atmosphere. *Tellus A*, **36 (2)**, 98–110.

Lorenz, E. N., 1987: Low-Order Models and Their Uses. *Irreversible Phenomena and Dynamical Systems Analysis in Geosciences*, C. Nicolis, and G. Nicolis, Eds., NATO ASI Series, Vol. 192, Springer Netherlands, 557–567, doi:10.1007/978-94-009-4778-8_28.

Lorenz, E. N., 1990: Can chaos and intransitivity lead to interannual variability? *Tellus A*, **42**, 378–389.

Lorenz, E. N., 1991a: Chaos, Spontaneous Climatic Variations and Detection of the Greenhouse Effect. *Greenhouse-Gas-Induced Climatic Change: A Critical Appraisal of Simulations and Observations*, M. E. Schlesinger, Ed., Developments in Atmospheric Science, Vol. 19, Elsevier, 445–453, doi:10.1016/B978-0-444-88351-3.50035-0.

Lorenz, E. N., 1991b: Dimension of weather and climate attractors. *Nature*, **353**, 241–244, doi:10.1038/353241a0.

Lorenz, E. N., 1995: Climate is what you expect. online, available at http://eaps4.mit.edu/research/Lorenz/publications.htm [online 10 February 2013].

Lovejoy, S., 2013: What Is Climate? *EOS, Trans. Am. Geophys. Union*, **94 (1)**, 1–2, doi:10.1002/2013EO010001.

Lovejoy, S., 2014: A voyage through scales, a missing quadrillion and why the climate is not what you expect. *Clim. Dyn.*, doi:10.1007/s00382-014-2324-0.

Lovejoy, S., and D. Schertzer, 1986: Scale invariance in climatological temperatures and the local spectral plateau. *Ann. Geophys.*, **4B (4)**, 401–410.

Lovejoy, S., and D. Schertzer, 1998: Stochastic chaos and multifractal geophysics. *Chaos Fractals and Models 96*, F. M. Guindani, and G. Salvadori, Eds., Italian University Press, 38–52.

Lovejoy, S., and D. Schertzer, 2010: Towards a new synthesis for atmospheric dynamics: Space–time cascades. *Atmos. Res.*, **96 (1)**, 1–52, doi:10.1016/j.atmosres.2010.01.004.

Lovejoy, S., and D. Schertzer, 2012: Stochastic and scaling climate sensitivities: Solar, volcanic and orbital forcings. *Geophys. Res. Lett.*, **39**, L11 702, doi:10.1029/2012gl051871.

Lovejoy, S., D. Schertzer, and D. Varon, 2013: Do GCMs predict the climate ... or macroweather? *Earth Syst. Dynam.*, **4 (2)**, 439–454, doi:10.5194/esd-4-439-2013.

Lovejoy, S., and Coauthors, 2009: Nonlinear Geophysics: Why We Need It. *EOS, Trans. Am. Geophys. Union*, **90 (48)**, 455–456, doi:10.1029/2009EO480003.

Lucarini, V., 2002: Towards a definition of climate science. *Int. J. Environ. Pollut.*, **18 (5)**, 413–422.

Ludescher, J., A. Bunde, C. E. Franzke, and H. Schellnhuber, 2015: Long-term persistence enhances uncertainty about anthropogenic warming of Antarctica. *Clim. Dyn.*, 1–9, doi:10.1007/s00382-015-2582-5.

Mahlstein, I., R. Knutti, S. Solomon, and R. W. Portmann, 2011: Early onset of significant local warming in low latitude countries. *Environ. Res. Lett.*, **6 (3)**, 034 009, doi:10.1088/1748-9326/6/3/034009.

Majda, A. J., 2012: Challenges in Climate Science and Contemporary Applied Mathematics. *Commun. Pur. Appl. Math.*, **65 (7)**, 920–948, doi:10.1002/cpa.21401.

Malherbe, J., W. Landman, and F. Engelbrecht, 2014: The bi-decadal rainfall cycle, Southern Annular Mode and tropical cyclones over the Limpopo River Basin, southern Africa. *Clim. Dyn.*, **42 (11 - 12)**, 3121–3138, doi:10.1007/s00382-013-2027-y.

Mann, M. E., and J. Park, 1994: Global-scale modes of surface temperature variability on interannual to century timescales. *J. Geophys. Res.*, **99 (D12)**, 25 819–25 833, doi:10.1029/94JD02396.

Mann, M. E., J. Park, and R. S. Bradley, 1995: Global interdecadal and century-scale climate oscillations during the past five centuries. *Nature*, **378 (6554)**, 266–270.

Mann, M. E., B. A. Steinman, and S. K. Miller, 2014: On forced temperature changes, internal variability, and the AMO. *Geophys. Res. Lett.*, **41 (9)**, 3211–3219, doi:10.1002/2014gl059233.

Mantua, N. J., S. R. Hare, and Y. Zhang, 1997: A Pacific Interdecadal Climate Oscillation with Impacts on Salmon Production. *Bull. Am. Meteorol. Soc.*, **78 (6)**, 1069–1079.

Maraun, D., and J. Kurths, 2004: Cross wavelet analysis: Significance testing and pitfalls. *Nonlin. Processes Geophys.*, **11 (4)**, 505–514, doi:10.5194/npg-11-505-2004.

Marini, C., C. Frankignoul, and J. Mignot, 2011: Links between the southern annular mode and the Atlantic meridional overturning circulation in a climate model. *J. Clim.*, **24 (3)**, 624–640.

Marshall, G. J., 2003: Trends in the Southern Annular Mode from observations and reanalyses. *J. Clim.*, **16 (24)**, 4134–4143, doi:10.1175/1520-0442(2003)016<4134:TITSAM>2.0.CO;2.

Martin, T., W. Park, and M. Latif, 2013: Multi-centennial variability controlled by Southern Ocean convection in the Kiel Climate Model. *Clim. Dyn.*, **40 (7-8)**, 2005–2022, doi:10.1007/s00382-012-1586-7.

Martin, T., W. Park, and M. Latif, 2014: Southern Ocean forcing of the North Atlantic at multi-centennial time scales in the Kiel Climate Model. *Deep Sea Res. II*, doi:10.1016/j.dsr2.2014.01.018.

Martyn, D., and P. Senn, 1992: *Climates of the world*. Developments in atmospheric science, Elsevier, Amsterdam.

Massey Jr., F. J., 1951: The Kolmogorov-Smirnov Test for Goodness of Fit. *J. Am. Stat. Assoc.*, **46 (253)**, 68–78, doi:10.1080/01621459.1951.10500769.

McCormack, J. P., S. D. Eckermann, K. W. Hoppel, and R. A. Vincent, 2010: Amplification of the quasi-two day wave through nonlinear interaction with the migrating diurnal tide. *Geophys. Res. Lett.*, **37 (16)**, doi:10.1029/2010GL043906.

McDonald, S. W., C. Grebogi, E. Ott, and J. A. Yorke, 1985: Fractal basin boundaries. *Physica D*, **17 (2)**, 125–153, doi:10.1016/0167-2789(85)90001-6.

McGregor, G. R., 2006: Climatology: Its scientific nature and scope. *Int. J. Climatol.*, **26 (1)**, 1–5, doi:10.1002/joc.1291.

McGuffie, K., and A. Henderson-Sellers, 2005: *A climate modelling primer*. J. Wiley.

Meehl, G. A., J. M. Arblaster, J. T. Fasullo, A. Hu, and K. E. Trenberth, 2011: Model-based evidence of deep-ocean heat uptake during surface-temperature hiatus periods. *Nat. Clim. Chang.*, **1 (7)**, 360–364.

Meehl, G. A., A. Hu, and B. D. Santer, 2009: The Mid-1970s Climate Shift in the Pacific and the Relative Roles of Forced versus Inherent Decadal Variability. *J. Clim.*, **22 (3)**, 780–792, doi:10.1175/2008jcli2552.1.

Meehl, G. A., W. M. Washington, W. D. Collins, J. M. Arblaster, A. Hu, L. E. Buja, W. G. Strand, and H. Teng, 2005: How Much More Global Warming and Sea Level Rise? *Science*, **307 (5716)**, 1769–1772, doi:10.1126/science.1106663.

Meehl, G. A., and Coauthors, 2014: Decadal climate prediction: an update from the trenches. *Bull. Am. Meteorol. Soc.*, **95 (2)**, 243–267, doi:10.1175/BAMS-D-12-00241.1.

Meijers, A. J. S., E. Shuckburgh, N. Bruneau, J.-B. Sallee, T. J. Bracegirdle, and Z. Wang, 2012: Representation of the Antarctic Circumpolar Current in the CMIP5 climate models and future changes under warming scenarios. *J. Geophys. Res.*, **117**, C12 008, doi:10.1029/2012jc008412.

Minobe, S., 1997: A 50–70 year climatic oscillation over the North Pacific and North America. *Geophys. Res. Lett.*, **24 (6)**, 683–686.

Minobe, S., 1999: Resonance in bidecadal and pentadecadal climate oscillations over the North Pacific: Role in climatic regime shifts. *Geophys. Res. Lett.*, **26 (7)**, 855–858, doi:10.1029/1999GL900119.

Mokhov, I. I., and D. A. Smirnov, 2006: El Niño–Southern Oscillation drives North Atlantic Oscillation as revealed with nonlinear techniques from climatic indices. *Geophys. Res. Lett.*, **33 (3)**, doi:10.1029/2005GL024557.

Monin, A., 1986: *An Introduction to the Theory of Climate*. Atmospheric and Oceanographic Sciences Library, Springer.

Moore, J. K., M. R. Abbott, and J. G. Richman, 1999: Location and dynamics of the Antarctic Polar Front from satellite sea surface temperature data. *J. Geophys. Res.*, **104 (C2)**, 3059–3073, doi:10.1029/1998JC900032/full.

Muller, R. A., and Coauthors, 2013: Decadal variations in the global atmospheric land temperatures. *J. Geophys. Res. Atmos.*, **118 (11)**, 5280–5286, doi:10.1002/jgrd.50458.

Neale, R. B., J. Richter, S. Park, P. H. Lauritzen, S. J. Vavrus, P. J. Rasch, and M. Zhang, 2013: The mean climate of the Community Atmosphere Model (CAM4) in forced SST and fully coupled experiments. *J. Clim.*, **26 (14)**, 5150–5168.

Neelin, J. D., D. S. Battisti, A. C. Hirst, F.-F. Jin, Y. Wakata, T. Yamagata, and S. E. Zebiak, 1998: ENSO theory. *J. Geophys. Res.*, **103 (C7)**, 14 261–14 290, doi:10.1029/97JC03424.

Neelin, J. D., and H. A. Dijkstra, 1995: Ocean-atmosphere interaction and the tropical climatology. Part I: The dangers of flux correction. *J. Clim.*, **8 (5)**, 1325–1342.

Nicolis, C., and G. Nicolis, 1984: Is there a climatic attractor? *Nature*, **311 (5986)**, 529–532.

Nicolis, C., and G. Nicolis, 1986: Reconstruction of the dynamics of the climatic system from time-series data. *Proc. Natl. Acad. Sci. U.S.A.*, **83 (3)**, 536–540, URL: http://www.pnas.org/content/83/3/536.abstract.

O'Brien, T., L. Sloan, and M. Snyder, 2011: Can ensembles of regional climate model simulations improve results from sensitivity studies? *Clim. Dyn.*, **37 (5 - 6)**, 1111 – 1118, doi:10.1007/s00382-010-0900-5.

Oreskes, N., D. A. Stainforth, and L. A. Smith, 2010: Adaptation to Global Warming: Do Climate Models Tell Us What We Need to Know? *Philos. Sci.*, **77 (5)**, 1012–1028, doi:10.1086/657428.

Orsi, A. H., T. Whitworth III, and W. D. Nowlin Jr, 1995: On the meridional extent and fronts of the Antarctic Circumpolar Current. *Deep Sea Res. I*, **42 (5)**, 641–673.

Otto, A., and Coauthors, 2013: Energy budget constraints on climate response. *Nat. Geosci.*, **6 (6)**, 415–416, doi:10.1038/ngeo1836.

Palmer, T., 1993: Extended-range atmospheric prediction and the Lorenz model. *Bull. Am. Meteorol. Soc.*, **74 (1)**, 49–65.

Palmer, T., 1999: A nonlinear dynamical perspective on climate prediction. *J. Clim.*, **12 (2)**, 575–591.

Palmer, T. N., 1996: Predictability of the Atmosphere and Oceans: From Days to Decades. *Decadal Climate Variability*, D. T. Anderson, and J. Willebrand, Eds., NATO ASI Series, Vol. 44, Springer Berlin Heidelberg, 83–155, doi:10.1007/978-3-662-03291-6_3.

Palmer, T. N., 2009: Edward Norton Lorenz. 23 May 1917– 16 April 2008. *Biogr. Mems Fell. R. Soc.*, **55 (0)**, 139–155, doi:10.1098/rsbm.2009.0004.

Palmer, T. N., A. D oring, and G. Seregin, 2014: The real butterfly effect. *Nonlinearity*, **27 (9)**, R123, doi:10.1088/0951-7715/27/9/R123.

Park, J., and M. E. Mann, 2000: Interannual temperature events and shifts in global temperature: A "multiwavelet" correlation approach. *Earth Interact.*, **4 (1)**, 1–36.

Park, W., and M. Latif, 2008: Multidecadal and multicentennial variability of the meridional overturning circulation. *Geophys. Res. Lett.*, **35 (22)**, doi:10.1029/2008GL035779.

Park, W., and M. Latif, 2012: Atlantic Meridional Overturning Circulation response to idealized external forcing. *Clim. Dyn.*, **39 (7 - 8)**, 1709–1726, doi:10.1007/s00382-011-1212-0.

Patara, L., and C. W. Böning, 2014: Abyssal ocean warming around Antarctica strengthens the Atlantic overturning circulation. *Geophys. Res. Lett.*, **41 (11)**, 3972–3978, doi:10.1002/2014gl059923.

Peixoto, P. J., Oort, and H. A., 1992: *Physics of climate*. New York: American Institute of Physics (AIP), 1992.

Peixóto, J. P., and A. H. Oort, 1984: Physics of climate. *Rev. Mod. Phys.*, **56 (3)**, 365.

Pelletier, J. D., 1997: Analysis and modeling of the natural variability of climate. *J. Clim.*, **10 (6)**, 1331–1342.

Philander, S. G. H., T. Yamagata, and R. C. Pacanowski, 1984: Unstable air-sea interactions in the tropics. *J. Am. Stat. Assoc.*, **41 (4)**, 604–613.

Phipps, S. J., and Coauthors, 2013: Paleoclimate data–model comparison and the role of climate forcings over the past 1500 years. *J. Clim.*, **26 (18)**, 6915–6936.

Pielke Sr., R. A., 1998: Climate prediction as an initial value problem. *Bull. Am. Meteorol. Soc*, **79 (12)**, 2743.

Pitcock, A. B., 1978: Concepts and Perspectives. *Climatic Change and Variability: A Southern Perspective*, A. Pitcock, L. Frakes, D. Jenssen, J. Peterson, and J. Zillman, Eds., Cambridge University Press, Cambridge, chap. 1, 1–3.

Quinlan, F. T., 1986: Comments on "Sahel: The Changing Rainfall Regime and the 'Normals' Used for its Assessment". *J. Clim. Appl. Meteorol.*, **25 (2)**, 257 –257.

R Development Core Team, 2014: *R: A Language and Environment for Statistical Computing*. Vienna, Austria, R Foundation for Statistical Computing, URL: http://www.r-project.org, ISBN 3-900051-07-0.

Rahmstorf, S., 1995: Climate drift in an ocean model coupled to a simple, perfectly matched atmosphere. *Clim. Dyn.*, **11 (8)**, 447–458.

Randall, D., and Coauthors, 2007: Cilmate Models and Their Evaluation. *Climate Change 2007: The Physical Science Basis. Contribution of Working Group I to the Fourth Assessment Report of the Intergovernmental Panel on Climate Change*, S. Solomon, D. Qin, M. Manning, Z. Chen, M. Marquis, K. Averyt, M. Tignor, and H. Miller, Eds., Cambridge University Press, Cambridge, United Kingdom and New York, NY, USA.

Reason, C. J. C., W. Landman, and W. Tennant, 2006: Seasonal to Decadal Prediction of Southern African Climate and Its Links with Variability of the Atlantic Ocean. *Bull. Am. Meteorol. Soc.*, **87 (7)**, 941–955, doi:10.1175/bams-87-7-941.

Reason, C. J. C., and M. Rouault, 2005: Links between the Antarctic Oscillation and winter rainfall over western South Africa. *Geophys. Res. Lett.*, **32**, L07 705, doi:10.1029/2005gl022419.

Rial, J. A., and Coauthors, 2004: Nonlinearities, feedbacks and critical thresholds within the Earth's climate system. *Clim. Chang.*, **65 (1-2)**, 11–38, doi:10.1023/B:CLIM.0000037493.89489.3f.

Rind, D., 1999: Complexity and Climate. *Science*, **284 (5411)**, 105–107, doi:10.1126/science.284.5411.105.

Risbey, J. S., S. Lewandowsky, C. Langlais, D. P. Monselesan, T. J. O'Kane, and N. Oreskes, 2014: Well-estimated global surface warming in climate projections selected for ENSO phase. *Nat. Clim. Chang.*, **4 (9)**, 835–840, doi:10.1038/nclimate2310.

Rodgers, K. B., P. Friederichs, and M. Latif, 2004: Tropical Pacific decadal variability and its relation to decadal modulations of ENSO. *J. Clim.*, **17 (19)**, 3761–3774.

Rogers, J. C., 1984: The association between the North Atlantic Oscillation and the Southern Oscillation in the northern hemisphere. *Mon. Weather Rev.*, **112 (10)**, 1999–2015.

Rose, B. E. J., K. C. Armour, D. S. Battisti, N. Feldl, and D. D. B. Koll, 2014: The dependence of transient climate sensitivity and radiative feedbacks on the spatial pattern of ocean heat uptake. *Geophys. Res. Lett.*, **41 (3)**, 1071–1078, doi:10.1002/2013gl058955.

Rouyer, T., J.-M. Fromentin, F. Ménard, B. Cazelles, K. Briand, R. Pianet, B. Planque, and N. C. Stenseth, 2008a: Complex interplays among population dynamics, environmental forcing, and exploitation in fisheries. *Proc. Natl. Acad. Sci. U.S.A.*, **105 (14)**, 5420–5425, doi:10.1073/pnas.0709034105.

Rouyer, T., J.-M. Fromentin, N. C. Stenseth, and B. Cazelles, 2008b: Analysing multiple time series and extending significance testing in wavelet analysis. *Mar. Ecol. Prog. Ser.*, **359**, 11–23, doi:10.3354/meps07330.

Sahay, A., and K. R. Sreenivasan, 1996: The Search for a Low-Dimensional Characterization of a Local Climate System. *Phil. Trans. R. Soc. A*, **354 (1713)**, 1715–1750, doi:10.1098/rsta.1996.0076.

Sawilowsky, S. S., and R. C. Blair, 1992: A more realistic look at the robustness and Type II error properties of the t test to departures from population normality. *Psychol. Bull.*, **111 (2)**, 352.

Scafetta, N., 2008: Comment on "Heat capacity, time constant, and sensitivity of Earth's climate system" by S.E. Schwartz. *J. Geophys. Res.*, **113**, D15 104.

Schellnhuber, H.-J., 1999: 'Earth system' analysis and the second Copernican revolution. *Nature*, **402**, C19–C23.

Schleussner, C. F., J. Runge, J. Lehmann, and A. Levermann, 2014: The role of the North Atlantic overturning and deep ocean for multi-decadal global-mean-temperature variability. *Earth Syst. Dynam.*, **5 (1)**, 103–115, doi:10.5194/esd-5-103-2014.

Schneider, S. H., and R. E. Dickinson, 1974: Climate modeling. *Rev. Geophys. Space Phys.*, **12 (3)**, 447–493.

Schwartz, S. E., 2007: Heat capacity, time constant, and sensitivity of Earth's climate system. *J. Geophys. Res.*, **112**, D24S05.

Schwartz, S. E., 2008a: Reply to comments by G. Foster et al., R. Knutti et al., and N. Scafetta on "Heat capacity, time constant, and sensitivity of Earth's climate system". *J. Geophys. Res.*, **113**, D15 105.

Schwartz, S. E., 2008b: Uncertainty in climate sensitivity: Causes, consequences, challenges. *Energ. Environ. Sci.*, **1 (4)**, 430–453, doi:10.1039/B810350J.

Schwartz, S. E., 2012: Determination of Earth's transient and equilibrium climate sensitivities from observations over the twentieth century: strong dependence on assumed forcing. *Surv. Geophys.*, **33 (3-4)**, 745–777, doi:10.1007/s10712-012-9180-4.

Schwartz, S. E., R. J. Charlson, R. A. Kahn, J. A. Ogren, and H. Rodhe, 2010: Why hasn't Earth warmed as much as expected? *J. Clim.*, **23 (10)**, 2453–2464, doi:10.1175/2009JCLI3461.1.

Sellers, W. D., 1969: A Global Climatic Model Based on the Energy Balance of the Earth-Atmosphere System. *J. Appl. Meteorol.*, **8 (3)**, 392–400, doi:10.1175/1520-0450(1969)008<0392:AGCMBO>2.0.CO;2.

Selvam, A. M., 2012: Nonlinear Dynamics and Chaos: Applications in Atmospheric Sciences. *J. Adv. Math. Appl.*, **1 (2)**, 181–205, doi:10.1166/jama.2012.1014.

Sen Gupta, A., N. C. Jourdain, J. N. Brown, and D. Monselesan, 2013: Climate Drift in the CMIP5 Models. *J. Clim.*, **26 (21)**, 8597–8615, doi:10.1175/jcli-d-12-00521.1.

Sen Gupta, A., L. C. Muir, J. N. Brown, S. J. Phipps, P. J. Durack, D. Monselesan, and S. E. Wijffels, 2012: Climate Drift in the CMIP3 Models. *J. Clim.*, **25 (13)**, 4621–4640, doi:10.1175/jcli-d-11-00312.1.

Sen Gupta, A., A. Santoso, A. S. Taschetto, C. C. Ummenhofer, J. Trevena, and M. H. England, 2009: Projected Changes to the Southern Hemisphere Ocean and Sea Ice in the IPCC AR4 Climate Models. *J. Clim.*, **22 (11)**, 3047–3078, doi:10.1175/2008jcli2827.1.

Shackleton, N. J., and J. Imbrie, 1990: The $\delta^{18}O$ spectrum of oceanic deep water over a five-decade band. *Clim. Chang.*, **16 (2)**, 217–230, doi:10.1007/BF00134658.

Shields, C. A., D. A. Bailey, G. Danabasoglu, M. Jochum, J. T. Kiehl, S. Levis, and S. Park, 2012: The low-resolution CCSM4. *J. Clim.*, **25 (12)**, 3993–4014.

Shilnikov, L. P., A. L. Shilnikov, D. V. Turaev, and L. O. Chua, 1998: *Methods of qualitative theory in nonlinear dynamics: Part I*, Vol. 5. World Scientific.

Sivakumar, B., 2004: Chaos theory in geophysics: past, present and future. *Chaos Soliton. Fract.*, **19 (2)**, 441–462, doi:10.1016/s0960-0779(03)00055-9.

Small, R. J., and Coauthors, 2014: A new synoptic scale resolving global climate simulation using the Community Earth System Model. *J. Adv. Model. Earth Syst.*, **6 (4)**, 1065–1094, doi:10.1002/2014MS000363.

Smith, L., 2000a: Disentangling Uncertainty and Error: On the Predictability of Nonlinear Systems. *Nonlinear Dynamics and Statistics*, A. Mees, Ed., Birkhauser.

Smith, L., 2000b: Limits to predictability in 2000 and 2100. *Adaptive Systems for Signal Processing, Communications, and Control Symposium 2000. AS-SPCC. The IEEE 2000*, IEEE, 129–134.

Smith, L., 2002: What might we learn from climate forecasts? *Proc. Natl. Acad. Sci. U.S.A.*, **99 (Suppl 1)**, 2487–2492.

Smith, R. S., R. Sutton, E. Hawkins, D. A. Stainforth, and J. M. Gregory, 2014: Irreducible uncertainty in regional near-term climate projections. *AGU Fall Meeting Abstracts*, Vol. 1, 3309.

Spiegel, E. A., 1987: Chaos: A Mixed Metaphor for Turbulence. *Proc. R. Soc. A*, **413 (1844)**, 87–95, doi:10.1098/rspa.1987.0102.

Stainforth, D., M. Allen, E. Tredger, and L. Smith, 2007a: Confidence, uncertainty and decision-support relevance in climate predictions. *Phil. Trans. R. Soc. A*, **365 (1857)**, 2145–2161.

Stainforth, D. A., T. E. Downing, R. Washington, A. Lopez, and M. New, 2007b: Issues in the interpretation of climate model ensembles to inform decisions. *Phil. Trans. R. Soc. A*, **365 (1857)**, 2163–2177, doi:10.1098/rsta.2007.2073.

Stainforth, D. A., and Coauthors, 2005: Uncertainty in predictions of the climate response to rising levels of greenhouse gases. *Nature*, **433 (7024)**, 403–406.

Steele, M., R. Morley, and W. Ermold, 2001: PHC: A global ocean hydrography with a high-quality Arctic Ocean. *J. Clim.*, **14 (9)**, 2079 –2087.

Stevens, B., and S. Bony, 2013: What Are Climate Models Missing? *Science*, **340 (6136)**, 1053–1054, doi:10.1126/science.1237554.

Stommel, H., 1961: Thermohaline convection with two stable regimes of flow. *Tellus*, **13**, 224–230.

Stone, D., A. J. Weaver, and R. J. Stouffer, 2001: Projection of climate change onto modes of atmospheric variability. *J. Clim.*, **14 (17)**, 3551–3565.

Stone, D. A., M. R. Allen, F. Selten, M. Kliphuis, and P. A. Stott, 2007: The detection and attribution of climate change using an ensemble of opportunity. *J. Clim.*, **20 (3)**, 504 – 516.

Stone, D. A., M. R. Allen, P. A. Stott, P. Pall, S.-K. Min, T. Nozawa, and S. Yukimoto, 2009: The Detection and Attribution of Human Influence on Climate. *Ann. Rev. Environ. Resour.*, **34 (1)**, 1–16, doi:10.1146/annurev.environ.040308.101032.

Strogatz, S., 1994: *Nonlinear dynamics and chaos: with applications to physics, biology, chemistry and engineering*. Perseus Books Group.

Swanson, K. L., G. Sugihara, and A. A. Tsonis, 2009: Long-term natural variability and 20th century climate change. *Proc. Natl. Acad. Sci. U.S.A.*, **106 (38)**, 16 120–16 123, doi:10.1073/pnas.0908699106, http://www.pnas.org/content/106/38/16120.full.pdf.

Swanson, K. L., and A. A. Tsonis, 2009: Has the climate recently shifted? *Geophys. Res. Lett.*, **36 (6)**, L06 711, doi:10.1029/2008gl037022.

Tang, Y., and Z. Deng, 2010: Low-dimensional nonlinearity of ENSO and its impact on predictability. *Physica D*, **239 (5)**, 258–268, doi:10.1016/j.physd.2009.11.006.

Tantet, A., and H. A. Dijkstra, 2014: An interaction network perspective on the relation between patterns of sea surface temperature variability and global mean surface temperature. *Earth Syst. Dynam.*, **5 (1)**, 1–14, doi:10.5194/esd-5-1-2014.

Taylor, K. E., R. J. Stouffer, and G. A. Meehl, 2012: An Overview of CMIP5 and the Experiment Design. *Bull. Am. Meteorol. Soc.*, **93 (4)**, 485–498, doi:10.1175/bams-d-11-00094.1.

te Raa, L. A., and H. . A. Dijkstra, 2002: Instability of the thermohaline ocean circulation on interdecadal timescales. *J. of Phys. Oceanogr.*, **32 (1)**, 138–160.

Teng, H., and G. Branstator, 2011: Initial-value predictability of prominent modes of North Pacific subsurface temperature in a CGCM. *Clim. Dyn.*, **36 (9-10)**, 1813–1834, doi:10.1007/s00382-010-0749-7.

Teng, H., G. Branstator, and G. A. Meehl, 2011: Predictability of the Atlantic Overturning Circulation and Associated Surface Patterns in Two CCSM3 Climate Change Ensemble Experiments. *J. Clim.*, **24**, 6054–6076, doi:10.1175/2011JCLI4207.1.

Thies, J., F. Wubs, and H. A. Dijkstra, 2009: Bifurcation analysis of 3D ocean flows using a parallel fully-implicit ocean model. *Ocean Modell.*, **30 (4)**, 287–297, doi:10.1016/j.ocemod.2009.07.005.

Thompson, D. W. J., S. Solomon, P. J. Kushner, M. H. England, K. M. Grise, and D. J. Karoly, 2011: Signatures of the Antarctic ozone hole in Southern Hemisphere surface climate change. *Nat. Geosci.*, **4 (11)**, 741–749, doi:10.1038/ngeo1296.

Todorov, A. V., 1985: Sahel: The changing rainfall regime and the "normals" used for its assessment. *J. Clim. Appl. Meteorol.*, **24 (2)**, 97–107.

Todorov, A. V., 1986: Reply. *J. Clim. Appl. Meteorol.*

Torrence, C., and G. P. Compo, 1998: A Practical Guide to Wavelet Analysis. *Bull. Am. Meteorol. Soc.*, **79 (1)**, 61–78.

Torrence, C., and P. J. Webster, 1998: The annual cycle of persistence in the El Niño/Southern Oscillation. *Q. J. R. Meteorol. Soc.*, **124 (550)**, 1985–2004, doi:10.1002/qj.49712455010.

Toth, Z., and E. Kalnay, 1993: Ensemble forecasting at NMC: The generation of perturbations. *Bull. Am. Meteorol. Soc*, **74 (12)**, 2317–2330.

Toth, Z., and E. Kalnay, 1997: Ensemble forecasting at NCEP and the breeding method. *Mon. Weather Rev.*, **125 (12)**, 3297–3319.

Trenberth, K. E., 1976: Spatial and temporal variations of the Southern Oscillation. *Q. J. R. Meteorol. Soc.*, **102 (433)**, 639–653, doi:10.1002/qj.49710243310.

Trenberth, K. E., 1990: Recent observed interdecadal climate changes in the Northern Hemisphere. *Bull. Am. Meteorol. Soc*, **71 (7)**, 988–993.

Trenberth, K. E., 1997: The Definition of El Niño. *Bull. Am. Meteorol. Soc.*, **78 (12)**, 2771–2777, doi:10.1175/1520-0477(1997)078<2771:TDOENO>2.0.CO;2.

Trenberth, K. E., and T. J. Hoar, 1996: The 1990–1995 El Niño-Southern Oscillation event: Longest on record. *Geophys. Res. Lett.*, **23 (1)**, 57–60.

Trenberth, K. E., and J. W. Hurrell, 1994: Decadal atmosphere-ocean variations in the Pacific. *Clim. Dyn.*, **9 (6)**, 303–319.

Trewin, B., 2007: *WCDMP– No. 61: The Role of Climatological Normlas in a Changing Climate*, WMO-TD, Vol. 1377. World Meteorological Organisation, Geneva, Switzerland.

Tsonis, A., J. Elsner, and K. Georgakakos, 1993: Estimating the dimension of weather and climate attractors: important issues about the procedure and interpretation. *J. Atmos. Sci.*, **50 (15)**, 2549–2555, doi:10.1175/1520-0469(1993)050<2549:ETDOWA>2.0.CO;2.

Tsonis, A. A., 1996: Dynamical systems as models for physical processes. *Complexity*, **1 (5)**, 23–33, doi:10.1002/cplx.6130010506.

Tsonis, A. A., 2001: The impact of nonlinear dynamics in the atmospheric sciences. *Int. J. Bifurcat. Chaos*, **11 (04)**, 881–902, doi:10.1142/S0218127401002663.

Tsonis, A. A., and J. B. Elsner, 1989: Chaos, strange attractors, and weather. *Bull. Am. Meteorol. Soc*, **70 (1)**, 14–23.

Tsonis, A. A., K. Swanson, and S. Kravtsov, 2007: A new dynamical mechanism for major climate shifts. *Geophys. Res. Lett.*, **34**, L13 705, doi:10.1029/2007gl030288.

Tsonis, A. A., and K. L. Swanson, 2012: Review article "On the origins of decadal climate variability: a network perspective". *Nonlin. Processes Geophys.*, **19 (5)**, 559–568, doi:10.5194/npg-19-559-2012.

Tsonis, A. A., K. L. Swanson, and P. J. Roebber, 2006: What Do Networks Have to Do with Climate? *Bull. Am. Meteorol. Soc.*, **87 (5)**, 585–595, doi:10.1175/bams-87-5-585.

Tsonis, A. A., G. N. Triantafyllou, and J. B. Elsner, 1994: Searching for determinism in observed data: A review of the issues involved. *Nonlin. Processes Geophys.*, **1 (1)**, 12 – 25, doi:10.5194/npg-1-12-1994.

Ujeneza, E., and B. Abiodun, 2015: Drought regimes in Southern Africa and how well GCMs simulate them. *Clim. Dyn.*, **44 (5–6)**, 1595–1609, doi:10.1007/s00382-014-2325-z.

van Veen, L., 2003: Overturning and wind-driven circulation in a low-order ocean–atmosphere model. *Dynam. Atmos. Oceans*, **37 (3)**, 197–221, doi:10.1016/S0377-0265(03)00032-0.

van Veen, L., T. Opsteegh, and F. Verhulst, 2001: Active and passive ocean regimes in a low-order climate model. *Tellus A*, **53A**, 616–628.

van Vuuren, D., and Coauthors, 2011: The representative concentration pathways: An overview. *Clim. Chang.*, **109 (1 - 2)**, 5–31, doi:10.1007/s10584-011-0148-z.

Veleda, D., R. Montagne, and M. Araujo, 2012: Cross-wavelet bias corrected by normalizing scales. *J. Atmos. Ocean. Tech.*, **29 (9)**, 1401–1408.

Vertenstein, M., A. Bertini, T. Craig, J. Edwards, M. Levy, A. Mai, and J. Schollenberger, 2013: CESM1.2 Release Series User's Guide. Tech. rep., NCAR. URL: http://www.cesm.ucar.edu/models/cesm1.2/cesm/doc/usersguide/book1.html.

von Storch, H., and F. W. Zwiers, 1999: *Statistical Analysis in Climate Research*. Cambridge University Press, Cambridge, UK.

Wallace, J., 1996a: Observed Climatic Variability: Spatial Structure. *Decadal Climate Variability*, D. T. Anderson, and J. Willebrand, Eds., NATO ASI Series, Vol. 44, Springer Berlin Heidelberg, 31–81, doi:10.1007/978-3-662-03291-6_2.

Wallace, J., 1996b: Observed Climatic Variability: Time Dependence. *Decadal Climate Variability*, D. T. Anderson, and J. Willebrand, Eds., NATO ASI Series, Vol. 44, Springer Berlin Heidelberg, 1–30, doi:10.1007/978-3-662-03291-6_1.

Ward, J. H., 1963: Hierarchical Grouping to Optimize an Objective Function. *J. Am. Stat. Assoc.*, **58 (301)**, 236–244, doi:10.1080/01621459.1963.10500845.

Watanabe, M., Y. Kamae, M. Yoshimori, A. Oka, M. Sato, M. Ishii, T. Mochizuki, and M. Kimoto, 2013: Strengthening of ocean heat uptake efficiency associated with the recent climate hiatus. *Geophys. Res. Lett.*, **40 (12)**, 3175–3179, doi:10.1002/grl.50541.

Weijer, W., and Coauthors, 2012: The Southern Ocean and its climate in CCSM4. *J. Clim.*, **25 (8)**, 2652–2675.

Werndl, C., 2014a: Definitions of climate and climate change under varying external conditions. *Earth Syst. Dynam. Discuss.*, **5 (1)**, 683–719, doi:10.5194/esdd-5-683-2014.

Werndl, C., 2014b: Interactive comment on `Definitions of climate and climate change under varying external conditions'. *Earth Syst. Dynam. Discuss.*, **5**, C355–C377, URL: http://www.earth-syst-dynam-discuss.net/5/683/2014/esdd-5-683-2014-discussion.html.

Werndl, C., 2015: On Defining Climate and Climate Change. *Brit. J. Philos. Sci.*, **0**, 1–28, doi:10.1093/bjps.

Wickham, H., 2009: *ggplot2: Elegant Graphics for Data Analysis*. Use R!, Springer.

Wittenberg, A. T., 2009: Are historical records sufficient to constrain ENSO simulations? *Geophys. Res. Lett.*, **36 (12)**, L12 702, doi:10.1029/2009gl038710.

Wittenberg, A. T., A. Rosati, T. L. Delworth, G. A. Vecchi, and F. Zeng, 2014: ENSO Modulation: Is It Decadally Predictable? *J. Clim.*, **27 (7)**, 2667–2681, doi:10.1175/jcli-d-13-00577.1.

WMO, 1983: *WMO - No. 100: Guide to Climatological Practices*. 2nd ed., World Meteorological Organisation.

WMO, 1988: *General Meteorological Standards and Recommended Practices*, WMO - No. 49: Technical Regulations, Vol. 1. World Meteorological Organisation, Geneva, Sitzerland.

WMO, 2010: *WMO - No. 100: Guide to Climatological Practices*. 3rd ed., World Meteorological Organisation.

WMO, 2012: METEOTERM. URL: http://wmo.multicorpora.net/MultiTransWeb/Web.mvc, [Online 2 June 2013].

Wu, Z., N. E. Huang, J. M. Wallace, B. V. Smoliak, and X. Chen, 2011: On the time-varying trend in global-mean surface temperature. *Clim. Dyn.*, **37 (3-4)**, 759–773, doi:10.1007/s00382-011-1128-8.

Wu, Z., E. Schneider, B. Kirtman, E. S. Sarachik, N. Huang, and C. Tucker, 2008: The modulated annual cycle: An alternative reference frame for climate anomalies. *Clim. Dyn.*, **31 (7 - 8)**, 823–841, doi:10.1007/s00382-008-0437-z.

Wunsch, C., 2003: The spectral description of climate change including the 100 ky energy. *Clim. Dyn.*, **20 (4)**, 353–363, doi:10.1007/s00382-002-0279-z.

Yeager, S. G., C. A. Shields, W. G. Large, and J. J. Hack, 2006: The low-resolution CCSM3. *J. Clim.*, **19 (11)**, 2545–2566.

Zhang, T., and D.-Z. Sun, 2014: ENSO Asymmetry in CMIP5 Models. *J. Clim.*, **27 (11)**, 4070–4093.

Zhang, T., D.-Z. Sun, R. Neale, and P. J. Rasch, 2009: An evaluation of ENSO asymmetry in the Community Climate System Models: A view from the subsurface. *J. Clim.*, **22 (22)**, 5933–5961.

Zhang, Y., J. M. Wallace, and D. S. Battisti, 1997: ENSO-like interdecadal variability: 1900-93. *J. Clim.*, **10 (5)**, 1004–1020.

Appendix A

Additional Methodological Details

A.1 CESM

CESM is available online for download at http://www2.cesm.ucar.edu/. The model set-up procedure for CESM1.2, the version used in this study, is explained in Vertenstein et al. (2013). Many different set-ups of the model are possible, making it suitable for a wide variety of modelling studies.

A.1.1 Component Sets

The component set or "compset" (see http://www.cesm.ucar.edu/models/cesm1.2/cesm/doc/modelnl/compsets.html) used for the present day controls ensembles is B_2000. B_1850 is used for the PIC. For the TFEs, B_RCP8.5_CN is used. Note, however, that because the CN-module is not used for PDCs, it is considered essential for comparability that this be deactivated for TFEs. Because all default RCP configurations of CESM1.2 include the CN-module, it had to be explicitly changed for CLM compilation. Otherwise the configurations used are as for the standard CESM RCP8.5 set-up.

A.1.2 CLM IC Perturbations Required in Certain Ensembles

Transient land BC files were not all available for use with the f45gx3 resolution. Consequently, the CESM regridding tools were used to produce compatible forcing files. However, the files thus produced are dimensionally incompatible with restart output from f45gx3 present day simulations. Hence, CLM restart output had to be interpolated for use in RCP8.5 simulations. Whereas this is unlikely to significantly affect the model's climate state, it does imply that the IC perturbations imposed on the CFEs and TFEs are not equivalent.

For Yr647, which used present day forcing conditions, but was initialised from restart files produced by an RCP8.5 run, roughly the reverse of the above process was conducted: restart files used as ICs for CLM, needed to be regridded from the grid compatible with the RCP8.5 regridded CLM BCs, to the grid used by CLM in the present day simulations.

A.2 Machines Used

The machines used at CHPC have 8 cores per node, the Edison machine at NERSC has 24. After performing load-balancing it was decided to run the CHPC Control with 64 cores (8 nodes); the CHPC ensemble runs on a single node (8 cores); and both the control run and ensemble runs at NERSC on 5 nodes (120 cores) each.

A.3 Wavelet Implementation

Version 0.17.5 of the `Biwavelet` package is used here; this version (and all other versions since 0.14) includes a bias correction in the wavelet power spectrum, after Liu et al. (2007) and—for the cross-wavelet and wavelet coherence functions—Veleda et al. (2012).

Appendix B

Model Drift and Internal Variability in the Pre-Industrial Control

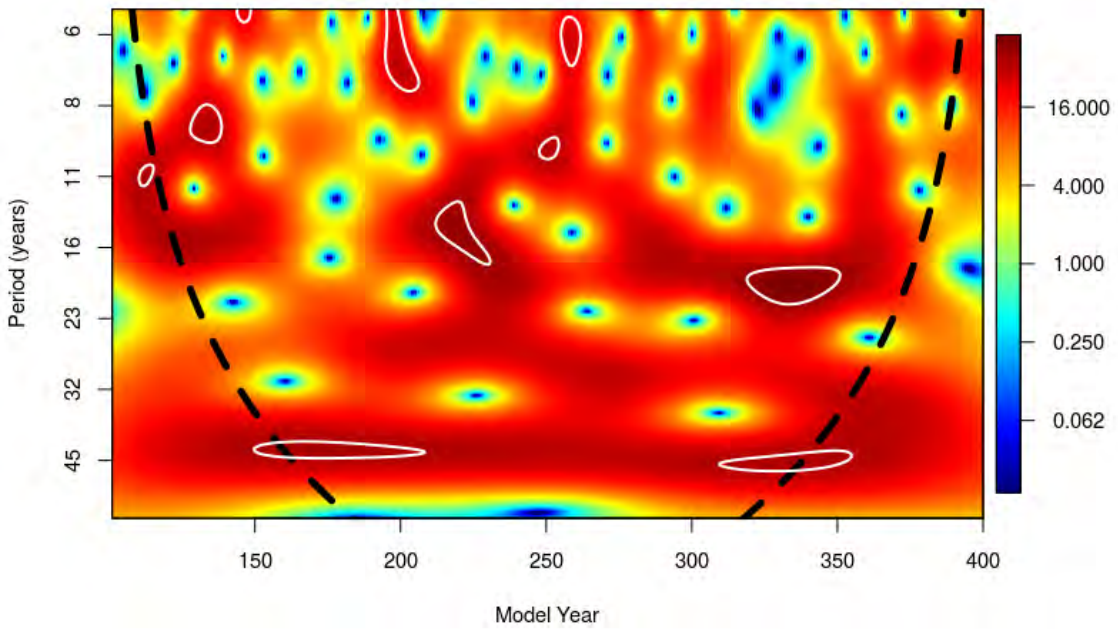

Figure B.1: As in Figure 4.3, but for NPa TS in the PIC.

The PIC appears to reach a relatively stable state, with much smaller subsequent TS drift than in the PDCs, immediately after the initial transient (see section 4.1). This should perhaps be expected, given that CCSM4 is initialised and parametrised for use

with pre-industrial forcing (see subsection 3.4.2). The apparent near-equilibrium state of the PIC is reached after about 70 to 100 model years, over all considered domains. The length of the PIC is, insufficient to verify whether model drift would remain negligible indefinitely—a shorter period of little drift in the PDCs is discussed in section 4.1.

Figure B.1 shows NPa TS wavelet power between model years 101 and 400 of the PIC. Unfortunately this is too short a period from which to draw robust conclusions, but it appears that a greater degree of lower-frequency ($\nu < \frac{1}{15}\text{yr}^{-1}$) variability occurs than during the earlier periods in the PDCs. Significant peaks occur in the interdecadal (15-20 year periods) and multidecadal bands ($\sim$ 45 year period), although the latter peaks straddle the COI. It is interesting to note that these peaks correspond quite well with peaks in lower-frequency NPa variability in the PDCs (see section 4.2).

As shown in Figure 4.1, there is some indication that NPa TS variability continues to increase over the duration of the PIC. Shifts occur between distinct colder and warmer model states, lasting—at times—for multiple decades. It is not clear whether this is simply an artefact of the relatively shorter run duration of the PIC.

Figure C.1 shows that, whereas Central Pacific ENSO variability does appear to increase during the PIC's 459-year duration, the variation in Niño-4 TS variance is not outside the bounds of what is exhibited by the PDCs. Further east, the change in variability is greater. In contrast, the PDCs exhibit relatively constant variability, over all domains, for at least the first 1000 years (see section 4.2).

It is possible (however, testing this hypothesis is beyond the scope of this work) that the increase in variability in the PIC is related to the model being allowed to explore more of its attractor space in the absence of strong model drift. This would have important implications for the interpretation of model output as indicative of a climatic possibility space.

The difference in ETP TS variability (which is closely linked to ENSO variability in the model) between the PIC and PDCs, considered from the end of the spin-up period to the 459$^{\text{th}}$ model year, appears to be considerable (Figure B.2). Initially there is little variability in the PIC, before spectral power increases rapidly across a broad range of periods, including more realistic ENSO frequencies ($\frac{1}{6}\text{yr}^{-1} \leq \nu \leq \frac{1}{4}\text{yr}^{-1}$) and interdecadal frequencies ($\nu \sim \frac{1}{15}\text{yr}^{-1}$). The PDCs never exhibit significant interdecadal spectral power.

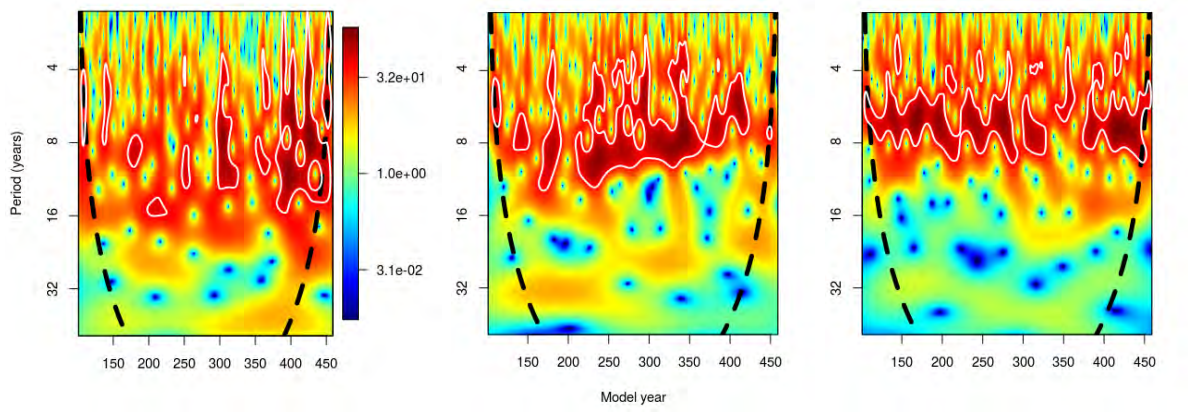

(a) Pre-Industrial (b) CHPC (c) NERSC

Figure B.2: Comparison of normalised ETP TS wavelet power between the three control runs, between model years 101 and 459. See Figure 4.3 for a more detailed discussion of wavelet plots.

Appendix C

Additional Figures and Results

C.1 Model ENSO modulations

In this section, modulations of the model ENSO are described. The 30-year moving Niño-4 TS variance (denoted by $\sigma^2_{N4}(t, 30)$) is used as a metric of such modulations. It is computed as follows:

$$\sigma^2_{N4}(t, 30) = \frac{1}{29} \sum_{\tau=t-14}^{t+15} \left(T_{N4}(\tau) - \overline{T_{N4}(t, 30)} \right)^2 \tag{C.1}$$

where t is discrete time, measured in model years, $T_{N4}(t)$ is defined as in Equation 4.1 and the centred moving average at time t, with window δt, is given by:

$$\overline{T_{N4}(t, \delta t)} = \frac{1}{\delta t} \sum_{\tau=[[t-0.5(\delta t-1)]]}^{[[t+0.5(\delta t)]]} T_{N4}(\tau) \tag{C.2}$$

where $[[x]]$ is the greatest integer less than or equal to x (i.e. floor$[x]$).

Figure C.1 shows the evolution of $\sigma^2_{N4}(t, 30)$ in the PIC and PDCs. It should be noted that, compared to observations (e.g., Zhang and Sun, 2014), the variance is generally about a factor of two too large. However, the relative range of σ^2_{N4} values obtained appear to be compatible with the observed running standard deviation time series obtained by Deser et al. (2012b). This suggests that the nature of model ENSO modulations are comparable with true ENSO modulation, implying that their influence on ensemble evolution can be considered to be relatively realistic.

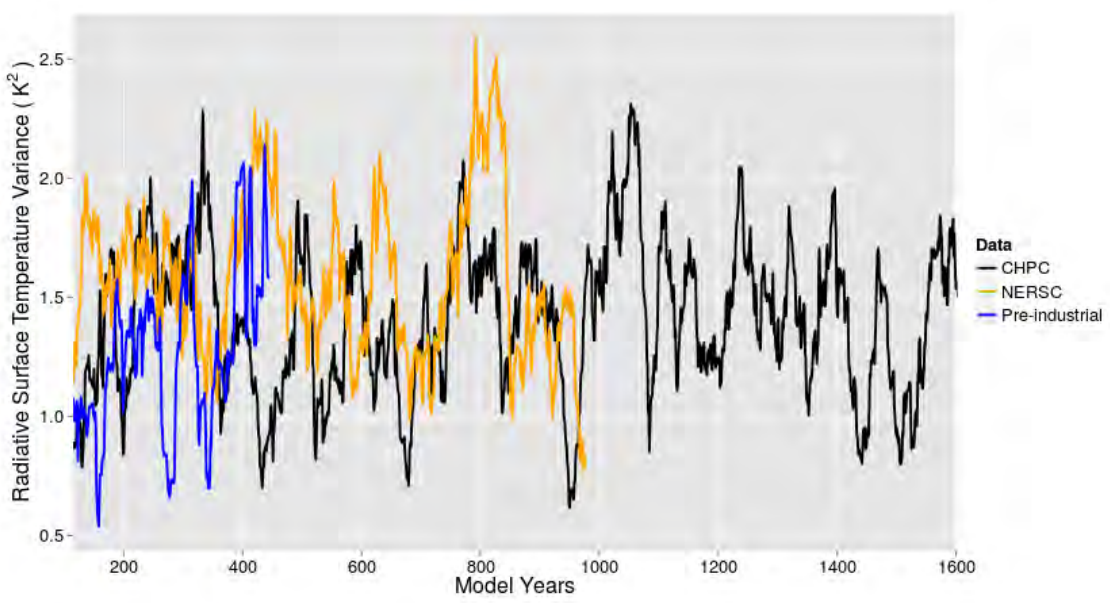

Figure C.1: Time series of centred 30-year variance of Niño4 TS ($\sigma^2_{N4}(t, 30)$) for the three control runs.

Comparison of the NPa TAS PDC time series shown in Figure 4.2 with the corresponding σ^2_{N4} time series in Figure C.1 appears to show a number of roughly co-occurring peaks (for example, model years: 400-430 and 800-850 of the NERSC Control; and 500-520, 580-600, 1020-1080, 1200-1250 and 1480-1500 in the CHPC Control—all periods containing strong EP events; see subsection 4.2.2). During such periods NPa TS variability also appears to increase (supported by wavelet analysis indicating increased—and at times statistically significant—PDC wavelet power in the 25-100 year periods). Consequently, the cross wavelet power and wavelet coherence between $\sigma^2_{N4}(t, 30)$ and NPa TS was investigated. Figure C.2 shows that significant peaks in cross-wavelet power over relatively long durations, at periods of around 50 years, as well as around 80 years, do occur in the CHPC Control. Generally, they show NPa TS leading $\sigma^2_{N4}(t, 30)$ by about a quarter phase ($\frac{\pi}{2}$). A similar phase relationship for regions of significant power is observed in the NERSC Control (not shown), but these regions are smaller (in time-frequency space) and the relationship less consistent. The wavelet coherence shows smaller regions of significance, sometimes at lower frequencies, but generally also at similar times and with the same phase relationship.

It should be noted that analysis conducted with $\sigma^2_{N4}(t, 30)$ involves a quantity which—by definition—has comparatively little variability at temporal scales shorter than 30 years. However, wavelet coherence between the Niño-4 TS index and NPa TS in the PDCs show similar patterns of variability. The Niño-4 TS index typically leads NPa TS by a quarter phase at the multidecadal time scales (consistent with the obtained anti-phase relationship between the Niño-4 TS index and $\sigma^2_{N4}(t, 30)$). Significant power is observed with 50-70

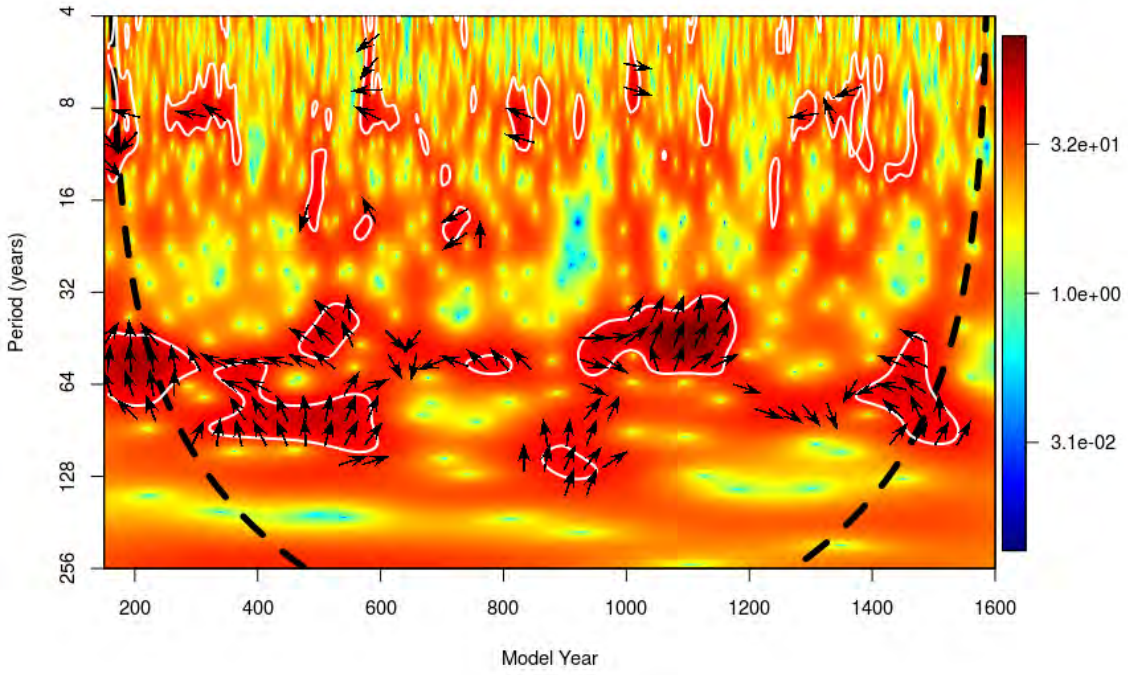

Figure C.2: As in Figure 4.5, but between $\sigma^2_{N4}(t, 30)$ (see text for details) and NPa TS.

year periods between model years 400 and 700 of the NERSC Control (not shown). In the CHPC Control longer-period coherence increases greatly after about model year 900, with peaks occur at periods of about 45, 80 and 125 years, during different time intervals (see Figure C.3). Periods with significant wavelet coherence at the decadal (∼8 year periods) and interdecadal (∼15-20 year periods) also occur, especially during model years 400-500 in the NERSC Control and during CHPC EP events. This may indicate intermittent interaction between extratropical and equatorial variability in the Pacific.

Additional significant wavelet coherence occurs at periods of around 200 years, although this is present only for the first 800 years in the CHPC Control (see Figure C.3) and mostly occurs in the COI. Hence it is assumed to be primarily a product of drift.

It is noteworthy that the model used in this study produces skewness values closer to observed values than any of the CMIP5 models studied by Zhang and Sun (2014). In this study, which compared 14 CMIP5 (20^{th} Century transient) simulations, CCSM4 (1°) best reproduced the observed 1950-1999 skew of the annual mean Niño-3 SST. In the present model set-up, during 50-year periods with high ENSO variability (such as between model years 1101 and 1150 in the CHPC Control, for which Niño-3.4 TS $b_1 \approx 0.87$), observed skewness is well approximated. It may be of value to attempt to understand

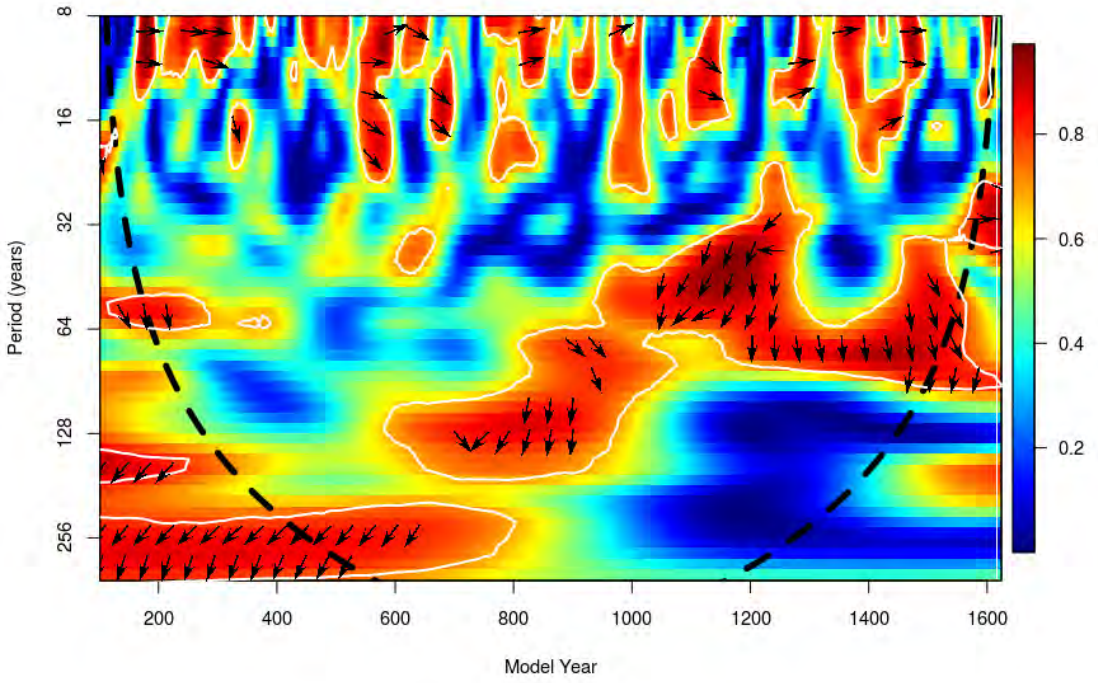

Figure C.3: As in Figure 4.4, but for the squared wavelet coherence between the Niño-4 TS index and NPa TS, from the CHPC Control.

why this model configuration simulates this ENSO characteristic accurately and determine whether this is simply a statistical artefact of the unrealistic ENSO variability produced by the low resolution used. It should be noted, however, that all analyses conducted here use annual-mean anomalies, rather than monthly-mean anomalies, used by, for example, Burgers and Stephenson (1999) and An (2009).

It should, however, be noted that the Niño-4 TS standard deviation (s) of this model is too large compared to observations used in Zhang and Sun (2014) (for the CHPC Control, $s \approx 1.2$K for model years 101-1624 and $s \approx 1.4$K for model years 1101-1150, compared to $s \approx 0.9$K for 1950-1999 observations).

C.2 Associations Between Southern and Northern Hemisphere Variability at Low-Frequencies

The lack of clear influence from the Southern Ocean on the northern Atlantic on well-defined time scales is perhaps surprising, given that spatial analysis shows the largest

multicentennial temperature changes occurring over the downwelling regions of the northern Atlantic and the Atlantic sector of the Southern Ocean (not shown). After model year 1000 there is some significant covariability at periods of 30-40 years between the NAO TS and SSA TS, with NAO variability leading SSA TS by about a $\frac{\pi}{4}$ ($\sim$ 5 years). However, such time frames are much shorter than would be expected for a relationship driven by variability in ocean transport.

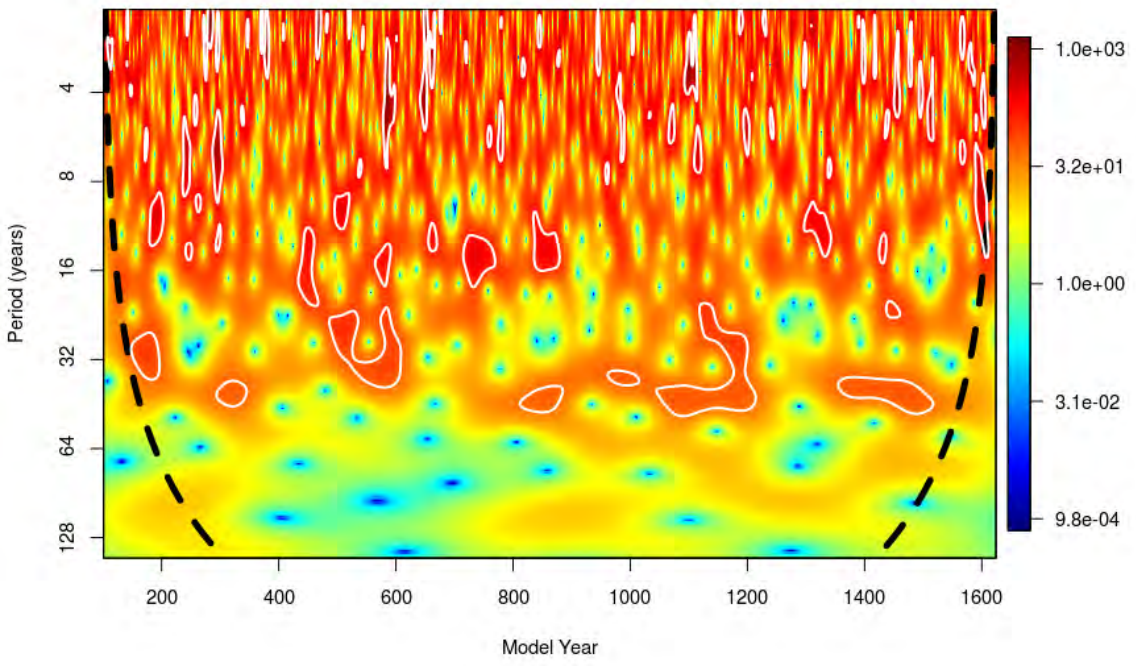

Figure C.4: As in Figure 4.3, but for the SAM PSL index.

Some of the difficulty in identifying significant wavelet power in the Southern Hemispheric extratropics may be a consequence of the magnitude of the influence of model drift over these domains, particularly earlier in the analysis period. More variability at longer periods is identified in the later stages of the CHPC Control. By limiting the analysis to model periods with lower magnitudes of drift (only after model year 600 or after model year 1000), sometimes previously unidentified variability emerges, probably in part because of the contribution of drift to autocorrelation coefficients. Additionally, PSL series, where internal variability is larger compared to drift, show generally more significant variability, especially in the 30-40 year periods— particularly during strong EP events. This is most clearly illustrated in the CHPC Control SAM PSL wavelet spectrum (Figure C.4).

Index

Glossary

almost-intransitivity A property exhibited by some transitive systems, which spend extended—but finite—periods of time in a particular subset of the system's attractor, before transitioning to a different attractor subset, thus creating the impression that the system is intransitive 8, 16, 21, 22, 24, 47–49, 92, 94, 122, 124, 130

attractor A minimal set of points in the state space, such that any trajectory initialised from a point in the set will remain in the set for all time. Strange attractors tend to exhibit chaotic dynamics. 6, 8, 20–23, 29, 30, 49, 50, 102, 129, 165, 173–175

basin of attraction The basin of attraction of some attractor A is the set of all points in the model state space which evolve, as $t \to \infty$, towards A. 21, 174

CAM The Community Atmosphere Model (CAM) is the atmospheric component of CESM. 41

CICE The Community Ice Code (CICE) model is the sea-ice component of CESM. 41

CLM The Community Land Model (CLM) is the land component of CESM. 41

dynamic core The part of a climate model which applies the numerical methods used to solve the PDEs that dictate fluid motions in the relevant climate system component. These equations are sometimes referred to as the primitive equations. 41

ensemble definition A quantification of climate employing climate variable distributions obtained by sampling from all members of an IC ensemble at a particular model time (this necessarily implies that annual averages are used to represent a point in time). 14, 15, 21–24, 124, 125, 131

ensemble-temporal definition A quantification of climate employing climate variable distributions obtained by sampling n time points (in this study, model years) from each of m IC ensemble member runs. first 15, 23, 24, 79, 122, 124, 125

EP event A small proportion ($\sim 4\%$) of model years exhibit an apparently distinct type of ENSO behaviour, characterised by much higher SST anomalies over the eastern equatorial Pacific than over the central and western equatorial Pacific. Such events are referred to as Eastern Pacific (EP) ENSO events. Quantitatively, EP events are defined as occuring during years when the annual-mean Niño-4 TS (T_{N4}) and Niño-1+2 TS (T_{N12}) indices for year t satisfy Equation 4.1. It should be noted that terminology is not intended to imply that these events are produced by dynamics associated with observed EP events, as the

term is conventionally applied in the literature, or that other ENSO events considered here could be considered to be CP ENSO events. 67, 69, 70, 72, 74, 83, 134, 168, 169, 171, 174

EP year A year that fall within an EP event 67, 69, 70

equilibrium climate sensitivity (λ) The change in mean surface temperature over a region resulting from a unit increase in radiative forcing, evaluated when interdecadal trend has become small compared to interannual variability. Measured in $\mathrm{K} \cdot (\mathrm{W} \cdot \mathrm{m}^{-2})^{-1}$. 37, 38

forcing Influences on climate that tend to produce a particular response from (model) climate system variables. In a low-dimensional dynamical system, these correspond roughly to control parameters 1, 3, 5, 8, 14–18, 21, 23, 28, 29, 31, 32, 35, 36, 38, 40, 43, 47, 50, 51, 63, 65, 68, 77, 79, 87, 94, 97, 99, 102, 103, 106, 109, 110, 112, 115, 116, 119, 120, 122–126, 129–131, 133, 135, 136, 162, 163

IC ensemble A collection of model runs, differing only in the state from which they are initialised. 1, 7, 8, 15, 24, 27, 28, 32, 33, 35, 38–40, 42–44, 50, 81, 114, 124, 129, 130, 133, 135, 136, 173, 174

IC influence The effects of IC differences on climate trajectories and quantifications. IC influence could be quantified by the length of time it takes for the "IC footprint" in climate system trajectories to decay to the extent that the system behaviour can no longer be directly attributed to particular aspects of the ICs used. IC influence could also be seen as reflecting the extent of qualitatively different behaviours of the system which are consistent with a particular ICU. 5, 7–9, 29, 31–33, 35, 48, 50, 71, 72, 79, 81, 83, 86–88, 90–92, 97, 103, 104, 110, 112, 115, 116, 120–124, 126–129, 133–136

IC predictability Potential predictability, attributable to a specified prior model state 31

initial transient The evolution of a model trajectory prior to reaching an approximate steady-state. In a dynamical systems context, the term refers to the period during which a model trajectory evolves from its initial state in the basin of attraction of some attractor A, towards that attractor A. After this transient, during which an initial perturbation decays (see relaxation behaviour), the state space distance between a model trajectory and the attractor becomes negligibly small. 20, 60–62, 174

intransitive An intransitive dynamical system possesses at least two attractors 8, 20, 21, 23, 24, 29, 47, 173

kairodic assumption Under the kairodic assumption, finite time temporal statistics from a single climate trajectory are indistinguishable from those derived from an IC ensemble. 7, 9, 23–25, 92, 125, 131, 135

lead time The model integration time prior to computing ensemble statistics 15, 21–23

model drift Trends observed in model output time series, which are not attributable to evolving external forcing or low-frequency internal variability of the model system. Model drift is generally associated with radiative disequilibrium and secular changes in model system heat storage. Transient or "spin-up" behaviour commonly results in model drift.

Acronyms

Notation	Description
ACC	the Antarctic Circumpolar domain 54, 55, 81–83, 86, 92, 96, 102, 103
Af	Africa 54, 106, 108–110, 116, 117
AMO	the Atlantic Multidecadal Oscillation 33, 34
AMOC	the Atlantic Meridional Overturning Circulation 3, 32, 34, 71
AMS	American Meteorological Society 11, 12
AR(1)	first-order autoregressive 31, 56
BC	boundary condition 18, 20, 162, 163
CAM	Community Atmosphere Model 41, 42, 46, 51, 54, 59, 64, *Glossary:* CAM
CAM4.0	Community Atmosphere Model, version 4.0 41, *Glossary:* CAM
CCSM3	the Community Climate System Model, version 3 32, 33, 36, 41
CCSM4	the Community Climate System Model, version 4 4, 35–37, 41, 46, 133, 164, 169
CDF	cumulative density function 79, 87
CESM	Community Earth System Model 7, 162
CESM-LE	CESM Large Ensemble Project 28, 46, *Glossary:* CESM
CESM1.2	the Community Earth System Model version 1.2 40–42, 51, 133, 162
CFE	present day constant forcing ensemble 45, 49–51, 61, 62, 67–69, 76, 81, 86, 87, 89, 95, 97, 101, 103–109, 111, 112, 115, 116, 119–121, 129, 133, 162
CHPC	South African Centre for High Performance Computing 42–46, 49, 59, 163
CICE	Community Ice Code 41, 46, *Glossary:* CICE
CICE4	Community Ice Code, version 4 41, *Glossary:* CICE
CLD	vertically integrated cloud cover 83, 85, 102
CLM	Community Land Model 41, 42, 51, 162, 163, *Glossary:* CLM
CLM4.0	Community Land Model, version 4.0 41, *Glossary:* CLM
CMIP5	Coupled Model Intercomparison Project phase 5 4, 28, 31–33, 35, 36, 41, 169
COI	cone of influence 57, 64, 71, 165, 169

Notation	Description
CSM	climate system model 1, 4, 8, 13, 15, 27, 28, 30–33, 35, 37, 41, 112, 123, 128, 133, 135, 136
dycore	dynamic core 41, 42, *Glossary:* dynamic core
EBM	energy balance model 17, 27
ENSO	El Niño-Southern Oscillation 13, 22, 26, 28, 30, 31, 33, 34, 41, 60, 64–69, 71–74, 82–84, 105, 108, 109, 116, 128, 134, 165, 167, 169, 170
EOF	emperical orthogonal function 33
ESM	Earth system model 27, 28, 30, 31, 35, 41, 128
ETP	the Eastern Tropical Pacific 65, 66, 69, 83, 87, 88, 90, 101, 106, 116, 119, 165, 166
FV	finite volume 41, 42
GCM	global circulation model 4, 27, 30–32, 35
GHG	greenhouse gas 20, 32, 34
Gl	global-mean 60, 61, 80, 102, 114
GMST	global-mean surface air temperature 17, 18, 22, 31, 34, 37, 38
IC	initial condition 1, 5, 8, 14, 15, 20, 21, 28, 31–33, 36, 37, 43, 44, 47–51, 59–61, 68, 76, 79–81, 83, 86–88, 92, 94, 97, 102–106, 110–112, 115, 116, 121–123, 126, 129, 132–136, 162, 163
ICP	IC predictability 31–33, 48, 103, 104, 106, 122, 128, 133–135, *Glossary:* IC predictability
ICU	initial condition uncertainty 4, 5, 7, 15, 24, 28, 38, 43, 122, 136
IPCC	Intergovernmental Panel on Climate Change 26
KS	Kolmogorov-Smirnov 58, 77, 87, 92, 110, 130
NAO	the North Atlantic Oscillation 33, 34, 54, 60, 63–66, 71, 82–84, 87, 88, 92, 110, 112, 120, 171
NAt	the North Atlantic 53, 60, 61, 63, 87, 89, 92, 101, 102, 110, 112
NERSC	National Energy Research Scientific Computing Center 42–45, 49, 59, 163
NH	the Northern Hemishpere 119, 126
NML	the Northern Midlatitudes 73, 97, 98, 102, 104, 110, 119, 126
NP	the Arctic 60, 73, 80, 87, 101, 110

Notation	Description
NPa	the North Pacific 53, 60–63, 69, 81, 82, 85–87, 92–94, 101, 102, 105, 110, 112, 164, 165, 168, 169
NPI	the North-West Pacific 53, 63, 81, 82, 85–87, 104, 105, 110–112, 116
ODE	ordinary differential equation 4, 30
OHC	ocean heat content 17, 36, 37, 102, 128
PDC	Present Day Control 43, 44, 46, 49–51, 55–57, 59–67, 69, 71–73, 81, 101, 112, 162, 164, 165, 167, 168
PDE	partial differential equation 4, 30
PDF	probability density function 25, 28, 68, 77, 79, 81, 86, 87, 94, 101, 106, 111, 112
PDV	Pacific Decadal Variability 22, 26, 33, 34, 84
PIC	Pre-Industrial Control 43, 45, 47, 59–61, 63, 65, 162, 164, 165, 167, *Glossary:* PIC
POP2	Parallel Ocean Program, version 2 41, 42, 71, *Glossary:* POP2
PPT	annual precipitation 87, 89, 102
PSL	sea-level pressure 24, 53–57, 64–67, 73, 74, 83, 84, 92, 94, 120, 171
RCP	Representative Concentration Pathway 28, 40, 43, 45, 50, 51, 103, 106, 109, 110, 115, 122, 162, 163
SA	Southern Africa 54, 94, 109, 116
SAM	Southern Annular Mode 34, 54, 55, 63, 171
SE	spectral element 41, 42
SH	the Southern Hemisphere 34, 61, 101, 119
SML	the Southern Midlatitudes 50, 60–62, 86, 92, 94, 101–103, 106–108, 110, 116, 117, 119
SO	the Southern Ocean 34–36, 54, 71, 72, 103, 110, 116
SOI	the Southern Oscillation Index 54, 64–67, 73, 109
SP	the Antarctic 86, 110, 112
SSA	the region South of southern Africa 54, 61–63, 86, 104, 105, 110, 115, 116, 171
SST	sea surface temperature 13, 54, 60, 64, 67, 87, 169
TAS	near-surface (2m) air temperature 50, 54, 55, 61–63, 66, 69, 76, 77, 79, 80, 86–88, 90, 93, 96, 97, 99, 101–104, 106–110, 115–117, 119, 168

Notation	Description
TFE	RCP8.5 transient forcing ensemble 44, 45, 49–51, 68, 76, 77, 87, 89, 103–111, 113–116, 119–121, 129, 133, 162, *Glossary:* RCP
TOA	top of the atmosphere 22, 36, 37
Tr	the Tropics 65, 73, 88, 90
TS	radiative surface temperature 56, 57, 60–64, 66–74, 81–83, 85–88, 92, 94, 95, 97, 98, 104–106, 108–112, 116, 126, 128, 164–171
WMO	World Meteorological Organisation 11–13, 24–26
WTP	the Western Tropical Pacific 65, 67, 73, 87, 101, 109